
# UNIVERSIDAD DE MURCIA

ESCUELA INTERNACIONAL DE DOCTORADO

Molecular Complexation of Several Bioactive Compounds with Cyclodextrins. *In vitro* and *in vivo* Applications

Encapsulación Molecular de Diferentes Compuestos Bioactivos con Ciclodextrinas. Aplicaciones *In vitro* e *in vivo*

**D. Adrián Matencio Durán**

**2020**

La presente tesis ha dado lugar a las siguientes publicaciones científicas:

*This thesis has given rise to the following scientific publications:*

1. Adrián Matencio, Silvia Navarro-Orcajada, Irene Conesa, Iván Muñoz-Sánchez, Lorena Laveda-Cano, Desiré Cano-Yelo, Francisco García-Carmona, José Manuel López-Nicolás: *Evaluation of Juice and Milk "food model" fortified with Oxyresveratrol and β-Cyclodextrin.* Food Hydrocolloids (Enviado/sent).
2. Adrián Matencio, María Alejandra Guerrero-Rubio, Fernando Gandía-Herrero, Francisco García-Carmona, José Manuel López-Nicolás: E*ncapsulation of a bioactive betalamic acid derivate by natural and modified cyclodextrin. A physicochemical, thermodynamic, computational and stabilizer study.* Food & Function (Enviado/Sent).
3. Silvia Navarro-Orcajada, Adrián Matencio, Francisco Garcia-Carmona, José Manuel López Nicolás: *Smart delivery of stilbenes: Synthesis and encapsulation of Resveratrol lipo-derivates. A complete study.* Journal of Agricultural and Food Chemistry (Enviado/sent).
4. Adrián Matencio, Nilesh K. Dhakar, José Manuel López-Nicolás, Federica Bessone, Francisco García-Carmona, Roberta Cavalli, Giorgia Musso, Francesco Trotta. *Obtaining complexation constants for ligand/cyclodextrin-basednanosponges.Application and study of oxyresveratrol complexes.* Journal of Controlled Release. (Enviado/sent).
5. Adrián Matencio, Francisco García-Carmona, José Manuel López Nicolás. *A characterization of the stilbene modulation of phosphodiesterase activity*. Molecular Nutrition and food research. (Enviado/sent).
6. Adrián Matencio, Fernando Gandía-Herrero, Fabrizio Caldera, Francesco Trotta, Francisco García-Carmona, José Manuel López Nicolás. *Lifespan extension in Caenorhabditis elegans by oxyresveratrol supplementation complexed in soluble cyclodextrin-based nanosponges.* Journal of Controlled Release. (Enviado/sent).
7. Adrián Matencio, Samanta Hernández-García, Francisco García-Carmona, José Manuel López-Nicolás: *A Way to Increase the*

*Bioaccesibility and Photostability of Roflumilast, a COPD Treatment, by Cyclodextrin Monomers*. Polymers 05/2019; 11(5):801., DOI:10.3390/polym11050801

8. Adrián Matencio, Francisco García-Carmona, José Manuel López-Nicolás: *An improved "ion pairing agent free" HPLC-RP method for testing cAMP Phosphodiesterase activity*. Talanta 09/2018; 192., DOI:10.1016/j.talanta.2018.09.058
9. Adrián Matencio, Silvia Navarro-Orcajada, Francisco Garcia-Carmona, José Manuel López Nicolás: *Ellagicacid-boraxfluorescenceinteraction. Application to a novel cyclodextrin-borax nanosensor for analyzing ellagic acid in food samples.*. Food & Function 06/2018; 9(7)., DOI:10.1039/C8FO00906F
10. Adrián Matencio, María Agustina Alcaráz-Gómez, Francisco García Carmona, Begoña Arias, José Manuel López-Nicolás: *Application of a simple methodology to analyze Hydroxypropyl-β-Cyclodextrin in urine using HPLC–LS in early Niemann–Pick disease type C patient*. Journal of Chromatography B 06/2018; 1093-1094., DOI:10.1016/j.jchromb.2018.06.051
11. Adrián Matencio, Francisco García-Carmona, José Manuel López-Nicolás: *The inclusion complex of oxyresveratrol in modified cyclodextrins: A thermodynamic, structural, physicochemical, fluorescent and computational study*. Food Chemistry 05/2017; 232:177–184., DOI:10.1016/j.foodchem.2017.04.027
12. Adrián Matencio, Francisco García-Carmona, José Manuel López-Nicolás: *Aggregation of t10, c12 Conjugated linoleic Acid in presence of natural and Modified Cyclodextrins. A physicochemical, thermal and Computational analysis*. Chemistry and Physics of Lipids 03/2017; 204., DOI:10.1016/j.chemphyslip.2017.03.008
13. Adrián Matencio, Samanta Hernandez-Garcia, Francisco Garcia-Carmona, José Manuel López Nicolás: *An integral study of cyclodextrins as solubility enhancers of α-methylstilbene, a resveratrol analogue*. Food & Function 12/2016; 8(1)., DOI:10.1039/C6FO01677D
14. Adrián Matencio, Mario J. Bermejo-Gimeno, Francisco García-Carmona, José Manuel López-Nicolás: *Separating and Identifying the Four*

*Stereoisomers of Methyl Jasmonate by RP-HPLC and using Cyclodextrins in a Novel Way*. Phytochemical Analysis 12/2016; 28(3)., DOI:10.1002/pca.2654

15. Adrián Matencio, Carlos Javier García Hernández-Gil, Francisco García-Carmona, José Manuel López-Nicolás: *Physicochemical, Thermal and Computational Study of the Encapsulation of Rumenic Acid by Natural and Modified Cyclodextrins*. Food Chemistry 08/2016; 216., DOI:10.1016/j.foodchem.2016.08.023
16. Adrián Matencio, Francisco Garcia-Carmona, José Manuel López-Nicolás: *Encapsulation of piceatannol, a naturally occurring hydroxylated analogue of resveratrol, by natural and modified cyclodextrins*. Food & Function 05/2016; 7(5)., DOI:10.1039/C6FO00557H

---

Y las siguientes publicaciones divulgativas:

*And the following popular science publications:*

1. Adrián Matencio: *Novel methods of chiral separation*. Mapping Ignorance. ISSN 2529-8992. <<https://mappingignorance.org/2017/09/25/novel-methods-chiral-separation>> (Reviewed 11/06/2019).
2. Adrián Matencio: Whe*n we forget basic science. An example concerning solubility*. Mapping Ignorance. ISSN 2529-8992. <<https://mappingignorance.org/2018/01/03/forget-basic-science-example-concerning-solubility/>> (Reviewed 11/06/2019).
3. Adrián Matencio: W*hen we forget basic science. Seeking the small details out.* Mapping Ignorance. ISSN 2529-8992. <<https://mappingignorance.org/2018/10/29/when-we-forget-basic-science-seeking-the-small-details-out/>> (Reviewed 11/06/2019).

**D. Francisco García Carmona** y **D José Manuel López Nicolás**, catedrático y profesor titular de Universidad respectivamente del Área de bioquímica y Biología Molecular en el departamento de Bioquímica y Biología Molecular-A.

**AUTORIZAN**:

La presentación de la tesis doctoral titulada ENCAPSULACIÓN MOLECULAR DE DIFERENTES COMPUESTOS BIOACTIVOS CON CICLODEXTRINAS. APLICACIONES IN VITRO E IN VIVO.*(Molecular complexation of several bioactive compounds with cyclodextrins. In vitro and in vivo applications).* Realizada por D. Adrián Matencio Durán, bajo nuestra inmediata dirección y supervisión para la obtención del grado de Doctor por la Universidad de Murcia.

En Murcia, a 08 de julio de 2019

D. Francisco García Carmona D. José Manuel López Nicolás.

Los trabajos de investigación recogida en esta memoria han sido financiados por los siguientes proyectos:

- AGL2014-57431-P (MEC, FEDER).
- Programa de ayudas a Grupos de Excelencia de la Región de Murcia, de la Fundación Séneca, Agencia de Ciencia y Tecnología de la Región de Murcia" No. 19893/GERM/2015.
- AGL2017-86526-P (MEC, FEDER).

Adrián Matencio disfrutó de un contrato FPU-UM para la realización de esta tesis doctoral (R1402-2015).

En Murcia, a 08 de julio de 2019

D. Adrián Matencio

*Do or do not. There is no try.*

*Master Yoda.*

## Agradecimientos

*Normalmente soy un hombre de pocas palabras, y no acostumbro a escribir agradecimientos. Así que, no va a ser una excepción. No obstante, me gustaría dedicar unas palabras a aquellos que en mayor o menor medida me han apoyado en este largo camino.*

*Agradecer como no a mi familia (mi padre, madre, hermano, abuelos, tíos…) su apoyo incondicional y su sacrificio diario para que pudiera estudiar con cierta tranquilidad y llegar a este día. Sin ellos no hubiera sido posible este momento.*

*También a mis amigos de toda la vida, y a los nuevos que he conocido durante este camino por sus consejos, paciencia, y animarme en los momentos difíciles.*

*A mi profesora de instituto Dra. Dña. Josefa María Balsalobre, sin la cual yo sería cualquier cosa, menos un biotecnólogo.*

*A los profesores que me han enseñado en la carrera, por lograr que tenga un pensamiento crítico e integral. Al departamento de Bioquímica y Biología molecular A, en especial a los miembros del grupo de Bioquímica y Biotecnología Enzimática: Juana, Fernando, Pepa, Álvaro, Manuela y Mercedes; por tener siempre un momento para resolver cualquier duda por mi tonta que fuera.*

*A los compañeros de mi departamento, los que están y los que estuvieron, que han sido apoyo, amigos y distracción beneficiosa.*

*A mi pupila Silvia Navarro Orcajada, te deseo lo mejor que la ciencia y el trabajo te puedan dar.*

*Al profesor Dr. Francesco Trotta y a su equipo de la Universidad de Turín por su agradable acogida y su buena disposición a trabajar juntos.*

*A Isabel María Guerrero Lozano, por estar conmigo en los buenos y los malos momentos y ser un gran pilar sin el cual esta tesis no podría haber sido posible. Gracias.*

*A mi director y profesor Dr. Francisco García Carmona. Uno de los hombres más inteligentes que he conocido. Siempre dispuesto a escucharme, no había día que no aprendiera algo nuevo. Confío llegar a tu nivel algún día e intentaré no olvidar nada de lo que me ha enseñado estos años. Gracias.*

*Y como no, a mi profesor, tutor, director y amigo Dr. José Manuel López Nicolás. Gracias por acogerme, por tus consejos y siempre darme la oportunidad de expresarme libremente. Gracias por confiar en mí cada día y lograr encontrar unos minutos de tu apretadísima agenda para atenderme cuando lo necesitaba y cuando no. Gracias por considerar mi palabra científica igualmente válida a la de un catedrático desde el primer día. No solo me has enseñado ciencia, me has enseñado vida. Gracias por todo.*

*Constancia, esfuerzo y superación.*

## Index

# Resumen/Summary

**Resumen de tesis doctoral**

Alimentos más saludables, fármacos más efectivos, cosméticos más seguros….el desarrollo de nuevos productos está en auge. Por esta razón diferentes sectores industriales intentan satisfacer las actuales demandas de la sociedad adicionando nuevas moléculas a sus productos que les otorguen un valor añadido que no tengan los productos de la competencia. En este marco de creciente competitividad empresarial y de alta investigación, desarrollo e innovación científica han emergido en los últimos años unas moléculas de uso multidisciplinar: las ciclodextrinas (CDs), compuestos glucídicos con singulares propiedades que se han hecho hueco en nuestra cesta de la compra, pudiendo encontrarlas en productos tan aparentemente dispares como barritas energéticas, desodorantes, colonias, medicinas, etc.

Las CDs son moléculas formadas por unidades de glucosa unidas por enlaces α-(1→4) glucosídicos. Aunque en la naturaleza solo existen tres tipos (α-, β-y γ-CD que contienen seis, siete y ocho unidades de glucosa respectivamente), son muchas las CDs modificadas que han sido sintetizadas a partir de las originales con distintos propósitos. Debido a su interior hidrofóbico y exterior hidrofílico, la propiedad más importante que presentan es su capacidad para incluir una amplia variedad de moléculas orgánicas e inorgánicas en su interior mediante procesos de encapsulación molecular. La formación de complejos de inclusión entre las CDs y las moléculas huésped tiene diferentes consecuencias para las moléculas encapsuladas. Entre ellas destacan un aumento de su estabilidad bajo condiciones de estrés biótico (enzimas) o abiótico (luz, oxidantes…), su liberación controlada, la eliminación

de sabores o propiedades desagradables, la separación quiral de isómeros, etc.

Al igual que cualquier aditivo, las CDs han tenido que pasar los exhaustivos controles que distintas administraciones como la FDA americana o EMA europea han establecido. Estos controles han limitado concentraciones seguras para su uso. Además, las tres ciclodextrinas naturales tienen reconocido el grado de aditivo alimentario (E-457, E-458 and E-459). El hecho de que su farmacocinética sea bastante rápida (un individuo sano puede eliminarlas del organismo en 24h) ha logrado, por ejemplo, que sean consideradas como fármaco huérfano para distintas enfermedades.

Como he comentado previamente, la capacidad de las CDs para encapsular moléculas hidrofóbicas ha provocado que diferentes sectores industriales las hayan incluido en las formulaciones de productos de muy diferente naturaleza. Sin embargo, antes de poder pensar en las aplicaciones industriales de los complejos de inclusión entre CDs y moléculas huésped hay que realizar una profunda investigación básica del proceso de encapsulación molecular. Dicha investigación básica abarca el conocimiento de las constantes implicadas en la interacción molecular, el estudio del efecto de distintos parámetros físico-químicos que afectan al proceso de encapsulación molecularcomo son el pH y la temperatura del medio de reacción, el análisis de estructura tridimensional del complejo de inclusión formado, etc.

Por ello el primer bloque de esta tesis doctoral estará dedicado a la investigación básica que se esconde tras los complejos de inclusión entre diferentes moléculas huésped (estilbenos, ácidos grasos, vitaminas, etc.) y

distintas CDs naturales y modificadas. Para ello se emplearán diversas técnicas analíticas como espectrofotometría, fluorescencia, cromatografía líquida, análisis computacional, etc. Esta información será clave para afrontar, en un segundo bloque, las aplicaciones prácticas de los complejos de inclusión en diferentes sectores como son la química analítica, la industria alimentaria o el sector médico-farmacéutico. Para concluir, en el tercer bloque de esta tesis doctoral haré una mirada hacia el futuro de las CDs, centrándome en el estudio de nanoesponjas basadas en CDs (CD-NS) y sus aplicaciones.

A continuación resumiré los principales resultados alcanzados en estos tres bloques:

Primer bloque

De forma resumida, en el primer bloque se usaron distintas CDs comerciales para encapsular compuestos bioactivos como ácidos grasos (ácido ruménico o su isómero, t10,c12 ácido linoléico conjugado) o de la familia de los estilbenos (piceatannol, trans-α-methylstilbene, oxyresveratrol, resveratrol esterato y resveratrol oleato).

El efecto de las CDs sobre la concentración micelar crítica (c.m.c., valor donde los ácidos pasan de estar de forma monomérica a agregarse) se usó para calcular su constante de encapsulación. Los efectos de distintas temperaturas y valores de pH sobre la constante también se evaluaron mostrando la constante gran dependencia conforme a su variación. Sorprendentemente, el ácido ruménico presentó un cambio sustancial de conformación intrínseco al variar la temperatura. No obstante, el otro ácido graso no mostró un comportamiento similar. De entre todas las CDs

estudiadas, HPβ-CD presentó el mejor resultado para ambos ácidos grasos aunque fue ligeramente superior con ácido ruménico.

Por otro lado, se estudió el complejo de inclusión de distintos estilbenos comerciales, además de algunos derivados hidrofóbicos del resveratrol que fueron sintetizados durante esta tesis, con CDs naturales y modificadas. Para su estudio, se usaron dos estrategias distintas basadas en medidas espectrofotométricas o HPLC. En general, los derivados de β-CD presentaron siempre los mejores valores de constantes. El efecto de pH y temperatura sobre la fuerza de la encapsulación fue estudiado para los estilbenos comerciales mostrando una gran influencia sobre la constante de encapsulación. El estilbeno conocido como Piceatannol fue estudiado mediante fluorescencia, produciéndose un incremento en su señal dependiente de la cantidad de CD (por el aumento de rigidez del sistema).

La encapsulación de trans-α-methylstilbene, oxyresveratrol y los derivados sintéticos del resveratrol se estudió mediante HPLC (debido a su menor solubilidad) obteniéndose una constante aparente. Por otro lado, se usó i) el desplazamiento de quinina de su complejo de inclusión con CD para demostrar la encapsulación de los estilbenos y que no era una mera adsorción, ii) resultados de RMN para corroborar la orientación del estilbeno dentro de la CD y iii) DSC para confirmar la formación de los complejos de inclusión.

Finalmente, se usaron técnicas de docking molecular para predecir y estudiar los distintos complejos de inclusión. Es importante mencionar que en esta tesis doctoral nuestro grupo por primera vez aplicó técnicas de modelado molecular para el estudio de complejos de inclusión.

Segundo bloque

En referencia al segundo bloque, las aplicaciones probadas se centraron en química analítica, ciencia alimentaria y farmacéutica.

En relación a la química analítica se separaron los cuatro isómeros del metil jasmonato, compuesto usado para la elicitación de cultivos vegetales y la producción de compuestos bioactivos, mediante una combinación de HPLC-RP, Mβ-CD y docking molecular. Se calcularon las constantes de encapsulación para los cuatro isómeros y se separaron los isómeros con un sencillo método. Para la identificación de los picos se usaron i) técnicas de docking molecular que identificaron los picos de HPLC en función de la fuerza con que Mβ-CD interaccionaba con cada uno y ii) una coinyección con aceite esencial de romero, que contenía cantidades descritas de un isómero mayoritario, que confirmó el orden predicho por docking molecular.

Por otro lado, en aplicaciones en la ciencia alimentaria en primer lugar sentamos las bases para un nuevo nanosensor basado en el complejo ternario bórax/ácido elágico/γ-CD para su determinación en alimentos. Después de desarrollar unos nuevos modelos matemáticos para obtener las constantes de encapsulación, se pudo comprobar que la unión entre bórax y ácido elágico tiene una estequiometria 2:1 en vez de 1:1, al contrario de lo que la bibliografía decía. Uno de esas moléculas de bórax sale para dejar entrar una ciclodextrina y así amplificar la señal. Finalmente descubrimos que la señal era lineal, precisa y sin interferencias usando como prueba una muestra cruda de arándanos para la determinación de este compuesto bioactivo.

En segundo lugar, estudiamos la estabilización de derivados del ácido betalámico (en concreto, feniletilamina betaxantina) a valores de pH cercanos a los zumos comerciales. Los resultados fueron concluyentes: los derivados del ácido betalámico presentan poca estabilidad en disoluciones ácidas y es necesaria su estabilización si queremos añadirlos en alimentos (como zumos por ejemplo). Por ello, estudiamos exhaustivamente su encapsulación con distintas CDs, en función de pH y temperatura para ver cómo estos parámetros afectarían a la constante de encapsulación. Los resultados verificaron que las CDs son capaces de proteger esta betalaína a valores de pH tan ácidos, resultados esenciales para la industria alimentaria si queremos suplementar zumos comerciales y el derivado betalámico llegue en perfecto estado al consumidor.

Y en tercer lugar, usamos la tecnología de los *food models* (tampones que asemejan las características de alimentos para facilitar su evaluación) para estudiar la fortificación de leche y zumos con oxyresveratrol y β-CD. Un total de 60 condiciones fueron evaluadas demostrando que las muestras fueron generalmente estables durante 5 semanas, con excepción de la muestra de leche sobresaturada con oxyresveratrol destapadas, que empezaron a degradarse a las 3 semanas. Almacenando las muestras en oscuridad, pueden preservarse durante al menos 5 semanas.

Así mismo, oxyresveratrol fue perfectamente bioaccesible y sus capacidades antimicrobianas aumentaron debido al incremento de solubilidad logrado por β-CD. Estos resultados son de gran importancia no solo para la industria alimentaria sino para nuestro departamento, porque suponen un paso

más en nuestros estudios con compuestos bioactivos encapsulados. Además suponen un valor añadido al trabajo de nuestro grupo de investigación al ser el primer trabajo de estas características que realizamos.

Por último, en esta parte se estudiaron dos aplicaciones farmacéuticas: la primera fue la creación de una novedosa metodología de HPLC con sensor de *light scattering* para el estudio de la eliminación de HPβ-CD en la enfermedad rara de Niemman Pick tipo C. El método se usó también para determinar la farmacocinética de este medicamento huérfano en un caso clínico. Los resultados sugieren que se podría aumentar la frecuencia de inyecciones de CD para mejorar sus resultados, ya que la CD se eliminaba en tres días sin mostrar toxicidad asociada a su administración.

La segunda aplicación fue la mejora de la bioaccesibilidad y fotoestabilidad de roflumilast, un potente fármaco contra las enfermedades pulmonares crónicas obstructivas (COPD). Se estudió la encapsulación de este fármaco con distintas CDs, además de determinar los parámetros cinéticos de su degradación por la luz. Los resultados sugieren que la dosis y las tabletas podrían ser reformuladas con menor cantidad al ser más bioaccesible.

Tercer bloque

Para terminar, el tercer bloque estudió la síntesis y aplicación de solubles e insolubles CD-NS para la encapsulación de oxyresveratrol. En primer lugar, los complejos de las CD-NS insolubles con oxyresveratrol fueron estudiados y utilizados en un ensayo anticancer. Se ideó un nuevo modelo para calcular por primera vez su constante de encapsulación. Distintos polímeros basados en el número de sus centros de unión o en el tipo de CD usada para su síntesis

fueron evaluados. Además, se comparó su constante con la del complejo resveratrol/CD-NS. Asimismo, el complejo fue caracterizado por TGA, DSC y FTIR.

Una liberación *in vitro* del compuesto demostró una liberación más lenta del mismo, lo cual es crucial para conseguir un efecto prolongado. Además, se realizó un estudio de su capacidad anticancer testando la inhibición del crecimiento sobre la línea celular PC-3 de cáncer de próstata, mostrando una mayor inhibición del complejo (58%) frente a oxyresveratrol solo (43%).

En segundo lugar, se estudio la encapsulación de oxyresveratrol por CD-NS solubles para el estudio de su efecto sobre la vida media del nematodo *Caenorhabditis elegans* (*C.elegans*). Se usó el desplazamiento de fluoresceína del interior de CD-NS para demostrar que oxyresveratrol estaba complejado dentro del polímero. Asimismo, se expresó heterólogamente en *E.coli*, purificó y plegó correctamente por primera vez la enzima completa fosfodiesterasa tipo 4 (PDE4) de *C.elegans* para estudiar sus parámetros cinéticos y su posible inhibición como diana terapéutica. Los resultados demostraron la capacidad de oxyresveratrol para afectar a la actividad fosfodiestarasa de la enzima inhibiendo la conversión de AMPc a AMP.

Además, el estudio *in silico* mediante docking molecular de la inhibición demostró que era una inhibición competitiva y recogió lo esencial de su actividad. La combinación de oxyresveratrol con CD-NS incrementó el efecto de oxyresveratrol sobre la vida media del gusano (9.6%). A diferencia que las CDs comerciales que afectaron negativamente a su vida, el polímero resultó ser inocuo para el nematodo.

En definitiva, esta tesis en su conjunto representa un importante avance en el conocimiento relacionado con CDs en distintos campos: nuevos métodos de separación de moléculas, de estabilización de alimentos y fármacos… Además, establece nuevas metodologías para trabajar con ellas en distintos campos como química analítica, ciencia alimentaria y farmacéutica.

Sin más dilación, espero disfrute de la lectura de esta tesis.

## Thesis summary (English Version)

Healthier foods, more effective drugs, safer cosmetics ... the development of new products are increasing. For this reason, different industrial fields try to satisfy the current demands of society by adding new molecules to their products that give them an added value. As a consequence, a molecule has taken huge impact in recent years, cyclodextrins (CDs). Indeed, it is not possible to imagine a world without CDs; they are present in many products of our life. CDs are torus-shaped oligosaccharides made up of α-(1,4) linked glucose units. The most common CDs are α, β and γ-CD, which contain six, seven and eight glucose units, respectively. Researches also have improved them modifying its structure with different radicals, adding functional molecules or creating novel materials. In general, CD forms inclusion complexes with hydrophobic and partially hydrophobic molecules, which improves the apparent solubility of the drug. Moreover, the complexation leads other positive properties such as increase of stability under abiotic (light, oxidants...) or biotic (enzymatic degradation) conditions, control release of molecules (e.g. volatiles), elimination of undesirable tastes and odours, chiral separation, directed chemical reactions, selective purification of molecules or alimentary fiber.

Before to introduce CDs in a product, it is important to know the ratio CDs/bioactive compounds necessary to achieve good protection without wasting money. In other words, is crucial to know the complexation constant between CD and our bioactive compound. Several techniques have been tuned up for studying this parameter. Among others, HPLC or spectrophotometric techniques has been used several years because they are i) easy, ii)

reproducible and iii) reliable. However, other techniques help and support their results (e.g. NMR, DSC, FTIR, TGA…)

As any additive, CDs have been approved and there are dose limits. The most important administrations such as FDA or EMA have written monographs about commercial available CDs explaining dose, adverse effects, etc. Indeed, natural CDs are considered as food additive (E-457, E-458 and E-459). Even some CDs derivates, such as HPβ-CD, are considered orphan drugs. An interesting point is that the pharmacokinetics of CDs is quick, being eliminated in more or less 24 hours in healthy subjects.

Bearing the above in mind, the uses of CDs in the last decades have considerably increased. Examples in analytical chemistry, pharmaceutical science or food science are published each day.

For that reason, this thesis will try to show the potential and applicability of CD knowledge: In our first block, several inclusion complexes characterizations will be carried out for understanding CDs capacities. After that, this knowledge will be used in the second block to study the application of CDs in different fields such as analytical chemistry, food science and pharmaceutical science. Finally, our third block will study the synthesis of a polymer called CDs-based nanosponge (CD-NS) and their applications.

First block

Different CDs were used to obtain and characterize the inclusion complex of some bioactive compounds such as fatty acids (rumenic acid and t10,c12

Conjugated linoleic acid) or stilbenes (piceatannol, trans-α-methylstilbene, oxyresveratrol, resveratrol sterate and resveratrol oleate).

To start with fatty acids, the effect of CDs on the critical micellar concentrations of the lipids was used to calculate the complexation constant of the fatty acids with CDs. The effect of temperature and pH were studied showing an interesting conformational changing in rumenic acid depending on temperature. The best CD tested was HPβ-CD in both cases giving similar $K_F$ results, although rumenic acid complex was the strongest.

According to stilbenes, commercial stilbenes and resveratrol derivates were studied using two principal strategies (spectrometric and HPLC) in combination with several techniques (DSC, NMR, molecular docking, quenching, etc.) to clarify the complex. In general, β-CD modified cyclodextrins were the best for stilbene complexing. Piceatannol was analyzed using its fluorescence signal, which increased in presence of CD due to its complexation and increase of rigidity. Trans-α-methylstilbene, oxyresveratrol and resveratrol derivates were analyzed using HPLC, obtaining and apparent complexation constant. Our results demonstrated that the displacement of quinine can be used to confirm the complexation of drugs in CD. In addition, NMR was used to study the structure of a complex for the first time in our research group. Finally, molecular docking strategy was applied to predict the interactions successfully. This technique was used for the first time during this thesis by our research group to characterize CDs inclusion complexes.

Second block

The applications of the second block were focused in three fields: analytical chemistry, food science and pharmaceutical science. Our analytical chemistry application was to study the enantioseparation of methyl jasmonate isomers using a combination of HPLC-RP, Mβ-CD and molecular docking technique. We separated and identified them successfully with an easy and reproducible method where Mβ-CD is added to mobile phase. Lastly, a rosemary essential oil sample was used in combination of molecular docking to number the isomers.

The applications of the food science studied three different uses of CDs: firstly, the ternary complex between ellagic acid, γ-CD and borax was evaluated and exhaustively studied to lay the foundations of a novel nanosensor tested in blueberries. A novel mathematical model was created to determine the encapsulation constant. The signal sensitivity was lineal and accurate. No interferences were observed in the application.

Secondly, the effect of CDs on betalain derivates protection at citric pH was evaluated. As it was obvious that the molecule presented low stability in acid pH values, the complex of Phenylethylamine-betaxanthin with different CDs was studied. β-CD derivates showed to be the best option to complex the molecule. Eventually, its complexation demonstrated to be a good strategy to protect the molecule in aqueous solutions.

Thirdly, the *food model* strategy was applied to fortify juice and milk with oxyresveratrol and β-CD. The results showed the samples to be perfectly stable for 5 weeks in all the conditions tested with the exception of the “oversaturated

non-darkness stored milk food model samples" after 3 week, when partial degradation started. Using dark storage an oversaturated oxyresveratrol solution solubilized by β-CD can be preserved at least 5 weeks. The samples were also perfectly bioaccessible and its antimicrobial properties were increased. This fact is important not only for food industry, but also for our research group because it represents a novel step in our work with complexed drugs.

Finally, the pharmaceutical applications will focus on i) to establish an easy methodology to measure HPβ-CD in Niemman Pick Type C patient. Indeed, the method is applied in a clinical case. An almost complete HPβ-CD elimination suggests that the dose can be increased to every four days. Ii) The increase of bioaccesibility and photostability of roflumilast, a potent Chronic obstructive pulmonary disease (COPD) treatment, was carried out complexing this drug with several CDs. These data could improve the tablets and therapy to improve the treatment.

Third block

To finish, the third block studied the synthesis and application of soluble and insoluble nanosponges on oxyresveratrol encapsulation and bioactivities. Insoluble nanosponges were used to complex oxyresveratrol, with a novel methodology to determine the complexation constant for the first time in nanosponges. The complexation efficiency and uptake were also obtained. TGA, DSC and FTIR experiments were carried out to check the complex. An *in vitro* controlled release showed slower release of complexated drug than free drug. Finally, an *in vivo* anticancer cell line experiment against PC-3 cell line

was carried out showing an increase of anticancer activity from 43 % (free drug) to 58 % (CD-NS complex)

Soluble nanosponges were used to study the lifespan of oxyresveratrol supplementation on Caenorhabditis *elegans* (*C.elegans*). A displacement of fluorescein was used to verify the encapsulation of oxyresveratrol on the nanosonges. Phosphodiesterase type 4 (PDE4) of *C.elegans* was heterologous expressed, purified and refolded to determine its enzymatic parameters and inhibition. An *in silico* study was carried out showing the essential of the inhibition. The combination of OXY and CD-NS increased the effect of OXY (9.6 %) on lifespan in contrast to CDs monomers that affected negatively to *C.elegans*.

In general terms, this thesis as a whole represent an important increase on CD knowledge in different fields: novel separating methods, nutraceutics stabilization… Moreover, novel methodologies to work with CDs were also studied.

Finally, I really hope you enjoy reading this thesis.

# Introduction

## 1. Cyclodextrin world.

Do you imagine a world “cyclodextrin-free”? No, I do not because Cyclodextrins (CDs, **Fig**. 1A) are used as invisible agent in common food products, cosmetics, textiles, and drug-excipient. CDs were discovered by Villiers in 1891 studing beautiful cristal formed as a degradation of starch [1]. Scientists were studying its molecule giving the first patent in 50s [2]. This fact started the huge increase of knowledge around CDs until days; for example, only in 2018 1530 research articles were published with CDs in the title and the word cyclodextrins appears in 4800 patents.

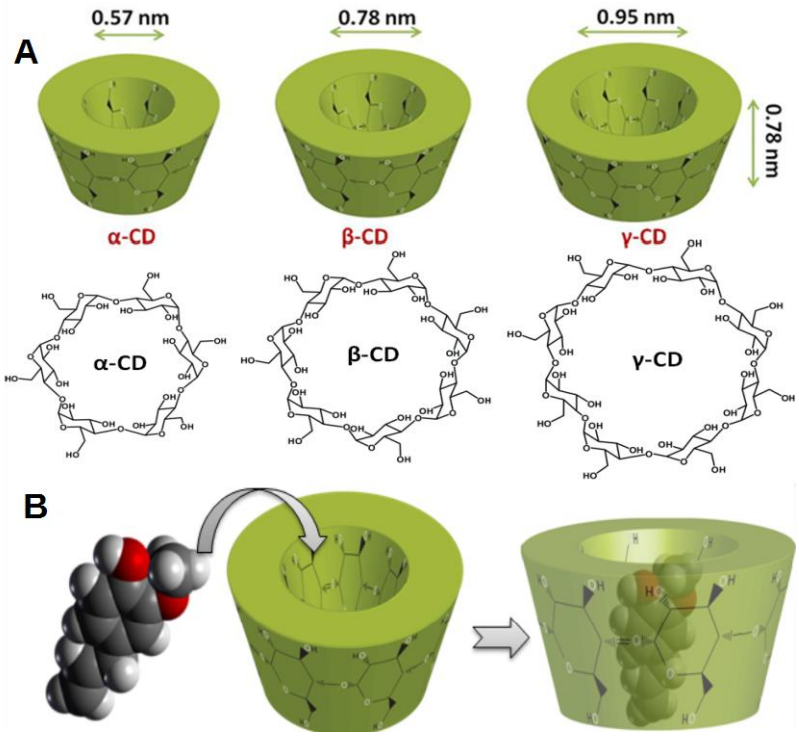


***Fig**. 1. (A) Natural CDs structure. (B) Inclusion complex formation.*

CDs are torus-shaped oligosaccharides made up of α-(1,4) linked glucose units thanks to cyclodextrin glucosil transferase from *Bacillus macerans* [3], among others. The most common CDs are α-, β- and γ-CD which contain six, seven and eight glucose units, respectively (**Fig**. 1A). The cavity of CDs is

covered by hydrogen atoms giving a hydrophobic nature and the outer part, where primary and secondary hydroxyl groups are exposed giving a hydrophilic nature. This characteristic was quickly investigated focused on complexing hydrophobic molecules, creating an “inclusion complex” (**Fig**. 1B) where CD get inside the molecule.

Although natural CDs are usually used, we can found some chemically derivates such us Methyl-β-cyclodextrin (Mβ-CD) or Hydroxypropyl-β-cyclodextrins (HPβ-CD), whose hydroxyl groups are modified. Generally, the derivates present better solubility than natural CDs. Indeed, these modifications could also change its complexation behavior (e.g. Mβ-CD can get more hydrophobic interactions). In addition, CDs polymers are also investigated to improve their complexation capacity and stability. Among others, we could cite β-cyclodextrin-epichlorohydrin polymers or CD- based nanosponges(CD-NS) [4,5].

### 1.1 General properties of CD/bioactive compound complexes

In aqueous solution, the “inclusion complex” is a dynamic equilibrium because it is a non-covalent union. In other words, complexes are continuously being formed and dissociated. This fact means predictable any dilution or aggregation of another hydrophobic drug may change the equilibrium rate.

In general, CD improves the apparent solubility of the drug increasing possibly the drug final concentration and bioavailability. Indeed, natural CDs are considered as food additive (E-457, E-458 and E-459). Moreover, the complexation leads other positive properties [6]:

1. Increase of stability under abiotic (light, oxidants...) or biotic (enzymatic degradation) conditions.
2. Control release of molecules (e.g. volatiles).
3. Elimination of undesirable tastes and odours.
4. Chiral separation.
5. Directed chemical reactions.
6. Selective purification of molecules.
7. Alimentary fiber [7] .

However, these properties could generate some adverse effects; for example, the release of a molecule could be too slow to get these effects (a perfume), or to enhance the degradation of a molecule. As a result of these facts, each complex must be exhaustively studied before to be used in industry.

## 1.2 Inclusion complex characterization

The capacity to form inclusion complexes of cyclodextrins (CDs) with bioactive compounds (BCs) is one of the most famous characteristics of this matrix. Indeed, many authors have focused its research to improve th analytical techniques to characterize the complex, in particular the complexion constant. Complexation constant ($K_F$), also called formation constant or encapsulation constant, is a crucial parameter for evaluating the effectiveness of the complexes because is related to the stability, the amount of each component of the equilibrium, etc.

This is not easy to evaluate and sometimes requires a combination of some techniques, such as show two recent reviews [8,9]. These studies could help to select the most interesting CD to use in your work.

The different available methods are generally based on a variation in any suitable physical or chemical property of the guest due to the inclusion complex formation. In that sense, we could find:

1. Spectroscopic techniques:
    a. Ultraviolet/Visible (UV).
    b. Circular dichroism.
    c. Fluorescence.
    d. Nuclear magnetic resonance (NMR).
    e. Electrons spin resonance (ESR).
    f. Fourier-transform infra-red (FTIR).
2. Electroanalytical techniques:
    a. Polarography.
    b. Voltammetry.
    c. Potentiometry.
    d. Conductimetry.
3. Separation techniques:
    a. High performance liquid chromatography (HPLC).
    b. Capillary electrophoresis (CE)
    c. Gas chromatography.
4. Thermal analysis techniques:
    a. Differential scanning calorimetry (DSC).
    b. Thermal gravimetric analysis (TGA).
    c. Isotermal titration calorimetry
5. Hot Stage microscopy (HSM).
6. X-ray diffraction:
    a. Single crystal X-ray diffraction (SCXRD).
    b. Powder X-ray diffraction (PXRD).
    c. Polarimetry.

However, the techniques used in this thesis will be only explained.

### *1.2.1 Techniques used*

#### 1.2.1.1 Ultraviolet/visible spectroscopy

UV-vis is a simple, easy and fast method for studing the host-guest complexation when its formation changes any particularity of the spectrum of the guest molecule. This change, depending on the chromophore, could originate new solute environment interactions. Moreover, the variation of the drug spectrum could be correlated with the formation of the complexes, but with some interference. The bathochromics shifts due to inclusion complex formation have been used several times to calculate the constant.

Is more common to found increasing in absorbance when the complex is formed, this fact is attributed to the shielding of chromophore group of the guest molecule in the CD cavity.

The stoichiometry and stability constant of complexes could be calculated, currently, using the job's plot or Benesi-Hildebrand method [10], these methods have demonstrated to be accurate. Complexes 1:1 or 1:2 are usually found (Table 1). Another quite used method is the Higuchi and Connors [11], but it only can study 1:1 complexes.

#### 1.2.1.2 Fluorescence techniques

Although could be considered as an extension of UV-Vis techniques, several authors consider these family of techniques different because is faster, simpler and more sensitive than UV-Vis. An enhancement in fluorescence is generally produced when a fluorescent molecule is complex by CDs, due to its quantum yield increase. As it can be observed, only fluorescence molecules

can be analyzed by this technique. These variation, can be used to obtain the stoichiometry and complexation constant of any fluorescence molecule using same model than UV-vis.

In any case, variation of these techniques has been several reported to increase their application and/or targets.

For example, a particular case showed in this thesis, its application to measure the complexation of fatty acids or high hydrophobic non-fluorescence molecules [12]. This technique is focused on measure the critical micellar concentration of fatty acids (cmc, the minimum concentration where fatty acids change from monomers to micelles), adding a fluorescence probe (generally 1,6-Diphenyl-1,3,5-hexatriene). The higher concentration of CDs is found, the higher cmc value. A relation between cmc and complexation constant could be used to obtain the constant.

Another one could be the fluorescence quenching method, an indirect probe to verify the complexation of any molecule in CDs. Solutions with any fluorescence molecule (able to be encapsulated) are prepared at fix concentrations the effect of our target molecule on the fluorescence of the other molecule is reported. Changes (currently decreasing) in fluorescence signal are related to the release of fluorescence molecule to enter the other one.

#### 1.2.1.3 Nuclear magnetic resonance (NMR) spectroscopy

NMR is one of the most powerful and useful techniques to obtain complete analytical information of the complexes. For example, this technique provide specific information on the orientation of the guest molecule inside the cavity,

while the other spectroscopic techniques previously described can give only indirect information on the molecular structure of the inclusion complexes.

#### 1.2.1.3.1 Usual 1H or 13C NMR

A comparative study of the chemical shifts (δ) of i) CD, ii) molecule and iii) the complex is the easiest experiment that can be carried out. This analysis can give important information not only about the complex formation but also give useful information about stoichiometry, stability, mechanism and geometry of the complex.

However, the technique present an important problem, the solubility of the drugs in water is not enough to get good signals so, the use of solvents are required that can modify the interactions.

#### 1.2.1.3.2 Nuclear overhauser effect experiments

NOE (nuclear overhauser effect) is a common phenomenon observed in NMR, consisting in the transfer of the spin polarization from one population of nuclear spins to another when atoms are close. This data are very useful to determine the 3D structure of a molecule or a complex.

Noe generates a 2D plot where a correlation between peaks is obtained, making easier the data interpretation. In addition, a higher sensitive NOE-1D can be done but the time required is longer and is only used when 2D does not results. The most common techniques exploiting the NOE are NOESY (Nuclear Overhauser Effect SpectroscopY) and ROESY (Rotational Overhauser Effect SpectroscopY), which have a strong application in CD inclusion complexes studies.

#### 1.2.1.4 Fourier-transform infra-red (FTIR)

This technique is usually used in solid complexes, to study which vibrational modes of the drug and CD are being changed during the inclusion complex formation. Changes in the characteristics bands of the guest molecule, such as disappearance, broadening, variations in peaks intensity and/or shifts in the wave number can indicate the formation of the complex.

The limited cost, wide diffusion, high sensibility and high selectivity of this technique, as well as the easy and relatively fast acquisition time of the spectra are among the main advantages of this technique.

#### 1.2.1.5. High performance liquid chromatography (HPLC)

Powerful, reproducible and versatile technique; HPLC is used to study as the stoichiometry as the encapsulation constant. It is focused on the interaction of stationary phase and its partition coefficient. However, the technique presents high use of materials may get high time of sample preparation and experiments.

CDs can be in the stationary phase bonded to the silica gel, or added in the mobile phase as a reactant. As a result of the interaction between CD and ligand, the retention time of the ligand will change, depending on the complexation and its interaction with the stationary according to Fujimura method [13]. Another approach, called Hummel-Dreyer method [14] uses a column equilibrated with an eluent carrying the guest molecule. When CD is added to the mobile phase, the chromatogram shows a positive peak due to the

complexation and a negative peak at the retention time of the free molecule, corresponding to the amount of complexed guest.

#### 1.2.1.6. Differential scanning calorimetry (DSC)

It is a very powerful analytical technique to characterize complexes. It has the ability to provide detailed information about their physical and energetic properties. The comparison of the thermal curves of single components, their physical mixture and the presumed inclusion compound ought to provide insight about modifications and interactions due to the formation of the inclusion complex. DSC of natural or amorphous CDs are characterized; they present an endothermal peak around 90-130 ºC corresponding to the dehydration, following a decomposition around 300 ºC. The peak corresponding to the fusion of guest molecule is usually hiding by their complexations. Modifications in the shape and temperature peak of the CD dehydration and/or with the disappearance of the drug melting peak, or the increase of the temperature of decomposition of the guest are probes of complex formation.

Table 1. Published mathematical models for complexation constants used in this thesis

| Stoichiometry | Equations for Benesi-Hildebrand/UV-VIS method |
|---|---|
| 1:1 | BC + CD ⇌ BC-CD |
| | $\frac{1}{F - F_0} = \frac{1}{(F_\infty - F_0)K_{11}[CD]} + \frac{1}{(F_\infty - F_0)}$ |
| 1:2 | BC + 2CD ⇌ BC-$CD_2$ |
| | $\frac{1}{F - F_0} = \frac{1}{(F_\infty - F_0)K_{11}[CD]^2} + \frac{1}{(F_\infty - F_0)}$ |
| | |
| Stoichiometry | Equations for Higuchi and Connors method |
| 1:1 | BC + CD ⇌ BC-CD |
| | $\mathrm{K}_{11} = \frac{\mathrm{Slope}}{\mathrm{S}_0(1 - \mathrm{Slope})}$ |
| | |
| Stoichiometry | Equations for Fijumura/HPLC method |
| 1:1 | BC + CD ⇌ BC-CD |
| | $\frac{1}{k} = \frac{1}{k_0} + \frac{K_{F11}}{k_0}\,[CD]$ |
| 1:2 | BC + 2CD ⇌ BC-$CD_2$ |
| | $\frac{1}{k} = \frac{1}{k_0} + \frac{K_{F12}}{k_0}\,[CD]^2$ |
| | |
| Stoichiometry | Equations for c.m.c. method |
| 1:1 | BC + CD ⇌ BC-CD |
| | $[c.m.c.*]_t = [c.m.c_0] + K_F[c.m.c_0][CD]$ |
| 1:2 | BC + 2CD ⇌ BC-$CD_2$ |
| | $[c.m.c.*]_t = [c.m.c_0] + K_{F12}[c.m.c_0][CD]^2$ |

#### 1.2.1.7. Thermogravimetric analysis (TGA)

TGA is ussualy used in combination with DSC analysis to support it. TGA allows determining the changes of weight with respect to temperature increases. The comparation of the weight lose profile of pure components, physical mixture and the complex shows differences correlatives to the complex formation. TGA of free CDs are characterized with a first stage around 100 ºC (dehydration) and the second at higher temperatures than 300 ºC due to its decomposition. As is expected, the weight loss profile of complexated drug will be different because an increase of stability; higher temperatures must be necessary.

#### 1.2.1.8. Molecular docking

Molecular docking is a technique that predicts non covalent bounds between a host and a guess. This knowledge may be used to check the binding affinity between two molecules, usually with a scoring function. Molecular docking is one of the most frequently used methods in structure-based drug design, due to its ability to predict the binding-conformation of small molecule ligands to the appropriate target binding site. Characterisation of the binding behaviour plays an important role in rational design of drugs as well as to elucidate fundamental biochemical processes. The general docking algorithm creates two initial positions (called pose) for host and guest and the software begins to approach them until a minimal energy. Later, a refinement with force fields is carrying out to get a better global pose of minimal scoring (energy).

With CDs, molecular docking techniques are recently employed to study the possible orientation and interaction between a bioactive compounds and

different CDs. Furthermore, the scoring ordination could help to test a few quantities of CDs instead of a lot of them.

### 1.3. Regulatory and safety of CDs

When our last objective is to use the product for human consumption like nutraceutical or pharmaceutical, we must know the real state of regulation, e.g. Quantity of CD, type of CD… An important aspect resting on the saccharide nature of CDs would be its non-toxicity; however, it must be studied.

The Food and Drug administration (FDA) of USA has published a list of inactive pharmaceutical ingredients such as CDs (https://www.fda.gov/Drugs/InformationOnDrugs/ucm113978.htm) that can be downloaded. In this list, the route, dosage form and maximum concentration is indicated. On the other hand, the European Medicines Agency (EMA) has published several reports on the use of different CDs in pharmaceutical products (https://www.ema.europa.eu/en/cyclodextrins). Indeed, a recent question and answer has been published about CDs and their uses [15]. Another organization, the Japanase Pharmacetical Codex (JPC) has published monographs about CDs. Regarding food products, the European Food Safety authority (EFSA) gave to α-CD the health claim dietary fiber, and the reduction of post prandial glycaemic responses and in 2012 [7] due to is competitive inhibition of α-amylase. In addition, the dosage of β-CD has been reevaluated in 2016 without modifications [16]. Finally, the natural CDs are commonly used as food additives and are included in FDA's "Generally recognized as safe" (GRAS) list and as food additives by the World Health Organization.

## 1.4. Pharmacokinetics and metabolism of CDs

As mentioned above, CDs are formed by saccharides. This fact suggests a possible metabolization into glucose. Although salivary α-amylase hydrolyzes dextrins quickly [17], the rapid transport to stomach makes this degradation insignificant. Unspecific pH dependent degradation can occur in stomach; however, the complexation with some molecule could delay its degradation [18]. After stomach, a pH neutral environment is found in small intestine where pancreatic amylase continues the hydrolysis. Finally, not digested subtracts are metabolized by microbioma digestion in the lower section of the digestion system.

A recent review discuss about pharmacokinetics of CDs [2]. Dextrins could also be administrated parenterally. For that reason, its pharmacokinetics has also been studied. As a result, monographs as the European Pharmacopoeia [19] has been written . CDs are no exception. Linear dextrin and CDs urinary clearance decreases with increasing molecular weight. Indeed, below 15 KDa are almost totally excreted by urine without important modifications [2].

All the natural CDs mentioned and its commercially available derivates are susceptible to bacterial digestion in the gastrointestinal tract. Between natural CDs, α-CD presents the lowest degradation rate. In healthy humans, the urinary clearance of HPβ-CD was studied showing an almost complete elimination of the dose injected parentally after 24h; however, kidney affected subjects could keep CD more time [20–22].

## 1.5 CD applications in different fields

The applicability of CDs is well known; indeed, a recent book is about this matter [23]. In this section, a contact with recent applications related with the work of this thesis is discussed.

### *1.5.1 Analytical chemistry*

In this field, CDs always show present in the separation of isomers and novel sensors. For example, recently has been applied the use of modified CDs with grapheme quantum dots to separate tyrosine enantiomers [24], which can be applied in depressed patients. The first step was to obtain β-CD quantum dot derivates in order to include them in an electrode. The method was validated using health and affected blood of patients showing significant difference in the oxidation peak current with ratio of L to D-Tyr reaching 2.35.

Not only hydrophobic molecules could be complexes by CDs, ions present susceptible encapsulation and this fact can also be used to create sensors. A recent work was published to analyze $Zn^{2+}$ and $CN^{-}$ in aqueous solution using magnetic CDs [25]. A modified fluorescein is used to selective bond $Zn^{2+}$ ion instead of others. This magnetic CDs presented high selectivity and increase of fluorescent signal. Moreover, the recycling of CDs was also studied showing a complete recovery of activity for at least 4 times.

The use of CDs in water treatment is also studied. Natural, chemically modified or polymeric CDs are used in this approach [23,26]. The most common strategy is to create different chemosensor focused on coloured or fluorescence CD (modified with a chromophore or fluorophore). CDs have demonstrated its

capacity to recognise and enantioseparate different water contaminant such as pesticides or 1-adamantanol. Indeed, mask can be also modified with CD to catch contaminants [27].

In a most common way, CDs can be used in chiral chromatography to separate isomers. This is very used in gas chromatography of essential oils [23,28]. There are commercially available CD columns where the degree of substitution or the type of CD can hugely modified the separation of isomers.

### *1.5.2. Food industry*

As was mentioned above, the most known application of CDs is to complex hydrophobic compounds. Consumers do not like bad organoleptic properties such us bitter or disgusting tastes and odors of food. Dietary nutraceuticals can be administrated in CD inclusion complexes [23] to mask its poor solubility or stability, or to increase some capacity such us antioxidant [29]; bioactive compounds such us vitamins, sterols or flavonoids are common targets for this strategy. The use of cyclodextrin in elicitation (alone or complexing) is also well studied, giving the possibility to obtain new bioactive compounds or an higher quantity of them [30].

A novel application is the use of “antimicrobial CDs”, where an antimicrobial has been complexed or linked to the CD [31,32]. Furthermore, another application of CDs in food can be the sequestrant of unpleasant odors like fish [33,34] or molecules like cholesterol [35]. These applications could help to decrease the concentration of undesirable compounds (e.g. coprecipitation of cholesterol by β-CD) or to reduce the amount of unpleasant properties.

### *1.5.3 Pharmaceutical industry*

Perhaps the most important application, the controlling release of a drug is a desirable characteristic making CDs a common used excipient. Desirable drug are classified in the Biopharmaceutics Classification System (BCS) as class I (highly soluble and permeable), however, the common drugs are class II (poorly soluble but highly permeable), III (soluble but not very permeable) or IV (poorly soluble and not very permeable); CDs can optimize these properties giving a good apparent solubility and permeability. For that reason, we could find CDs in a lot of pharmaceutical approved drugs such as steroids, Dozolamide, Disoxaril, insulin, Rifampicin or Salmon Calcitonin [23,36]. CDs Polymers could presents better results than CDs because its release is slower [37]. Moreover, CDs derivates could help to get the drug in the target tissue (e.g. magnetic CDs). One aspect that must be taken into account is the osmolarity. CDs could increase the osmolarity of a solution and, of course, blood tissue. You must always to work in the legal limits established by the FDA or the EMA.

By the moment, we are always talking about CDs/drug complexes but, can CD be use as a drug? Yes. Trappsol® (HPβ-CD) is an orphan drug approved for treating the rare disease Niemman Pick Type C (disease cause by a deficient *npc1* or *npc2*, accumulating cholesterol in tissues) due to its capacity to remove cholesterol.

## 2. Concluding Remarks

In the introduction, the fundamental aspects of CDs and its work have been showed. CDs present a lot of benefits complexing bioactive compounds or drug, such as increase of solubility or stability which makes interesting its study. Moreover, there are several techniques to calculate the inclusion complex strength giving its complexation constant. In addition, common applications have been discussed.

However, many articles only scratch the surface of CD potential during its work. For that reason, this thesis will go to try to go further. Several inclusion complexes will be exhaustively studied to show how different techniques and procedures could complement its basic work. Moreover, the application of CDs (natural, modified and polymeric) in different fields will be carried out showing the importance of the previous basic work and a novel strategy to solve crucial problems.

Specifically, in our first block, several inclusion complexes characterizations will be carried out for understanding CDs capacities. After that, in the second block we will study the application of CDs in different fields such as analytical chemistry, food science and pharmaceutical science. Finally, our third block will study the synthesis of a polymer called CDs-based nanosponge and their applications.

## REFERENCES

[1] Antoine Villiers, Sur la fermentation de la fécule par l'action du ferment butyrique, Comptes Rendus Académie Sci. 112 (1981) 536–538.

[2] S.V. Kurkov, T. Loftsson, Cyclodextrins, Int. J. Pharm. 453 (2013) 167–180. doi:10.1016/j.ijpharm.2012.06.055.

[3] A. Tonkova, Bacterial cyclodextrin glucanotransferase, Enzyme Microb. Technol. (1998) 678–686. doi:10.1016/S0141-0229(97)00263-9.

[4] A.P. Sherje, B.R. Dravyakar, D. Kadam, M. Jadhav, Cyclodextrin-based nanosponges: A critical review, Carbohydr. Polym. 173 (2017) 37–49. doi:10.1016/j.carbpol.2017.05.086.

[5] X. Yao, P. Huang, Z. Nie, Cyclodextrin-Based Polymer Materials: from Controlled Synthesis to Applications, Prog. Polym. Sci. (2019). doi:10.1016/j.progpolymsci.2019.03.004.

[6] W.J. Shieh, A.R. Hedges, Properties and Applications of Cyclodextrins, J. Macromol. Sci. Part A. 33 (1996) 673–683. doi:10.1080/10601329608010886.

[7] Scientific Opinion on the substantiation of health claims related to alpha cyclodextrin and reduction of post prandial glycaemic responses (ID 2926, further assessment) pursuant to Article 13(1) of Regulation (EC) No 1924/2006, EFSA J. 10 (2012) 2713. doi:10.2903/j.efsa.2012.2713.

[8] P. Mura, Analytical techniques for characterization of cyclodextrin complexes in aqueous solution: A review, J. Pharm. Biomed. Anal. 101 (2014) 238–250. doi:10.1016/j.jpba.2014.02.022.

[9] P. Mura, Analytical techniques for characterization of cyclodextrin complexes in the solid state: A review, J. Pharm. Biomed. Anal. 113 (2015) 226–238. doi:10.1016/j.jpba.2015.01.058.

[10] H.A. Benesi, J.H. Hildebrand, A Spectrophotometric Investigation of the Interaction of Iodine with Aromatic Hydrocarbons, J. Am. Chem. Soc. 71 (1949) 2703–2707. doi:10.1021/ja01176a030.

[11] H.T. Connors KA, Phase solubility techniques, Adv. Anal. Chem. Instrum. 4 (1965) 117–210.

[12] R. Bru, J.M. López-Nicolás, F. García-Carmona, Aggregation of polyunsaturated fatty acids in the presence of cyclodextrins, Colloids Surf. Physicochem. Eng. Asp. 97 (1995) 263–269. doi:10.1016/0927-7757(95)03091-Q.

[13] K. Fujimura, T. Ueda, M. Kitagawa, H. Takayanagi, T. Ando, Reversed-phase retention behavior of aromatic compounds involving .beta.-cyclodextrin inclusion

complex formation in the mobile phase, Anal. Chem. 58 (1986) 2668–2674. doi:10.1021/ac00126a020.

[14] S.F. Sun, C.L. Hsiao, Hummel-Dreyer method in high-performance liquid chromatography for the determination of drug-protein binding parameters, J. Chromatogr. A. 648 (1993) 325–331. doi:10.1016/0021-9673(93)80414-4.

[15] Questions and answers on cyclodextrins used as excipients in medicinal products for human use, (n.d.) 9.

[16] A. Mortensen, F. Aguilar, R. Crebelli, A.D. Domenico, B. Dusemund, M.J. Frutos, P. Galtier, D. Gott, U. Gundert-Remy, J.-C. Leblanc, O. Lindtner, P. Moldeus, P. Mosesso, D. Parent-Massin, A. Oskarsson, I. Stankovic, I. Waalkens-Berendsen, R.A. Woutersen, M. Wright, M. Younes, P. Boon, D. Chrysafidis, R. Gürtler, P. Tobback, D. Arcella, A.M. Rincon, C. Lambré, Re-evaluation of β-cyclodextrin (E 459) as a food additive, EFSA J. 14 (2016) e04628. doi:10.2903/j.efsa.2016.4628.

[17] J. John Marshall, I. Miwa, Kinetic difference between hydrolyses of γ-cyclodextrin by human salivary and pancreatic α-amylases, Biochim. Biophys. Acta BBA - Enzymol. 661 (1981) 142–147. doi:10.1016/0005-2744(81)90093-0.

[18] J. Singh, A. Dartois, L. Kaur, Starch digestibility in food matrix: a review, Trends Food Sci. Technol. 21 (2010) 168–180. doi:10.1016/j.tifs.2009.12.001.

[19] European Pharmacopoeia (Ph. Eur.) 9th Edition | EDQM, (n.d.). https://www.edqm.eu/en/european-pharmacopoeia-ph-eur-9th-edition (accessed April 3, 2019).

[20] H.W. Frijlink, J. Visser, N.R. Hefting, R. Oosting, D.K.F. Meijer, C.F. Lerk, The Pharmacokinetics of β-Cyclodextrin and Hydroxypropyl-β-cyclodextrin in the Rat, Pharm. Res. 7 (1990) 1248–1252. doi:10.1023/A:1015929720063.

[21] D.A. Hamilton, C.C. Ernst, W.G. Kramer, D. Madden, E. Lang, E. Liao, P.G. Lacouture, A. Ramaiya, D.B. Carr, Pharmacokinetics of Diclofenac and Hydroxypropyl-β-Cyclodextrin (HPβCD) Following Administration of Injectable HPβCD-Diclofenac in Subjects With Mild to Moderate Renal Insufficiency or Mild Hepatic Impairment, Clin. Pharmacol. Drug Dev. 7 (2018) 110–122. doi:10.1002/cpdd.417.

[22] D.R. Luke, N.D. Wood, K.E. Tomaszewski, B. Damle, Pharmacokinetics of sulfobutylether-β-cyclodextrin (SBECD) in subjects on hemodialysis, Nephrol. Dial. Transplant. Off. Publ. Eur. Dial. Transpl. Assoc. - Eur. Ren. Assoc. 27 (2012) 1207–1212. doi:10.1093/ndt/gfr472.

[23] S. Fourmentin, G. Crini, E. Lichtfouse, eds., Cyclodextrin Applications in Medicine, Food, Environment and Liquid Crystals, Springer International Publishing, 2018. https://www.springer.com/la/book/9783319761619 (accessed April 4, 2019).

[24] S. Dong, Q. Bi, C. Qiao, Y. Sun, X. Zhang, X. Lu, L. Zhao, Electrochemical sensor for discrimination tyrosine enantiomers using graphene quantum dots and β-cyclodextrins composites, Talanta. 173 (2017) 94–100. doi:10.1016/j.talanta.2017.05.045.

[25] Q. Li, Y. Zhang, Y. Jin, Q. Yang, J. Du, Y. Li, Fluorescent magnetic nanosensors for Zn2+ and CN− in aqueous solution prepared from adamantane-modified fluorescein and β-cyclodextrin-modified Fe3O4@SiO2 via host–guest interactions, RSC Adv. 5 (2015) 68815–68821. doi:10.1039/C5RA12258A.

[26] S. Salazar, D. Guerra, N. Yutronic, P. Jara, Removal of Aromatic Chlorinated Pesticides from Aqueous Solution Using β-Cyclodextrin Polymers Decorated with Fe3O4 Nanoparticles, Polymers. 10 (2018) 1038. doi:10.3390/polym10091038.

[27] D.M. Alzate-Sánchez, B.J. Smith, A. Alsbaiee, J.P. Hinestroza, W.R. Dichtel, Cotton Fabric Functionalized with a β-Cyclodextrin Polymer Captures Organic Pollutants from Contaminated Air and Water, Chem. Mater. 28 (2016) 8340–8346. doi:10.1021/acs.chemmater.6b03624.

[28] V.S. Pragadheesh, A. Yadav, C.S. Chanotiya, Role of substituents in cyclodextrin derivatives for enantioselective gas chromatographic separation of chiral terpenoids in the essential oils of Mentha spicata, J. Chromatogr. B. 1002 (2015) 30–41. doi:10.1016/j.jchromb.2015.07.034.

[29] J.M. López-Nicolás, P. Rodríguez-Bonilla, F. García-Carmona, Cyclodextrins and Antioxidants, Crit. Rev. Food Sci. Nutr. 54 (2014) 251–276. doi:10.1080/10408398.2011.582544.

[30] K. Ramirez-Estrada, H. Vidal-Limon, D. Hidalgo, E. Moyano, M. Golenioswki, R.M. Cusidó, J. Palazon, Elicitation, an Effective Strategy for the Biotechnological Production of Bioactive High-Added Value Compounds in Plant Cell Factories, Molecules. 21 (2016) 182. doi:10.3390/molecules21020182.

[31] P. Wen, D.-H. Zhu, K. Feng, F.-J. Liu, W.-Y. Lou, N. Li, M.-H. Zong, H. Wu, Fabrication of electrospun polylactic acid nanofilm incorporating cinnamon essential oil/β-cyclodextrin inclusion complex for antimicrobial packaging, Food Chem. 196 (2016) 996–1004. doi:10.1016/j.foodchem.2015.10.043.

[32] C. Abril-Sánchez, A. Matencio, S. Navarro-Orcajada, F. García-Carmona, J.M. López-Nicolás, Evaluation of the properties of the essential oil citronellal nanoencapsulated by cyclodextrins, Chem. Phys. Lipids. 219 (2019) 72–78. doi:10.1016/j.chemphyslip.2019.02.001.

[33] H.-S. Na, J.-N. Kim, J.-M. Kim, K.-Y. Lee, Encapsulation of fish oil using cyclodextrin and whey protein concentrate, Biotechnol. Bioprocess Eng. 16 (2011) 1077–1082. doi:10.1007/s12257-011-0099-2.

[34] H. Hashimoto, Application of Cyclodextrins to Foods, Toiletries and Other Products in Japan, in: O. Huber, J. Szejtli (Eds.), Proc. Fourth Int. Symp. Cyclodext., Springer Netherlands, 1988: pp. 533–543.

[35] D. Castagne, M. Fillet, L. Delattre, B. Evrard, B. Nusgens, G. Piel, Study of the cholesterol extraction capacity of β-cyclodextrin and its derivatives, relationships with their effects on endothelial cell viability and on membrane models, J. Incl. Phenom. Macrocycl. Chem. 63 (2008) 225–231. doi:10.1007/s10847-008-9510-9.

[36] P. Jansook, N. Ogawa, T. Loftsson, Cyclodextrins: structure, physicochemical properties and pharmaceutical applications, Int. J. Pharm. 535 (2018) 272–284. doi:10.1016/j.ijpharm.2017.11.018.

[37] R. Cavalli, F. Trotta, W. Tumiatti, Cyclodextrin-based Nanosponges for Drug Delivery, J. Incl. Phenom. Macrocycl. Chem. 56 (2006) 209–213. doi:10.1007/s10847-006-9085-2.

# Block I

## Study and characterization of different inclusion complexes with commercially available cyclodextrins

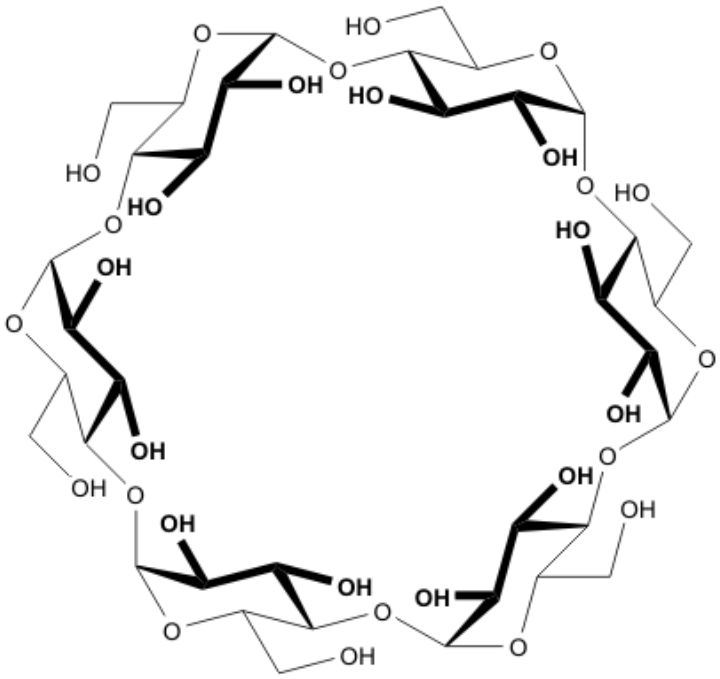

## Block Introduction

In this block, several inclusion complexes will be characterized. Two families of compounds (fatty acids and stilbenes) were studied using different techniques and mathematical models. Spectrophotometric measurements and chromatographic will be used depending on the molecule properties to calculate the complexation constant and combined with other techniques to complete the characterization.

# Block I Part I

## *Fatty acids*

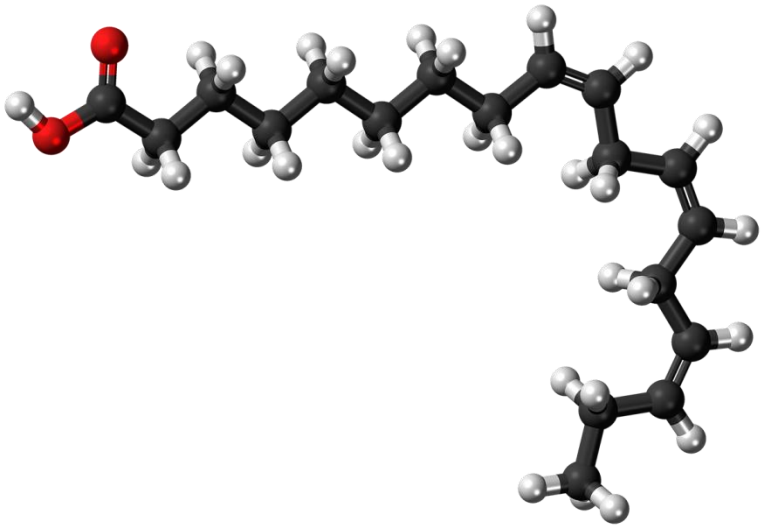

**Introduction**

Another family with recognized bioactivies is dietary fatty acids. There are a lot of products fortified with these fatty acids. Indeed, ω-3 fatty acids such as EPA (eicosapentanoic acid) or DHA (docosahexaenoic acid) are well known targets for food industry because FDA and EFSA awarded their food health claims. For example, Swanson *et al.,* wrote <<*Studies have shown that EPA and DHA are important for proper fetal development, including neuronal, retinal, and immune function. EPA and DHA may affect many aspects of cardiovascular function including inflammation, peripheral artery disease, major coronary events, and anticoagulation. EPA and DHA have been linked to promising results in prevention, weight management, and cognitive function in those with very mild Alzheimer's disease*.>> [1]. Recently, their relationship with sperm quality was also reported [2]. As a consequence, it is a family quite used to create new products

Despite all these healthy properties, there are several problems related with the chemical properties of dietary fatty acids prevent its use as fortifier of nutraceutical or functional foods. This bioactive molecule presents low solubility in water. In other words, the fortified products commonly have a considerable quantity of other fatty products (e.g. milk). Poor bioavailability and is easily oxidized, making it necessary to look for new strategies which may increase its bioavailability, solubility and stability in the face of pro-oxidant agents.

Bearing these problems in mind, it is obvious that its complexation in CDs could, at least, solve many of them. For that reason, in the present part of the thesis we are going to study the complexation of two promising fatty acids,

Rumenic acid ((c9,t11)-octadeca-9,11-dienoic acid) and (t10, c12)-octadeca-9,11-dienoic acid).

## References

[1] D. Swanson, R. Block, S.A. Mousa, Omega-3 Fatty Acids EPA and DHA: Health Benefits Throughout Life1, Adv. Nutr. 3 (2012) 1–7. doi:10.3945/an.111.000893.

[2] V. Esmaeili, A.H. Shahverdi, M.H. Moghadasian, A.R. Alizadeh, Dietary fatty acids affect semen quality: a review, Andrology. 3 (2015) 450–461. doi:10.1111/andr.12024.

[3] G. Navarro, E. Martínez -Pinilla, R. Ortiz, V. Noé, C.J. Ciudad, R. Franco, Resveratrol and Related Stilbenoids, Nutraceutical/Dietary Complements with Health-Promoting Actions: Industrial Production, Safety, and the Search for Mode of Action: Stilbenoids and food industry…, Compr. Rev. Food Sci. Food Saf. 17 (2018) 808–826. doi:10.1111/1541-4337.12359.

# Block I part I

## Chapter I

## *Rumenic acid inclusion complexes characterization*

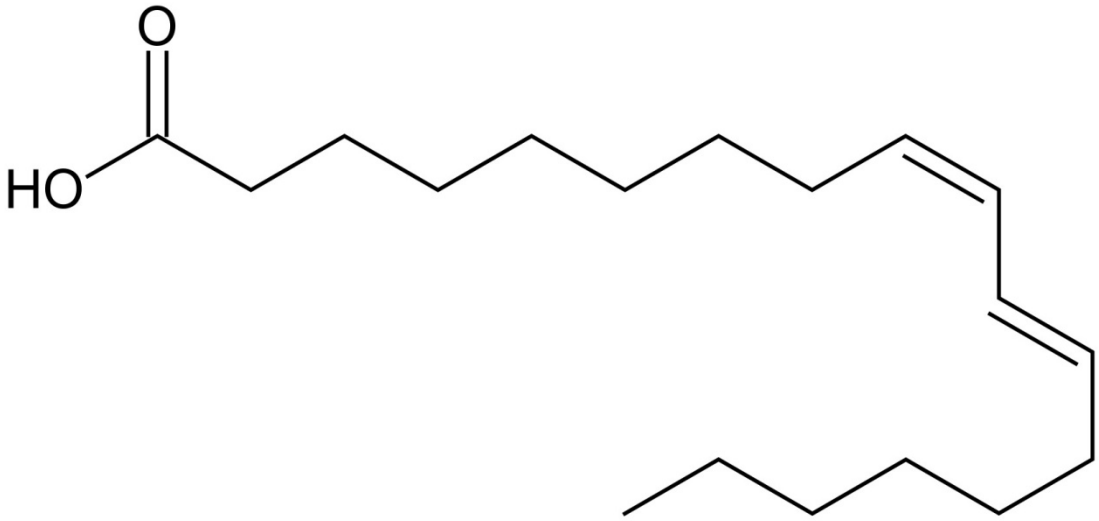

**Abstract**

In this chapter the aggregation behavior of Rumenic acid (RA) is presented for the first time. The results point to a c.m.c. of 35 μM at pH 8 and 25 ºC. This behavior can be modified by introducing CDs into the system to encapsulate the RA. The encapsulation process presented a 1:1 stoichiometry in all the cases studied but the complexation constants were strongly dependent on the type of CDs used, the pH and temperature.

The effect of the type of CD on the encapsulation process was studied. Among the natural and modified CDs analyzed HPβ-CD was the best for encapsulating RA. The $pK_a$ determined for RA was 4.31. The $K_F$ showed different behavior below and above 25 ºC due to changes in the stoichiometry. Finally, molecular docking calculations provided further insights into how the different interactions influence the complexation constant.

## Index

## 1. Contextualization.

Rumenic acid (RA, **Fig**. 1A *insert*) is, a conjugated linoleic acid (CLA) found in the fat of ruminants and in dairy products. Along with vaccenic acid, it is formed by the biohydrogenation of dietary polyunsaturated fatty acids in the rumen. RA can be considered as the principal dietary form of CLA, accounting for as much as 85-90 % of the total CLA content of dairy products, while the other isomer of CLA (t10,c12) only represents 1 % of milk fat CLA [1].

A recent revision of the properties of RA in health and disease [1] emphasized the role of RA in cancer. In vivo the dietary supplementation of RA at 0.05-1 % chemically inhibits induced tumors in many tissues [2–4] or their metastasis [5,6] . Furthermore, in vitro studies have demonstrated its anti-proliferative effect against a range of different cells lines [7–9]. RA can decreases 5-lipoxygenase and cyclooxygenase expression, leading to decreased levels of prostanglandin E2 and thromboxane B2 [9], and can inhibit NF-kB activation [10]. In addition, RA might have therapeutic potential in the treatment of Th1 mediated diseases [11]. A study in humans showed that the RA found in butter exerted immune-modulatory effects on healthy young adults, reducing the production of inflammatory biomarkers associated with overweight and obesity [12].

## 2. Objectives

1. To analyze the aggregation behavior of RA studying the possible existence of monomers or aggregates
2. To discover the mechanism involved in RA complexation with different types of natural (α-CD and β-CD) and modified (HPβ-CD and Mβ-CD) just as the complexation constant ($K_F$)
3. To analyze the effect of pH and temperature on the encapsulation behavior. CDs under various experimental conditions (temperature and pH) are studied.
4. To use molecular docking for studying the molecular interaction established in the complexation process.

## 3. Materials and methods

### 3.1 Materials

RA, β-CD, HPβ-CD and Mβ-CD were purchased from Sigma Aldrich (Madrid, Spain). α-CD was purchased from Shanghai Soyoung Biotechnology (Shanghai, China). Diphenylhexatriene (DPHT) was a product of Fluka (Madrid, Spain) and tetrahydrofuran was from Merck (Darmstadt, Germany).

### 3.2 Fluorimetric determination of critical micellar concentration (c.m.c)

The c.m.c. of RA was determined as a function of pH and temperature by means of the fluorescence spectroscopy method [13]. The required concentration of CD and RA was added to the desire buffer with 0.88 μM of DPHT (supplied in tetrahydrofuran). The samples were incubated for an hour at the desired temperature in the dark to reach equilibrium and to prevent photoisomerization of the fluorescent probe.

Fluorescence intensity was measured at 430 nm (358 nm excitation wavelength) in a Kontron SFM-25 spectrofluorimeter equipped with thermostatically controlled cells. 430 and 358 nm are the emission and excitation wavelengths of DPHT, respectively. The relative fluorescence intensity values were plotted against RA concentration, and the c.m.c. was determinated as the intersection between the lines defining fluorescence intensity in the pre- and post-micellar regions

For each pH, three different buffers were used for pH 2 sodium citrate 0.1 M, for pH (3-4) sodium acetate 0.1 M, for pH (5.5-8) sodium phosphate 0.1 M. For the temperature study, the study was carried out in sodium phosphate 0.1

M pH 8 at 15, 20, 25, 30 and 37 ºC , using a Thermomixer Comfort (Eppendorf Ibérica, Madrid, Spain).

3.3 Determination of stoichiometry and complexation constants of the encapsulation process

For 1:1 model (one CD per RA), a correlation between apparent "critical micellar concentration" (c.m.c.) in presence of CD (c.m.c.*) and CD concentration was used [14]:

$$[\mathrm{c.m.c.}*]_t = [\mathrm{c.m.c}_0] + K_F[\mathrm{c.m.c}_0][\mathrm{CD}] \quad (1)$$

The linear representation of eqn 1, [c.m.c*] vs [CD], give a linear regression coefficient. Values close to 1 mean that the complex is 1:1 (1 CD per RA).

Secondly, for a 1:2 stoicheiometry, a variation of the 1:1 complex was used.

$$[\mathrm{c.m.c.}*]_t = [\mathrm{c.m.c}_0] + K_{F12}[\mathrm{c.m.c}_0][\mathrm{CD}]^2 \quad (2)$$

The linear representation of eqn 14, [c.m.c*] vs $[CD]^2$, provides a linear regression coefficient. Values far from 1 mean that the complex is not 1:2 (1 RA per 2 CD).

3.4 Molecular modeling and molecular docking

The molecular structures used in this work were built using Avogadro Software [15] or were obtained from different databases. α-CD and β-CD structures were extracted from a crystal of Protein Data Bank (PDB ID: 3EDD and 1Z0N). RA was obtained from CACTUS database (NCI/CADD group, USA).

HPβ-CD and Mβ-CD were built by adding hydroxypropyl or methyl group**s** to the β-CD. pH simulation was carried out manually using Avogadro. Molecular docking was done using Autodock Vina [16]. All CDs were considered as rigid. Graphical representations of the docking results were prepared using PyMOL (Molecular GraphicsSystem, version 1.3, Schrödinger, LLC).

### 3.5 Data Analysis

All experiments were carried out three times. Regressions were made using SigmaPlot (Systat Software, version 10.0). Other mathematical operations were made using wxMaxima software (version 12.04.0).

## 4. Results and discussion

### 4.1 Effect of CDs on the RA monomer/aggregate equilibrium

The monomer/aggregate behavior of RA in dissolution has not been studied. Because of RA is not fluorescent, the appearance of the aggregates at increased concentrations of RA can be detected by measuring the fluorescence of a probe such as diphenylhexatriene, whose quantum yield increases when it finds an apolar environment as the aggregation core [17]. As is shown in **Fig.** 1A, RA forms aggregates above a certain critical concentration called “critical micellar concentration” (c.m.c.) below which, RA forms monomers but not aggregate structures. Similar results were obtained by our group for LA, AA and LNA [13,18], pointing to the dual behaviors of fatty acids (monomer/aggregate) depending on the fatty acid concentration.

**Fig.** 1B shows that, in the presence of CDs, RA/CD complexes are formed. At high concentrations of RA equilibrium is established between the aggregates and the free and complexed RA. As occurs with detergents in the presence of CD [14], the concentration of the free amphiphile equals the c.m.c when no CDs are present ($c.m.c._0$). However, the complexed RA contributes to the apparent c.m.c* and causes it to increase. The greather the CD concentrations, the higher the apparent c.m.c* of RA, perhaps the RA enters the intern cavity of the CD, preventing the formation of micelles, **Fig**. 1C**)**

The formation of inclusion complexes between CDs and RA leads to the expansion of the premicellar region due to the establishment of a pool of nonaggregated RA. This is important in several respects. The resulting RA/CD

complexes can be used to increase the sensitivity of polarographic and spectrophotometric methods for example.

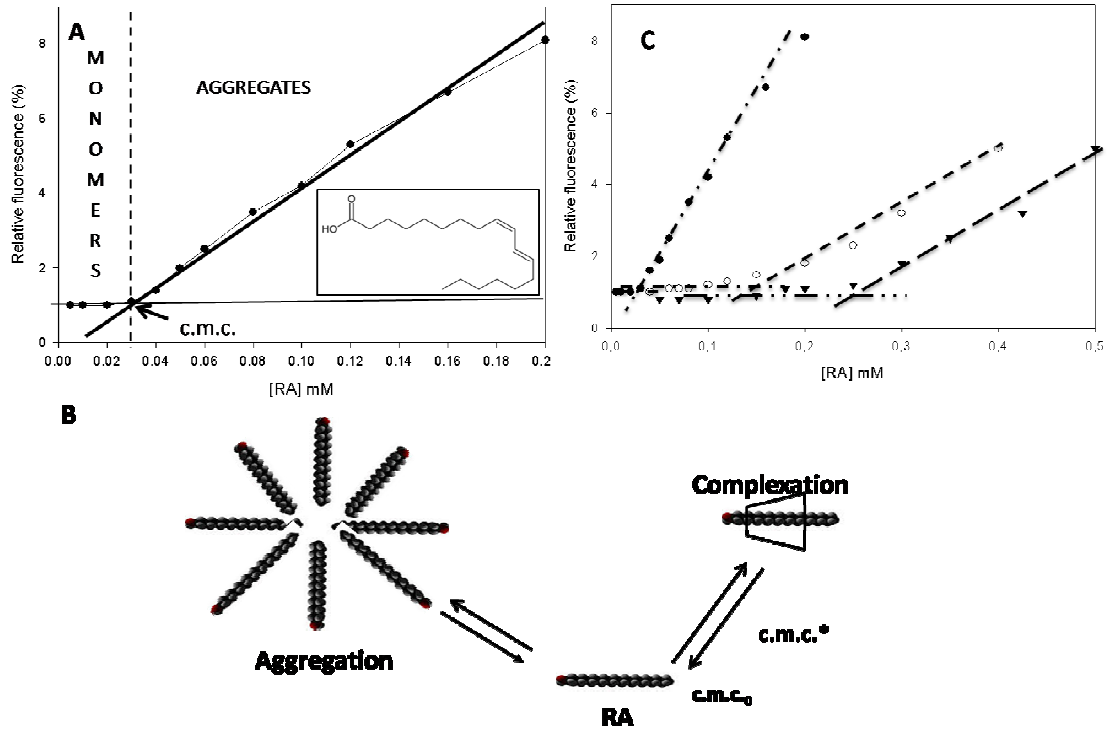


***Fig. 1**. (A) Dependence of relative fluorescence intensity of diphenyl-hexatriene at 430 nm (excitatlon wavelength 358 nm) on RA concentration (pH 8 at 25 ºC). Insert: Structure of RA. (B). Interaction of RA with CDs. RA exists in three states: aggregated, free and complexed. When the RA concentration is sufficiently high to form aggregates, the concentration of free RA is c.m.c.$_0$, independently of whether CDs are present or not. CDs trap a certain amount of RA which is not available for aggregation but which is indistinguishable from free RA when the c.m.c is determined. Therefore, the observed c.m.c.* consists of c.m.c.$_0$ plus the trapped concentration of RA. When the concentration of RA is lower than c.m.c.*, only free RA is available for the enzyme reaction and its concentration is ruled by the complexation constants of the interaction with CDs. (C) Effect of increasing HPβ-CD on c.m.c. of RA.*

4.2 Study of stoichiometry and complexation constant ($K_F$)

In order to study the stoichiometry of RA encapsulation, the c.m.c.* values of this fatty acid were calculated with increasing concentrations of CD added to the medium, using HPβ-CD as CD model. The linear dependence of c.m.c.* on the HPβ-CD concentration ($R^2 > 0.99$) indicated that a 1:1 model is the optimum for the encapsulation of RA by HPβ-CD. However, it can be seen that a 1:2 stoichiometry for the inclusion compound (RA/HPβ-CD) can be directly ruled out as this would have yielded a non linear dependence of c.m.c.* values on the CD concentration ($R^2 \approx 0.92$). Based on these results, eq. 1 was used to calculate the complexation constants of the 1:1 encapsulation process. In the case of HPβ-CD the complexation constant determined was 8347 +/- 417 $M^{-1}$.

4.3 Effect of the cyclodextrin structure on the complexation constants

The complexation constants between RA and CDs were determined with different CDs in an attempt to obtain better RA-CD complexes. Different types of natural (α-CD and β-CD) and modified (HPβ-CD and Mβ-CD) CDs were used. All the complexes studied showed a 1:1 stoichiometry (1 RA per CD) with an $R^2$>0.99. Table 1 shows that β-CD provided a better $K_F$ than α-CD. However, chemical modifications of the β-CD led to an increase in the complexation constants of the encapsulation process. For example, the encapsulation of RA in Mβ-CD and HPβ-CD was more efficient than when natural CDs were used. In all cases the encapsulation process carried involving modified CDs was more efficient than when natural CDs were used.

Since the highest $K_F$ calculated (8347 +/- 417 $M^{-1}$) was that obtained for the complex HPβ-CD/RA, this type of modified CD was regarded as the

optimum CD for encapsulating RA and was therefore selected for the next step of the study.

**Table 1**. Experimental $K_F$ values with each CD, regression coefficient for each model (pH 8 and 25 ºC) and molecular score docking results.

| | $K_F$ ($M^{-1}$) | SD (+/-) ($M^{-1}$) | $R^2$ (1:1) | $R^2$ (1:2) | Score |
|---|---|---|---|---|---|
| α-CD | 3859.00 | 192.00 | 0.99 | 0.91 | -2.30 |
| β-CD | 5846.00 | 292.00 | 0.97 | 0.86 | -3.20 |
| Mβ-CD | 6814.00 | 340.00 | 0.99 | 0.91 | -3.70 |
| HPβ-CD | 8347.00 | 417.00 | 0.99 | 0.94 | -3.90 |

4.4 Effect of pH on the complexation constant

The importance to evaluate the effect of pH increases when one of the main objectives of the complexation of bioactive molecules, such as RA, is a fatty acid and are suitable to form aggregates. In this work, the effect of pH on the complexation constant was studied for the RA/HPβ-CD complex at 25 ºC using pH values of 2.0, 3.0, 4.0, 5.5, 7.0 and 8.0 . The results (**Fig.** 2A) point to the strong pH dependence of $K_F$, which passes from a stable value of about 13585 +/- 682 $M^{-1}$ to another stable value of about 8329 +/- 431 $M^{-1}$ in just 2.5 pH units, as happens during the titration of a weak ionizable group. For this reason the next step of this investigation was to calculate the $pK_a$ of RA.

Applying the second derivative to the third degree polynomial regression of **Fig**. 2A, ($R^2 \approx 0.97$, data not shown) provided an experimental $pK_a$ of 4.31. Using Avogadro software, a $pK_a$ of around 4.1 was obtained manually which is very close to the experimental value. As **Fig.** 2A shows, at pH values below the

experimental $pK_a$ the encapsulation process is better than at pH values above the $pK_a$. A likely explanation for the dependence of $K_F$ on pH is that the carboxyl group of the protonated FA forms a hydrogen bond with hydrophilic groups of CD at pH values below the $pK_a$ value, as in the case of other ionized weak electrolytes [19]. The non-deprotoned form of RA is more hydrophobic than the deprotoned form, which favors encapsulation in the hydrophobic internal cavity of CDs.

### 4.5 Effect of temperature on the complexation constant

Usually small changes in temperature can lead to large changes in the complexation constants. For that reason, the effect of temperature on the complexation constant was also studied for the RA/HPβ-CD complex at pH 8. To prevent the results from being affected by changes in the buffer $pK_a$ due to variations in temperature, the pH of the buffer was adjusted to the indicated temperature.

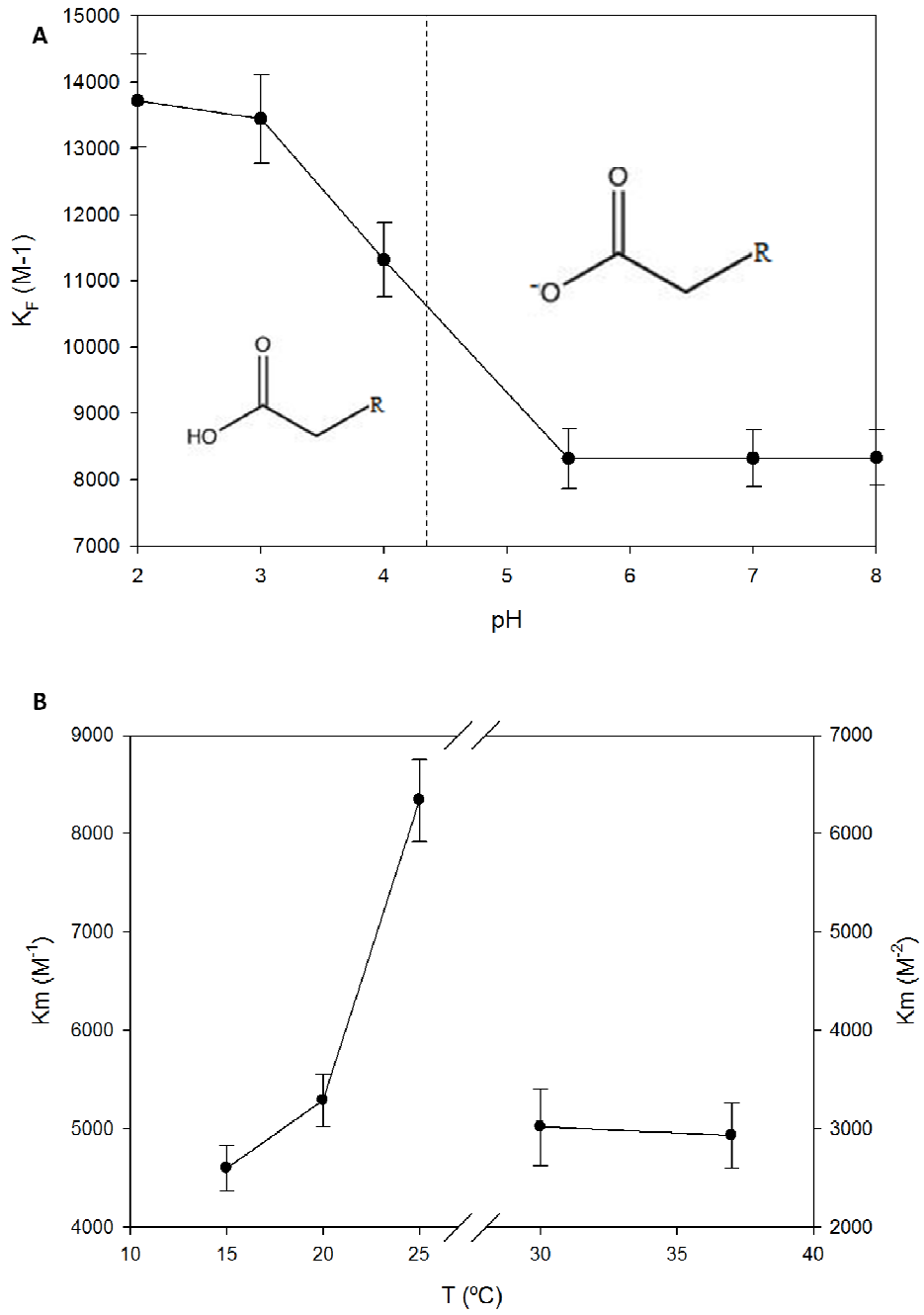


***Fig. 2**. (A) Effect of pH on complexation constant. Separation corresponds to the experimental pKa . (B) Effect of temperature on complexation constant at pH 8.*

The results point to the unusual behavior of encapsulation compared with other FAs [13,18], where the dependence of $K_F$ with the pH was lineal. As shown in **Fig**. 2B, the process of RA encapsulation by HPβ-CD presented a critical value at 25 ºC, below which the $K_F$ increased with temperature.

However, at temperatures higher than 25 ºC the $K_F$ values behaved differently, perhaps due to the different stoichiometries of the RA/HPβ-CD complexes. **Fig**. 3 depicts how the c.m.c. values obtained at 15 ºC fitted a 1:1 stoichiometry ($R^2$ > 0.99). However, at 37 ºC the model cannot be adjusted to fit a 1:1 stoichiometry ($R^2$ < 0.95). These data suggested a 1:1 complexation below to 25 ºC and a 1:2 above 25 ºC, perhaps due to a possible structural conformational change in RA at increasing temperatures as shown by the strong increase in the c.m.c. value observed in **Fig**. 3 *insert*.

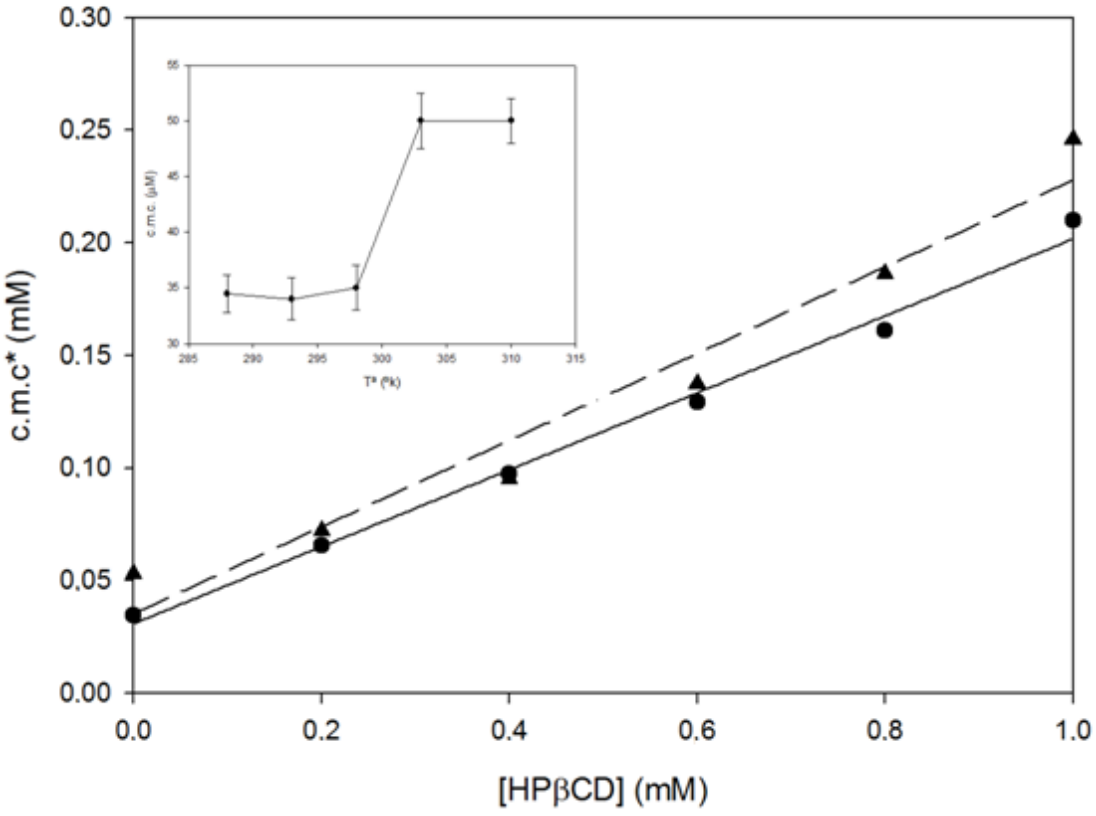


***Fig. 3****. Effect of HPβCD concentration on c.m.c. of RA at different temperatures: 15 ºC (●) and 37 ºC (▲). Inset: Effect of temperature on c.m.c. of RA in the absence of CDs at pH 8.*

4.6 Molecular docking

To increase our knowledge of the RA-CD complex, molecular modeling was used. Scoring functions are fast mathematical methods used to predict the strength of the non-covalent interaction (also referred to as binding affinity) between two molecules after they have docked. This matter let us to compare our score results with our experimental $K_F$ values. The results (Table 1) showed good correlation between the computed scores and experimental values for the complexes (which always followed the same orders).

Moreover, the poses of Vina reflect the possible interaction between RA and each CD. The docking results (**Fig.** 4) showed that α-CD (**Fig.** 4A) unlike natural and modified β-CDs might not be encapsulated perfectly, and was always the least effective CD in the experimental results. As β-CD and Mβ-CD (**Fig.** 4B and 4C) presented identical number of hydrogen bonds, perhaps the differences may have been the results of the increase in hydrophobicity due to the methyl radical. The HPβ-CD complex (**Fig.** 4D) has fewer hydrogen bonds than β-CD. However, the increase in hydrophobicity due to the presence of the hydroxypropyl radical may explain the different scores between HPβ-CD on the one hand, and β-CD and the MβCD complexes on the other. To justify what was said in the Temperature section (**3.5**) concerning the particular behavior of RA/CD complexes at temperatures higher than 25 ºC, a special docking with HPβ-CD was run (**Fig.** 4E and 4F). The results showed that RA could be complexed by 2 molecules of HPβ-CD depending on the RA conformation.

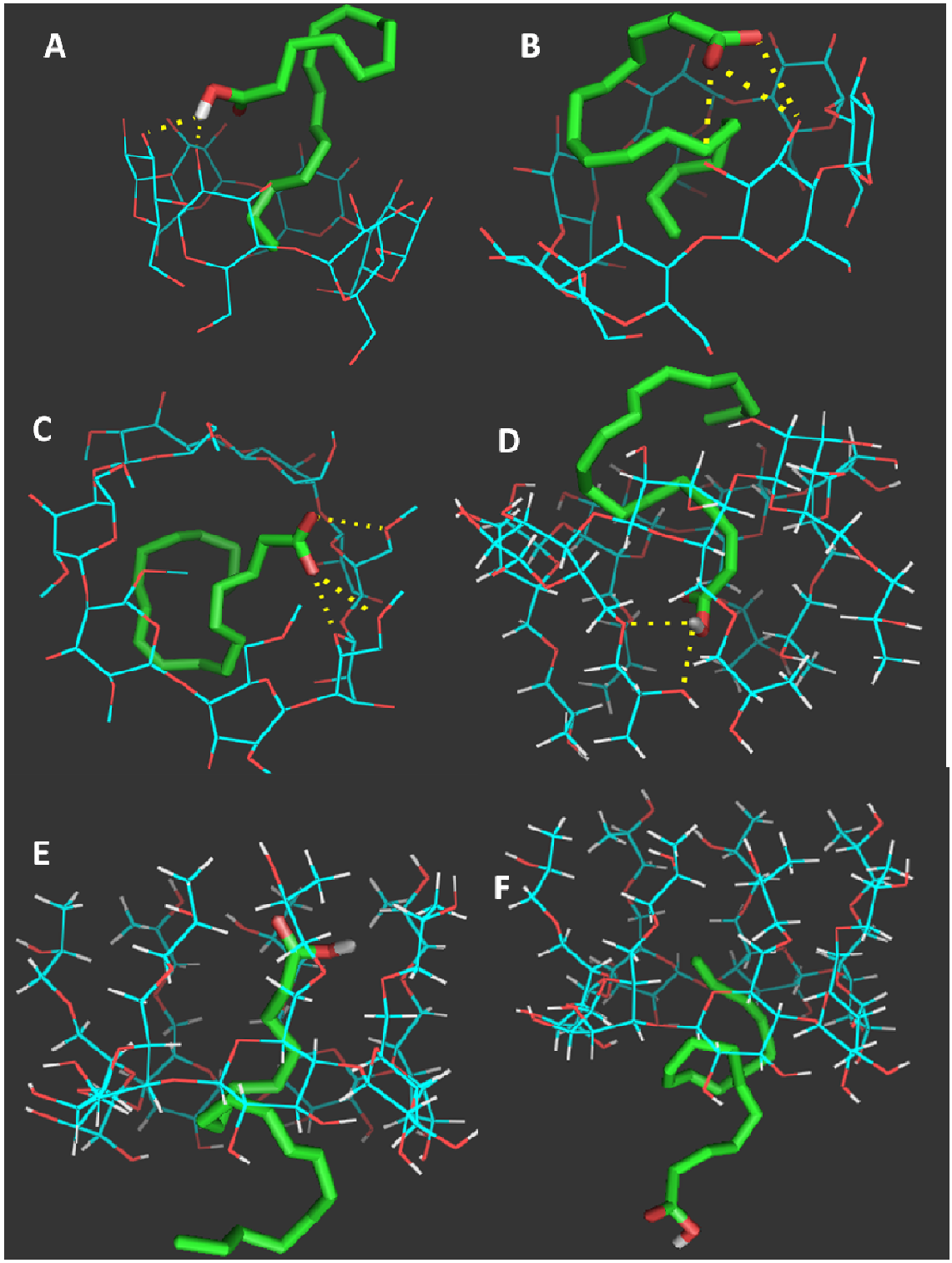


***Fig. 4**. Docking results of RA with: (A) α-CD; (B) β-CD; (C) Mβ-CD and (D) HPβ-CD. (E) and (F) poses RA/HPβ-CD showing different possible orientations. In yellow, hydrogens bonds.*

In conclusion, this work studied the monomer/aggregate equilibrium of RA and its encapsulation by CDs. Many types of natural (α- and β-) and modified (HPβ- and Mβ-) CDs were used and the stoichiometry of their complexes in equilibrium was found. Among the natural and modified CDs analyzed HPβ-CD was the best for encapsulating RA, showing the highest $K_F$. In all cases studied the encapsulation process presented a 1:1 stoichiometry. In addition, the effects on the complexation constants of factors that typically affect biochemical processes, such as pH and temperature, were studied. The $K_F$ showed a strong dependence on the determined $pK_a$ of RA (4.31). Moreover, the $K_F$ showed different behavior below and above 25 ºC due to changes in the stoichiometry. To increase our understanding of the complex, *in silico* molecular docking was used.

## References

[1] B. Yang, H. Chen, C. Stanton, R.P. Ross, H. Zhang, Y.Q. Chen, W. Chen, Review of the roles of conjugated linoleic acid in health and disease, J. Funct. Foods. 15 (2015) 314–325. doi:10.1016/j.jff.2015.03.050.

[2] A. Białek, M. Jelińska, A. Tokarz, Influence of maternal diet enrichment with conjugated linoleic acids on lipoxygenase metabolites of polyunsaturated fatty acids in serum of their offspring with 7,12-dimethylbenz[a]anthracene induced mammary tumors, Prostaglandins Other Lipid Mediat. 116–117 (2015) 10–18. doi:10.1016/j.prostaglandins.2014.10.001.

[3] B.-Q. Chen, Inhibition of conjugated linoleic acid on mouse forestomach neoplasia induced by benzo (a) pyrene and chemopreventive mechanisms, World J. Gastroenterol. 9 (2003) 44. doi:10.3748/wjg.v9.i1.44.

[4] A. Stawarska, A. Białek, I. Stanimirova, T. Stawarski, A. Tokarz, The effect of conjugated linoleic acids (CLA) supplementation on the activity of enzymes participating in the formation of arachidonic acid in liver microsomes of rats--probable mechanism of CLA anticancer activity, Nutr. Cancer. 67 (2015) 145–155. doi:10.1080/01635581.2015.967875.

[5] B.-Q. Chen, Y.-M. Yang, Y.-H. Gao, J.-R. Liu, Y.-B. Xue, X.-L. Wang, Y.-M. Zheng, J.-S. Zhang, R.-H. Liu, Inhibitory effects of c9, t11-conjugated linoleic acid on invasion of human gastric carcinoma cell line SGC-7901, World J. Gastroenterol. 9 (2003) 1909–1914.

[6] Y. Sakai, T. Sasahira, H. Ohmori, K. Yoshida, H. Kuniyasu, Conjugated linoleic acid reduced metastasized LL2 tumors in mouse peritoneum, Virchows Arch. Int. J. Pathol. 449 (2006) 341–347. doi:10.1007/s00428-006-0249-7.

[7] F. Beppu, M. Hosokawa, L. Tanaka, H. Kohno, T. Tanaka, K. Miyashita, Potent inhibitory effect of trans9, trans11 isomer of conjugated linoleic acid on the growth of human colon cancer cells, J. Nutr. Biochem. 17 (2006) 830–836. doi:10.1016/j.jnutbio.2006.01.007.

[8] A. Koronowicz, J. Dulińska-Litewka, P. Pisulewski, P. Laidler, [Effect of conjugated linoleic acid isomers on proliferation of mammary cancer cells], Rocz.

Państw. Zakładu Hig. 60 (2009) 261–267.

[9] J.J. Ochoa, A.J. Farquharson, I. Grant, L.E. Moffat, S.D. Heys, K.W.J. Wahle, Conjugated linoleic acids (CLAs) decrease prostate cancer cell proliferation: different molecular mechanisms for cis-9, trans-11 and trans-10, cis-12 isomers, Carcinogenesis. 25 (2004) 1185–1191. doi:10.1093/carcin/bgh116.

[10] M.A. Rakib, W.S. Lee, G.S. Kim, J.H. Han, J.O. Kim, Y.L. Ha, Antiproliferative Action of Conjugated Linoleic Acid on Human MCF-7 Breast Cancer Cells Mediated by Enhancement of Gap Junctional Intercellular Communication through Inactivation of NF-κB, Evid. Based Complement. Alternat. Med. 2013 (2013) e429393. doi:10.1155/2013/429393.

[11] C.E. Loscher, E. Draper, O. Leavy, D. Kelleher, K.H.G. Mills, H.M. Roche, Conjugated linoleic acid suppresses NF-kappa B activation and IL-12 production in dendritic cells through ERK-mediated IL-10 induction, J. Immunol. Baltim. Md 1950. 175 (2005) 4990–4998.

[12] L.A. Penedo, J.C. Nunes, M.A.S. Gama, P.E.C. Leite, T.F. Quirico-Santos, A.G. Torres, Intake of butter naturally enriched with cis9,trans11 conjugated linoleic acid reduces systemic inflammatory mediators in healthy young adults, J. Nutr. Biochem. 24 (2013) 2144–2151. doi:10.1016/j.jnutbio.2013.08.006.

[13] J.M. López-Nicolás, R. Bru, A. Sánchez-Ferrer, F. García-Carmona, Use of “soluble lipids” for biochemical processes: linoleic acid-cyclodextrin inclusion complexes in aqueous solutions., Biochem J. 308 (1995) 151–154.

[14] E. Junquera, E. Aicart, G. Tardajos, Inclusional complexes of decyltrimethylammonium bromide and .beta.-cyclodextrin in water, J. Phys. Chem. 96 (1992) 4533–4537. doi:10.1021/j100190a074.

[15] M.D. Hanwell, D.E. Curtis, D.C. Lonie, T. Vandermeersch, E. Zurek, G.R. Hutchison, Avogadro: an advanced semantic chemical editor, visualization, and analysis platform, J. Cheminformatics. 4 (2012) 17. doi:10.1186/1758-2946-4-17.

[16] O. Trott, A.J. Olson, AutoDock Vina: improving the speed and accuracy of docking with a new scoring function, efficient optimization, and multithreading, J. Comput. Chem. 31 (2010) 455–461. doi:10.1002/jcc.21334.

[17] J. Serth, A. Lautwein, M. Frech, A. Wittinghofer, A. Pingoud, The inhibition of the GTPase activating protein-Ha-ras interaction by acidic lipids is due to physical association of the C-terminal domain of the GTPase activating protein with micellar structures., EMBO J. 10 (1991) 1325–1330.

[18] R. Bru, J.M. López-Nicolás, F. García-Carmona, Aggregation of polyunsaturated fatty acids in the presence of cyclodextrins, Colloids Surf. Physicochem. Eng. Asp. 97 (1995) 263–269. doi:10.1016/0927-7757(95)03091-Q.

[19] F.Y. Liu, D.O. Kildsig, A.K. Mitra, Cyclodextrin/weak-electrolyte complexation: interpretation and estimation of association constants from phase solubility diagrams, Pharm. Res. 9 (1992) 1671–1672.

# Block I part I

## Chapter II

## *Characterization of t10,c12 conjugated linoleic acid inclusion complexes.*

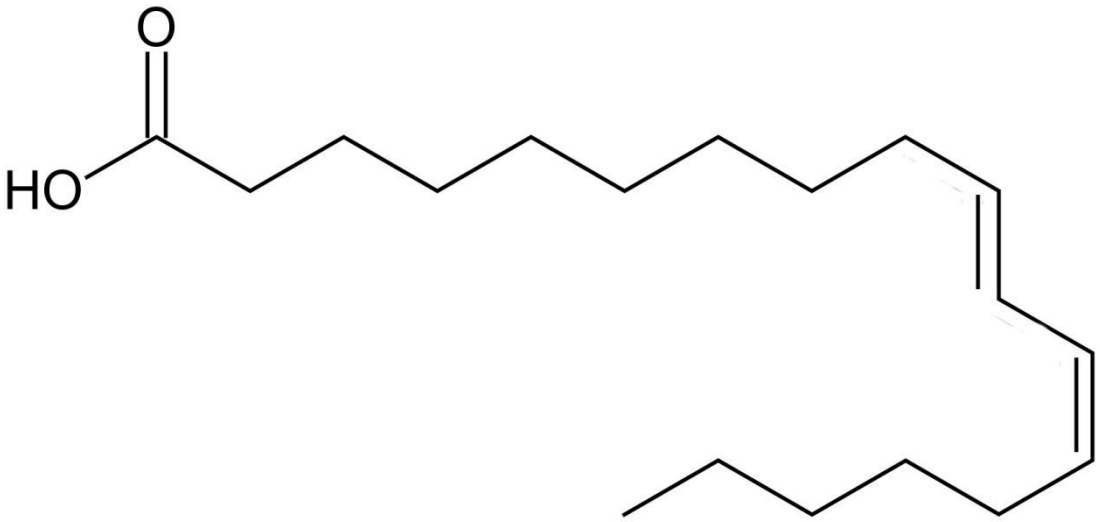

**Abstract**

In this chapter the aggregation behavior of t10,c12 Conjugated linoleic acid (t10,c12-CLA) is presented for first time. The results show a c.m.c. of 25 µM at pH 8 and 25ºC. The encapsulation process with cyclodextrins (CDs) presented a 1:1 stoichiometry in all cases studied but the complexation constants were strongly dependent on the type of CDs used, the pH and temperature. Hydroxypropyl-beta-Cyclodextrin (HPβ-CD) was the best CD studied for encapsulating t10,c12-CLA.

The resulting t10,c12-CLA/HPβ-CD complex showed a very high dependency on pH, which explains why a $pK_a$ of 4.08 was found for first time, which was very close to the simulated value. Furthermore, the effect of temperature on the t10,c12-CLA-HPβ-CD was studied. The complexation constant ($K_F$) showed an increase behavior with the temperature. In addition, molecular docking calculations provided further insights into how the different interactions influence the complexation constant. Finally, a comparative study with rumenic acid, an isomer, was carried out.

## Index

## 1. Contextualization

A recent revision talked about the role of t10,c12 Conjugated linoleic acid (t10,c12-CLA, **Fig**. 1) in cancer [1]: *In vivo* the dietary supplementation of t10,c12-CLA at 0.05-1% chemically inhibits induced tumors of many tissues. Furthermore, *in vitro* studies have demonstrated its anti-proliferative effect against a range of different cells lines. In addition, t10,c12-CLA seems to work through modulation of apoptosis and cell cycle control preferably activating caspase-9 and 3 or Bcl-2 [1], among others. Furthermore, t10,c12-CLA has showed as a good body fat reductor in a lot of animal models like mice, rats, hamster, pigs and also human [2–5]; whereas Rumenic acid (RA, c9,t11-CLA, **Fig**. 1) has demonstrated no positive effect on lean body mass [6]. In addition, t10,c12-CLA exhibits higher antioxidant capacity than c9,t11-CLA [7].

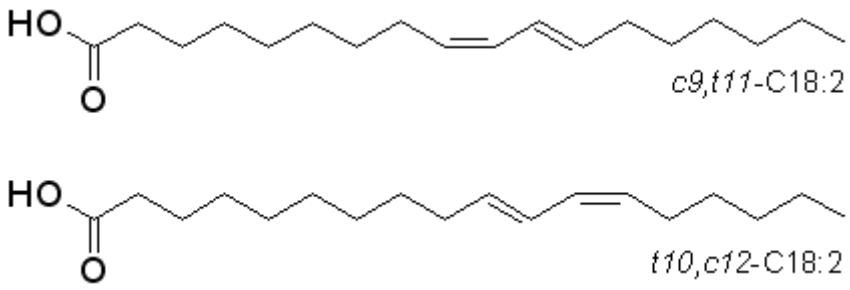


***Fig**. 1. Structures of Conjugated linoleic acid isomers: c9,t11 (RA) and t10,c12.*

Moreover, t10,c12-CLA shows very poor solubility in water, (although it is more soluble in ethanol and other organic solvents), possesses low bioavailability and is easily oxidized by physico-chemical agents[8]. Its complexation with molecules which might increase its bioavailability, solubility and stability in the face of prooxidant agents, as cyclodextrins (CDs), is strongly desirable.

## 2. Objectives

1. To analyze the aggregation behavior of t10,c12-CLA studying the possible existence of monomers or aggregates of t10,c12-CLA.
2. To understand the complexation mechanism of t10,c12-CLA with different types of natural (α-CD and β-CD) and modified CDs (HPβ-CD and Mβ-CD) under various experimental conditions of temperature and pH were studied.
3. To evaluate the stoichiometry, $K_F$ values and thermal behavior of the t10,c12-CLA-CD complexes.
4. To predict the molecular interaction established in the complexation process using *in silico* molecular docking is studied. To compare our results with with rumenic acid (RA), the isomer characterized previously.

## 3. Materials and methods

### 3.1 Materials

t10,c12-CLA (CID 5282800), β-CD, modified HPβ-CD Mβ-CD were purchased from Sigma Aldrich (Madrid, España). α-CD was purchased from Shanghai Soyoung Biotechnology (Shanghai, China). Diphenylhexatriene was a product of Fluka (Madrid, Spain) and tetrahydrofuran was from Merck (Darmstadt, Germany).

### 3.2 Fluorimetric determination of critical micellar concentration (c.m.c)

The c.m.c. of t10,c12-CLA was determined by means of a fluorescence spectroscopy method [9]. The required concentration of CD and t10,c12-CLA was added to the desire buffer with 0.88μM of DPH (supplied in tetrahydrofuran). The samples were incubated for an hour at the desired temperature in the dark to reach equilibrium and, to prevent photoisomerization of the fluorescent probe.

Fluorescence intensity was measured at 430 nm (358 nm excitation wavelength) in a Kontron SFM-25 spectrofluorimeter equipped with thermostatically controlled cells. 430 and 358 nm are the emission and excitation wavelengths of DPHT, respectively. The relative fluorescence intensity values were plotted against t10,c12-CLA concentration, and the c.m.c. was determinated as the intersection between the lines defining fluorescence intensity in the pre- and post-micellar regions

This values were related to the intensity of the lowest t10,c12-CLA concentration. For each pH, different types of buffer were used: pH (2-3) sodium citrate 0.1 M, pH (3-4) sodium acetate 0.1 M, pH (5-8) sodium phosphate 0.1 M.

3.3 Determination of stoichiometry and complexation constants of the encapsulation process.

For 1:1 model (one CD per t10,c12-CLA), a correlation between apparent "critical micellar concentration" (c.m.c.) in presence of CD (c.m.c.*) and CD concentration was used [10]:

$$[\mathrm{c.m.c.}*]_t = [\mathrm{c.m.c_0}] + \mathrm{K_F}[\mathrm{c.m.c_0}][\mathrm{CD}] \qquad (1)$$

The linear representation of eqn 1, [c.m.c*] vs [CD], give a linear regression coefficient. Values close to 1 mean that the complex is 1:1 (1 CD per t10,c12-CLA).

Secondly, for a 1:2 stoicheiometry, a variation of the 1:1 complex was used.

$$[\mathrm{c.m.c.}*]_t = [\mathrm{c.m.c_0}] + \mathrm{K_{F12}}[\mathrm{c.m.c_0}][\mathrm{CD}]^2 \qquad (2)$$

The linear representation of eqn 14, [c.m.c*] vs $[CD]^2$, provides a linear regression coefficient. Values far from 1 mean that the complex is not 1:2 (1 t10,c12-CLA per 2 CD).

3.4 Molecular modeling and molecular docking.

The molecular structures used in this work were built using Avogadro Software [11] or were obtained by different databases. α-CD and β-CD

structures were extracted from a crystal of Protein Data Bank (PDB ID: 3EDD and 1Z0N). t10,c12-CLA and RA were obtained from CACTUS database (NCI/CADD group, USA). HPβ-CD and Mβ-CD were built by adding Hydroxypropyl or Methyl group**s** to the β-CD. pH simulation was carried out manually using Avogadro. Molecular docking was done using Autodock Vina [12]. Input files for Vina was obtained using AutodockTools (version 1.5.6) All CDs were considered as rigid. Graphical representations of the docking results were prepared using PyMOL (Molecular GraphicsSystem, version 1.3, Schrödinger, LLC).

2.5 Data Analysis.

All experiments were made three times. Regressions were made using SigmaPlot (Systat Software, version 10.0). Other mathematical operations were carried out using wxMaxima software (version 12.04.0).

## 4. Results and discussion

### 4.1 Study of monomer/aggregate equilibrium in presence of CDs

**Fig**. 2A inset shows that t10,c12-CLA forms aggregates above a certain critical concentration called “critical micellar concentration” (c.m.c.). Below the c.m.c., t10,c12-CLA forms monomers but not aggregates structures [13]. The results that follow may help clarify the different properties of t10,c12-CLA depending on its concentration in the reaction medium.

The formation of inclusion complexes between CDs and t10,c12-CLA could lead to the expansion of the premicellar region through the establishment of a pool of nonaggregated t10,c12-CLA. **Fig**. 2A, showed that increasing the CD concentrations led to a concomitant increase of the apparent c.m.c* of t10,c12-CLA perphaps t10,c12-CLA enters in CD intern cavity preventing the formation of micelles. **Fig**. 2A shows such an effect of different CDs on the aggregating behavior of t10,c12-CLA in different conditions. These data demonstrated CDs can solubilize t10,c12-CLA in aqueous products.

### 4.2 Study of stoichiometry and complexation constant ($K_F$)

Previously was explained to different mechanismin order to study the stoichiometry of t10,c12-CLA encapsulation. After obtaining the c.m.c.* values of this fatty acid with increasing concentrations of CD (HPβ-CD was used as CD model) added to the medium. **Fig**. 2B shows the fitting of the experimental data to Eqs. (1) and (2) for the 1:1 and 1:2 models, respectively.

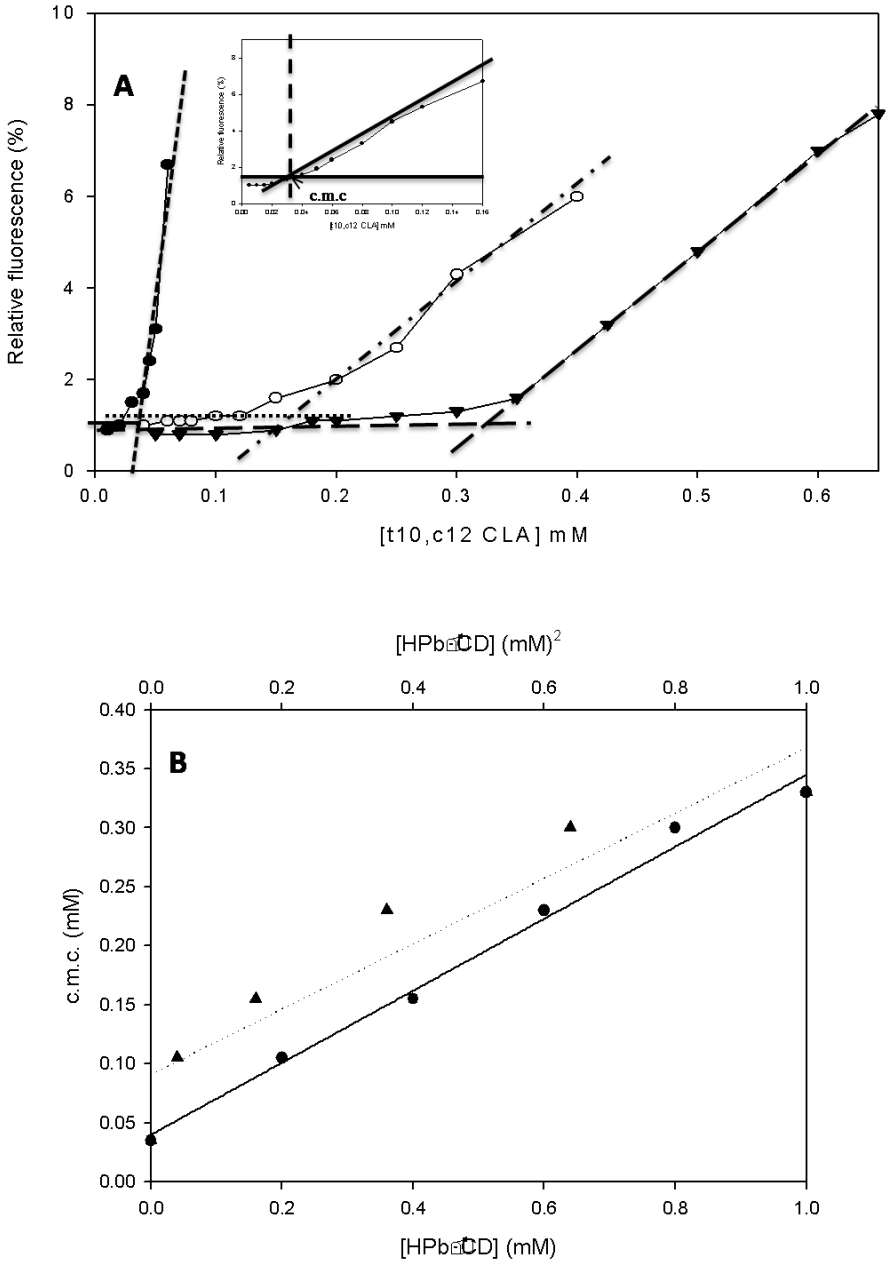


***Fig**. 2. (A) Dependence of relative fluorescence intensity on t10,c12-CLA concentration with different HPβ-CD concentrations: 0mM (●), 0.4mM (○) and 1 mM (▲). Inset. Dependence of relative fluorescence intensity of diphenyl-hexatriene at 430 nm (excitatlon wavelength 358 nm) on t10,c12-CLA concentration, conditions: pH 8 at 25ºC. (B) Effect of HPβ-CD concentration on t10,c12-CLA c.m.c. values. Stoichiometry 1:1 (●) and 1:2 (▲) at 25ºC pH 8.*

The linear dependence of c.m.c.* values on the HPβ-CD concentration ($R^2$ > 0.99) indicates that a 1:1 model is the optimum for the encapsulation of t10,c12-CLA by HPβ-CD. In this results can be seen that a 1:2 stoichiometry for the inclusion compound, t10,c12-CLA/HPB-CD cannot be directly considered ($R^2$ ≈ 0.89). Based on these results, a 1:1 is the most plausible stoichiometry. In the case of HPβCD the complexation constant determined was 7400 +/- 370 $M^{-1}$. Although linoleic acid was a 1:2 complex [9], it is clear that our coefficient ($R^2$) demonstrated a 1:1 complex between t10,c12-CLA and CDs. It suggests that changes in the place of secondary bonds could affect the complexation with CDs.

Table 1. Experimental $K_F$ values with each CD regression coefficient for each model (pH 8 and 25ºC) and Score results.

| | **$K_F$ ($M^{-1}$)** | **SD (+/-)($M^{-1}$)** | **$R^2$ (1:1)** | **$R^2$ (1:2)** | **Score** |
|---|---|---|---|---|---|
| α-CD | 1560 | 78 | 0.99 | 0.92 | -2.90 |
| Mβ-CD | 3387 | 169 | 0.97 | 0.93 | -3.30 |
| β-CD | 4499 | 220 | 0.99 | 0.95 | -3.50 |
| HPβ-CD | 7400 | 370 | 0.99 | 0.89 | -3.60 |

### 4.3 Effect of different CDs on the complexation constant

The complexation constants between t10,c12-CLA and different CDs were determined. In an attempt to obtain better t10,c12-CLA-CD complexes, different types of natural (α- and β-) and modified (HPβ-CD and Mβ-CD) CDs were used.

1:1 stoichiometry (1 t10,c12-CLA per CD) with an $R^2$>0.99 was obtained for all CDs tested. The results (Table 1) show that, for natural CDs, β-CD provided a better $K_F$ than α-CD. Indeed, β-CD was better than Mβ-CD due to a stearic-hindrance or less hydrogens bonds possibly. However, chemical modifications on HPβ-CD led to an increase in the complexation constants of the encapsulation process.

Since the highest $K_F$ calculated (7400 +/- 370 $M^{-1}$) was for the complex HPβ-CD/t10,c12-CLA, this type of modified CD was regarded as the optimum CD for encapsulating t10,c12-CLA and was therefore selected for the next step of the study.

4.4 Effect of pH on the complexation constant

The pH can affect the stability of some compounds and it can be considered previously to its use. In this work the effect of pH on the complexation constant was studied for the t10,c12-CLA/HPβ-CD complex at 25ºC using pH values of 2.0, 2.5, 3.0, 4.0, 5.0, 5.5, 7.0 and 8.0 . The results (**Fig**. 3A) demonstrate the strong dependence of $K_F$ on pH, passing from a stable value of about 10760 +/- 538 $M^{-1}$ to another stable value of about 7993 +/- 374 $M^{-1}$ in just 2.5 pH units, as happens during the titration of a weak ionizable group. For this reason the next step of this investigation was to calculate the $pK_a$ of t10,c12-CLA.

After a mathematical treatment to pH data, an experimental $pK_a$ of 4.08 was calculated. Using Avogadro software, a $pK_a$ of around 4.1 was obtained which is much closed to the experimental value. As **Fig**. 3A shows, at pH values below the $pK_a$ calculated the encapsulation process is better than at pH values above

the $pK_a$. A likely explanation for the dependence of $K_F$ on pH is that the protonated FA carboxyl group forms a hydrogen bond with hydrophilic groups of CD at pH values below the $pK_a$ value, as with other ionized weak electrolytes [14]. In this work the non-deprotoned t10,c12-CLA is more hydrophobic than the deprotoned t10,c12-CLA, which favors the encapsulation in the hydrophobic cavity intern of CDs.

### 4.5 Effect of temperature on the complexation constant

Another factor that must be considered when using encapsulated bioactive compounds in the food and nutraceutical industry is the temperature. Even small changes in temperature can lead to large changes in the complexation constants. In the present work the effect of temperature on the complexation constant was studied for the t10,c12-CLA/HPβ-CD complex at pH 8.

The results showed a similar behavior to the published for other guest molecules encapsulated by CDs such as other fatty acids [9] where the dependence of $K_F$ with temperature was increasing the $K_F$ value with temperature (**Fig**. 3B). This might be interpreted as a higher degree of interaction at higher temperatures. Hydrogens bonds are usually weakened by heating [15], although in this case the contrary seems to be true. In addition, hydrophobic interactions could decrease when temperature is higher [16], so a combination of both factors could be occurred.

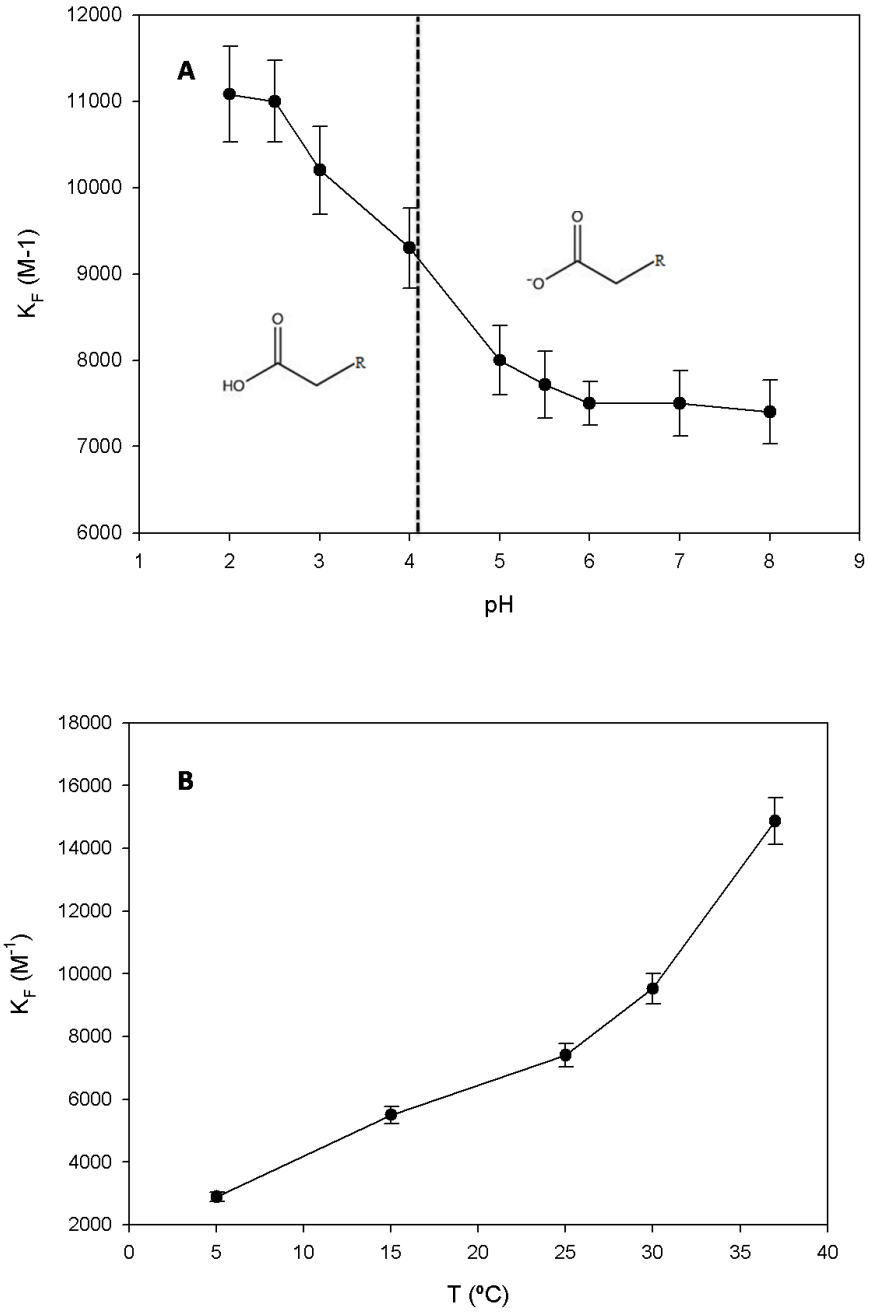


***Fig**. 3. (A) Effect of pH on complexation constant. Separation corresponds to the experimental pKa .(B) Effect of temperature on complexation constant at pH 8.*

## 4.6 Molecular docking

To increase our knowledge of the t10,c12-CLA/CD complex, a molecular modeling technique was used. The lower score, the stronger affinity predicted. Score results (Table 1) showed good correlation between the computed scores and experimental values with different CDs.

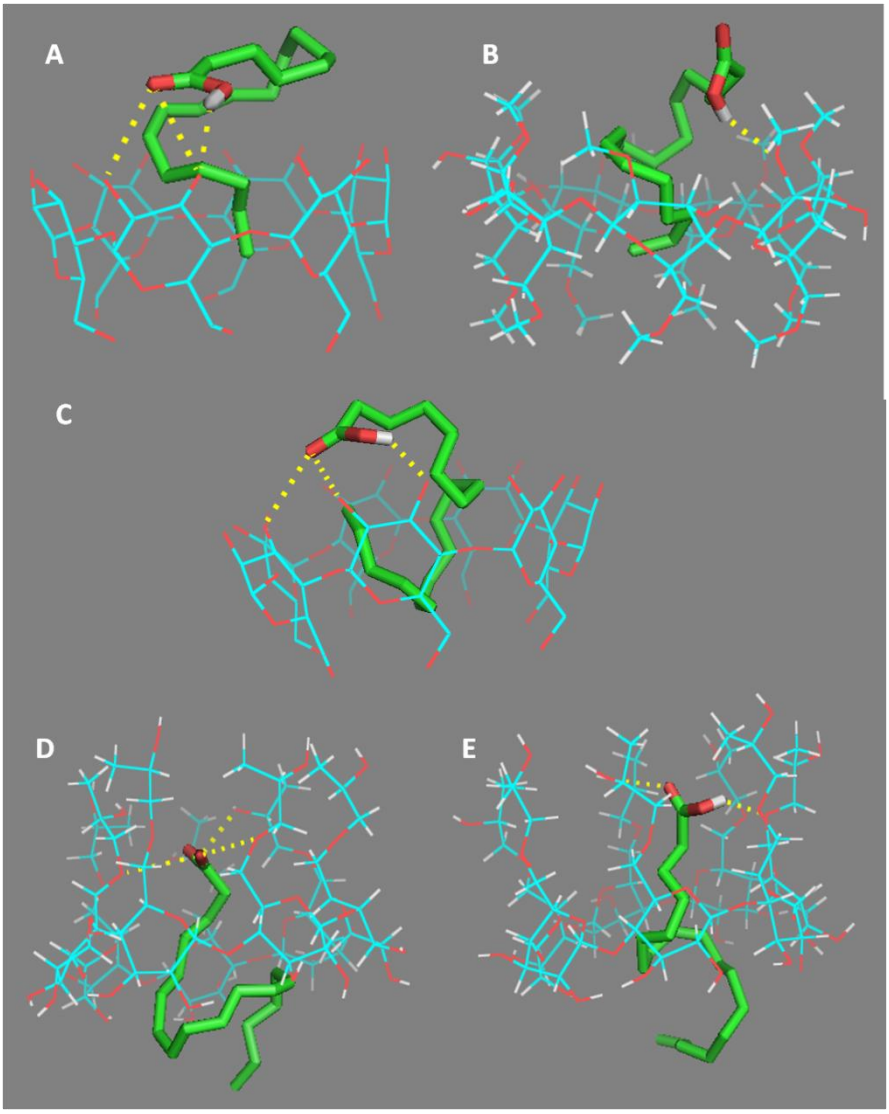


***Fig**. 4. Docking results of t10,c12-CLA with: (A) α-CD; (B) Mβ-CD; (C) β-CD and (D) HPβ-CD. (E): Docking results for RA/HPβ-CD complex. In yellow, hydrogens bonds.*

The docking results (**Fig**. 5) showed that α-CD (**Fig**. 5A) might not encapsulate perfectly in contrast to natural and modified β-CDs. β-CD present a high number of hydrogen bonds than Mβ-CD (**Fig**. 5C and 5B), it could be an important factor for the better $K_F$ values of β-CD. Furthermore, the HPβ-CD docking was the best (**Fig**. 5D). It presented a same number of hydrogen bonds than β-CD; however, the increase in hydrophobicity due to the Hydroxypropyl radical may explain the different scores between HPβ-CD and -CD or the Mβ-CD complexes.

3.8 Comparative encapsulation with Rumenic acid, an isomer of t10,c12-CLA

As we have been mentioned in the introduction, t10,c12-CLA is only one of the LA isomers, another one is Rumenic acid (c9,t11-CLA, RA) which complexation with different CDs was studied in previous chapter. It can be considered as the principal dietary form of CLA, accounting for as much as 85-90% of the total CLA [1] content in dairy products.

Although in both cases HPβ-CD was the best CD tested, the $K_F$ of RA obtained at the same conditions of t10,c12-CLA (pH 8 at 25ºC) was lower (7400 +/- 362 $M^{-1}$ ) than the obtained by RA (8347 +/- 417 $M^{-1}$), in both cases with a 1:1 complexation. Different interactions between CD and fatty acid, or the different collocation of unsaturated bond could justify the differences between the two isomers. To understand better this interaction, a molecular docking with HPβ-CD and RA was done. Score results showed good correlation between the computed scores and experimental values, obtaining a higher score for RA complex (-3.90) in contrast of t10,c12-CLA complex (-3.60). **Fig**. 5E shows the

docking result for RA/HPβ-CD complex. It presented a low number of hydrogen bonds in contrast with t10,c12-CLA/HPβ-CD (Fig. 5D) however the best collocation of RA into CD could justify the differences. Moreover, pKa of Ra was slightly higher (4.31) than t10,c12-CLA (4.08). Moreover, the effect of temperature in RA showed a change of conformation around 25 ºC not showed with t10,c12-CLA. This point reflects the importance on insaturation localization on FA.

In conclusion, we studied the monomer/aggregate equilibrium of t10,c12-CLA and its encapsulation by cyclodextrin, a well-known encapsulant agent that improves the stability and solubility of hydrophobic compounds in aqueous solutions. Many types of natural (α- and β-) and modified (Hydroxypropyl-β- and Methyl-β-) cyclodextrins were used and the stoichiometry of their complexes in equilibrium were found. The complexation constants ($K_F$) were determinate in an attempt to characterize the system. Knowledge of the complexation constants is essential if t10,c12-CLA/CDs complexes are to be used in the food industry. In addition, the effects on the complexation constants of factors that typically affect biochemical processes, such as pH, temperature and CD structure, were studied. To Increase our understanding of the complex, *in silico* molecular docking was used. Finally, a comparative study with RA was done, justifying the $K_F$ values differences.

## References

[1] B. Yang, H. Chen, C. Stanton, R.P. Ross, H. Zhang, Y.Q. Chen, W. Chen, Review of the roles of conjugated linoleic acid in health and disease, J. Funct. Foods. 15 (2015) 314–325. doi:10.1016/j.jff.2015.03.050.

[2] J.H. Kim, J.H. Pan, H.G. Park, H.G. Yoon, O.-J. Kwon, T.W. Kim, D.H. Shin, Y.J. Kim, Functional comparison of esterified and free forms of conjugated linoleic acid in high-fat-diet-induced obese C57BL/6J mice, J. Agric. Food Chem. 58 (2010) 11441–11447. doi:10.1021/jf102164j.

[3] W. Gilbert, V. Gadang, A. Proctor, V. Jain, L. Devareddy, trans-trans Conjugated linoleic acid enriched soybean oil reduces fatty liver and lowers serum cholesterol in obese zucker rats, Lipids. 46 (2011) 961–968. doi:10.1007/s11745-011-3585-6.

[4] V. Navarro, J. Miranda, I. Churruca, A. Fernández-Quintela, V.M. Rodríguez, M.P. Portillo, Effects of trans-10,cis-12 conjugated linoleic acid on body fat and serum lipids in young and adult hamsters, J. Physiol. Biochem. 62 (2006) 81–87.

[5] I. Fernández-Fígares, M. Lachica, A. Martín, R. Nieto, L. González-Valero, J.M. Rodríguez-López, J.F. Aguilera, Impact of dietary betaine and conjugated linoleic acid on insulin sensitivity, protein and fat metabolism of obese pigs, Anim. Int. J. Anim. Biosci. 6 (2012) 1058–1067. doi:10.1017/S1751731111002308.

[6] N.M. Racine, A.C. Watras, A.L. Carrel, D.B. Allen, J.J. McVean, R.R. Clark, A.R. O'Brien, M. O'Shea, C.E. Scott, D.A. Schoeller, Effect of conjugated linoleic acid on body fat accretion in overweight or obese children, Am. J. Clin. Nutr. 91 (2010) 1157–1164. doi:10.3945/ajcn.2009.28404.

[7] Y.H. Leung, R.H. Liu, trans-10,cis-12-Conjugated Linoleic Acid Isomer Exhibits Stronger Oxyradical Scavenging Capacity than cis-9,trans-11-Conjugated Linoleic Acid Isomer, J. Agric. Food Chem. 48 (2000) 5469–5475. doi:10.1021/jf991163d.

[8] L. Giua, F. Blasi, M.S. Simonetti, L. Cossignani, Oxidative modifications of conjugated and unconjugated linoleic acid during heating, Food Chem. 140 (2013) 680–685. doi:10.1016/j.foodchem.2012.09.067.

[9] J.M. López-Nicolás, R. Bru, A. Sánchez-Ferrer, F. García-Carmona, Use of "soluble lipids" for biochemical processes: linoleic acid-cyclodextrin inclusion complexes in aqueous solutions., Biochem J. 308 (1995) 151–154.

[10] E. Junquera, E. Aicart, G. Tardajos, Inclusional complexes of decyltrimethylammonium bromide and .beta.-cyclodextrin in water, J. Phys. Chem. 96 (1992) 4533–4537. doi:10.1021/j100190a074.

[11] M.D. Hanwell, D.E. Curtis, D.C. Lonie, T. Vandermeersch, E. Zurek, G.R. Hutchison, Avogadro: an advanced semantic chemical editor, visualization, and analysis platform, J. Cheminformatics. 4 (2012) 17. doi:10.1186/1758-2946-4-17.

[12] O. Trott, A.J. Olson, AutoDock Vina: improving the speed and accuracy of docking with a new scoring function, efficient optimization, and multithreading, J. Comput. Chem. 31 (2010) 455–461. doi:10.1002/jcc.21334.

[13] A. Chattopadhyay, E. London, Fluorimetric determination of critical micelle concentration avoiding interference from detergent charge, Anal. Biochem. 139 (1984) 408–412. doi:10.1016/0003-2697(84)90026-5.

[14] F.Y. Liu, D.O. Kildsig, A.K. Mitra, Cyclodextrin/weak-electrolyte complexation: interpretation and estimation of association constants from phase solubility diagrams, Pharm. Res. 9 (1992) 1671–1672.

[15] L. Sun, C.D. Wick, J.I. Siepmann, M.R. Schure, Temperature Dependence of Hydrogen Bonding: An Investigation of the Retention of Primary and Secondary Alcohols in Gas−Liquid Chromatography, J. Phys. Chem. B. 109 (2005) 15118–15125. doi:10.1021/jp0512006.

[16] P.L. Privalov, S.J. Gill, Stability of Protein Structure and Hydrophobic Interaction, in: J.T.E. C.B. Anfinsen Frederic M. Richards and David S. Eisenberg (Ed.), Adv.

Protein Chem., Academic Press, 1988: pp. 191–234. doi:10.1016/S0065-

3233(08)60377-0.

# Block I Part II

## *Stilbenes*

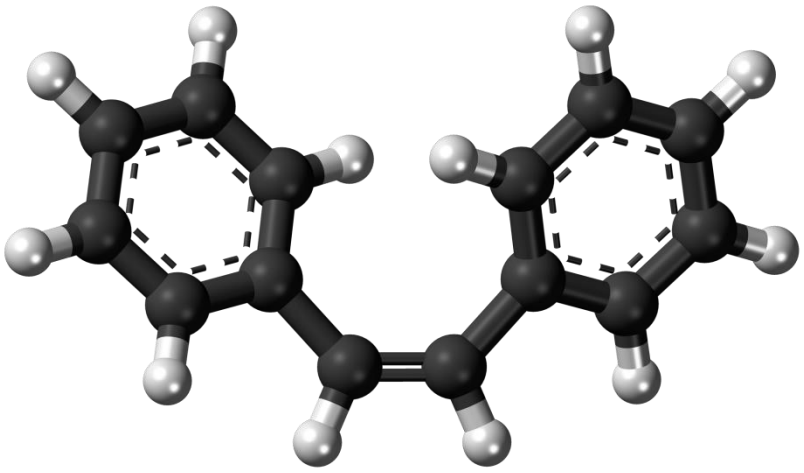

## Introduction

Stilbenes are a well known polyphenols family due to their bioactivities. For example, we can find resveratrol, which is responsible of wine benefits. A recent review is focused on their bioactivities [1]. Despite the mechanistic is not completely understood, stilbenes presents, in general, several bioactivities like anti-inflammatory, antioxidant and neuroprotective Moreover, they are promising drugs from diabetes mellitus, obesity, cancer or cardiovascular diseases. Stilbenes also demonstrated to extend the lifespan in different animal models, creating an evidence of potential benefits in age-derived conditions. Moreover they are presents also in some skin products to protect against chronic ultraviolet hyper-pigmentation.

Despite all these healthy properties, there are several problems related with the chemical properties of stilbenes prevent its use as fortifier of nutraceutical or fuctional foods. This bioactive molecule presents low solubility in water, poor bioavailability and is easily oxidized, making it necessary to look for new strategies which may increase its bioavailability, solubility and stability in the face of pro-oxidant agents.

Bearing these problems in mind, it is obvious that its complexation in CDs could, at least, solve many of them. For that reason, in the present part of thesis we are going to study the complexation of three commercial stilbenes (piceatannol, trans-α-methylstilbene and oxyresveratrol) and two derivates (resveratrol-sterate and resveratrol-oleate).

## References

[1] T. El Khawand, A. Courtois, J. Valls, T. Richard, S. Krisa, A review of dietary stilbenes: sources and bioavailability, Phytochem. Rev. 17 (2018) 1007–1029. doi:10.1007/s11101-018-9578-9.

# Block I part II

## Chapter I

## *Characterization of Piceatannol inclusion complexes*

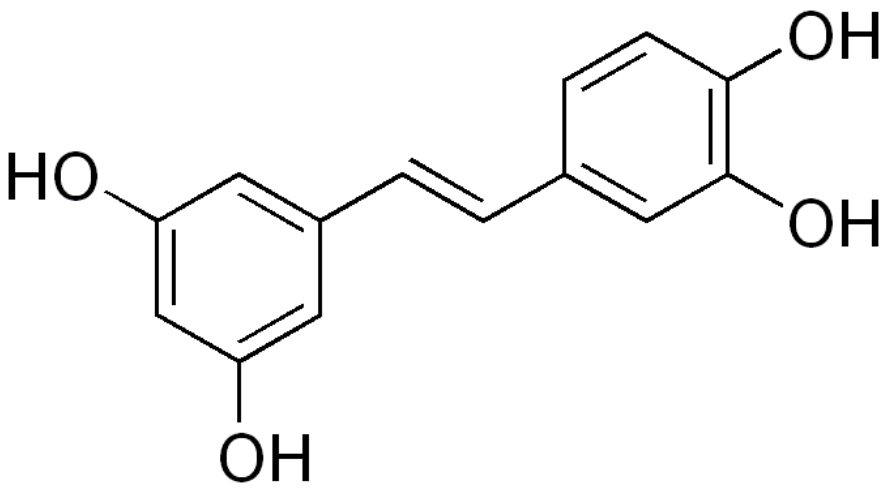

**Abstract**

In this chapter, an in-depth study of the interaction between piceatannol and different natural and modified cyclodextrins (CDs) is made, using steady state fluorescence. This bioactive molecule forms a 1:1 complex with all the natural (α-CD, β-CD and γ-CD) and modified (HPβ-CD, HEβ-CD and Mβ-CD) tested. Among natural CDs, the interaction of piceatannol with β-CD was the most efficient. However, the modified CDs showed higher complexation constants ($K_F$) than β-CD, except Mβ-CD; the highest $K_F$ being found for HPβ-CD (14048 ± 702 $M^{-1}$). The encapsulation of piceatannol in the internal cavity of CDs showed a strong dependence on pH and temperature. The interaction between HP-β-CD and piceatannol was less effective in the pH region where the stilbene begins to suffer deprotonation of its hydroxyl group. Moreover, the values of $K_F$ decreased as the system temperature increased.

To obtain information on the mechanism involved in piceatannol affinity for CD, the thermodynamic parameters of the complexation ($\Delta H^o$, $\Delta S^o$ and $\Delta G^o$) were studied, the results showed negative entropy (-3.7 +/- 0.2 J $mol^{-1}$ $K^{-1}$), enthalpy (–24.6 +/- 1.2 kJ $mol^{-1}$) and Gibbs free energy change at 25ºC (-23.5 +/- 1.2 J $mol^{-1}$). Finally, molecular docking calculations provided further insights into how the different interactions influence the complexation constant. High degree of correlation was observed between computed scores and experimental values can be observed.

## Index

## 1. Contextualization

Piceatannol (3',4',3,5-Tetrahydroxy-trans-stilbene) (**Fig**. 1), is an hydroxylated analogue of resveratrol that has been less well studied than other members of stilbenes family but, is known to display a wide spectrum of biological activity [1]. In detail, Piceatannol exhibits potential anticancer properties, as suggested by its ability to suppress proliferation of a wide variety of tumor cells, including leukemia, lymphoma; breast, prostate and colon cancer, and melanoma [1–3]. The pharmacological properties of piceatannol, especially its antitumor, antioxidant, and anti-inflammatory activities, suggest that piceatannol might be a potentially useful nutritional and pharmacological biomolecule.

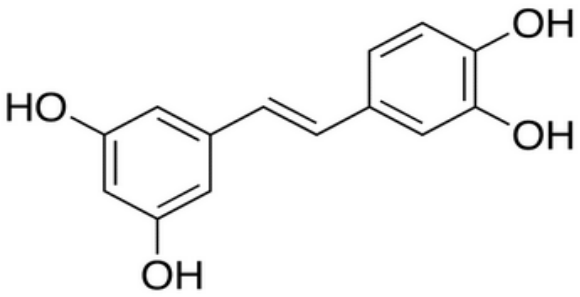


*Fig. 1. Structure of Piceatannol*

## 2. Objectives

1) To analyze the complexation mechanism of piceatannol by different types of natural (α-, β- and γ-CD) and modified (HP-β-CD, M-β-CD and HE-β-CD) CDs.

2) To evaluate the effect of temperature and pH on the complexation mechanism of piceatannol.

3) Determine the stoichiometry, $K_F$ values and thermodynamic parameters for the piceatannol-CD complexes.

4) To study the types of interaction between piceatannol and CD using molecular docking.

## 3. Materials and methods

### 3.1 Materials

Natural (α-, β- and γ-CD), modified CDs (HPβ-CD, HEβ-CD and Mβ-CD) and piceatannol were purchased from Sigma-Aldrich (Madrid, Spain) and used as received. Piceatannol was stored in darkness.

### 3.2 Equipment and Experimental Procedure

#### *3.2.3 Fluorescence studies*

Fluorescence intensity was measured in a Kontron SFM-25 spectrofluorimeter (Zurich, Switzerland) equipped with thermostatically controlled cells and with a xenon lamp source and quartz cell, which were used to perform all the fluorescence measurements. Excitation and emission bandwidths were both set at 2 nm. The excitation and emission wavelengths for piceatannol were 343 nm and 395 nm, respectively. The relative fluorescence intensity values were recorded at 25 ºC. The concentration of piceatannol was fixed at 25 µM and the CD concentration was between 0-2.5 mM. All reagents were dissolved in water.

#### *3.2.4 Complexation constant determination*

To determine the stoichiometry of the CD-piceatannol interaction, two mathematical models were proposed: a 1:1 model, where one molecule of CD complexes one molecule of piceatannol and a 1:2 model, where one molecule of piceatannol is encapsulated by two molecules of CDs.

Fluorescence intensities changes due to the interaction between piceatannol and CD can be used to quantify the strength of the complexation. For this, the Benesi-Hildebrand method [4], which permits the complexation constant ($K_F$) to be obtained, was used.

Assuming that the composition of the complex to be 1:1, the following expression can be written:

Piceatannol + HPβ-CD ⇆ HPβ-CD-Piceatannol

The complexation constant, $K_F$ is given by:

$$K_F = \frac{[HP\beta\text{-}CD/Piceatannol]}{[Piceatannol]\,[HP\beta\text{-}CD]} \quad (1)$$

where [HPβ-CD], [Piceatannol] and [HPβ-CD/Piceatannol] are equilibrium concentrations.

To calculate $K_F$ firstly the increase in relative fluorescence of piceatannol was plotted for increasing concentrations of HPβ-CD added to the medium. Then, the difference in the intensity of the emission fluorescence of piceatannol in the absence and presence of different amounts of HPβ-CD was plotted vs the HPβ-CD concentration. Finally, the expression corresponding to the Benesi–Hildebrand method was used to determine the $K_F$ value.

$$\frac{1}{F-F_0} = \frac{1}{(F_\infty - F_0)K_F\,[HP\beta\text{-}CD]} + \frac{1}{F_\infty - F_0} \quad (2)$$

where [HPβ-CD] denotes the HPβ-CD concentration; $F_0$ the fluorescence intensity of piceatannol in the absence of HPβ-CD; $F_\infty$ the fluorescence intensity when all of the piceatannol molecules are essentially complexed with HPβ-CD;

and F, is the observed fluorescence intensity at each β-CD concentration tested.

In order to study the possible presence of higher order complexes between HPβ-CD and piceatannol, a plot of $1/F\text{-}F_0$ as a function of $1/ [HP\beta\text{-}CD]^2$ was also analyzed. Assuming the stoichiometry of the inclusion complex to be 1:2, the following expression is obtained [5]:

$$\frac{1}{F-F_0} = \frac{1}{(F_\infty - F_0)K_{F12}([HP\beta-CD])^2} + \frac{1}{F_\infty - F_0} \quad (3)$$

For temperature studies, the $K_F$ values for the complex were determined at the following temperatures 288, 298, 303 and 310 K **(**15 ºC, 25 ºC, 30 ºC and 37 ºC)**,** using a Thermomixer Comfort (Eppendorf Ibérica, Madrid, Spain).

For pH studies, the $K_F$ values for the complex were determined in the pH range 5.5-13.0. For each pH, different types of buffer were used: pH (5.5-8.0) sodium phosphate 0.1 M; pH (8.0-12.0) sodium borate 0.1 M; pH 13.0 potassium chloride-NaOH 0.1 M.

3.5 Thermodynamic parameters determination

The thermodynamic parameters Δ*H*º, Δ*S*º and ΔG*º* can be calculated using the following thermodynamic relationship:

$$Ln\ K_F = \frac{-\Delta H^\circ}{RT} + \frac{-\Delta S^\circ}{R} \quad (4)$$

where $K_F$ is the complexation constant of the inclusion complex, T is the temperature, R is the gas constant and Δ*H*º and Δ*S*º are standard enthalpy and entropy changes of complex formation in the mobile phase. The Gibbs free

energy change for the interactions that take place during the inclusion process may be found by the following equation:

$$\Delta G^{\circ} = \Delta H^{\circ} - T\Delta S^{\circ} \quad (5)$$

### 3.6 Molecular docking

The molecular structures used in this work were built using Avogadro Software [6] or were obtained by different databases. The α-CD and β-CD structures were extracted from a crystal from the Protein Data Bank (PDB ID: 2XFY and 1Z0N), and the γ-CD was extracted from London South Bank University website. Piceatannol was obtained from the CACTUS database (NCI/CADD group, USA). HPβ-CD, HEβ-CD and Mβ-CD were built by adding Hydroxypropyl, Hydroxyethyl or Methyl group**s** to the β-CD. Molecular docking was carried out using Autodock Vina [7]. All CDs were considered as rigid. Graphical representations of the docking results were prepared using PyMOL (Molecular GraphicsSystem, version 1.3, Schrödinger, LLC).

### 3.7 Data Analysis

All experiments were carried out three times. Regressions were made using SigmaPlot (Systat Software, version 10.0). ANOVA and a Tukey Test were applied using Rstudio (version 0.99.878) with a significance of $P<0.05$. Other mathematical operations were carried out using wxMaxima software (version 12.04.0).

## 4. Results and discussion

4.1 Study of the stoichiometry and determination of the complexation constants.

To calculate $K_F$ firstly the increase in relative fluorescence of piceatannol was plotted for increasing concentrations of HPβ-CD added to the medium (**Fig**. 2). **Fig**. 2 *inset* showed (filled circles) a linear correlation higher than 0.99 for eq. 2, indicating that the presumed stoichiometry of the HPβ-CD/piceatannol complexes was 1:1. In order to study the possible presence of higher order complexes (1:2) between HPβ-CD and piceatannol, a plot of $1/F\text{-}F_0$ as a function of $1/ [HP\beta\text{-}CD]^2$ was also analyzed with worse results (linear correlation of 0.95). Indeed, a nonlinear relationship was obtained (**Fig**. 2 *inset*, filled squares). These results indicate that the stoichiometry of the inclusion complex was not 1:2.

Using eq. 2, the $K_F$ value for this pH was 14048 ± 702 $M^{-1}$. These results are in agreement with those previously obtained for the 1:1 complexes between HPβ-CD and several compounds with structures similar to piceatannol, such as resveratrol, pterostilbene, pinosilvyn or oxyresveratrol [8–11].

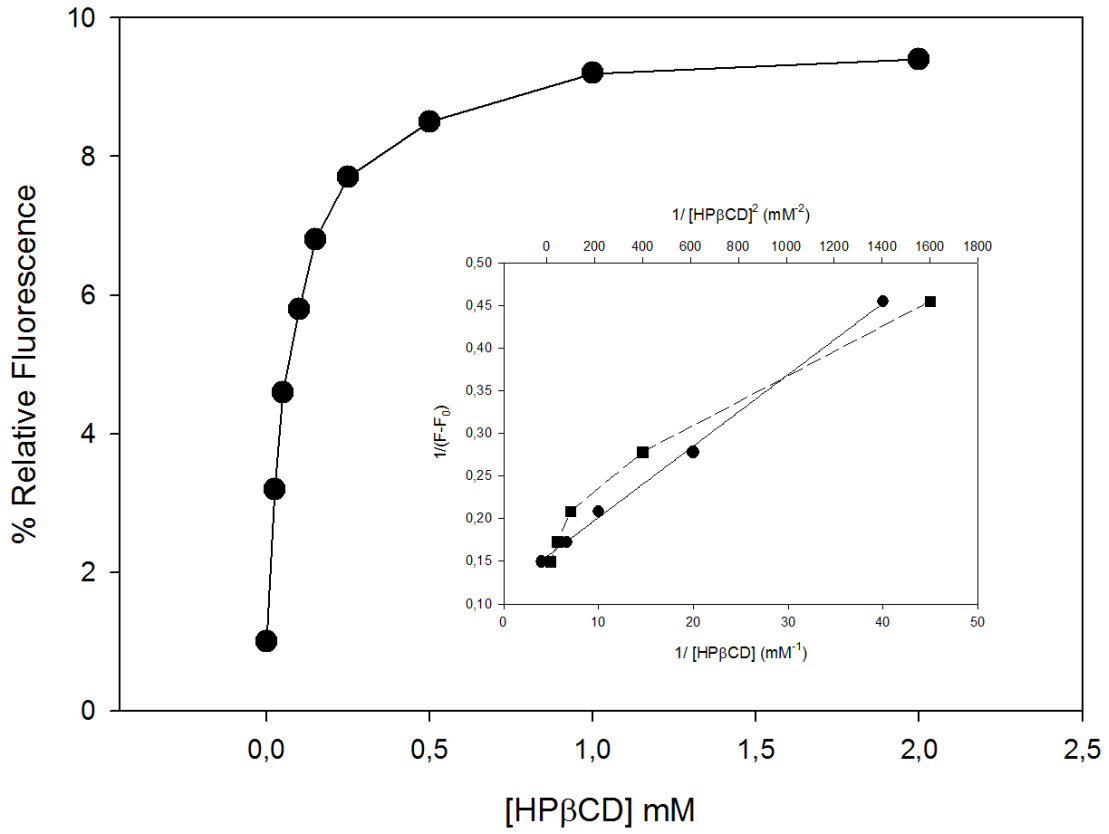


***Fig. 1.*** *Dependence of emission fluorescence intensities of piceatannol (25 μM) on HPβ-CD concentrations at pH 7 and 25ºC. Inset: Double reciprocal plot of piceatannol complexed to HPβ-CD for determining the stoichiometry of HPβ-CD/piceatannol complexes: 1/(F-F$_0$) versus 1/ [HPβ-CD] (assumption of 1:1 complex) (filled circles); (b) 1/(F-F$_0$) versus 1/ [HPβ-CD]$^2$ (hypothesis of 1:2 complex) (filled squares).*

4.2 Selection of the optimum type of cyclodextrin for the complexation of piceatannol

The next step in our investigation was to calculate the $K_F$ values between piceatannol and different types of CDs. In Table 1 it is observed that the highest $K_F$ value ($K_F$ =9797 ± 489 M$^{-1}$) was for β-CD, followed by γ-CD ($K_F$ =4370 ± 524 M$^{-1}$) and, finally, α-CD ($K_F$ = 2383 ± 357 M$^{-1}$). These results show that the inner diameter of the CD formed by six units of glucose (β-CD: 6.0-6.4 Å) fitted

piceatannol better than the inner diameter of five units (α-CD: 4.7-5.2 Á) or seven units (γ-CD: 7.5-8.3 Á) of glucose.

Table 1. Experimental KF values, correlation coefficients arising from equations (4) and (5) (for 1:1 and 1:2 Piceatannol/CD complexes, respectively) at 25 ºC at pH 7.0; and Docking Score.

| CD type | $K_F$ ($M^{-1}$) | Correlation coefficient | | **Score** |
|---|---|---|---|---|
| | | *1:1* | *1:2* | |
| HPβ-CD | 14048 ± 702 | 0.99 | 0.95 | *-6.10* |
| HEβ-CD | 12310 ± 615 | 0.98 | 0.86 | -5.80 |
| β-CD | 9797 ± 489 | 0.98 | 0.83 | -5.60 |
| Mβ-CD | 7757 ± 387 | 0.99 | 0.96 | -5.20 |
| γ-CD | 4370 ± 524 | 0.99 | 0.95 | -5.0 |
| α-CD | 2383 ± 357 | 0.99 | 0.87 | -2.8 |

The next step was to study the effect of chemical by modifying of β-CD on the complexation constants of the piceatannol/CD complexes. For this HPβ-CD, HEβ-CD and Mβ-CD, three modified CDs obtained by the addition of different functional groups to the macrocyclic ring, were used.

In Table 1 it is observed that the $K_F$ values obtained with theses modified CDs were higher than those obtained when natural CDs were tested. Indeed HPβ-CD (14048 ± 702 $M^{-1}$) showed the highest $K_F$ value, followed by HEβ-CD (12310 ± 6115 $M^{-1}$). As can be seen, the $K_F$ for the complexation of piceatannol by different modified CDs is dependent on the length of the aliphatic chain of the β-CD substituent: the greater the number of carbon atoms in the substituent, the higher the $K_F$ value for the resulting complex.

However, Mβ-CD $K_F$ was lower than β-CD (7757 ± 387 $M^{-1}$) indicating that hydroxyl group may affect stability drastically. Then, the dramatic changes occurring in the hydrophobicity of the CD torus provoked by the substitution of the internal –OH groups would also explain the behaviour of $K_F$. Additionally, these results were corroborated using ANOVA (for the group) and Tukey analysis (for each 2 $K_F$). For this reason, HPβ-CD was chosen as host CD for the following sections of the paper.

4.3 Effect of temperature on the complexation of piceatannol by HPβ-CD.

The effect of the temperature in the $K_F$ values of the piceatannol/HPβ-CD complexes was studied. Temperature is one of the most important physicochemical factors that must be taken into account. This may affect the stability of the complex.

For different molecules, conflicting results for the effect of temperature on the $K_F$ values of inclusion complexes can be obtained. Normally, inclusion complexes are dissociated when temperature is increased [12,13]. However, the complexation of polyunsaturated fatty acids by CDs is favoured by an increase in temperature [14].

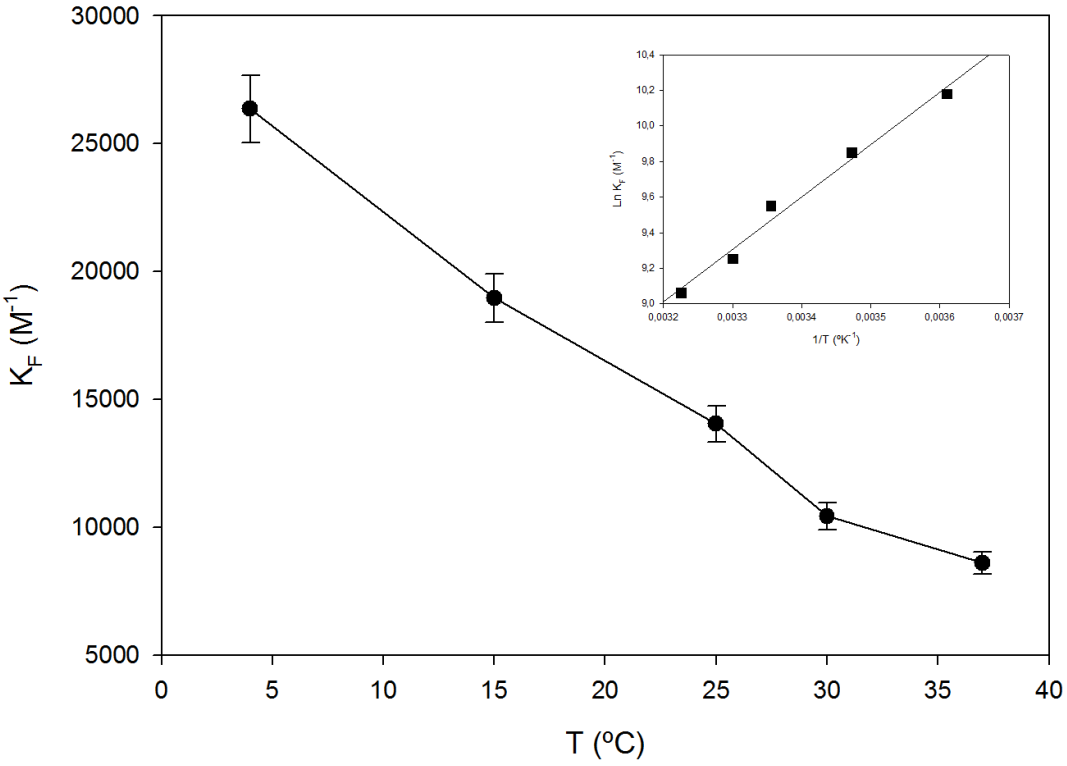


*Fig. 3. Effect of temperature on the complexation constant ($K_F$) of piceatannol-HPβ-CD complexes at pH 7.0. Inset: Van´t Hoff plot (ln $K_F$ vs. 1/T) for piceatannol-HPβ-CD complexes in 0.1 M sodium phosphate buffer pH 7.0.*

**Fig**. 3 represents the effect of four different temperatures, 288, 298, 303 and 310 K **(**15 ºC, 25 ºC, 30 ºC and 37 ºC), on the $K_F$ values for the piceatannol/HPβ-CD complex. An increase in temperature led to a strong decrease in the complexation constant values. This behaviour is in good agreement with other stilbenoids [8–11]. This lower degree of interaction at higher temperatures could be attributed to the fact that hydrogen bonds are usually weakened by heating.

*4.3.1 Thermodynamic parameters for the piceatannol-HPβ-CD complexes.*

To gain information on mechanistic aspects of the affinity of piceatannol for HPβ-CD, the thermodynamic parameters ($\Delta H^o$, $\Delta S^o$ and $\Delta G^o$ at 25ºC) of the complexation were obtained. **Fig**. 3 *inset* shows that the relation is linear, with a correlation coefficient higher than 0.99. From the same figure different conclusions may be obtained:

Changes of entropy are negative in these processes (-3.7 ± 0.2 J $mol^{-1}K^{-1}$). This can be justified due to the fact that complexation decreases the translational and rotational degrees of freedom of the complexed piceatannol compared with the free ones, leading to more ordered system.

Moreover, the negative values obtained for enthalpy changes (-24.6 ± 1.2 kJ $mol^{-1}$) indicate the exothermic nature of the interaction processes. This behaviour is typical of three types of hydrophobic interactions, due to the displacement of water molecules from the cavity of HP-β-CD; increased van der Waals interactions between the molecules and the formation of hydrogen bonds and other interactions [15].

Concerning the spontaneity of the complexation process, our data show that the inclusion process is spontaneous due to the negative value obtained (–23.5 ± 1.2 kJ $mol^{-1}$) using the Gibbs free energy change at 25ºC .

## 4.4 Effect of pH on the complexation of piceatannol by HPβ-CD.

Several authors have shown that the protonation state has a great influence on the complexation constants [9]. As shown in **Fig**. 4, there is a strong dependence of $K_F$ on pH, passing from a stable value of 14039 ± 700 $M^{-1}$ (5.5 < pH < 7.5) to about 2557 ± 120 $M^{-1}$ (10 < pH < 13), as occurs during the titration of a weak ionizable group.

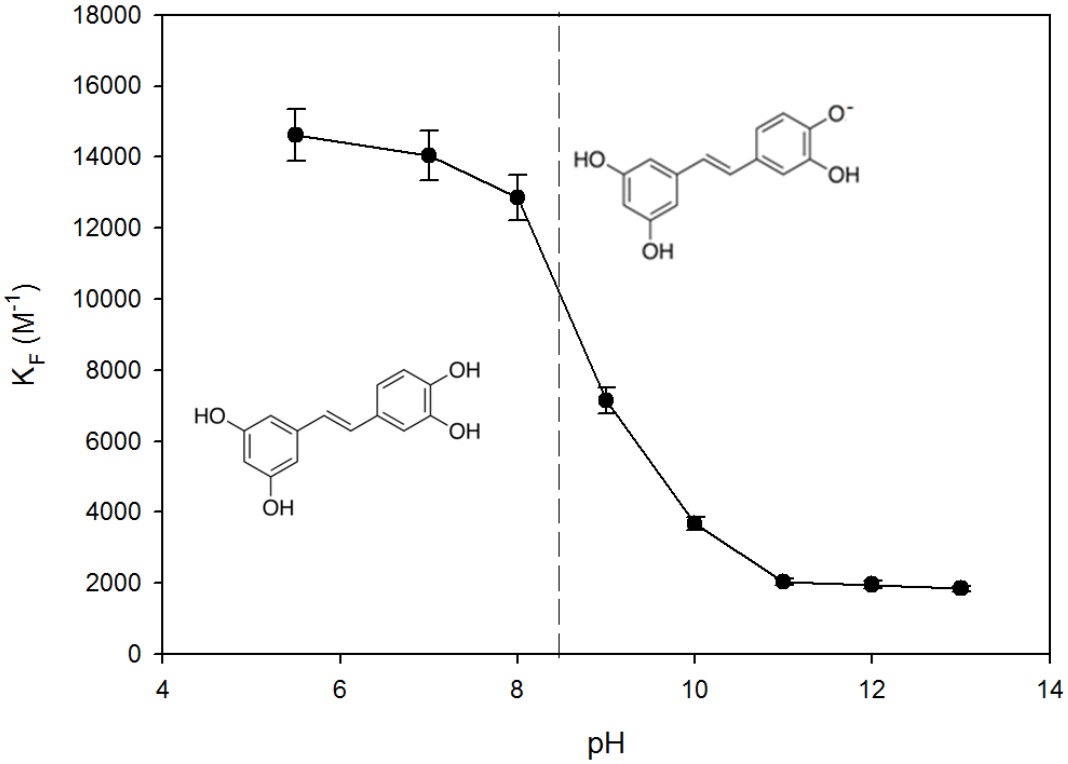


*Fig.4. Effect of pH on the complexation constant ($K_F$) of piceatannol-HPβ-CD complexes at 25 ºC.*

The sharp decrease in the $K_F$ value shown in **Fig**. 4 might coincide with the region where the piceatannol begins deprotonation of its hydroxyl groups. A possible cause for this dependence of $K_F$ on pH is that the hypothetical formation of a hydrogen bond between the hydroxyl group of the piceatannol

and the hydrophilic groups of CD [13,16] at pH values below the $pK_a$ value (8.34, calculated).

The fact that the complexes between HPβ-CD and the protonated form of piceatannol were more stable than the interaction with the deprotonated forms of this lipophilic antioxidant is of great interest for the food industry, because the protonated form of stilbenes presents several beneficial biological effects on human health [17].

4.5 Molecular modelling of the piceatannol/ CD complexes.

In order to understand how piceatannol interacts with CDs, docking simulations were carried out. Table 1 shows that the docking scores were directly proportional to the $K_F$ values. A good correlation between computed scores and experimental values can be observed, suggesting that our modelling methodology captures the essentials of the host-guest energetic interactions. Additionally, the structural information concerning the different binding poses obtained by docking, and shown in **Fig**. 5, might explain experimental data obtained.

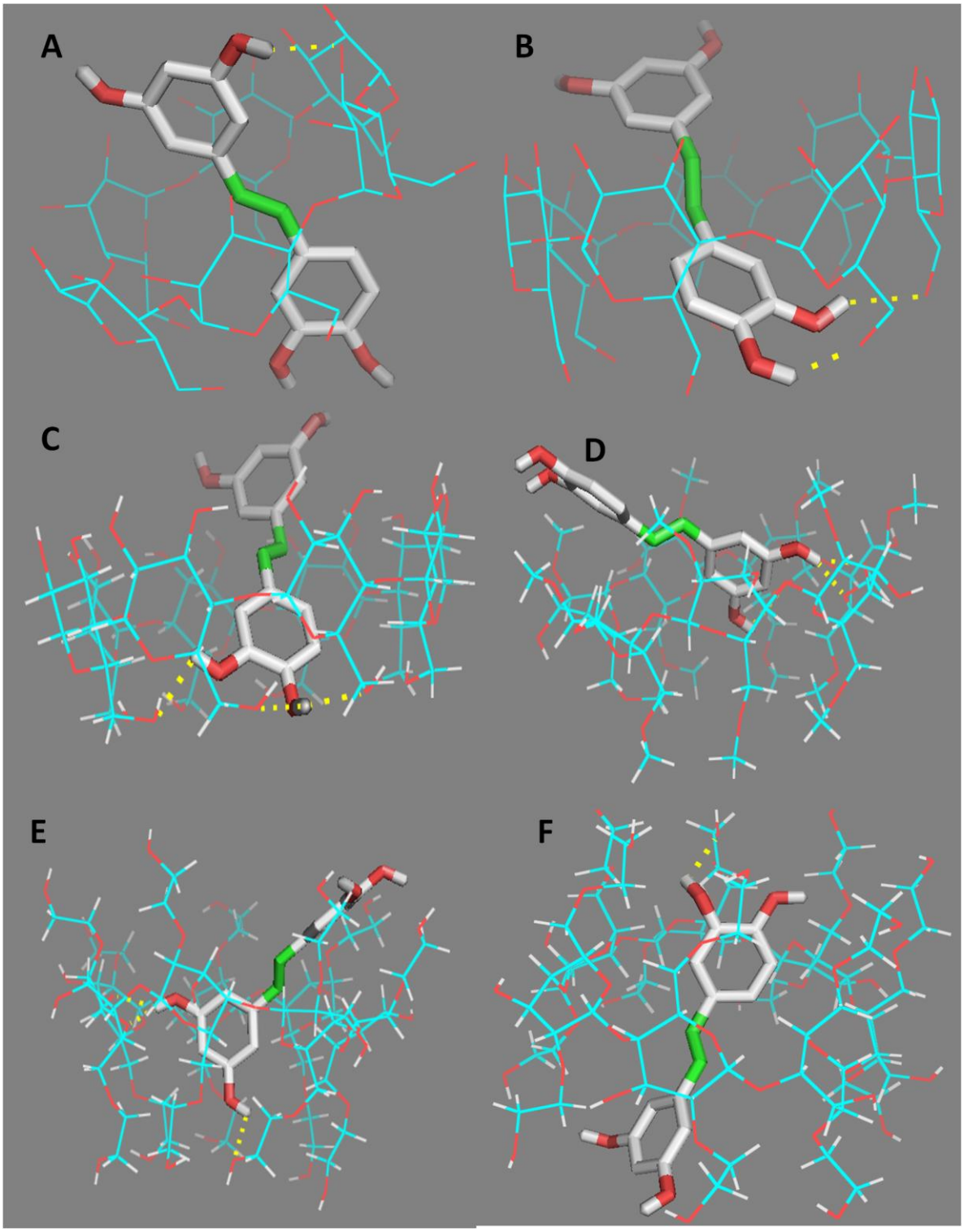


*Fig. 5. Docking Results of A: α-CD, B: β-CD, C: γ-CD, D: Mβ-CD, E: HEβ-CD and F: HPβ-CD. In yellow, hydrogens bonds.*

As regards the ring size of the different CDs, the weakest interaction corresponds to the complex with α-CD, as depicted in **Fig**. 5A. The main reason for this worked be the weak hydrophobic stabilisation due to the poor host-guest fit. The γ-CD is more stable (**Fig**. 4C) due to the hydrogen bonds established with the primary hydroxy rim, but, in general terms, the stability of the complexation increases with β-CD and its derivatives Mβ-CD, HEβ-CD and HPβ-CD (**Figs**. 5B, 5D, 5E and 5F) since the fit is better in the Piceatannol/CD.

For CDs with seven sugar rings, the most stable combination corresponds to β-CD followed by its derivatives HEβ-CD and HPβ-CD, though Mβ-CD was lower than β-CD. The Mβ-CD complex has fewer hidrogens bonds than the β-CD complex, which might explain the lower $K_F$ obtained. In the case of HEβ-CD and HPβ-CD, there might be less entropic stabilization than in β-CD due to the loss of degrees of freedom of the additional hydroxyethyl and hydroxypropyl groups. As regards energy contributions, the reason for the greater stability of HPβ-CD with respect to HEβ-CD could be due to the additional hydrophobic stabilization of the extra methyl groups of HPβ-CD, which can point to the inner cavity.

In conclusion, this chapter presents a physico-chemical, thermodynamic and computational study of the complexation of piceatannol, a member of a family of bioactive compounds of potential use in the food and nutraceutical industries. Piceatannol forms 1:1 complexes with natural and modified CDs, showing the highest complexation constant with HPβ-CD. The complexation process was more efficient in the pH region where the hydroxyl group of this stilbene is protonated. The study of temperature´s effect on the

CDs/piceatannol complexes showed that the efficacy of the complexation increased as the system temperature decreased. Moreover the results showed a negative entropy and enthalpy changes and negative Gibbs free energy value at 25ºC for the complexation process. A computational study carried out using molecular docking calculations showed a high degree of correlation between computed scores and experimental values.

## References

[1] H. Piotrowska, M. Kucinska, M. Murias, Biological activity of piceatannol: Leaving the shadow of resveratrol, Mutat. Res. Mutat. Res. 750 (2012) 60–82. doi:10.1016/j.mrrev.2011.11.001.

[2] M.A. Seyed, I. Jantan, S.N.A. Bukhari, K. Vijayaraghavan, A Comprehensive Review on the Chemotherapeutic Potential of Piceatannol for Cancer Treatment, with Mechanistic Insights, J. Agric. Food Chem. (2016). doi:10.1021/acs.jafc.5b05993.

[3] H. Song, J.I. Jung, H.J. Cho, S. Her, S.-H. Kwon, R. Yu, Y.-H. Kang, K.W. Lee, J.H.Y. Park, Inhibition of tumor progression by oral piceatannol in mouse 4T1 mammary cancer is associated with decreased angiogenesis and macrophage infiltration, J. Nutr. Biochem. 26 (2015) 1368–1378. doi:10.1016/j.jnutbio.2015.07.005.

[4] H.A. Benesi, J.H. Hildebrand, A Spectrophotometric Investigation of the Interaction of Iodine with Aromatic Hydrocarbons, J. Am. Chem. Soc. 71 (1949) 2703–2707. doi:10.1021/ja01176a030.

[5] A.M. Rimando, M. Cuendet, C. Desmarchelier, R.G. Mehta, J.M. Pezzuto, S.O. Duke, Cancer Chemopreventive and Antioxidant Activities of Pterostilbene, a Naturally Occurring Analogue of Resveratrol, J. Agric. Food Chem. 50 (2002) 3453–3457. doi:10.1021/jf0116855.

[6] M.D. Hanwell, D.E. Curtis, D.C. Lonie, T. Vandermeersch, E. Zurek, G.R. Hutchison, Avogadro: an advanced semantic chemical editor, visualization, and analysis platform, J. Cheminformatics. 4 (2012) 17. doi:10.1186/1758-2946-4-17.

[7] O. Trott, A.J. Olson, AutoDock Vina: improving the speed and accuracy of docking with a new scoring function, efficient optimization, and multithreading, J. Comput. Chem. 31 (2010) 455–461. doi:10.1002/jcc.21334.

[8] J.M. López-Nicolás, F. García-Carmona, Rapid, simple and sensitive determination of the apparent formation constants of trans-resveratrol complexes with natural cyclodextrins in aqueous medium using HPLC, Food Chem. 109 (2008) 868–875. doi:10.1016/j.foodchem.2008.01.022.

[9] J.M. López-Nicolás, P. Rodríguez-Bonilla, F. García-Carmona, Complexation of pinosylvin, an analogue of resveratrol with high antifungal and antimicrobial activity, by different types of cyclodextrins, J. Agric. Food Chem. 57 (2009) 10175–10180. doi:10.1021/jf902519d.

[10] J.M. López-Nicolás, P. Rodríguez-Bonilla, L. Méndez-Cazorla, F. García-Carmona, Physicochemical study of the complexation of pterostilbene by natural and modified cyclodextrins, J. Agric. Food Chem. 57 (2009) 5294–5300. doi:10.1021/jf900285e.

[11] P. Rodríguez-Bonilla, J.M. López-Nicolás, F. García-Carmona, Use of reversed phase high pressure liquid cromatography for the physicochemical and thermodynamic characterization of oxyresveratrol/β-cyclodextrin complexes, J. Chromatogr. B. 878 (2010) 1569–1575. doi:10.1016/j.jchromb.2010.04.016.

[12] D.W. Armstrong, S.M. Han, Y.I. Han, Separation of optical isomers of scopolamine, cocaine, homatropine, and atropine, Anal. Biochem. 167 (1987) 261–264. doi:10.1016/0003-2697(87)90161-8.

[13] W. Saenger, Cyclodextrin Inclusion Compounds in Research and Industry, Angew. Chem. Int. Ed. Engl. 19 (1980) 344–362. doi:10.1002/anie.198003441.

[14] J.M. López-Nicolás, R. Bru, A. Sánchez-Ferrer, F. García-Carmona, Use of “soluble lipids” for biochemical processes: linoleic acid-cyclodextrin inclusion complexes in aqueous solutions., Biochem J. 308 (1995) 151–154.

[15] C. Ravelet, A. Geze, A. Villet, C. Grosset, A. Ravel, D. Wouessidjewe, E. Peyrin, Chromatographic determination of the association constants between nimesulide and native and modified β-cyclodextrins, J. Pharm. Biomed. Anal. 29 (2002) 425–430. doi:10.1016/S0731-7085(02)00088-2.

[16] R. Bru, J.M. López-Nicolás, E. Núñez-Delicado, D. Nortes-Ruipérez, A. Sánchez-Ferrer, F. Garciá-Carmona, Cyclodextrins as hosts for poorly water-soluble compounds in enzyme catalysis, Appl. Biochem. Biotechnol. 61 (1996) 189–198. doi:10.1007/BF02785701.

[17] H. Cao, X. Pan, C. Li, C. Zhou, F. Deng, T. Li, Density functional theory calculations for resveratrol, Bioorg. Med. Chem. Lett. 13 (2003) 1869–1871. doi:10.1016/S0960-894X(03)00283-X.

# Block I part II

## Chapter II

## *Trans-alpha-methylstilbene inclusion complexes characterization*

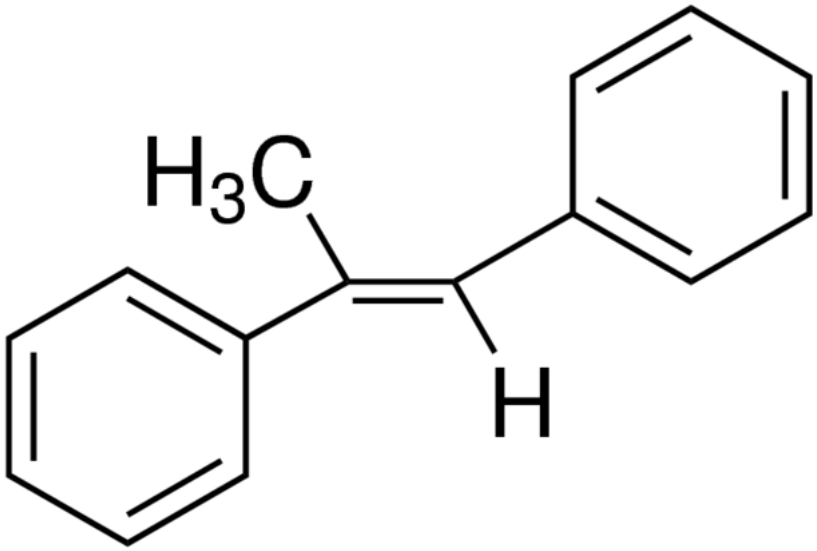

**Abstract**

Trans-α-Methylstilbene (tMS), a resveratrol analogue, has recently been studied in a search of new bioactivities. However, such studies do not take into account that the poor solubility of tMS in aqueous solutions could affect its bioactivity. For this reason, we propose, for first time, using cyclodextrins (CDs) as solubilizers to increase tMS solubility, in aqueous solutions.

The HPLC-RP results obtained, point to a 1:1 stoichiometry for all the natural (α-, β- and γ-CD) and modified (HPβ-CD and Mβ-CD) CDs tested. The $K_{Fapp}$ (Apparent formation constant) for the tMS-CD complexes was seen to be closely dependent on several factors, including temperature and type of CD. Indeed, the highest $K_{Fapp}$ value was obtained for Mβ-CD, while the $K_{Fapp}$ decreased with increasing temperature. In addition, the results showed negative entropy ($-8.86 \cdot 10^{-3} \pm 0.40$ kJ $mol^{-1}K^{-1}$) and enthalpy (-16.70 +/- 0.98 kJ $mol^{-1}$) changes and a negative Gibbs free energy value at 25ºC (–14.00 ± 0.55 kJ $mol^{-1}$) for the encapsulation process.

A computational study carried out using molecular docking calculations showed a high degree of correlation between the computed scores and experimental values. Finally, the complexation of trans-stilbene and pinosylvin with HPβCD was compared with tMS.

## Index

## 1. Contextualization

One of the less well known stilbenes is trans-α-Methylstilbene (tMS, **Fig**. 1), an analogue of resveratrol used in chemical synthesis [1,2]. Recently the National Cancer Institute (NIH) of USA studied the bioactivity of tMS for use in the fight against cancer, with disappointing results [4]. However, the hydrophobic nature of tMS and it low solubility was not taken into account. Indeed, this problem could hinder the bioavailability of the compound, preventing the discovery of its bioactivities. It is therefore clear that tMS solubility needs to be improved if it is to be used in aqueous solutions. One possibility would be to use a polymer or matrix to encapsulate tMS creating a substrate reservoir that would improve release efficiency [6]. Of the mocules available, cyclodextrins (CDs) could be considered a good option.

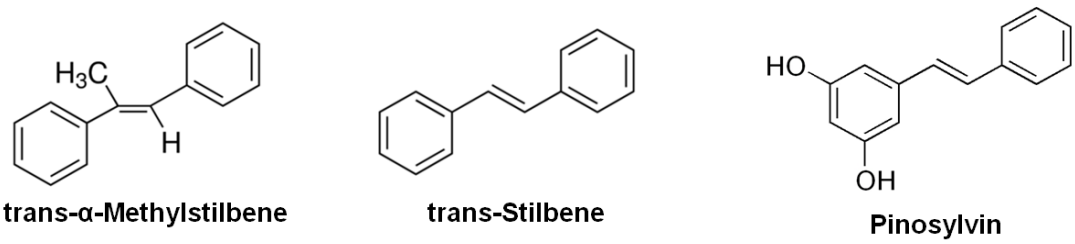


***Fig 1.*** *Structures of trans-α-Methylstilbene, trans stilbene, pinosylvin*

## 2. Objectives

The main objectives of this work were to:

1. Analyse the encapsulation mechanism of tMS with different types of natural (α-, β- and γ-CD) and modified (HPβCD and MβCD) CDs.
2. Evaluate the effect of temperature on the encapsulation mechanism of tMS.
3. Determine the stoichiometry, $K_F$ values and thermodynamic parameters for the tMS-CD complexes.
4. Study the types of interaction between tMS and CD using molecular docking.
5. Compare the $K_F$ values of tMS, trans-stilbene and pinosilvyn.

## 3. Materials and methods

### 3.1 Materials

Quinine (purity ≥ 90 % Pubchem CIF 145904), natural CDs (α-, β- and γ-CD, purity ≥ 97 % Pubchem CIFs 444913, 444041 and 5287407), modified CDs (HPβCD and MβCD, purity ≥ 95 % Pubchem CIF 44134771 and 51051622) were purchased from Sigma-Aldrich (Madrid, Spain). tMS (purity ≥ 98 % Pubchem CIF 1549166) was purchased from Alfa Aesar (Karlsruhe, Germany) and used as received. Ethanol (analysis grade) was purchased from Merck (Madrid, Spain). The samples were stored in darkness. Methanol (HPLC grade) was purchased from Fisher (Madrid, Spain). MQ water was obtained using a Milli-Q Advantage A10 system by Merck Millipore (Madrid, Spain). Binary mixtures of water/methanol, with methanol percentages of 40-80%, were used without further purification.

### 3.2 Equipment and Experimental Procedures.

#### *3.2.1 Inclusion complex characterization.*

10 µL of a 1 mg/mL tMS solution in ethanol was analysed in an Agilent 1100 series HPLC system (CA, USA) and a 1200 series module UV-VIS detector with a Kromasil 150 C18 column (Análisis Vínicos S.L.Tomelloso, Spain) (150 mm x 4,6 mm, 5µm particle size). The mobile phase flow rate was set and automatically controlled at 1.50 ± 0.01 mL/min with Methanol/Water (60/40 v/v) at different concentrations of CDs at 25 ºC. The UV detector was operated at 306 nm.

To determine the $K_F$ value for the tMS / CD complexes, Equation 1, which relates the capacity factor, *k*, and the CDs mobile-phase concentration, [CD], was used[16]. In this equation two conditions are assumed: 1) the complex has a 1:1 stoichiometry and 2) any interaction of the tMS / CD complexes with the stationary phase is negligible [15] as explained Jujimura *et al.,* (1986), where its $t_R$ for the CD used was nearly the same as that of potassium nitrite used as a marked for measuring the column dead volume.

$$\frac{1}{k} = \frac{1}{k_0} + \frac{K_F}{k_0}[CD] \quad (1)$$

where *k* is the capacity factor of the solute, $k_0$ is the solute capacity factor in the absence of CD, $K_F$ is the apparent formation constant of the inclusion complex and [CD] is the CD mobile-phase concentration. Values of $R^2$ close to 1 indicate a 1:1 model.

We also studied the possible formation of a 1:2 tMS / CD complex. Eq. 2 is an extension of Eq. 1 and includes a second-order term that accounts for the possibility of a 1:2 tMS / CDs complex formation[17]:

$$\frac{1}{k} = \frac{1}{k_0} + \frac{K_{F12}}{k_0}[CD]^2 \quad (2)$$

where $k_0$ is the capacity factor of tMS in the absence of CD modifier and $K_{F12}$ is the apparent formation apparent for the 1:2 tMS / CD complex. Values of $R^2$ close to 1 indicate a 1:2 model.

The column void volume, $t_0$, was determined using a reagent grade copper sulphate (0.01 mg/mL) solution [18]. The HPLC-RP method gives us an apparent $K_F$ ($K_{Fapp}$) because of methanol/CD interactions [19].

*3.2.2 Temperature studies*

To study the effect of the temperature on the encapsulation process of tMS by CD, increasing temperatures of; 288, 293, 298, 303 and 310 K (15, 20, 25, 30 and 37 ºC) were selected. The thermodynamic relationship shown in eq. 3 was used to determine the standard thermodynamic parameters: enthalpy and entropy of transfer of the tMS from the mobile phase to the CD:

$$Ln\ K_F = \frac{-\Delta H^{\circ}}{RT} + \frac{-\Delta S^{\circ}}{R} \quad (3)$$

where $K_F$ is the apparent formation constant of the inclusion complex, T is the temperature in Kelvin degrees, R is the gas constant, Δ*H*º and Δ*S*º are standard enthalpy and entropy changes of complexes formed in the mobile phase. For a linear plot of ln $K_F$ *versus* 1/T, the slope and intercept are –ΔHº/R and ΔSº/R, respectively. To determine the Gibbs free energy change for the interactions that take place during the inclusion process, we used eq. 4:

$$\Delta G^{\circ} = \Delta H^{\circ} - T\Delta S^{\circ} \quad (4)$$

*3.2.3 Solubility studies*

0.5 mL of 5mM tMS dissolved in ethanol was placed in Falcon tubes until complete evaporation leaving only tMS. Later, increasing concentrations of Mβ-CD (0, 10, 20, 25, 30, 35, 40 and 50 mM) were dissolved in a fixed 0.5 mM tMS concentration. These tubes were incubated 24 h at 14 ºC and 400 rpm using a thermomixer comfort (Eppendorf Ibérica, Madrid, Spain) to control the temperature. Then, 0.5 mL were filtered through a 0.22 μm mesh filter and 50 μL of each tube was analysed in an Agilent 1100 series HPLC system (CA,

USA) and a 1200 series module UV-VIS detector with a Kromasil 150 C18 column (Análisis Vínicos S.L.Tomelloso, Spain) (150 mm x 4,6 mm, 5µm particle size). The mobile phase flow rate was set and automatically controlled at 1.00 ± 0.01 mL/min with Methanol/Water (80/20 v/v) at different concentrations of CDs at 25 ºC. The UV detector was operated at 306 nm.

*3.2.4 Quinine quenching*

Different tubes with i) 10 µM of quinine, ii) 5 mM of Mβ-CD and iii) increasing quantities of tMS obtained from a suspension of 0.1 mg in 50 mL of pH 5.5 phosphate-sodium 0.1 M buffer were mixed vigorously. Then, the samples were incubated 24 h at 25 ºC and 400 rpm in darkness using a thermomixer comfort (Eppendorf Ibérica, Madrid, Spain) to control the temperature. The samples were filtered using 0.22 µm diameter filters. The fluorescence was measured using a Kontron SFM-25 spectrofluorimeter (Zurich, Switzer-land). The excitation and emission wavelengths for quinine were 350 nm and 450 nm, respectively. The relative fluorescence intensity values were recorded at 25 °C and pH 5.5 in a phosphate-sodium 0.1 M buffer.

*3.2.5 Molecular docking.*

The molecular structures used in this work were built using Avogadro Software [20] or were obtained by different databases. The α-CD, β-CD and γ-CD structures were extracted from the Protein Data Bank (PDB ID: 3EDD, 4RER and 5E70). tMS and Pinosylvin molecules were obtained from PubChem database (NCBI, USA). HPβ-CD and Mβ-CD were built by adding hydroxypropyl or methyl group to the β-CD. The topology of HPβ-CD and Mβ-

CD was obtained using PRODRG [21] with default parameters. Molecular docking was carried out using Autodock Vina [22] using default parameters. All CDs were considered as flexible. Graphical representations of the docking results were prepared using PyMOL (Molecular GraphicsSystem, version 1.3, Schrödinger, LLC).

### *3.2.6 Data analysis.*

All experiments were carried out in triplicate. Graphical representations were made using SigmaPlot (Version 10.0). An ANOVA and a Holm Test were applied using Rstudio (version 0.99.878) fixing the significance level at $P < 0.05$. Other mathematical operations were carried out using wxMaxima software (version 12.04.0).

## 4. Results and discussion

### 4.1 Selection of the optimal conditions to characterize the encapsulation of tMS with different CDs.

The use of CDs as additives in the mobile phases in reversed-phase high performance liquid chromatography (RP-HPLC) decreases the retention time of the guest as a result of host-guest interactions [13]. However, changes in retention are strongly dependent on factors such as flow rate due to the host-guest complex stability or the type of organic modifier. For this reason, the first step was to select the most suitable composition of the mobile phase to be used for the analysis.

The formation of CD inclusion complexes in the liquid phase proceeds more easily in an aqueous solution. However, In this analysis an aqueous-organic solvent was used because when water alone was used as mobile phase, very long retention times, with the associated experimental error and a column deterioration, were observed.

In the selection of the most appropriate organic solvent for this work, two parameters were born in mind i) the affinity of the organic modifier for the CD cavity and the solubility of CDs in the organic solvent, due their influence on the retention value, and ii) the resolution of the sample solute and the binding constant of inclusion complexes of the solute. We decide to introduce methanol in the corresponding mobile phases for the following reasons: i) the very weak association of methanol with β-CD, as represented by the low value of $K_m$, the constant which describes the affinity of the organic modifier for the CD cavity [19]. Indeed the $K_m$ value described for the interaction between methanol and β-

CD ($K_m$ = 0.32 $M^{-1}$) or α-CD ($K_m$ = 0.93 $M^{-1}$) makes it a more favourable medium for tMS-CD encapsulation process than other alcohols such as ethanol ($K_m$ for β-CD = 0.93 $M^{-1}$; $K_m$ for α-CD = 5.62 $M^{-1}$) or 1-propanol ($K_m$ for β-CD = 3.71 $M^{-1}$; $K_m$ for α-CD = 23.44 $M^{-1}$); ii) the fact that the solubility of β-CD in methanol is greater than in acetonitrile and THF permits the concentration of the β-CD in the mobile phase to be increased, thus facilitating characterization of the tMS/β-CD complexes. For these reasons, binary mixtures of methanol:water were used as the optimum composition of the mobile phase in RP-HPLC to study the encapsulation process of tMS by β-CD.

4.2 Effect of Mβ-CD on the retention time of tMS in HPLC-RP

The retention time (tR) was 75.06 +/- 3.02 min without CDs. Although *tR* could have been shortened using higher methanol concentrations, this would decrease the encapsulation efficiency. Injecting different concentrations of Mβ-CD (**Fig** 2A), tMS *tR* decreased (from 75.06 +/- 3.02 to 8.78 +/- 0.5 at 40 mM of Mβ-CD), perhaps because the encapsulation of tMS affects at the solubility of hydrophobic compounds in aqueous solutions [24].

To validate our result, we needed to confirm that the effect of CDs on the tMS *tR* was not due to the glucidic nature of the CDs, but to their ability to complex hydrophobic compounds.

Thus, different amounts of D-glucose (14 and 280 mM), corresponding to 2 and 40 mM of Mβ-CD, were added to the 60:40 (v/v) (methanol:water) mobile phase and the *tR* of tMS was ascertained. The tMS *tR* in the absence of any additive was 75.06 +/- 3.02 min. but decreased in the presence of 2 mM (59.62

+/- 2.87 min.) and 40 mM (8.78 +/- 0.5 min) Mβ-CD, whereas the addition of D-glucose did not significantly alter the retention times (74.37 min).

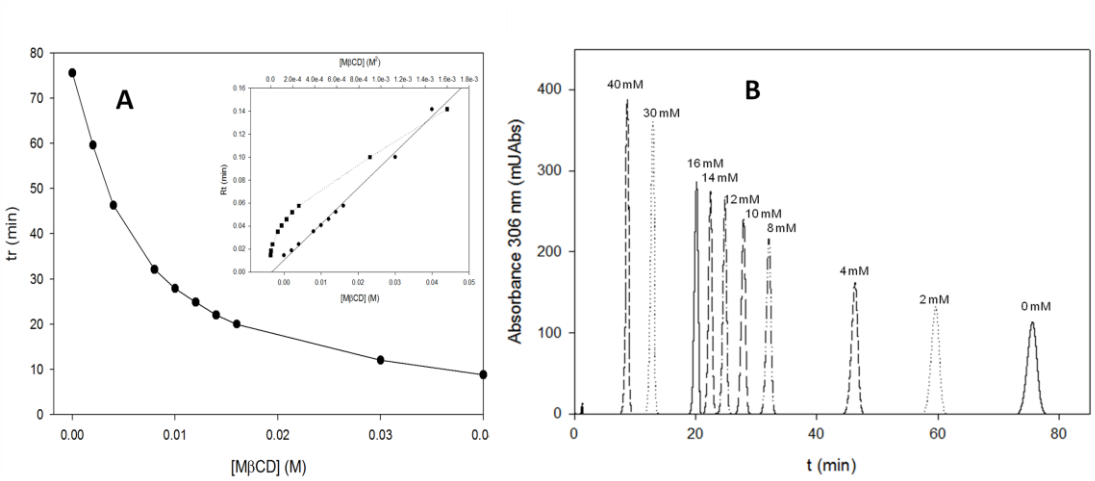


***Fig 2.*** *(A) Effect of increasing concentration of Mβ-CD on retention time of tMS (C18 column, 60:40 MeOH/water 1.5 mL/min at 25ºC). Inset: linear fit of tMS complexed with Mβ-CD to determine the stoichiometry of tMS/Mβ-CD complexes: 1/k vs [Mβ-CD] (circles, 1:1 complex) and representation of the curve fit of the1:2 complex (squares,). (B) HPLC chromatograms for increasing concentration of Mβ-CD (0-40 mM) at 25 ºC, 60/40 MeOH/Water and 1.5 mL/min in C18 column.*

As expected, the addition of CD to the mobile phase reduces the tMS *tR* due to its capacity to complex hydrophobic substances since no glucose/tMS complexes are formed.

4.3 Stoichiometry and apparent complexation constant of tMS by natural and modified CDs.

In general, knowing the $K_F$ is important for optimizing the quantity of each reactant to be added, for which reason the encapsulation process was studied with a high number of natural (α-, β- and γ-CD) and modified (HPβ-CD and Mβ-CD) CDs. Table 1 shows the different $K_{Fapp}$ (apparent $K_F$) values obtained and,

their stoichiometry (1 CD per tMS or 2 CDs per tMS) obtained using eq. 1 for a 1:1 encapsulation process or eq. 2 for a 1:2 encapsulation process (**Fig**. 2B). The highest $K_{Fapp}$ value was obtained using MβCD (298.01 +/- 15.03 $M^{-1}$). The results showed that tMS/MβCD complex has a 1:1 stoichiometry ($R^2$ > 0.99, **Fig** 2 *inset*) and not a 1:2 stoichiometry ($R^2$ ≈ 0.95, **Fig** 2A *inset*). Furthermore, the best $K_{Fapp}$ for natural CDs was β-CD followed by γ- and α-CD, all with a 1:1 stoichiometry.

**Table 1**. Experimental $K_{Fapp}$ values and correlation coefficients arising from equations (1) and (2) (for 1:1 and 1:2 *tMS/CD* complexes, respectively) at 25 ºC in C18 column and 60:40 MeOH:water; and Vina simulated binding energy.

| Type de CD | $K_{Fapp}$ ($M^{-1}$) | SD (+/-) | $R^2$ (1:1) | $R^2$ (1:2) | Binding energy (kJ/mol) |
|---|---|---|---|---|---|
| **MβCD** | 298.01 | 15.03 | 0.99 | 0.95 | -35.98 |
| **HPβCD** | 108.65 | 6.02 | 0.99 | 0.95 | -24.28 |
| **βCD** | 82.67 | 4.01 | 0.99 | 0.95 | -23.85 |
| **γCD** | 23.16 | 1.12 | 0.99 | 0.96 | -23.01 |
| **αCD** | 12.15 | 0.80 | 0.99 | 0.95 | -21.34 |

## 4.4 Effect of CD structure on complexation

In the previous section the $K_{Fapp}$ value and stoichiometry of different complexes of tMS with natural and modified CDs of differing structure, size and number of glucose units were determined. Table 1 shows the effect of adding α-, β- and γ-CD concentrations on the $K_{Fapp}$ value. As can be observed, the highest $K_{Fapp}$ was obtained with β-CD, followed by γ-CD and α-CD.

At the molecular level, our data show that the inner diameter of the CD formed by seven units of glucose (β-CD: 6.0-6.4 Å) fitted tMS better than the inner diameter of six (α-CD: 4.7-5.2 Å) or eight (γ-CD: 7.5-8.3 Å) glucose units.

The higher $K_{Fapp}$ observed for the tMS/modified CD complexes could be due to increase hydrophobicity with no steric hindrances, as a result of the long chain presented by HPβ-CD. The results were corroborated using ANOVA (for all $K_{Fapp}$s) and Holm [31] test (for pairs of $K_{Fapp}$). All the $K_{Fapp}$ values differed significantly ($P < 0.05$) except the difference between α-CD and γ-CD ($P \approx 0.1$), which might be explained by a minimal interaction between these CDs and tMS. As the strongest $K_{Fapp}$ was obtained with Mβ-CD, this was chosen as host CD for the following sections of the paper.

4.5 Increase of solubility of tMS by CDs, a direct measurement.

As mentioned above, the decrease in tMS tR with increasing CD concentration was assumed to be due to the encapsulation of tMS in the cavity of CDs, which improves solubility. However, a direct measurement of the tMS concentration in aqueous solution was carried out to confirm this hypothesis. Different aqueous solutions at a fixed tMS concentration were incubated with increasing Mβ-CD concentrations at 14 ºC for 24 h at 400 rpm. The results (**Fig** 3A) demonstrated that i) the solubility of tMS in water is negligible and ii) CD can increase the solubility of tMS to give a 1:1 complex, which is demonstrated by the linear behaviour of the diagram ($R^2 > 0.98$). Moreover, the phase-solubility reflected a negative deviation at low concentrations of Mβ-CD (below 20 mM), perhaps because very hydrophobic compounds generate dimers in

aqueous solutions until the CD concentration is sufficient to separate the dimers and so encapsulate them [25].

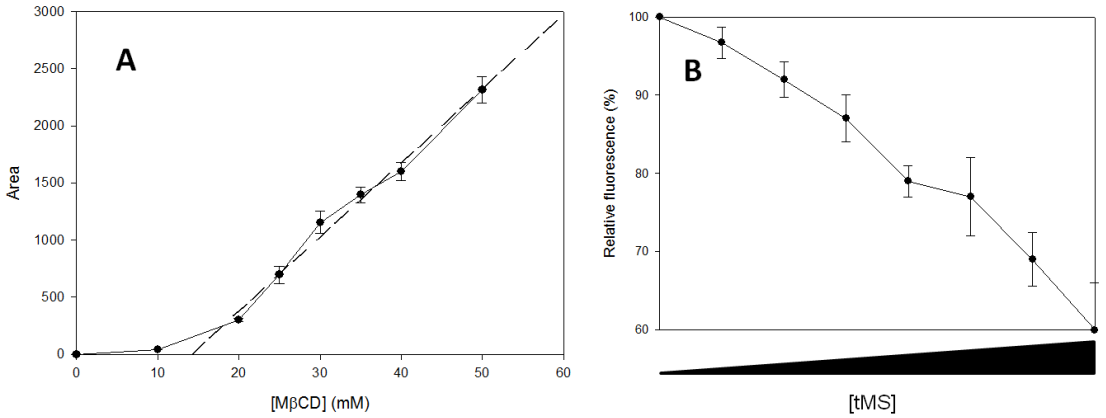


***Fig 3**. (A) Effect of increasing concentrations of Mβ-CD on tMS solubility (represented by HPLC absorbance peak area); the discontinuous line represents a linear fit. (B) Effect of tMS on quinine/Mβ-CD complex fluorescence (pH 5.5 at 25 ºC).*

4.6 tMS/Mβ-CD complex demonstrated by quinine fluorescence quenching

There is also a slight possibility that adsorption or another non-specific interaction could have occurred. For that reason, in this section the quenching of quinine, a well know CD guest [26,27], encapsulated by Mβ-CD at increasing concentrations of tMS was studied. When tMS was not present, the quinine/Mβ-CD complex showed no alteration in fluorescence (**Fig** 3B). However, when tMS was added the equilibrium was displaced and a tMS/Mβ-CD complex was formed, releasing free quinine. The decrease in the fluorescence signal was probably due to a decrease in quantum yield [28]. On the other hand, if tMS were absorbed by MβCD there would have been no differences in the signal

[29]. Hence, we can safely say that CDs increased the solubility of tMS by forming a complex.

### 4.7 Effect of temperature on complexation constant of tMS/MβCD complex

One of the most important physicochemical parameters studied in bioavailability is temperature, which is closely related, for example, with the release or integrity. For this reason, it is interesting to study the behaviour of the complex at different temperatures. **Fig** 4 shows the effect of temperature on the complexation constant. The relationship between temperature and $K_{Fapp}$ observed was inversely proportional. Applying eq 1 a stoichiometry of 1:1 was observed for all the temperatures tested, leading us to conclude that the encapsulation process is more efficient at low temperatures.

### 4.8 Thermodynamic parameters for the tMS/Mβ-CD complex

The next step of this study was to obtain the thermodynamic parameters of the encapsulation process (ΔHº, ΔSº and ΔGº at 25 ± 0.2 ºC) in order to complete the temperature study. A Van´t Hoff plot (eq. 3) showed a linear correlation ($R^2 > 0.98$, **Fig**. 4 *inset*).

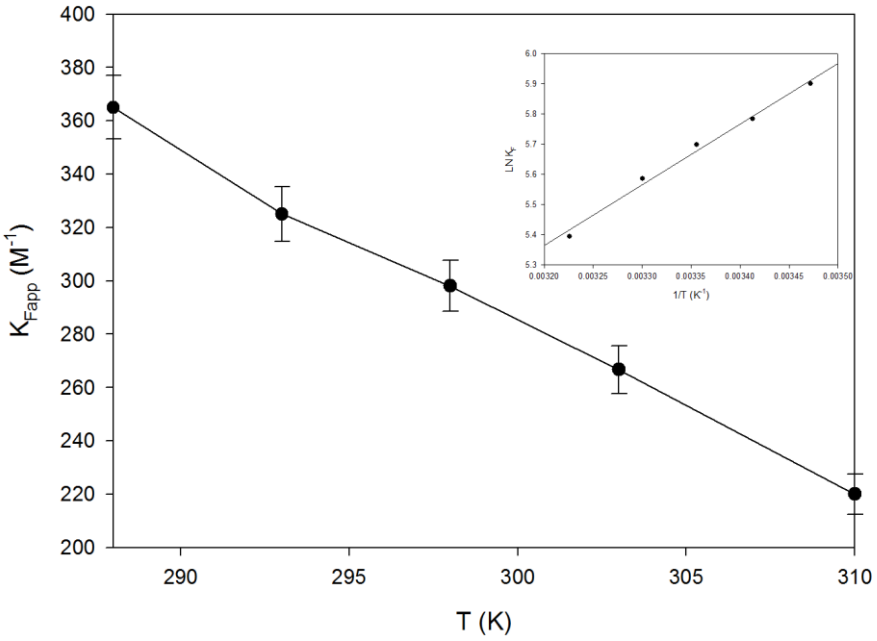


***Fig. 4.*** *Effect of temperature on the complexation constant ($K_F$) of tMS/MβCD complexes (C18 column, 60:40 MeOH/water 1.5 mL/min). Inset: Van´t Hoff plot (ln $K_F$ vs. 1/T) for tMS/MβCD complexes.*

The results led to three main conclusions being reached concerning the nature of the encapsulation process of tMS by Mβ-CD: 1) the process is *exothermic* (-16.70 +/- 0.98 kJ $mol^{-1}$). This response is typical of several changes such us hydrophobic interactions, the release of water molecules from Mβ-CD cavity or the formation of hydrogen bonds; 2) The process presents a negative entropy changes (-8.86 · $10^{-3}$ ± 0.40 · $10^{-3}$ kJ $mol^{-1}K^{-1}$) due to a decrease in the degrees of freedom of the complexes; 3) The process is *spontaneous*, as seen for the negative value obtained for the Gibbs free energy change (–14.00 ± 0.55 kJ $mol^{-1}$) for the interactions that take place during the inclusion process at 25 ± 0.2 ºC.

4.9 Molecular modelling of the complexes established between tMS and CDs.

Docking simulations were carried out to study the possible the interactions between tMS and CDs. Scoring functions are fast approximate mathematical methods used to predict the strength of the non-covalent interaction (also referred to as binding affinity) between two molecules after they have docked. Table 1 shows that the binding affinities were directly proportional to the Gibbs free energy of the encapsulation process and, thus, to the $K_{Fapp}$ values. A good correlation observed between the binding affinities and experimental values was observed. This point suggests that our modelling methodology captures the essentials of the host-guest energetic interactions.

Additionally, our experimental data might be explained using the structural information concerning the different binding poses obtained by docking (**Fig**. 5). As regards the ring size of the different CDs, the weakest interaction corresponds to the complex with α-CD, as depicted in **Fig**. 5A and γCD (**Fig**. 5C) respectively. The main reason for this was weak hydrophobic stabilisation due to the poor host-guest fit. Nevertheless, in general terms, the stability of the encapsulation process was greater with β-CD and its derivatives HPβ-CD and Mβ-CD (**Fig**.s 5B, 5D and 5E). For these CDs, the most stable combination corresponded to β-CD followed by its derivatives HPβ-CD and MβCD. The possible optimal diameter of β-CD, could explain the better $K_F$ than γ-CD. HPβ-CD provided a worse fit than Mβ-CD; perhaps because of steric hindrances between tMS and hydroxypropyl groups or the increase of polar contacts with hydroxypropyl groups; in fact, tMS almost does not enter into the cyclodextrin.

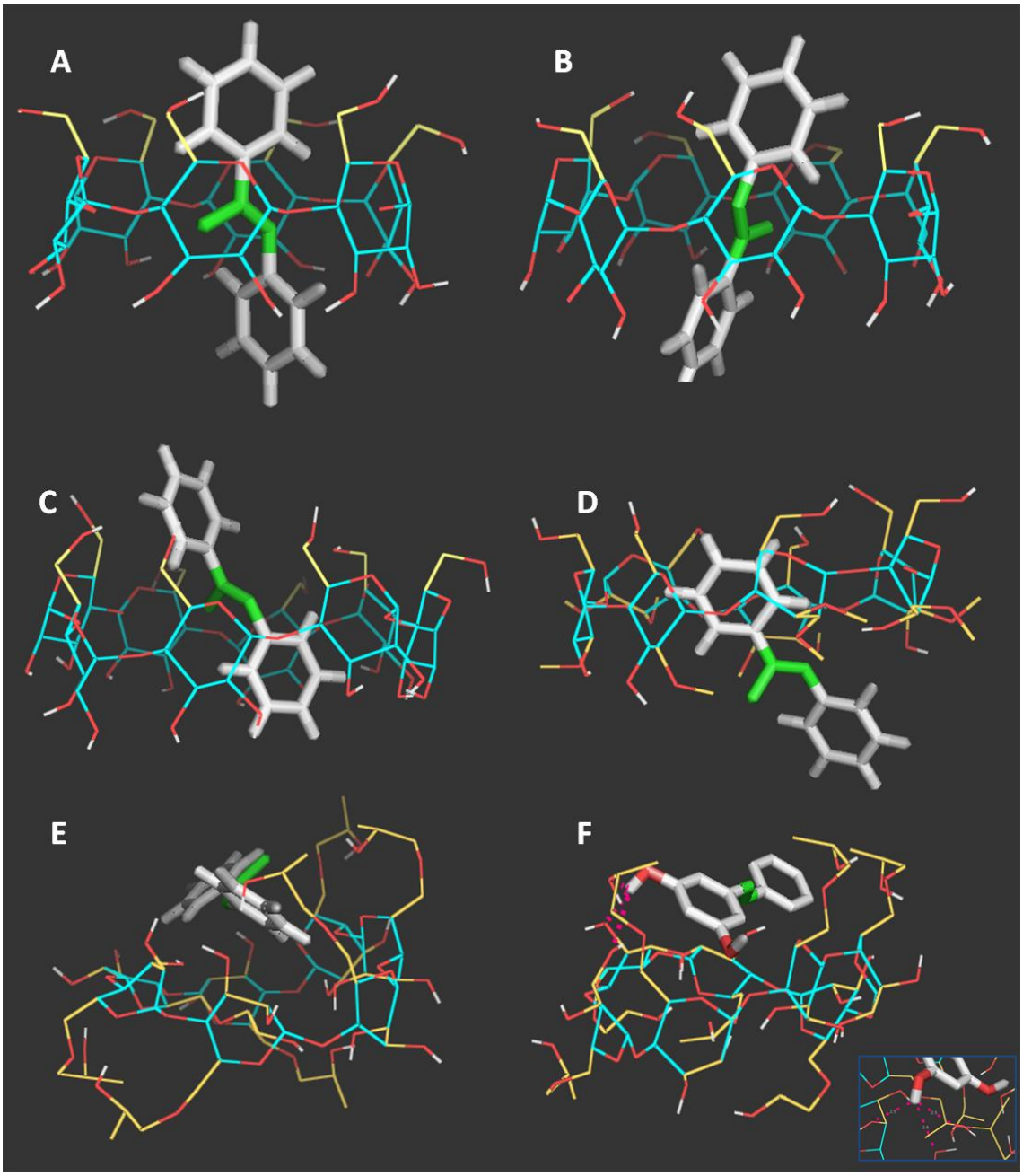


***Fig. 5.*** *Results for tMS/αCD (A), tMS/βCD (B), tMS/γCD (C), tMS/MβCD (D), tMS/HPβCD (E) Pinosylvin/HPβCD (F) with the hydrogen bond in magenta (Inset, Hydrogen bonds donor-acceptor distances 2.5, 2.6 and 2.5 Å). Flexible atoms are coloured pale-yellow.*

## 4.10 Comparative study of tMS, trans stilbene and pinosylvin encapsulation process with HPβ-CD

Previous to this thesis, many complexes of stilbenes with CDs were studied by this research group. The slight differences observed between stilbenes (hydroxyl groups, methyls, etc.) led us to compare their $K_F$ values. For that reason, we compared the complexation of HPβCD with tMS, trans-stilbene [33] and pinosylvin [34], whose structures are depicted in **Fig** 1.

One obvious detail is that tMS ($K_{Fapp}$ = 108.65 +/- 6.02 $M^{-1}$) and pinosylvin ($K_F$ = 12112 +/-761 $M^{-1}$) have a 1:1 stoichiometry whereas trans-stilbene ($K_{F12}$ = 1.01 · $10^9$ +/- 0.67 · $10^6$ $M^{-2}$) has 1:2 stoichiometry, perhaps because any substituent in the structure affects the fitting with two CDs. If we try to compare the experimental $K_F$ values of tMS and Pinosylvin, we will make a mistake due to the apparent value of tMS $K_F$ (Pinosylvin was studied using a fluorescence technique, which provides a real $K_F$). However, we could carry out a computational study. The binding energy for tMS/HPβ-CD (-24.28 kJ/mol, **Fig** 5E) was far lower than Pinosylin/HPβ-CD (-33.47 kJ/mol, **Fig** 5F), perhaps due to the existence of hydrogen bonds in the pinosylvin/HPβ-CD complex, hydrogen bonds is one of the most important types of interaction for the stabilization of inclusion complexes of guest molecules with CDs [35,36]. Furthermore, a better fit was obtained for the simulation of Pinosylvin, helping the stabilization.

In summary, in this chapter we propose using CDs to increase the solubility of tMS in aqueous solution. Our results show that, although the stoichiometry of the complex is 1:1 for all the conditions used, the best $K_F$ values obtained for

the CDs tested was for Mβ-CD which was chosen for the study. Furthermore the $K_{Fapp}$ values for the tMS/CD complexes are strongly dependent on several factors, such as temperature, type of CD and structure of the guest molecule. For example, an inverse relationship between temperature and $K_F$ was observed.

Moreover, the results showed negative entropy ($-8.86 \cdot 10^{-3} \pm 0.40$ kJ mol$^{-1}$K$^{-1}$) and enthalpy (-16.70 +/- 0.98 kJ mol$^{-1}$) changes and a negative Gibbs free energy value at 25ºC (–14.00 ± 0.55 kJ mol$^{-1}$) for the encapsulation process. A computational study carried out using molecular docking calculations showed a high degree of correlation between the computed binding affinities and the experimental values. The same numerical order of the complexation was predicted. Finally, a comparison between tMS, trans-stilbene and pinosylvin encapsulation process with HPβ-CD was carried out finding that any modification of the stilbene structure affected the complexation.

## References

[1] G. Berti, F. Bottari, B. Macchia, The direction of ring opening of trans-α-methylstilbene oxide by organic acids, Tetrahedron. 20 (1964) 545–550. doi:10.1016/S0040-4020(01)98616-8.

[2] X. Quan, V.S. Parihar, M. Bera, P.G. Andersson, Iridium Catalysts with Chiral Bicyclic Pyridine–Phosphane Ligands for the Asymmetric Hydrogenation of Olefins, Eur. J. Org. Chem. 2014 (2014) 140–146. doi:10.1002/ejoc.201301141.

[3] K.M. Kasiotis, H. Pratsinis, D. Kletsas, S.A. Haroutounian, Resveratrol and related stilbenes: their anti-aging and anti-angiogenic properties, Food Chem. Toxicol. Int. J. Publ. Br. Ind. Biol. Res. Assoc. 61 (2013) 112–120. doi:10.1016/j.fct.2013.03.038.

[4] Pubchem, AID 248 - NCI In Vivo Anticancer Drug Screen. Data for tumor model L1210 Leukemia (intraperitoneal) in B6D2F1 (BDF1) mice - PubChem, (2016). https://pubchem.ncbi.nlm.nih.gov/bioassay/248#section=Data-Table (accessed November 3, 2016).

[5] Pubchem, alpha-Methylstilbene Biological Test Results, (2016). https://pubchem.ncbi.nlm.nih.gov/compound/1549166#section=Biological-Test-Results (accessed November 3, 2016).

[6] C.M. Bernards, Effect of (hydroxypropyl)-β-cyclodextrin on flux of morphine, fentanyl, sufentanil, and alfentanil through the spinal meninges of monkey, J. Pharm. Sci. 83 (1994) 620–622. doi:10.1002/jps.2600830504.

[7] L. Szente, J. Szejtli, Cyclodextrins as food ingredients, Trends Food Sci. Technol. 15 (2004) 137–142. doi:10.1016/j.tifs.2003.09.019.

[8] E.M.M. Del Valle, Cyclodextrins and their uses: a review, Process Biochem. 39 (2004) 1033–1046. doi:10.1016/S0032-9592(03)00258-9.

[9] J.M. López-Nicolás, P. Rodríguez-Bonilla, F. García-Carmona, Cyclodextrins and Antioxidants, Crit. Rev. Food Sci. Nutr. 54 (2014) 251–276. doi:10.1080/10408398.2011.582544.

[10] A. Matencio, C.J.G. Hernández-Gil, F. García-Carmona, J.M. López-Nicolás, Physicochemical, thermal and computational study of the encapsulation of rumenic acid by natural and modified cyclodextrins, Food Chem. 216 (2017) 289–295. doi:10.1016/j.foodchem.2016.08.023.

[11] N. Vilanova, C. Solans, Vitamin A Palmitate–β-cyclodextrin inclusion complexes: Characterization, protection and emulsification properties, Food Chem. 175 (2015) 529–535. doi:10.1016/j.foodchem.2014.12.015.

[12] A. Matencio, F. García-Carmona, J.M. López-Nicolás, Encapsulation of piceatannol, a naturally occurring hydroxylated analogue of resveratrol, by natural and modified cyclodextrins, Food Funct. 7 (2016) 2367–2373. doi:10.1039/c6fo00557h.

[13] J.M. López-Nicolás, M. Escorial Camps, H. Pérez-Sánchez, F. García-Carmona, Physicochemical and Thermodynamic Characterization of the Encapsulation of Methyl Jasmonate by Natural and Modified Cyclodextrins Using Reversed-Phase High-Pressure Liquid Chromatography, J. Agric. Food Chem. 61 (2013) 11347–11354. doi:10.1021/jf402920p.

[14] A. Matencio, M.J. Bermejo-Gimeno, F. García-Carmona, J.M. López-Nicolás, Separating and Identifying the Four Stereoisomers of Methyl Jasmonate by RP-HPLC and using Cyclodextrins in a Novel Way, Phytochem. Anal. (2016) n/a-n/a. doi:10.1002/pca.2654.

[15] K. Fujimura, T. Ueda, M. Kitagawa, H. Takayanagi, T. Ando, Reversed-phase retention behavior of aromatic compounds involving .beta.-cyclodextrin inclusion complex formation in the mobile phase, Anal. Chem. 58 (1986) 2668–2674. doi:10.1021/ac00126a020.

[16] J.M. López-Nicolás, E. Núñez-Delicado, A.J. Pérez-López, A.C. Barrachina, P. Cuadra-Crespo, Determination of stoichiometric coefficients and apparent formation constants for beta-cyclodextrin complexes of trans-resveratrol using reversed-phase liquid chromatography, J. Chromatogr. A. 1135 (2006) 158–165. doi:10.1016/j.chroma.2006.09.013.

[17] C. Moeder, T. O'Brien, R. Thompson, G. Bicker, Determination of stoichiometric coefficients and apparent formation constants for α- and β-CD complexes of terpenes using reversed-phase liquid chromatography, J. Chromatogr. A. 736 (1996) 1–9. doi:10.1016/0021-9673(95)01276-1.

[18] I. Clarot, D. Clédat, S. Battu, P.J. Cardot, Chromatographic study of terpene derivatives on porous graphitic carbon stationary phase with beta-cyclodextrin as mobile phase modifier, J. Chromatogr. A. 903 (2000) 67–76.

[19] Y. Matsui, K. Mochida, Binding Forces Contributing to the Association of Cyclodextrin with Alcohol in an Aqueous Solution, Bull. Chem. Soc. Jpn. 52 (1979) 2808–2814.

[20] M.D. Hanwell, D.E. Curtis, D.C. Lonie, T. Vandermeersch, E. Zurek, G.R. Hutchison, Avogadro: an advanced semantic chemical editor, visualization, and analysis platform, J. Cheminformatics. 4 (2012) 17. doi:10.1186/1758-2946-4-17.

[21] A.W. Schüttelkopf, D.M.F. van Aalten, PRODRG: a tool for high-throughput crystallography of protein-ligand complexes, Acta Crystallogr. D Biol. Crystallogr. 60 (2004) 1355–1363. doi:10.1107/S0907444904011679.

[22] O. Trott, A.J. Olson, AutoDock Vina: improving the speed and accuracy of docking with a new scoring function, efficient optimization, and multithreading, J. Comput. Chem. 31 (2010) 455–461. doi:10.1002/jcc.21334.

[23] M.E. Juan, R.M. Lamuela-Raventós, M.C. de la Torre-Boronat, J.M. Planas, Determination of trans-resveratrol in plasma by HPLC, Anal. Chem. 71 (1999) 747–750.

[24] P. Rodríguez-Bonilla, J.M. López-Nicolás, F. García-Carmona, Use of reversed phase high pressure liquid cromatography for the physicochemical and thermodynamic characterization of oxyresveratrol/β-cyclodextrin complexes, J. Chromatogr. B. 878 (2010) 1569–1575. doi:10.1016/j.jchromb.2010.04.016.

[25] T. Loftsson, D. Hreinsdóttir, M. Másson, Evaluation of cyclodextrin solubilization of drugs, Int. J. Pharm. 302 (2005) 18–28. doi:10.1016/j.ijpharm.2005.05.042.

[26] Z. Fan, C.-H. Diao, H.-B. Song, Z.-L. Jing, M. Yu, X. Chen, M.-J. Guo, Encapsulation of Quinine by β-Cyclodextrin: Excellent Model for Mimicking Enzyme−Substrate Interactions, J. Org. Chem. 71 (2006) 1244–1246. doi:10.1021/jo052183j.

[27] X.-M. Wang, H.-Y. Chen, Investigation of the β-cyclodextrin-quinine inclusion complex in aqueous solution by spectroscopic study, Spectrochim. Acta. A. Mol. Biomol. Spectrosc. 51 (1995) 333–339. doi:10.1016/0584-8539(94)00137-Z.

[28] M. Hoshino, M. Imamura, K. Ikehara, Y. Hama, Fluorescence enhancement of benzene derivatives by forming inclusion complexes with .beta.-cyclodextrin in aqueous solutions, J. Phys. Chem. 85 (1981) 1820–1823. doi:10.1021/j150613a012.

[29] T. Kuwabara, A. Nakamura, A. Ueno, F. Toda, Inclusion Complexes and Guest-Induced Color Changes of pH-Indicator-Modified .beta.-Cyclodextrins, J. Phys. Chem. 98 (1994) 6297–6303. doi:10.1021/j100076a011.

[30] D.W. Armstrong, S.M. Han, Y.I. Han, Separation of optical isomers of scopolamine, cocaine, homatropine, and atropine, Anal. Biochem. 167 (1987) 261–264. doi:10.1016/0003-2697(87)90161-8.

[31] S. Holm, A Simple Sequentially Rejective Multiple Test Procedure, Scand. J. Stat. 6 (1979) 65–70.

[32] J.M. López-Nicolás, R. Bru, A. Sánchez-Ferrer, F. García-Carmona, Use of “soluble lipids” for biochemical processes: linoleic acid-cyclodextrin inclusion complexes in aqueous solutions., Biochem J. 308 (1995) 151–154.

[33] J.M. López-Nicolás, P. Rodríguez-Bonilla, L. Méndez-Cazorla, F. García-Carmona, Physicochemical study of the complexation of pterostilbene by natural and modified cyclodextrins, J. Agric. Food Chem. 57 (2009) 5294–5300. doi:10.1021/jf900285e.

[34] J.M. López-Nicolás, P. Rodríguez-Bonilla, F. García-Carmona, Complexation of pinosylvin, an analogue of resveratrol with high antifungal and antimicrobial activity, by different types of cyclodextrins, J. Agric. Food Chem. 57 (2009) 10175–10180. doi:10.1021/jf902519d.

[35] W.L. Hinze, Applications of Cyclodextrins in Chromatographic Separations and Purification Methods, Sep. Purif. Rev. 10 (1981) 159–237. doi:10.1080/03602548108066011.

[36] W. Saenger, Cyclodextrin Inclusion Compounds in Research and Industry, Angew. Chem. Int. Ed. Engl. 19 (1980) 344–362. doi:10.1002/anie.198003441.

# Block I part II

# Chapter III

# Characterization of Oxyresveratrol inclusion complexes

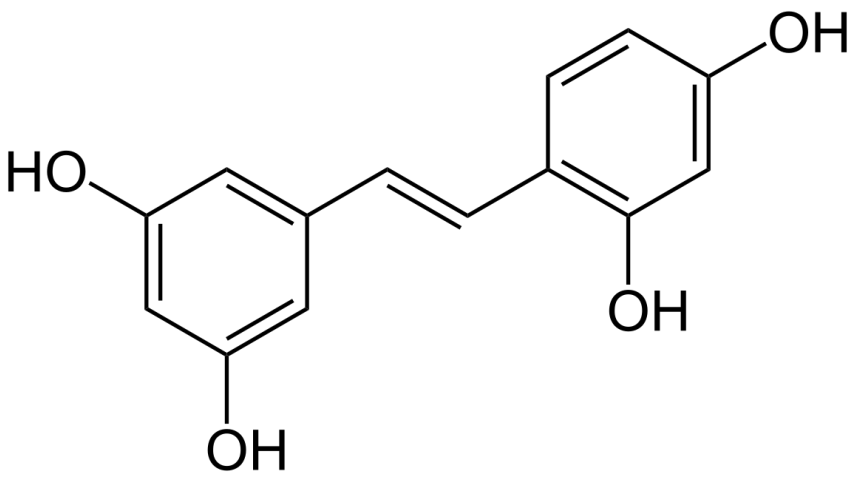

**Abstract**

The interaction between oxyresveratrol (a type of stilbene with high biological activity) and modified cyclodextrins (CDs) was studied. Using HPLC-RP was seen to form a 1:1 complex with all the CDs tested. The best CD in this respect was Mβ-CD ($K_F$ = 606.65 +/- 30.18 $M^{-1}$). The complexation showed a strong dependence on pH and temperature: The complexation constant ($K_F$) decreased as the pH and temperature increased. The thermodynamic parameters studied (ΔHº, ΔSº and ΔGº) showed negative entropy, enthalpy and Gibbs free energy change at 25 ºC.

In addition, fluorescence signal of oxyresveratrol increased when Mβ-CD was added. The oxyresveratrol emission and excitation spectra were obtained for first time. A $^1$H-NMR was carried out to study the structure of the complex and, DSC studied demonstrated the complexation. A computational study by molecular docking was made to complement the structural study.

## Index

## 1. Contextualization

Oxyresveratrol (*trans*-3,5,2′,4′-tetrahydroxystilbene, OXY, **Fig**. 1A) a stilbenoid presents in mulberry fruits (*Morus alba* L.) and twigs is a naturally occurring resveratrol (3,5,4′-trihydroxy-trans-stilbene) analogue with an additional hydroxyl group in the aromatic ring (**Fig** 1A). A recent review [1] is about its pharmacological properties: including a wide range of biological activities, such as antioxidant, antiviral, anti-inflammation, anti-obesity, cholesterol lowering, hepato- and neuroprotection and photo-protective effects . Futhermore, OXY presents cyclooxygenase and tyrosinase-inhibitory activities. Indeed, OXY has demonstrated great potential in several pre-clinical studies [2,3].

Despite all these health-related properties, several problems related with the chemical properties of OXY prevent its use as a fortifier of nutraceutical or functional foods. This bioactive molecule presents low solubility in aqueous solutions, poor bioavailability and is easily oxidized, making it necessary to seek new strategies to improve its solubility, bioavailability and resistance to oxidation. In this chapter we analyzed the encapsulation of OXY by cyclodextrins (CDs).

## 2. Objectives

1) To determine the effect of temperature and pH on the encapsulation mechanism of OXY.

2) To study the effect of the addition of CDs on OXY fluorescence behavior.

3) To determine the stoichiometry, $K_F$ values and thermodynamic parameters for the OXY-CD complexes.

4) To study the physical interactions between OXY and CD using NMR and molecular docking.

## 3. Materials and methods.

### 3.1 Materials

Hydroxypropyl-beta- and methyl-beta-cyclodextrin (HPβ-CD and Mβ-CD) were purchased from Carbosynth (Berkshire, UK). Oxyresveratrol was purchased from Sigma-Aldrich (Madrid, Spain) and used as received. The samples were stored in darkness. Methanol (HPLC grade) was purchased from Fisher (Madrid, Spain). MQ water was obtained using a Milli-Q Advantage A10 system by Merck Millipore (Madrid, Spain). Binary mixtures of water/methanol were used without further purification.

### 3.2 Equipment and Experimental Procedure

#### *3.2.1 Inclusion complex characterization.*

The methodology was used as Rodriguez-Bonilla et al., (2010) said, with slight modifications as follows: 0.5 μL of OXY (0.01 g/mL in Methanol) was injected in an Agilent 1100 series HPLC system (CA, USA) and a 1200 series module UV-VIS detector with a Kromasil 150 C18 column (Análisis Vínicos S.L.Tomelloso, Spain) (150 mm x 4,6 mm, 5μm particle size). The flow rate was set and automatically controlled at 1.00 ± 0.01 mL/min with Methanol/Water (30/70 v/v - pH 7 20 mM Tris-HCl) with different concentrations of CDs at 25 ºC. The UV detector was operated at 328 nm [4].

To determine the complexation constant ($K_F$) value for the OXY / CD complexes, Eq. 1, which relates the capacity factor, *k*, and the CDs mobile-phase concentration, [CD], was used. In this equation two conditions are

assumed: 1) the complex has a 1:1 stoichiometry and 2) any interaction of the OXY / CD complexes with the stationary phase is negligible [5].

$$\frac{1}{k} = \frac{1}{k_0} + \frac{K_F}{k_0}[CD] \quad (1)$$

where *k* is the capacity factor of the solute, $k_0$ is the solute capacity factor in the absence of CD, $K_F$ is the apparent formation constant of the inclusion complex and [CD] is the CD mobile-phase concentration. Values of $R^2$ close to 1 indicate a 1:1 model.

Eq. 2 is an extension of Eq. 1 and includes a second-order term that accounts for the possibility of a 1:2 OXY / CDs complex formation [6]:

$$\frac{1}{k} = \frac{1}{k_0} + \frac{K_{F12}}{k_0}[CD]^2 \quad (2)$$

where $k_0$ is the capacity factor of OXY in the absence of CD modifier and $K_{F12}$ is the apparent formation apparent for the 1:2 OXY / CD complex. Values of $R^2$ close to 1 indicate a 1:2 model. The column void volume, $t_0$, was determined using a reagent grade copper sulphate solution (0.01 mg/mL). The HPLC-RP method gives an apparent $K_F$ ($K_{Fapp}$) due to the methanol/CD interactions that take place [7].

### *3.2.2 Temperature and pH*

To study the effect of the temperature on the encapsulation process of OXY by CD, increasing temperatures of; 288, 293, 298, 303 and 313 K (15, 20, 25, 30 and 40 ºC) were selected. The thermodynamic relationship shown in eq. 3 was used to determine the standard thermodynamic parameters: enthalpy and entropy of transfer of the OXY from the mobile phase to the CD:

$$Ln\ K_F = \frac{-\Delta H^{\circ}}{RT} + \frac{-\Delta S^{\circ}}{R} \quad (3)$$

where $K_F$ is the apparent formation constant of the inclusion complex, T is the temperature in Kelvin degrees, R is the gas constant, $\Delta H^{o}$ and $\Delta S^{o}$ are standard enthalpy and entropy changes of complexes formed in the mobile phase. For a linear plot of ln $K_F$ *versus* 1/T, the slope and intercept are $-\Delta H^{o}/R$ and $\Delta S^{o}/R$, respectively. To determine the Gibbs free energy change for the interactions that take place during the inclusion process, we used eq. 4:

$$\Delta G^{\circ} = \Delta H^{\circ} - T\Delta S^{\circ} \quad (4)$$

For the pH studies, the same method as that explained in the previous section was used at pH 7, 9 and 10 using i) pH 7 20 mM Tris-HCl and ii) pH {9-10} 20 mM Borate-phosphate buffers.

### *3.2.3 Differential scanning microcalorimetry (DSC).*

Thermograms were measured using a Microcal VP Differential Scanning Calorimeter (VP-DSC, Microcal, Northampton, MA, USA). Reference buffer (pH 7 0.05 M sodium-phosphate buffer at 1% of MeOH) with 100 μM OXY, 8 mM MβCD or a mixture of both were degassed under vacuum for 10 min before loading in the corresponding calorimeter cell (0.5 ml approximately each).

After 10 min of equilibration time at the star temperature, the samples were heated from 10 to 140 ºC at a rate of 1 ºC/min with a filtering period of 10 seconds and a High Feedback Gain mode. Cooling scans were also recorded in the same conditions. The Origin 5.0 software package supplied by Microcal was

used for data collection and analysis. Cp values were measured with respect to the reference cell (which contained reference buffer).

### *3.2.4 Fluorescence study*

A Shimazdu RF-6000 spectrofluorimeter (Shimadzu, Kyoto, Japan) equipped with thermostatically controlled cells was used to obtain its fluorescence spectra. Excitation and emission bandwidths were both set at 5 nm. The excitation and emission wavelengths for OXY were 288 nm and 400 nm, respectively. The relative fluorescence intensity values were recorded at 25 ºC. To avoid inner filter effects, 2-mm quartz cells were used. The concentration of OXY was fixed at 25 µM and the CD concentration varied between 0 and 20 mM. All reagents were dissolved in pH 7 0.1 M sodium-phosphate buffer.

### *3.2.5 Proton and Carbon nuclear magnetic resonance spectroscopy and Nuclear Overhauser effect spectroscopy (NOESY)*

OXY (2 mg) and Mβ-CD (40mg) were added to 0.6mL of $D_2O$/DMSO (85/15 v/v). Nuclear magnetic resonance was measured using a Bruker Avance 600MHz (Bruker, Germany) in 5 mm tubes. Chemical Shifts (δ) were reported as ppm and referenced to $D_2O$ (for $^{1}$H-NMR and NOESY) and DMSO (for $^{13}$C-NMR). Mixing and delay times of the NOESY test were 1.00 and 1.70 s, respectively.

### *3.2.6 Molecular docking*

The molecular structures used in this work were built using Avogadro Software (version 2.3.2) or were obtained by different databases. MβCD were built by adding methyl group to a β-CD obtained from the Protein Data Bank

(PDB ID: 4RER). OXY molecule was downloaded from the PubChem database (NCBI, USA). Input files for docking were generated using Autodock tools (version 1.5.6) with default parameters and charges. Molecular docking was carried out using Autodock Vina [8] using default parameters. MβCD was considered as flexible. Graphical representations of the docking results were prepared using PyMOL (Molecular GraphicsSystem, version 1.3, Schrödinger, LLC) with default parameters to display hydrogen bonds.

*3.2.7 Data analysis.*

The NMR experiments were carried out once, while the remaining experiments were carried out in triplicate. Graphical representations were made using SigmaPlot (Version 10.0). A t-test was applied using Rstudio (version 0.99.878) fixing the significance level at $P < 0.05$. Other mathematical operations were carried out using wxMaxima software (version 12.04.0).

## 4. Results and discussion

### 4.1 The presence of Mβ-CD affects the retention time of OXY in HPLC-RP

As our research group previously established the optimal conditions for studing the encapsulation of OXY with natural CDs [4] so, the same conditions were used here. The first step was to obtain the retention time (tR) of OXY without CDs, the results were 16.98 +/- 0.85 min Although retention time (*tR*) could have been shortened using higher methanol concentrations, this would have decreased the encapsulation efficiency [4]. When the injection of OXY was tested with increasing concentrations of Mβ-CD (**Fig** 1B) *tR* decreased (from 16.98 +/- 0.85 to 3.14 +/- 0.17 at 12 mM of Mβ-CD), perhaps because the encapsulation of OXY affects its *tR*.

To confirm that the reduction the OXY retention time was not due to the presence of D-glucose (component of CDs) in the reaction it is necessary to dismiss any adsorption of OXY to the CD instead of complex formation. Thus, different amounts of D-glucose (14 and 84 mM), corresponding to 2 and 12 mM of Mβ-CD (each molecule of Mβ-CD contains seven units of D-glucose in a ring), were added to the 30:70 (v/v) (methanol:water) mobile phase and the *tR* of OXY was ascertained. It was found that in the absence of any additive OXY *tR* was 16.58 +/- 0.95min but decreased in the presence of 2 mM (7.52 +/- 0.35 min.) and 12 mM (3.2 +/- 0.16 min) MβCD, whereas the addition of D-glucose did not significantly alter the retention times (16.6 min.).

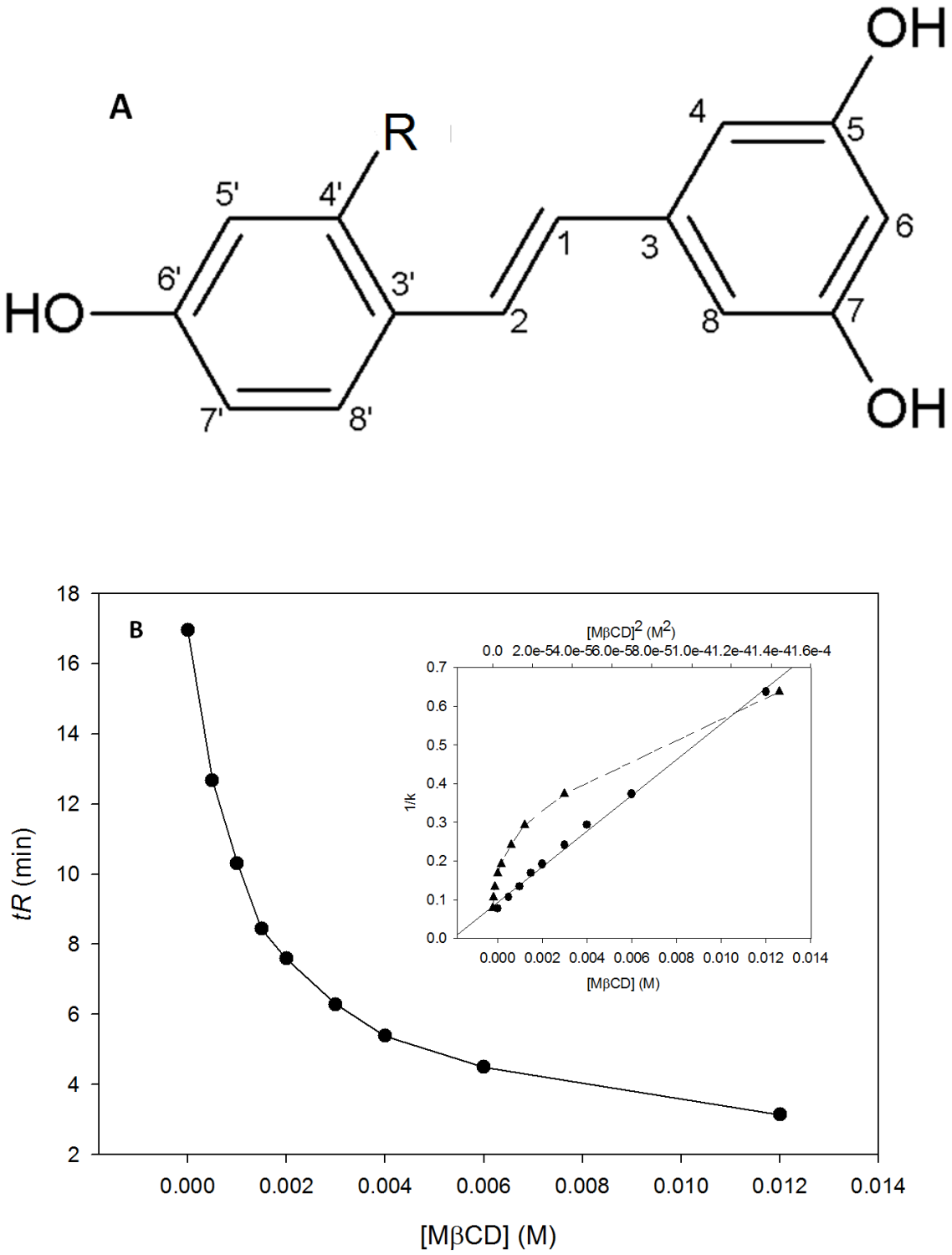


***Fig 1**. (A) Structure of Oxyresveratrol (R = -OH) or Resveratrol (R = -H). (B) Effect of increasing concentration of MβCD on retention time of OXY (C18 column, 30:70 MeOH/water 1.0 mL/min at 25ºC). Inset: linear fit of OXY complexed with MβCD to determine the stoichiometry of OXY/MβCD complexes: 1/k vs*

These results suggest that, firstly, the *tR* is reduced by the addition of CD to the mobile phase due to its capacity to complex OXY. And secondly, A variation on solvent strength cannot justify the elution modification of OXY.

4.2 Stoichiometry and apparent complexation constant of OXY by modified CDs

The inclusion complexes of OXY with natural CDs were previously characterized [4]; however, natural CDs are not the most useful for clinical cases due to their intravenous toxicity, among other reasons [9,10]. For this reason the encapsulation process was studied with modified CD such as HPβ-CD and Mβ-CD, both of which are widely used in the nutraceutical industry [11–14]. Table 1 shows the different $K_F$ (apparent $K_F$) values obtained and, their stoichiometry (1 CD per OXY or 2 CDs per OXY) obtained using eq 1 for a 1:1 encapsulation process or eq 2 for a 1:2 process. The highest $K_F$ value was obtained using Mβ-CD (606.65 +/- 30.18 $M^{-1}$). The results showed that the OXY/Mβ-CD complex has a 1:1 stoichiometry ($R^2 > 0.99$, **Fig** 1B *inset*) and not a 1:2 stoichiometry ($R^2 \approx 0.89$, **Fig** 1B *inset*).

At the molecular level, the previous work of our research group showed that the inner diameter of the CD formed by seven units of glucose (β-CD: 6.0-6.4 Å) fitted OXY better than the inner diameter of six (α-CD: 4.7-5.2 Å) or eight (γ-CD: 7.5-8.3 Å) glucose units.

Table 1. Apparent $K_F$ values and correlation coefficients for OXY/CD complexes at 25 °C and pH 7 in a methanol:water (30:70%) medium.

| Complex | $K_F$ ($M^{-1}$) | SD (+/-) | 1:1 model | 2:1 model | Pass t-test? (P≤0.05) |
|---|---|---|---|---|---|
| **OXY/Mβ-CD** | 606.65 | 30.18 | 0.99 | 0.89 | Yes |
| **OXY/HPβ-CD** | 435.53 | 21.78 | 0.99 | 0.87 | Yes |
| **OXY/β-CD*** | 590.00 | 23.00 | 0.99 | 0.86 | - |

* Obtained from Rodriguez-Bonilla *et al.;* (2010), It was not possible to obtain the $K_F$ of OXY with α- and γ-CD due to the low encapsulation efficiency.

The higher $K_F$ observed for the OXY/Mβ-CD complex could be due to the absence of steric hindrances, as a result of the long chain presented by HPβ-CD, or any alteration due to methanol [7]. Furthermore, a slight difference was found between the previously reported OXY/β-CD and OXY/Mβ-CD complexes. A t-test was used to check the results with modified CDs; this result was significant ($P \leq 0.05$). As the highest $K_F$ with modified CD was obtained with Mβ-CD, this was chosen as host CD for the following series of experiments.

## 4.3 Effect of temperature on complexation constant of the OXY/Mβ-CD complex

### *4.3.1 HPLC analysis.*

The effect of temperature is an interesting variable to study because the release or the stability of complexes or drugs could be affected. **Fig** 2A shows the effect of temperature on the complexation constant. An inverse relationship between temperature and $K_F$ was observed. By applying eq. 3, a stoichiometry of 1:1 was observed for all the temperatures tested, leading us to conclude that the encapsulation process is more efficient at low temperatures.

*4.3.2 DSC determination*

DSC can be used for the recognition of inclusion complexes. When guest molecules were embedded into CD cavities, their melting, boiling or sublimating points generally shifted to different temperature or disappear [15]. **Fig** 2B showed the DSC results for a) OXY, b) Mβ-CD and c) the OXY/Mβ-CD complex. The endothermics peaks centred at 118 ºC and 115 ºC in OXY and Mβ-CD respectively could be due to a conformational change of OXY [16] and the loss of solvation water from the Mβ-CD cavity [17]. On the other hand, the inflection point close to 103 ºC for MβCD is reached before in the OXY/MβCD complex; furthermore, the peak of sample “a” (OXY) and the drastic changed at 120 ºC disappeared, demonstrating an endothermic behavior. The results evidenced that OXY was protected into the cavity of the Mβ-CD.

4.4 Thermodynamic parameters for the OXY/Mβ-CD complexes

To further study the affinity of OXY for Mβ-CD the principal thermodynamic parameters of the complexation process (***ΔHº, ΔSº*** and ***ΔGº*** at 25 ± 0.2 ºC) was analysed a van´t Hoff plot (eq. 3) and plotting the Ln $K_F$ *vs* 1/T. The lineal behavior of the data was accompanied by a correlation coefficient > 0.99 (**Fig**. 2A *inset*).

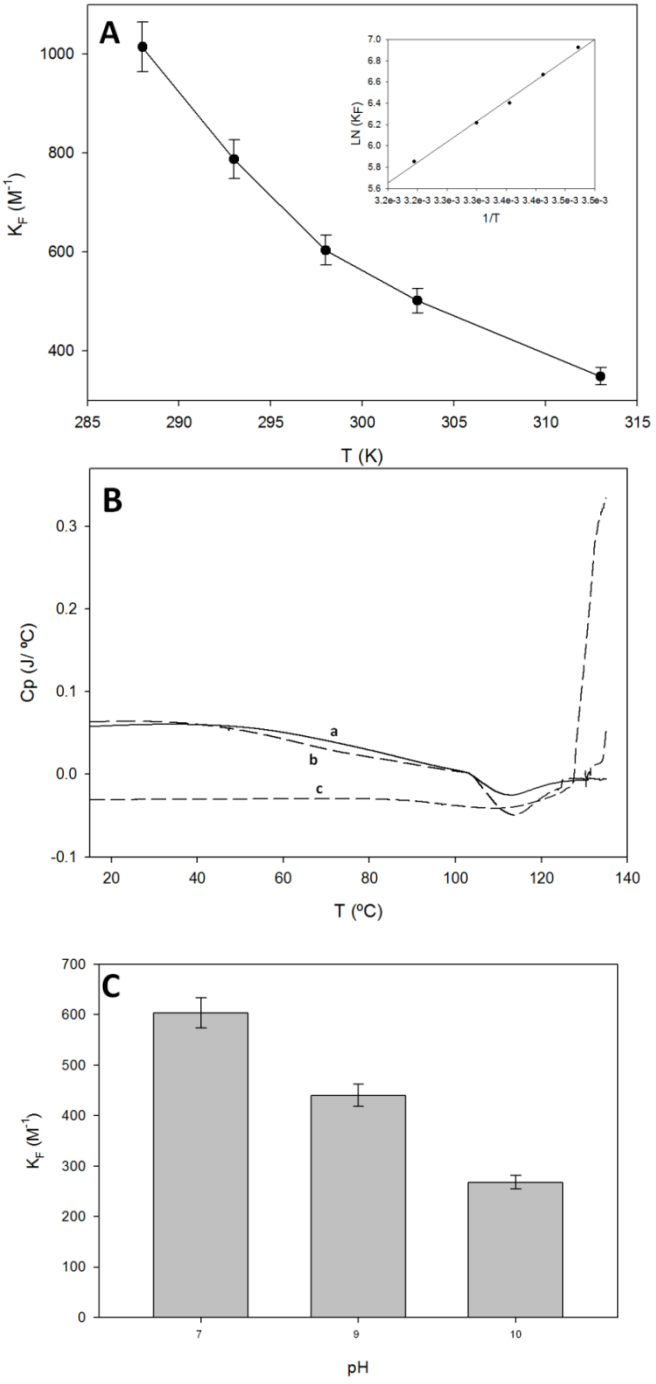


***Fig 2. (A)*** *Effect of temperature on the complexation constant ($K_F$) of OXY/MβCD complexes (C18 column, 30:70 MeOH/water 1.0 mL/min). Inset: Van´t Hoff plot (ln KF vs. 1/T) for OXY/MβCD complexes. (**B**) Thermograms of (a) OXY, (b) MβCD and (c) OXY/MβCD complex. (**C**)Effect of pH on the complexation constant (KF) of OXY/MβCD complexes (C18 column, 30:70 MeOH/water 1.0 mL/min)*

The main conclusions reached concerning the complexation of OXY by Mβ-CD were that the process is *exothermic*, spontaneous and shows negative Gibbs free energy. The negative values obtained for the enthalpy changes (–31.99 +/- 1.59 KJ $mol^{-1}$) confirm the exothermic nature of the interaction of OXY with Mβ-CD behavior that is typical of hydrophobic interactions, van der Waals interactions, the formation of hydrogen bonds or the displacement of water molecules from the cavity. The negative value for entropy changes (-53.76 +/- 2.69 J $mol^{-1}$ $K^{-1}$) are due the complexated OXY having lower translational and rotational degrees of freedom that the free product. Finally, the spontaneity of the interaction is reflected in the negative value of the Gibbs free energy change (-15.96 +/- 0.79 KJ $mol^{-1}$) at 25 ± 0.2 ºC.

## 4.5 Effect of pH on complexation constant of the OXY/Mβ-CD complex

Before a guest molecule/CD complex can be used in the food or nutraceutical industry, the pH of the medium must be taken into account because any deprotonation could affect the complexation. As **Fig**. 2C shows, $K_F$ closely depends on the pH, 606.65 +/- 30.18 $M^{-1}$, when the medium pH is 7 and about 267.72 +/- 13.39 $M^{-1}$ at pH 10, as occurs when a weak ionizable group is titrated.

The $K_F$ observed in **Fig**. 2C sharply decreased in region where deprotonation of the hydroxyl groups of OXY begins. One reason for the pH-dependence of $K_F$ might be that a hydrogen bond is formed between the hydroxyl group of the OXY and the hydrophilic groups of CD at pH values below $pK_a$ [18,19]. These results suggest that complexes formed between Mβ-CD and

the protonated form of OXY were more stable than those formed with the deprotonated forms.

## 4.6 Structural characterization

### *4.6.1 RMN and NOESY*

The formation of an OXY/Mβ-CD complex through insertion of OXY into the cavity was studied. Table 2 shows the chemical shifts of OXY, Mβ-CD and the OXY/Mβ-CD complex. The complexation was clearly demonstrated by chemical shifts (Δδ) of Mβ-CD protons, for example H-3 (-0.020) and H-5 (0.030), because the insertion of an aromatic ring had an effect on the chemical shifts of protons in the cavity [20] However, the highest Δδ was obtained for methyl radicals (-0.098 and -0.025) possibly because they rotate to encapsulate OXY. In addition, OXY presented a high degree of Δδ changes due to its complexation in the cavity, which was more important in H-1 and H-8 (-0.174 and -0.157 respectively). On the other hand, the chemical shift of Mβ-CD carbon atoms and OXY carbon atoms was considerable, reflecting the formation of a complex.

Table 2. $^{1}H$ and $^{13}C$ nuclear magnetic resonance shifts of the OXY/MβCD and free OXY and MβCD in $D_2O$/DMSO (85:15 v/v). The corresponding shifts (Δδ) represent the chemical shift differences (ppm) between two states. Negative values indicate high field. Inserted, structures of OXY and MβCD glucose units.

| Proton | OXY | | Proton | Mβ-CD | | Proton | OXY/MβCD | | | |
|---|---|---|---|---|---|---|---|---|---|---|
| | H | C | | H | C | | H | Δδ | C | Δδ |
| **1** | 6.871 | 126.960 | | | | **1** | 6.7 | -0.171 | 126.293 | -0.667 |
| **2** | 7.220 | 124.827 | | | | **2** | 7.177 | -0.043 | 124.426 | -0.401 |
| **3** | - | 141.805 | | | | **3** | - | - | 141.49 | -0.315 |
| **4** | 6.541 | 106.226 | | | | **4** | 6.365 | -0.162 | 105.69 | -0.536 |
| **5** | - | 158.384 | 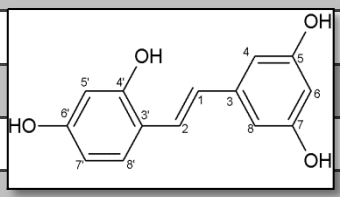 | | | **5** | - | - | 158.784 | 0.400 |
| **6** | 6.213 | 102.736 | | | | **6** | 6.19 | -0.023 | 103.009 | 0.273 |
| **7** | - | 158.384 | | | | **7** | - | - | 158.784 | 0.400 |
| **8** | 6.541 | 106.226 | | | | **8** | 6.365 | -0.162 | 105.69 | -0.536 |
| **3'** | - | 117.744 | | | | **3'** | - | - | 117.443 | -0.301 |
| **4'** | - | 156.081 | | | | **4'** | - | - | 156.941 | 0.860 |
| **5'** | 6.363 | 103.912 | | | | **5'** | 6.379 | 0.016 | 103.724 | -0.188 |
| **6'** | - | 157.996 | | | | **6'** | - | - | 158.104 | 0.108 |
| **7'** | 6.410 | 109.349 | | | | **7'** | 6.342 | -0.068 | 108.69 | -0.659 |
| **8'** | 7.424 | 129.238 | | | | **8'** | 7.267 | -0.157 | 128.073 | -1.165 |
| | | | | | | | | | | |
| 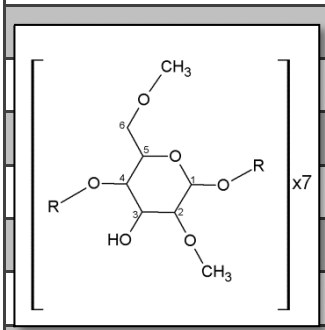 | | | **1** | 5.148 | 102.725 | **1** | 5.134 | -0.014 | 102.543 | -0.182 |
| | | | **2** | 3.307 | 82.18 | **2** | 3.278 | -0.029 | 82.413 | 0.233 |
| | | | **3** | 4.960 | 79.47 | **3** | 4.940 | -0.020 | 79.401 | -0.069 |
| | | | **4** | 3.69 | 83.52 | **4** | 3.668 | -0.022 | 83.635 | 0.115 |
| | | | **5** | 3.801 | 74.19 | **5** | 3.831 | 0.030 | 74.263 | 0.073 |
| | | | **6** | 3.783 | 72.98 | **6** | 3.774 | -0.009 | 73.076 | 0.096 |
| | | | **C2O** | 3.584 | 60.29 | **C2O** | 3.486 | -0.098 | 60.045 | -0.245 |
| | | | **C6O** | 3.496 | 61.18 | **C6O** | 3.471 | -0.025 | 61.022 | -0.158 |

In addition, a 2D NOESY (a powerful technique used to study the internal interaction in inclusion complexes, since it distinguishes inclusion complex from other interactions [21]) of the OXY/Mβ-CD complex of was carried out (**Fig**. 3). The 2D NOESY identified strong interactions between C4H4, C5H5 and C6H6 of the Mβ-CD and H{4,8} of OXY, and also between C2OCH3 and H5' of OXY. These results suggest that the most frequent conformation involved interaction between the most hydrophobic part of the aromatic ring and the internal cavity of Mβ-CD. There was a lower degree of contact between C4H4 and C6H6 of Mβ-CD and H2 and H8' of OXY. It could be because two different complex were formed: one, the major, between C4H4, C5H5 and C6H6 of the Mβ-CD with H{4,8} of OXY) and another, minor, between C4H4 and C6H6 of Mβ-CD and H2 and H8' of OXY. These results are in accordance for example with Chlorogenic Acid/ β-cyclodextrin Complexes [22], where two possible 1:1 complexes were found.

### *4.6.2 Molecular Docking*

After purchasing or constructing the molecules, Vina software was run. Scoring functions are fast mathematical methods used to predict the strength of the non-covalent interaction (also referred to as binding affinity) between two molecules after they have docked, for which reason the binding affinity was compared with the ΔGº obtained previously.

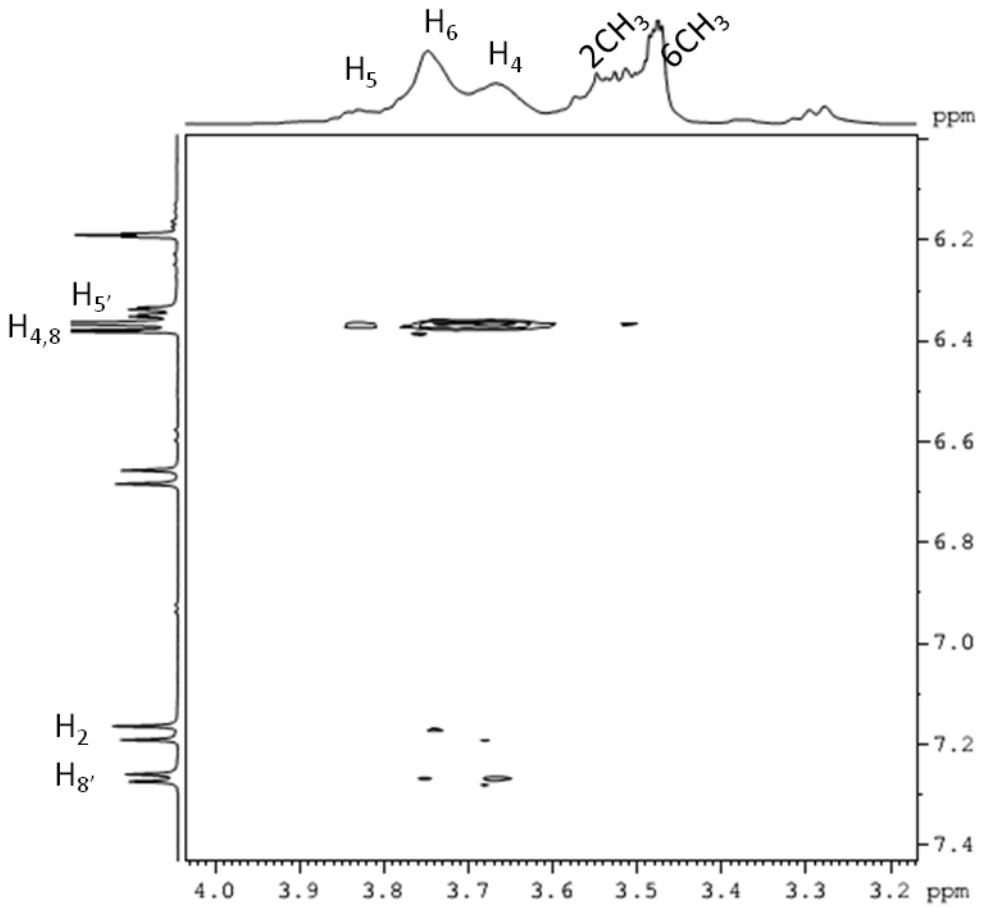


***Fig. 3**. NOESY spectrum of the OXY/MβCD inclusion complex.*

The results showed that the simulated binding affinity (-38. 91 KJ $mol^{-1}$) was higher than experimental ΔG° (-15.96 +/- 0.79 KJ $mol^{-1}$), perhaps because methanol is used in the HPLC method (30:70 v/v), which Vina software did not take it into account in docking simulations [8]. **Fig**. 4 showed the two most probable poses of Vina, which are very close to the NOESY results. In **Fig**. 4A, a Vina pose was obtained with similar conformation to the major complex obtained by NMR; indeed, the distances between the atoms shown in the NOESY complex are small (**Fig**. 4B). Furthermore, a second pose was obtained where by the atoms were related with the second complex shown by NOESY (**Fig**. 4C and D). On the other hand, molecular docking calculations predicted

one hydrogen bond between OXY and Mβ-CD in each complex. The deprotonation of hydroxyl groups, which would eliminate the hydrogen bonds, might explain the results obtained in the pH section because, as already mentioned, hydrogen bonding is one of the most important types of interaction in the stabilization of inclusion complexes [18,19].

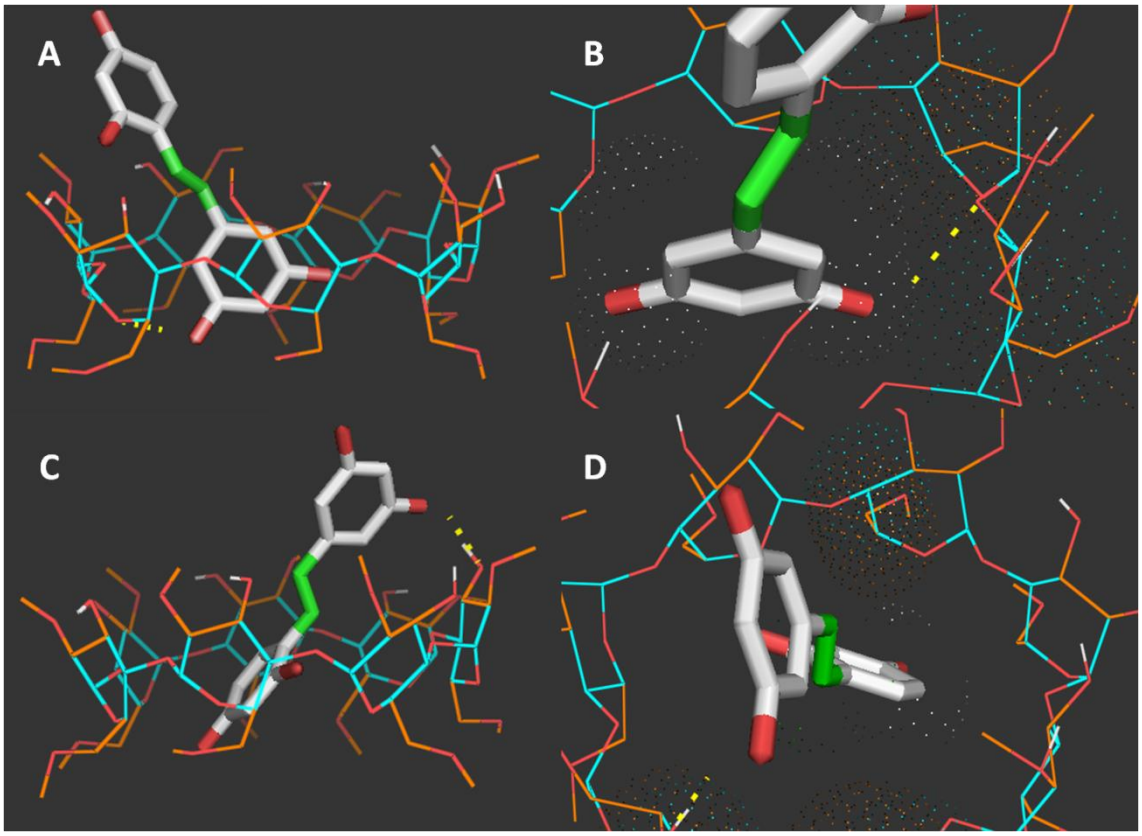


***Fig.4*** *Results for OXY/MβCD (A and B) and interaction zones for each pose (C and D), with the hydrogen bond in yellow (dots indicated the interaction sphere of atoms). Flexible atoms are coloured orange.*

## 4.7 Effect of Mβ-CD on the fluorescence behavior of OXY

Stilbenes are well documented as fluorescence molecules [23]. This intrinsic characteristic can be used to identify them [24], which is why the effect of Mβ-CD on the fluorescence signal of OXY was studied. For first time, maxima of excitation and emission were obtained at 288 and 400 nm respectively, at

least in our conditions. The emission maxima are very near of the obtained for Resveratrol (em 388 nm). However, the excitation is more displayed in resveratrol (ex 334 nm) [25]. These differences might be caused by their different structure. The results (**Fig**. 5) pointed to an increase in fluorescence as Mβ-CD concentrations increased at pH 7, possibly as a result of the enhanced quantum yield obtained for OXY complexation in Mβ-CD [26]. However, when the concentration of Mβ-CD was increased to 2 mM, an important scattering effect appeared near the emission maximum at 25 μM OXY. This effect displaced the maximum of fluorescence and increased the signal to/at around 350 nm. In addition, signal decreased above 2 mM Mβ-CD. Several conclusions drawn from this section: i) enhancement of the fluorescence signal is limited because no more OXY can be encapsulated, ii) the fluorescence signal is affected by high CD concentrations, and iii) CDs could be used as fluorescence enhancers of OXY signal.

4.8 Comparative evaluation of the apparent $K_F$ value and complexation behavior between OXY and resveratrol.

In previous works [4,27] our research group has encapsulated OXY and Resveratrol with β-CD. For that reason it could be interesting to compare these results. $K_{Fapp}$ values obtained for OXY/β-CD (590 +/- 23 $M^{-1}$) and resveratrol/β-CD (≈ 1800 $M^{-1}$) were quite different.

There is only one difference between these molecules, and it is an extra –OH (**Fig**. 1A), this fact suggest that the extra –OH not form a favorable hydrogen bond with bCD, but it may have any steric hindrances that decrease the encapsulation efficiency. Although several authors has study the

complexation of Resveratrol with CDs [27,28], even using NMR [29], no one has found two possible complexes for these type of molecules until now.

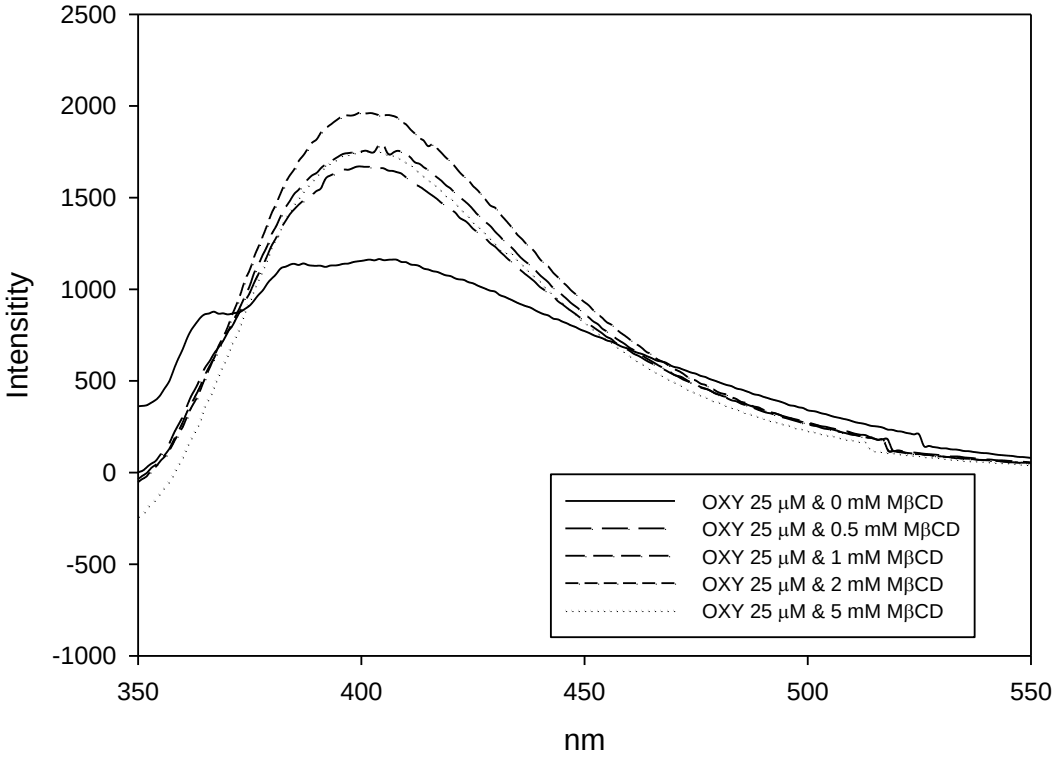


***Fig.5**. Differential fluorescence emission spectrums of OXY/MβCD complexes against MβCD at the same concentration (ex 288 nmpH 7 25 ºC).*

In conclusion, a study of the interaction between oxyresveratrol (a type of stilbene with high biological activity) and modified cyclodextrins (CDs) was made. This bioactive molecule was seen to form a 1:1 complex with both the modified (HPβ-CD, and Mβ-CD) CDs tested using HPLC-RP. The best CD was Mβ-CD ($K_F$ = 606.65 +/- 30.18 $M^{-1}$). The encapsulation of oxyresveratrol in the internal cavity of CDs showed a strong dependence on pH and temperature. $K_F$ increased as pH decreased (due to protonation of the hydroxyl groups) and as the system temperature decreased. Furthermore, a study of the thermodynamic parameters of the complexation (ΔHº, ΔSº and ΔGº) showed negative entropy (-53.76 +/- 2.69 J $mol^{-1}$ $K^{-1}$), enthalpy (–31.99 +/- 1.59 KJ $mol^{-1}$) and Gibbs free

energy change (-15.96 +/- 0.79 KJ $mol^{-1}$) at 25 ºC. In addition, the fluorescence signal of oxyresveratrol increased when Mβ-CD was added. An $^{1}$H-NMR of the complex was carried out, complemented by molecular docking to throw light on the interactions between OXY and Mβ-CD. Finally, the effect of its extra hydroxyl group was compared with the efficiency of resveratrol encapsulation suggesting a decrease of it due to the hydroxyl group.

## References

[1] Y.H. Lim, K.H. Kim, J.K. Kim, Source, biosynthesis, biological activities and pharmacokinetics of oxyresveratrol, Korean J. Food Sci. Technol. 47 (2015) 545–555. doi:10.9721/KJFST.2015.47.5.545.

[2] R.M. Bertram, J.K. Takemoto, C.M. Remsberg, K.R. Vega-Villa, S. Sablani, N.M. Davies, High-performance liquid chromatographic analysis: applications to nutraceutical content and urinary disposition of oxyresveratrol in rats, Biomed. Chromatogr. 24 (2010) 516–521. doi:10.1002/bmc.1320.

[3] W. Chen, S.C.M. Yeo, M.G.A.A. Elhennawy, H.-S. Lin, Oxyresveratrol: A bioavailable dietary polyphenol, J. Funct. Foods. 22 (2016) 122–131. doi:10.1016/j.jff.2016.01.020.

[4] P. Rodríguez-Bonilla, J.M. López-Nicolás, F. García-Carmona, Use of reversed phase high pressure liquid cromatography for the physicochemical and thermodynamic characterization of oxyresveratrol/β-cyclodextrin complexes, J. Chromatogr. B. 878 (2010) 1569–1575. doi:10.1016/j.jchromb.2010.04.016.

[5] K. Fujimura, T. Ueda, M. Kitagawa, H. Takayanagi, T. Ando, Reversed-phase retention behavior of aromatic compounds involving .beta.-cyclodextrin inclusion complex formation in the mobile phase, Anal. Chem. 58 (1986) 2668–2674. doi:10.1021/ac00126a020.

[6] C. Moeder, T. O'Brien, R. Thompson, G. Bicker, Determination of stoichiometric coefficients and apparent formation constants for α- and β-CD complexes of terpenes using reversed-phase liquid chromatography, J. Chromatogr. A. 736 (1996) 1–9. doi:10.1016/0021-9673(95)01276-1.

[7] Y. Matsui, K. Mochida, Binding Forces Contributing to the Association of Cyclodextrin with Alcohol in an Aqueous Solution, Bull. Chem. Soc. Jpn. 52 (1979) 2808–2814.

[8] O. Trott, A.J. Olson, AutoDock Vina: improving the speed and accuracy of docking with a new scoring function, efficient optimization, and multithreading, J. Comput. Chem. 31 (2010) 455–461. doi:10.1002/jcc.21334.

[9] R. Challa, A. Ahuja, J. Ali, R.K. Khar, Cyclodextrins in drug delivery: An updated review, AAPS PharmSciTech. 6 (2005) E329–E357. doi:10.1208/pt060243.

[10] S. Gould, R.C. Scott, 2-Hydroxypropyl-beta-cyclodextrin (HP-beta-CD): a toxicology review, Food Chem. Toxicol. Int. J. Publ. Br. Ind. Biol. Res. Assoc. 43 (2005) 1451–1459. doi:10.1016/j.fct.2005.03.007.

[11] S.S. Jambhekar, P. Breen, Cyclodextrins in pharmaceutical formulations II: solubilization, binding constant, and complexation efficiency, Drug Discov. Today. 21 (2016) 363–368. doi:10.1016/j.drudis.2015.11.016.

[12] T. Loftsson, D. Duchêne, Cyclodextrins and their pharmaceutical applications, Int. J. Pharm. 329 (2007) 1–11. doi:10.1016/j.ijpharm.2006.10.044.

[13] C.-D. Radu, O. Parteni, L. Ochiuz, Applications of cyclodextrins in medical textiles — review, J. Controlled Release. 224 (2016) 146–157. doi:10.1016/j.jconrel.2015.12.046.

[14] G. de O. Makson, A.G. Guimarães, A.A. Adriano, S.Q. Jullyana, M.R. Santos, L.J. Quintans-Júnior, Cyclodextrins: improving the therapeutic response of analgesic drugs: a patent review, Expert Opin. Ther. Pat. 25 (2015) 897–907. doi:10.1517/13543776.2015.1045412.

[15] R.L. Abarca, F.J. Rodríguez, A. Guarda, M.J. Galotto, J.E. Bruna, Characterization of beta-cyclodextrin inclusion complexes containing an essential oil component, Food Chem. 196 (2016) 968–975. doi:10.1016/j.foodchem.2015.10.023.

[16] Y. Sangsen, K. Wiwattanawongsa, K. Likhitwitayawuid, B. Sritularak, R. Wiwattanapatapee, Modification of oral absorption of oxyresveratrol using lipid based nanoparticles, Colloids Surf. B Biointerfaces. 131 (2015) 182–190. doi:10.1016/j.colsurfb.2015.04.055.

[17] L.M.A. Pinto, L.F. Fraceto, M.H.A. Santana, T.A. Pertinhez, S.O. Junior, E. de Paula, Physico-chemical characterization of benzocaine-β-cyclodextrin inclusion complexes, J. Pharm. Biomed. Anal. 39 (2005) 956–963. doi:10.1016/j.jpba.2005.06.010.

[18] R. Bru, J.M. López-Nicolás, E. Núñez-Delicado, D. Nortes-Ruipérez, A. Sánchez-Ferrer, F. Garciá-Carmona, Cyclodextrins as hosts for poorly water-soluble compounds in enzyme catalysis, Appl. Biochem. Biotechnol. 61 (1996) 189–198. doi:10.1007/BF02785701.

[19] W. Saenger, Cyclodextrin Inclusion Compounds in Research and Industry, Angew. Chem. Int. Ed. Engl. 19 (1980) 344–362. doi:10.1002/anie.198003441.

[20] H.-J. Schneider, F. Hacket, V. Rudiger, NMR STUDIES OF CYCLODEXTRINS AND CYCLODEXTRIN COMPLEXES, Chem. Rev. 98 (1998) 1755–1785.

[21] L. Gong, T. Li, F. Chen, X. Duan, Y. Yuan, D. Zhang, Y. Jiang, An inclusion complex of eugenol into β-cyclodextrin: Preparation, and physicochemical and antifungal characterization, Food Chem. 196 (2016) 324–330. doi:10.1016/j.foodchem.2015.09.052.

[22] E. Álvarez-Parrilla, R. Palos, L.A. de la Rosa, B.A. Frontana-Uribe, G.A. González-Aguilar, L. Machi, J.F. Ayala-Zavala, Formation of Two 1:1 Chlorogenic Acid: β-cyclodextrin Complexes at pH 5: Spectroscopic, Thermodynamic and Voltammetric study, J. Mex. Chem. Soc. 54 (2010) 103–110.

[23] J.M. López-Nicolás, P. Rodríguez-Bonilla, F. García-Carmona, Complexation of pinosylvin, an analogue of resveratrol with high antifungal and antimicrobial activity, by different types of cyclodextrins, J. Agric. Food Chem. 57 (2009) 10175–10180. doi:10.1021/jf902519d.

[24] P. Rodríguez-Bonilla, J.M. López-Nicolás, L. Méndez-Cazorla, F. García-Carmona, Development of a reversed phase high performance liquid chromatography method based on the use of cyclodextrins as mobile phase additives to determine pterostilbene in blueberries, J. Chromatogr. B. 879 (2011) 1091–1097. doi:10.1016/j.jchromb.2011.03.025.

[25] J.M. López-Nicolás, F. García-Carmona, Aggregation state and pKa values of (E)-resveratrol as determined by fluorescence spectroscopy and UV-visible absorption, J. Agric. Food Chem. 56 (2008) 7600–7605. doi:10.1021/jf800843e.

[26] M. Hoshino, M. Imamura, K. Ikehara, Y. Hama, Fluorescence enhancement of benzene derivatives by forming inclusion complexes with .beta.-cyclodextrin in aqueous solutions, J. Phys. Chem. 85 (1981) 1820–1823. doi:10.1021/j150613a012.

[27] J.M. López-Nicolás, F. García-Carmona, Rapid, simple and sensitive determination of the apparent formation constants of trans-resveratrol complexes with natural cyclodextrins in aqueous medium using HPLC, Food Chem. 109 (2008) 868–875. doi:10.1016/j.foodchem.2008.01.022.

[28] J.M. López-Nicolás, E. Núñez-Delicado, A.J. Pérez-López, A.C. Barrachina, P. Cuadra-Crespo, Determination of stoichiometric coefficients and apparent formation constants for beta-cyclodextrin complexes of trans-resveratrol using reversed-phase liquid chromatography, J. Chromatogr. A. 1135 (2006) 158–165. doi:10.1016/j.chroma.2006.09.013.

[29] V. Bertacche, N. Lorenzi, D. Nava, E. Pini, C. Sinico, Host–Guest Interaction Study of Resveratrol With Natural and Modified Cyclodextrins, J. Incl. Phenom. Macrocycl. Chem. 55 (2006) 279–287. doi:10.1007/s10847-006-9047-8.

# Block I part II

# Chapter IV

# Characterization of *Resveratrol lipo-derivates* inclusion complexes

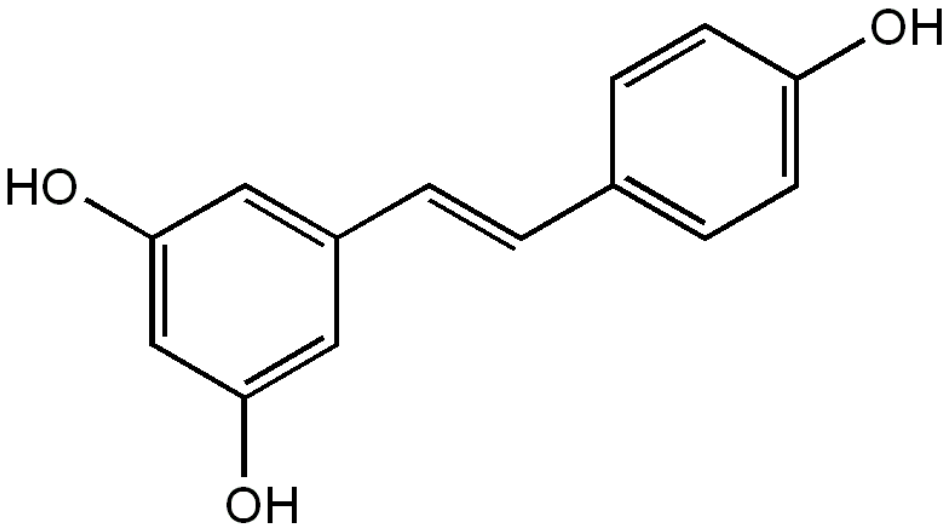

**Abstract**

In this chapter, the synthesis of resveratrol sterate and resveratrol oleate was carried out to study their complexation with HPβ-CD. A Steglich esterification was used to obtain both derivates with a yield around 70%. A mixture of isomers was obtained with a resveratrol 4'-OH majority derivation (confirmed by NMR and logP calculation). HPLC-RP system was used to obtain the constants and stoichiometry. All derivates showed a 1:1 stoichiometry. The stearic acid derivates presented higher complexation constant ($K_F$). The 4'-derivate obtained the highest $K_F$ value.

A molecular docking study showed that the fatty acid is curved to enter in the CD cavity. The molecular docking results provided further insights into how the different interactions influence the complexation constant. High degree of correlation was observed between computed scores and experimental values.

## Index

## 1. Contextualization

Resveratrol (RES) is a well known bioactive compound [1,2]. Recent reviews are about its *in vivo* and *in vitro* pharmacological properties: including a wide range of biological activities, such as antioxidant, antiviral, anti-inflammation, anti-obesity, anticancer, hepato- and neuroprotection and photo-protective effects. It is a molecule that you can find in local markets easily as food supplement. Recently the adipogenesis inhibition by stilbenes was studied with promising results [3,4]. However, the metabolism of stilbenes are considerably fast in humans [5], for that reason different strategies to introduce these molecules are desirable. A chemically modification with fatty acids could create an interesting opportunity because fatty acids are directly transported to the adipocyte, where esterases would liberate the stilbene [6].

For that reason, in this chapter we are going to modify resveratrol with stearic acid (C18:0) and oleic acid (C18:1) and the derivates will be complexed with cyclodextrins (CDs) to protect then for degradation. This fact might be crucial to not decrease the digestion bioaccessibility of derivates.

## 2. Objectives

1) To modify resveratrol with some fatty acids using the steglich esterification and identify them.

2) To determine the stoichiometry and $K_F$ values for the resveratrol-derivates/CD complexes.

3) To study the physical interactions between derivates and CD using molecular docking.

## 3. Materials and methods.

### 3.1 Materials

Hydroxypropyl-beta-cyclodextrin (HP-βCD) was purchased from Carbosynth (Berkshire, UK). Resveratrol was purchased from TCI (Belgium) and used as received. Stearic acid and oleic acid (reactant grade) were purchased from Merck (Madrid, Spain). Dicyclohexylcarbodiimide (DCC) and 4-dimethylaminopyridine (DMAP) were purchased from Sigma-Aldrich (Madrid, Spain). The samples were stored in darkness. Methanol (HPLC grade), chloroform (analytical grade) and dimethylformamide (DMF, analytical grade) were purchased from Fisher (Madrid, Spain). MQ water was obtained using a Milli-Q Advantage A10 system by Merck Millipore (Madrid, Spain). Binary mixtures of water/methanol were used without further purification.

### 3.2 Equipment and Experimental Procedure

#### *3.2.1 Resveratrol derivates synthesis*

A steglich esterification was carried out to get the derivates. In a three-necked flask equipped with condenser, dropping funnel and stirrer maintained under inner atmosphere were added 100 mL of dry 94:6 chloroform:DMF and molecular sieve. After, 0.125 g of fatty acid ($4.4 \times 10^{-4}$ mols), 0.09 g of DCC ($4.4 \times 10^{-4}$ mols) and $5.4 \times 10^{-4}$ g of DMAP ($4.4 \times 10^{-6}$ mols) were added and finally 0.1 g of resveratrol ($4.4 \times 10^{-4}$ mols) dissolved in chloroform previously. The mixture was left for 24 h and the results were checked by TLC using Chloroform/methanol 9:1 and LC-MS using an Agilent HPLC 1200 series equipped with a TOF 6220 (acquisition range 100-1100) in negative mode. One

microlitres of the reaction was injected using 40/60 H2O/MeOH with 20 mM ammonium acetate as mobile phase at 0.6 mL/min and 25 ºC. Yield was obtained using a calibration with initial resveratrol quantity. In order to inject samples in HPLC, the solution was evaporated and dissolved in 55:10:35 Methanol:water:THF.

NMR analysis were carried out adding 0.4 mL of DMSO at RES (1.2 mg) and 4'-RO/E (0.4mg). Nuclear magnetic resonance was measured using a Bruker Avance 600MHz (Bruker, Germany) in 5 mm tubes.

### *3.2.2 Inclusion complex characterization.*

5 μL of the final solution was injected in an Agilent 1100 series HPLC system (CA, USA) and a 1200 series module UV-VIS detector with a Kromasil 150 C18 column (Análisis Vínicos S.L.Tomelloso, Spain) (150 mm x 4,6 mm, 5μm particle size). The flow rate was set and automatically controlled at 1.00 ± 0.01 mL/min with Methanol/Water (85/15 v/v) with different concentrations of CDs at 25 ºC. The UV detector was operated at 310 and 220 nm.

To determine the complexation constant ($K_F$) value for the derivates/CD complexes, Eq. 1, which relates the capacity factor, *k*, and the CDs mobile-phase concentration, [CD], was used. In this equation two conditions are assumed: 1) the complex has a 1:1 stoichiometry and 2) any interaction of the Derivate / CD complexes with the stationary phase is negligible [7].

$$\frac{1}{k} = \frac{1}{k_0} + \frac{K_F}{k_0}[CD] \quad (1)$$

where *k* is the capacity factor of the solute, $k_0$ is the solute capacity factor in the absence of CD, $K_F$ is the apparent formation constant of the inclusion complex and [CD] is the CD mobile-phase concentration. Values of $R^2$ close to 1 indicate a 1:1 model.

Eq. 2 is an extension of Eq. 1 and includes a second-order term that accounts for the possibility of a 1:2 derivate / CDs complex formation [8]:

$$\frac{1}{k} = \frac{1}{k_0} + \frac{K_{F12}}{k_0}[CD]^2 \quad (2)$$

where $k_0$ is the capacity factor of OXY in the absence of CD modifier and $K_{F12}$ is the apparent formation apparent for the 1:2 derivate / CD complex. Values of $R^2$ close to 1 indicate a 1:2 model. The column void volume, $t_0$, was determined using a reagent grade copper sulphate solution (0.01 mg/mL). The HPLC-RP method gives an apparent $K_F$ ($K_{Fapp}$) due to the methanol/CD interactions that take place [9].

### *3.2.3 Molecular docking*

The molecular structures used in this work were built using Avogadro Software (version 2.3.2) or were obtained by different databases. HPβ-CD was built by adding hydroxypropyl group to a β-CD [10] obtained from the Protein Data Bank (PDB ID: 4RER). Resveratrol molecule was downloaded from the PubChem database (NCBI, USA) and modified using Avogadro. Input files for docking were generated using Autodock tools (version 1.5.6) with default parameters and charges. Molecular docking was carried out using Autodock Vina [11] using default parameters. HPβ-CD was considered as flexible.

Graphical representations of the docking results were prepared using PyMOL (Molecular GraphicsSystem, version 1.3, Schrödinger, LLC) with default parameters to display hydrogen bonds.

### *3.2.4. Determination of Lipophilicity*

The lipophilicity (LogP) was computationally obtained using ALOGPS 2.1 [12]. The structures of resveratrol derivates were uploaded as .mol2 generated by Pymol (Molecular GraphicsSystem, version 1.3, Schrödinger, LLC).

### *3.2.5 Data analysis.*

The experiments were carried out in triplicate. Graphical representations were made using SigmaPlot (Version 10.0). A t-test was applied using Rstudio (version 0.99.878) fixing the significance level at $P < 0.05$. Other mathematical operations were carried out using wxMaxima software (version 12.04.0).

## 4. Results and discussion

### 4.1 Synthesis of resveratrol:fatty acid derivates

Our first step was to synthesize the derivates. We selected steglich esterification due to their no-aggressive conditions. **Fig**. 1A shows the TLC results of our reactions (Oleic acid = RO and Stearic acid = RS), only two peaks were detected in both cases. Although there must be three products, due to the isomerism there are only two derivates, 3- and 4'-, **Fig**. 1B. In addition, the quantity of diesters was minimal (**Fig**. 2A and B, peak 721 for RS and 755 for RO) in LC-MS analysis indicating a majority 1:1 esterification. The yield of 1:1 esterification was around 70% in both cases and the abundance. Our results obtained better yield than others in bibliography using chloride derivates [13]. This suggests a new, cleaner and easy protocol not only by our yield but also by our absence of diesters.

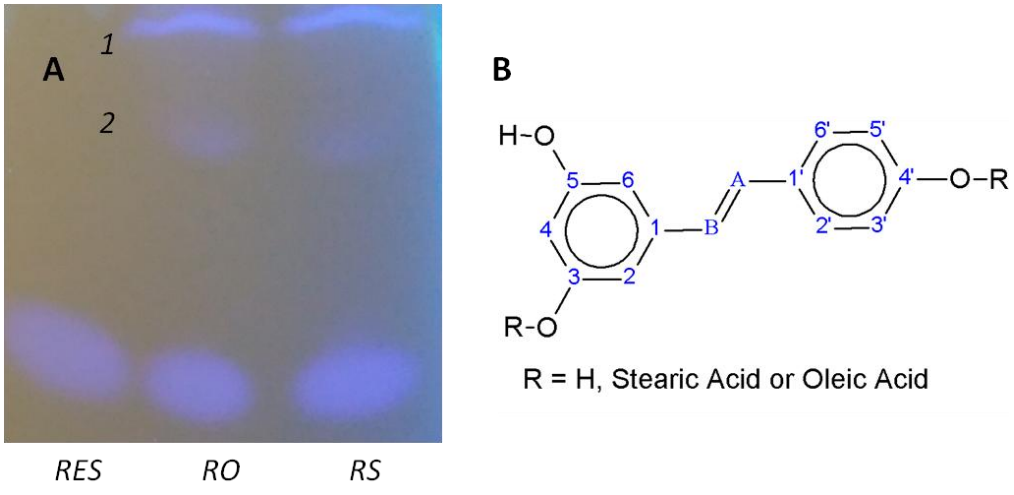


***Fig** 1. (A) TLC of RES and reactions after 24 h. (B) Structure of Resveratrol and derivates.*

## 4.2 Selecting the optimal conditions on HPLC

As in this thesis has been written, the effectiveness of HPLC system to obtain $K_F$ depends on methanol quantity [9]. For that reason, different methanol proportions (50-100%) were evaluated at 25 ºC to obtain a good $t_R$ without using too much methanol. As the hydrophobicity of derivates is around 3.6 [13] times higher than resveratrol, at least an 85 % of methanol was necessary to obtain a compressive $t_R$ with both derivates (**Fig**. 3A and B).

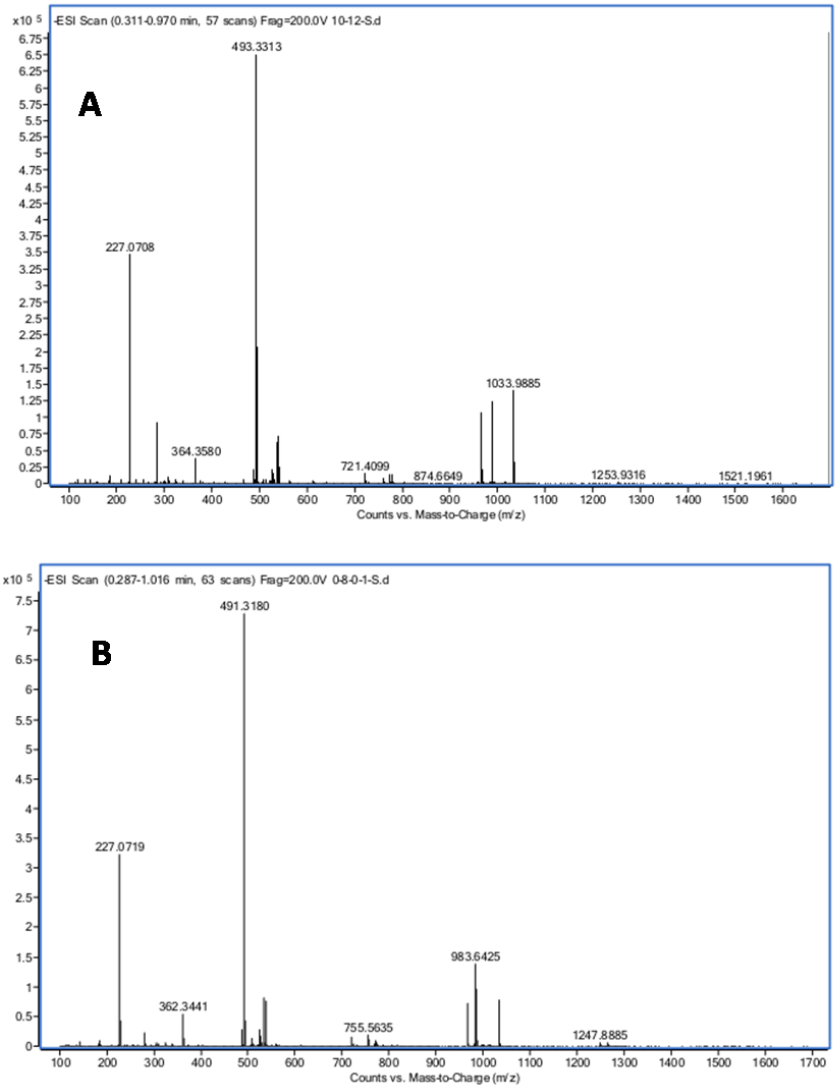

***Fig** 2. LC-MS direct injection in negative for (A) RS and (B) RO reaction, m/z 227 is RES, 493 and 491 are RS and RO, 1033 is the internal standard.*

Two peaks were displayed in both samples, with $t_R$ of 122.15 +/- 6.10 min and 135.42 +/- 6.70 min for resveratrol sterates (RS) and 67.50 +/- 3.40 min and 75.53 +/- 3.70 min for resveratrol oleates (RO). The lipophilicity of derivates was also calculated (Table 1) giving that in both case, the 4'- derivates are more hydrophobic than 3-. The abundance of 4'- was around 70% in both derivates.

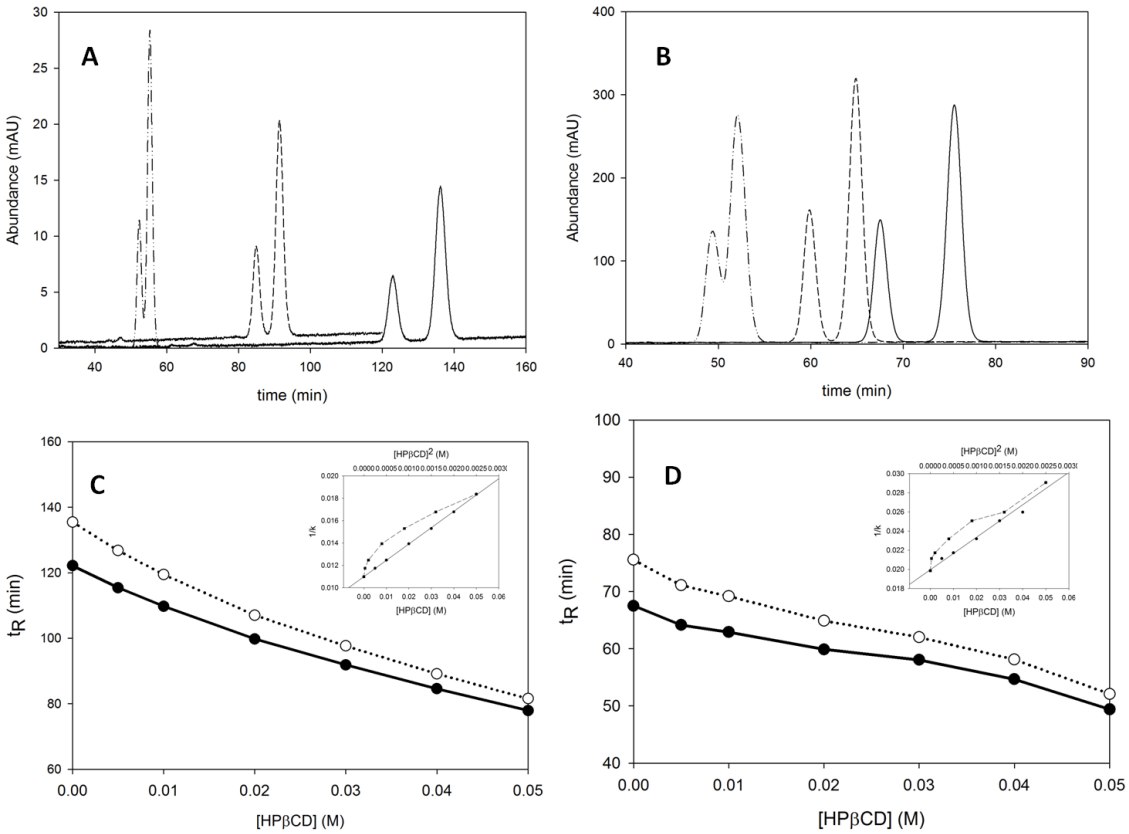


***Fig** 3. HPLC chromatograms of (A) RS and (B) RO derivates at increasing HPβ-CD concentrations. Conditions: 85:15 methanol:water 25ºC at 1 mL/min. Effect of HPβ-CD concentrations on (C) RS tR and (D) RO tR. Inserts: linear fit of RS and RO complexed with HPβ-CD to determine the stoichiometry of complexes: 1/k vs [HPβ-CD] (circles, 1:1 complex) and representation of the curve fit of the1:2 complex (squares,).*

As HPLC-RP separates molecules due to its hydrophobicity, the major isomers might be the 4' isomer in both cases. This is supported by the fact 4'-OH of resveratrol is the more reactive –OH [14] of the molecule, promoting the esterification in this hydroxyl group. However, to completely verify this hypothesis, we realized an NMR of the supposed 4'- peak: the absence of 4'-OH signal in the sample (data not showed) certify the esterification on this site.

### 4.3 Stoichiometry and apparent complexation constant of resveratrol derivates by HPβ-CD

The solubility of several natural and modified CDs were tested at 85 % methanol showing that only HPβ-CD could be used in our current conditions. Indeed, HPβ-CD is one of the most useful CDs due to its low toxicity [15–17]. For this reason the encapsulation process was studied with HPβ-CD. The effect of different HPβ-CD concentration on $t_R$ was evaluated (**Fig**. 3C and D) giving a decrease on $t_R$. Plotting these data using eq. 1 and 2 (**Fig** 3C and D *inserts*) we could obtain their $K_F$ Table 1 shows the different $K_F$ (apparent $K_F$) values obtained and, their stoichiometry.

Table 1. Apparent $K_F$ values, relative derivate abundance, lipophilicity, correlation coefficients and score docking for RS/HPβ-CD and RO/HPβ-CD complexes at 25 °C in a methanol:water (85:15%) medium.

| Complex | Abundance (%) | $K_F$ ($M^{-1}$) | SD (+/-) | 1:1 model | 2:1 model | Lipophilicity of derivate | Score |
|---|---|---|---|---|---|---|---|
| **3-RS/HPβ-CD** | 30 | 11.4 | 0.5 | 1.0 | 0.93 | 9.3 | -4.3 |
| **4'-RS/HPβ-CD** | 70 | 13.3 | 0.6 | 1.0 | 0.93 | 9.34 | -4.8 |
| **3-RO/HPβ-** | 33 | 6.7 | 0.3 | 0.96 | 0.94 | 8.91 | -4.5 |

| | | | | | | | |
|---|---|---|---|---|---|---|---|
| **CD** | | | | | | | |
| **4'-RO/HPβ-CD** | 67 | 8.5 | 0.4 | 0.98 | 0.94 | 9.13 | -5.2 |

The highest $K_F$ value was obtained for the stearic acid derivates, perhaps due to higher hydrophobicity of derivate. The 4'- derivates showed the highest $K_F$ value (t-test, $p<0.05$).

4.4 Molecular modeling of RS/HPβ-CD and RO/HPβ-CD complexes

After purchasing or constructing the molecules, Vina software was run. Scoring functions are fast mathematical methods used to predict the strength of the non-covalent interaction (also referred to as binding affinity) between two molecules after they have docked.

The results showed that the score values are perfectly correlated with our $K_F$ values intra-derivates but they are not able to discern between RS or RO chain. However, the data supports our product ordination. **Fig**. 4 showed the two most probable poses of Vina. According to RS/HPβ-CD complexes (4'-, 4A and 3-, 4B), it can be seen as only 5/3 derivates establish some hydrogen bonds, perhaps this fact increase the stability the complex. However, some steric hydrances could be happened in 5/3 derivates because the molecule did not fit perfectly. Another interesting data is that the fatty acid chain is completely curved to enter in the CD in the case of 4'-RS. On the other hand, **Fig.** 4C and **Fig.** 4D present the results for 4'-RO/HPβ-CD and 3-RO/HPβ-CD complexes. In this case, both molecules have a perfect fit in the CD cavitiy, however, 4'-RO presents a hydrogen bond that could increase the stability of the complex

because hydrogen bonding is one of the most important types of interaction in the stabilization of inclusion complexes [18,19].

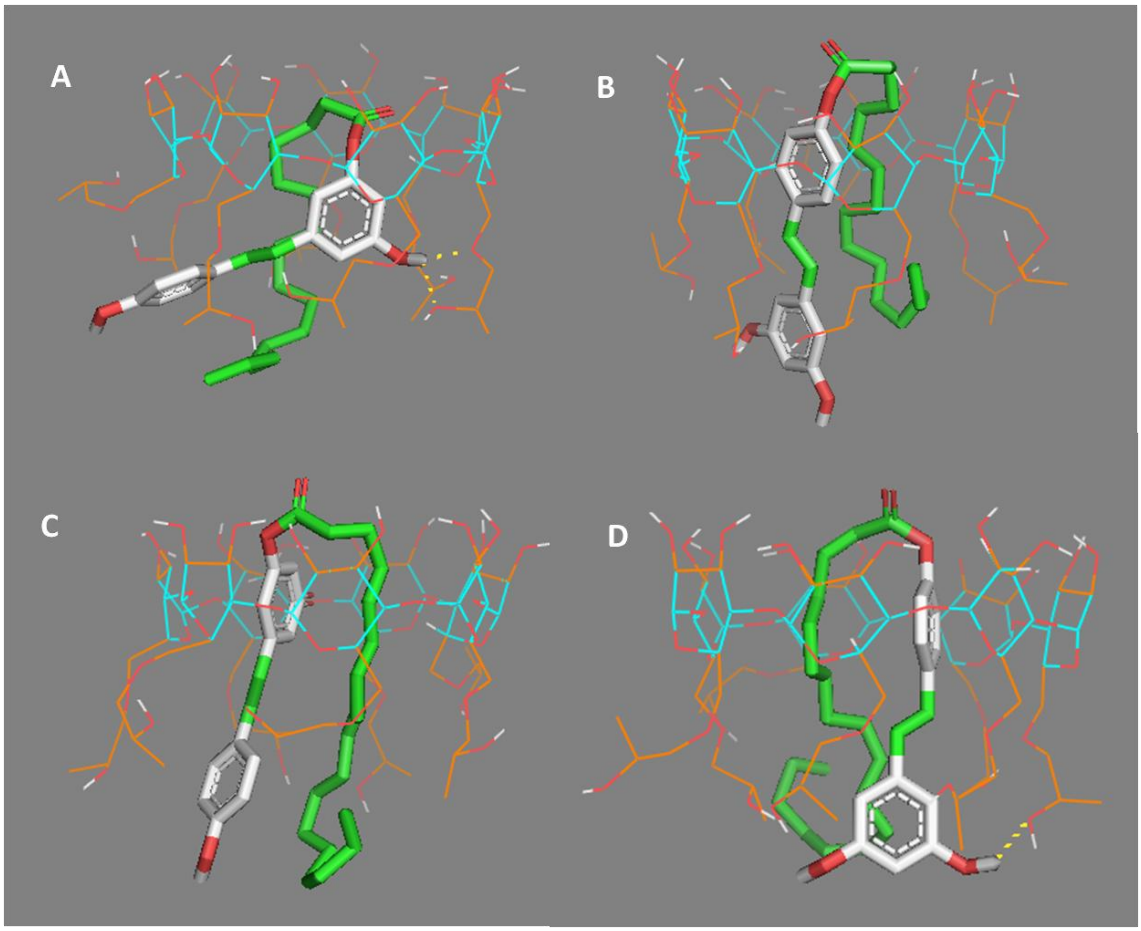


***Fig** 4. Docking poses for (A) 3-RS/HPβ-CD, (B) 4'-RS/HPβ-CD, (C) 3-RO/HPβ-CD and (D) 4'-RO/HPβ-CD. In orange flexible atoms and in yellow hydrogen bonds.*

4.5 Comparative evaluation of the apparent $K_F$ value and complexation behavior between RS and RO derivates

Both derivates derivates presents similar HPLC profile of peaks, giving two peaks when the second is the major. Analyzing the lipophicity, $K_F$ and score docking data (Table 1), we can say that the second peaks are the 4'- derivates. On the other hand, the insaturation presented in oleic acid decrease the

encapsulation strength as our experimental data reported. The RS derivates would get a stronger complexation than RO derivates. Although the internal docking score ordination is correct, the comparation between RS and RO is inverse, perhaps the software cannot measure differences caused by a simple hydrogenation.

In conclusion, in the present chapter we have easily synthesized some resveratrol derivates adding stearic acid and oleic acid chemically with a yield of 70% without important diesters to study its complexation behavior with 3-RO/HPβ-CD. RS/HPβ-CD and RO/HPβ-CD always gave 1:1 stoichiometry. The 4' derivates presented higher $K_F$ value than 3- derivates, and RS complexation was better than RO. Molecular docking simulations showed the essential of the complexation process, fatty acids chain were curved to fit with HPβ-CD.

## References

[1] G. Navarro, E. Martínez -Pinilla, R. Ortiz, V. Noé, C.J. Ciudad, R. Franco, Resveratrol and Related Stilbenoids, Nutraceutical/Dietary Complements with Health-Promoting Actions: Industrial Production, Safety, and the Search for Mode of Action: Stilbenoids and food industry…, Compr. Rev. Food Sci. Food Saf. 17 (2018) 808–826. doi:10.1111/1541-4337.12359.

[2] A.Y. Berman, R.A. Motechin, M.Y. Wiesenfeld, M.K. Holz, The therapeutic potential of resveratrol: a review of clinical trials, Npj Precis. Oncol. 1 (2017) 35. doi:10.1038/s41698-017-0038-6.

[3] C. Carpéné, H. Pejenaute, R. Del Moral, N. Boulet, E. Hijona, F. Andrade, M.J. Villanueva-Millán, L. Aguirre, J.M. Arbones-Mainar, The Dietary Antioxidant Piceatannol Inhibits Adipogenesis of Human Adipose Mesenchymal Stem Cells and Limits Glucose Transport and Lipogenic Activities in Adipocytes, Int. J. Mol. Sci. 19 (2018). doi:10.3390/ijms19072081.

[4] C. Carpéné, F. Les, G. Cásedas, C. Peiro, J. Fontaine, A. Chaplin, J. Mercader, V. López, Resveratrol Anti-Obesity Effects: Rapid Inhibition of Adipocyte Glucose Utilization, Antioxid. Basel Switz. 8 (2019). doi:10.3390/antiox8030074.

[5] T. Walle, F. Hsieh, M.H. DeLegge, J.E. Oatis, U.K. Walle, High absorption but very low bioavailability of oral resveratrol in humans, Drug Metab. Dispos. Biol. Fate Chem. 32 (2004) 1377–1382. doi:10.1124/dmd.104.000885.

[6] B.R. Thompson, S. Lobo, D.A. Bernlohr, Fatty acid flux in adipocytes; the in's and out's of fat cell lipid trafficking, Mol. Cell. Endocrinol. 318 (2010) 24–33. doi:10.1016/j.mce.2009.08.015.

[7] K. Fujimura, T. Ueda, M. Kitagawa, H. Takayanagi, T. Ando, Reversed-phase retention behavior of aromatic compounds involving .beta.-cyclodextrin inclusion complex formation in the mobile phase, Anal. Chem. 58 (1986) 2668–2674. doi:10.1021/ac00126a020.

[8] C. Moeder, T. O'Brien, R. Thompson, G. Bicker, Determination of stoichiometric coefficients and apparent formation constants for α- and β-CD complexes of terpenes using reversed-phase liquid chromatography, J. Chromatogr. A. 736 (1996) 1–9. doi:10.1016/0021-9673(95)01276-1.

[9] Y. Matsui, K. Mochida, Binding Forces Contributing to the Association of Cyclodextrin with Alcohol in an Aqueous Solution, Bull. Chem. Soc. Jpn. 52 (1979) 2808–2814.

[10] J.M. López-Nicolás, M. Escorial Camps, H. Pérez-Sánchez, F. García-Carmona, Physicochemical and Thermodynamic Characterization of the Encapsulation of Methyl Jasmonate by Natural and Modified Cyclodextrins Using Reversed-Phase High-Pressure Liquid Chromatography, J. Agric. Food Chem. 61 (2013) 11347–11354. doi:10.1021/jf402920p.

[11] O. Trott, A.J. Olson, AutoDock Vina: improving the speed and accuracy of docking with a new scoring function, efficient optimization, and multithreading, J. Comput. Chem. 31 (2010) 455–461. doi:10.1002/jcc.21334.

[12] I.V. Tetko, J. Gasteiger, R. Todeschini, A. Mauri, D. Livingstone, P. Ertl, V.A. Palyulin, E.V. Radchenko, N.S. Zefirov, A.S. Makarenko, V.Y. Tanchuk, V.V. Prokopenko, Virtual computational chemistry laboratory--design and description, J. Comput. Aided Mol. Des. 19 (2005) 453–463. doi:10.1007/s10822-005-8694-y.

[13] W.Y. Oh, F. Shahidi, Lipophilization of Resveratrol and Effects on Antioxidant Activities, J. Agric. Food Chem. 65 (2017) 8617–8625. doi:10.1021/acs.jafc.7b03129.

[14] S. Xu, G. Wang, H.-M. Liu, L.-J. Wang, H.-F. Wang, A DMol3 study on the reaction between trans-resveratrol and hydroperoxyl radical: Dissimilarity of antioxidant activity among O–H groups of trans-resveratrol, J. Mol. Struct. THEOCHEM. 809 (2007) 79–85. doi:10.1016/j.theochem.2007.01.036.

[15] R. Challa, A. Ahuja, J. Ali, R.K. Khar, Cyclodextrins in drug delivery: An updated review, AAPS PharmSciTech. 6 (2005) E329–E357. doi:10.1208/pt060243.

[16] S. Gould, R.C. Scott, 2-Hydroxypropyl-beta-cyclodextrin (HP-beta-CD): a toxicology review, Food Chem. Toxicol. Int. J. Publ. Br. Ind. Biol. Res. Assoc. 43 (2005) 1451–1459. doi:10.1016/j.fct.2005.03.007.

[17] P. Jansook, N. Ogawa, T. Loftsson, Cyclodextrins: structure, physicochemical properties and pharmaceutical applications, Int. J. Pharm. 535 (2018) 272–284. doi:10.1016/j.ijpharm.2017.11.018.

[18] R. Bru, J.M. López-Nicolás, E. Núñez-Delicado, D. Nortes-Ruipérez, A. Sánchez-Ferrer, F. Garciá-Carmona, Cyclodextrins as hosts for poorly water-soluble compounds in enzyme catalysis, Appl. Biochem. Biotechnol. 61 (1996) 189–198. doi:10.1007/BF02785701.

[19] W. Saenger, Cyclodextrin Inclusion Compounds in Research and Industry, Angew. Chem. Int. Ed. Engl. 19 (1980) 344–362. doi:10.1002/anie.198003441.

# Block II

# Application of cyclodextrin in different fields: analytical chemistry, food science and pharmaceutics.

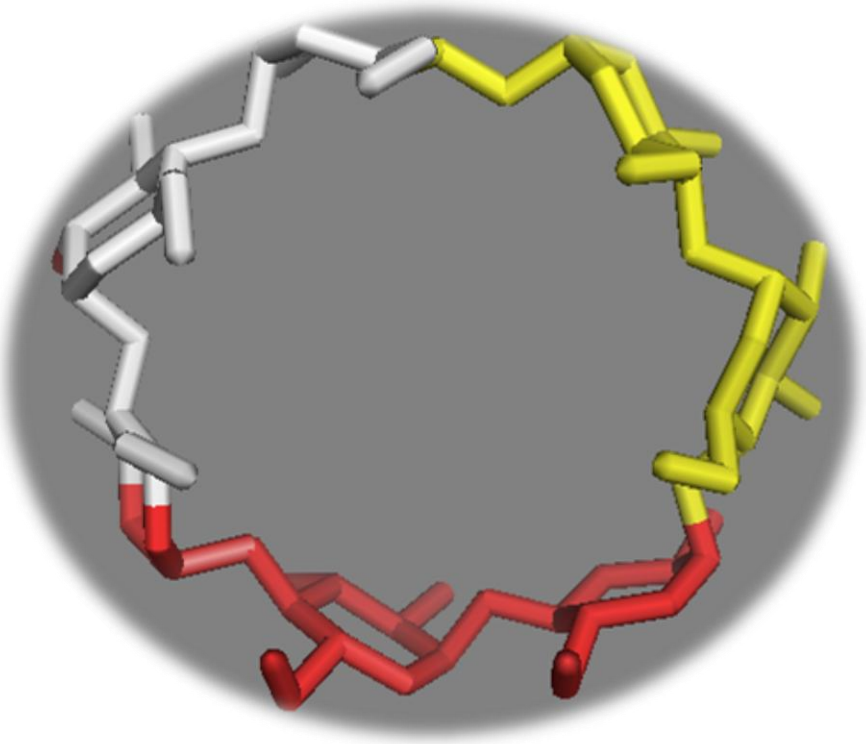

## Block Introduction

In this block, several applications of CDs in different field will be carried out. We are focused on three matters such as analytical chemistry, food science and pharmaceutics. From enantioseparation to rare diseases, the use of CDs will demonstrate its versatility and possibilities.

# Block II Part I

# Application of cyclodextrins in analytical chemistry.

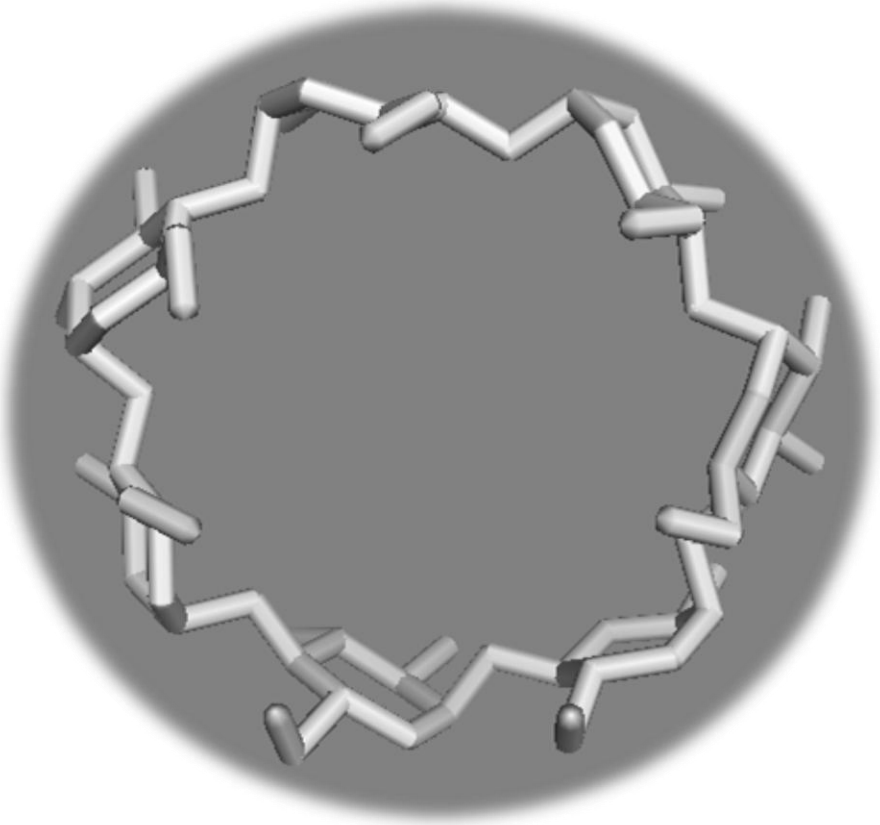

## Introduction

Analytical chemistry is a part of science that studies different methods to separate, identify, and quantify matter. The separation, identification or quantification may constitute the entire analysis or be combined with another method.

It is always desirable to get faster, cheaper and more precise methods to identify drugs or metabolites. Cyclodextrins has a great potential in this part application as our thesis introduction showed.

In this section we are going to show an application of CDs in HPLC to separate and identify the four isomers of methyl jasmonate, an important elicitor in plant cell cultures.

# Block II part I

# Chapter I

## *Separating and identifying the four stereoisomers of Methyl Jasmonate by RP-HPLC and using cyclodextrins in a novel way.*

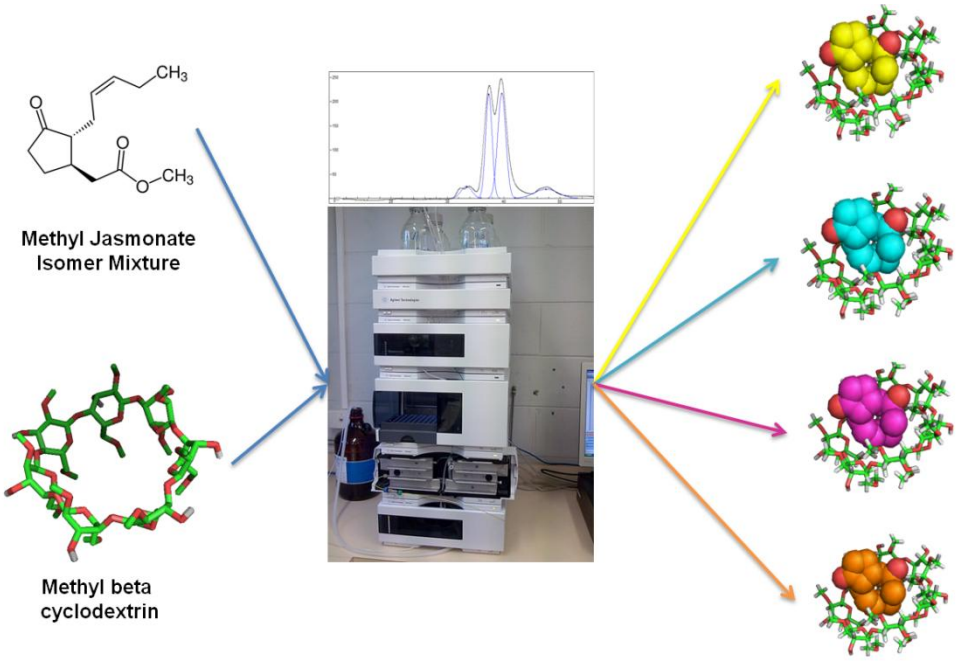

**Abstract**

In this chapter we propose a simple, precise and cheap method for separating and identifying the four stereoisomers present in commercial racemic mixtures of methyl jasmonate (MeJA), an elicitor widely used in plant cell cultures. Our method is based on adding cyclodextrins (CDs) as encapsulant agents to the mobile phase of a RP-HPLC system. No previous treatment of the sample, derivatizacion or chiral columns is necessary.

The results show that the best conditions for the enantioseparations of MeJA stereoisomers are: 20% methanol in the mobile phase, a temperature of 45 ºC and a 16 mM concentration of MβCD. A simple C18 250 mm column and a flow rate of 1.25 mL/min were used. The reduction in the *tR* of MeJA when MβCD is added to the mobile phases was used to determine the complexation constants of the guest/CD complex and compared with the obtained when other CDs were used. The value of $K_F$ for Mβ-CD (117.49 +/- 5.9 $M^{-1}$) is the highest value our group has obtained for all the cyclodextrins investigated to date. In all the cases tested the stoichiometry of the complex was 1:1.

The four stereoisomers were identified by molecular docking techniques and coinjection of a commercial rosemary essential oi. In order to understand how MβCD interacts with the different stereoisomers of MeJA, molecular modelling studies were carried out.

## Index

## 1. Contextualization

In recent years many researchers have focused on improving the production of bioactive secondary metabolites from natural plants. One of the methods most widely reported for enhancing the biosynthesis of plant and fruit components such as carotenes and chlorophylls [1] , vitamins [2], stilbenes [3,4], and aromatic compounds [5], has been the elicitation of plant cell cultures using molecules such as methyl jasmonate (MeJA).

Although this molecule is present in a great variety of higher plants, where it plays an important role in the defence mechanism against insect attack or in the control of plant responses to stimuli such us mechanical stress [6], most researchers use commercial preparations of MeJA for their experiments. However, these preparations have the inconvenience that the stereochemistry of their chiral centres means that they occur as a mixture of four stereoisomers with different properties: (+) epiMeJA, (-) epiMJA; (+) MeJA and (-) MeJA (**Fig. 1**). Indeed, one paper mentions the effect of postharvest treatment with stereoisomers of MeJA on the bioformation of myricetin, quercetin and kaempferol in red raspberry, the results obtained depending on the stereoisomers used [4,7,8].

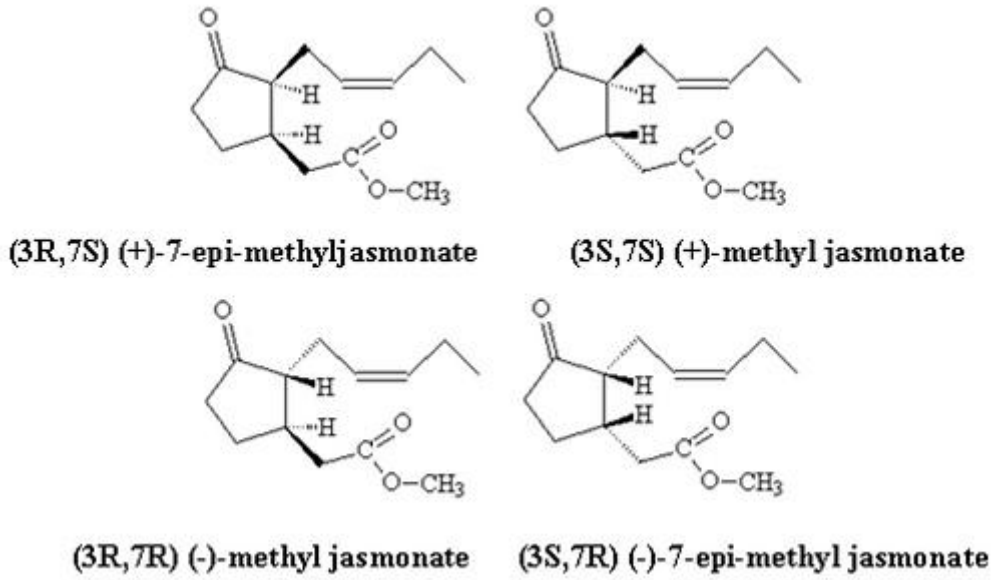


***Fig.** 1. Structure of the four stereoisomers of MeJA.*

For this reason, it is necessary to develop effective methods to resolve and obtain pure MeJA stereoisomers, for which it is important to know the compositions of MeJA solutions so that the most powerful stereoisomer can be used.

In recent years several methods have been developed for separating the four stereoisomers of MeJA although they all have disadvantages concerning the difficulty involved in sample preparation and the time and cost of analysis. As reported by Flores et al. (2013) several methods to obtain pure MeJA stereoisomers have centred on asymmetric synthesis [9,10], enzymatic resolution [11] and HPLC resolution prior to diastereoisomer formation [12]. However, not all these methods permit separation of the four stereoisomers of MeJA.

In this paper we propose a cheap and sensitive method for separating and identifying the four stereoisomers of MeJA based on the use of cyclodextrins (CDs) added to the mobile phase of an RP-HPLC system.

It should be emphasised at this point that the use of CDs for separating MeJA stereoisomers is not new. In 2009, for example, Blanch et al (2009) and Flores et al (2013) used these encapsulant agents with the same objective [13,14], although, in a chiral CD column phase of the HPLC system and not in the mobile phase. Such a method has serious inconveniences, including the cost of the stationary phase used. By contrast, in the present study the CDs were added to the mobile phase and a simple C18 column, which can be reused for other purposes, was used as stationary phase.

## 2. Objectives

1. To study the retention mechanism of MeJA in a reversed-phase system involving the formation of different CD inclusion complexes in the mobile phase.
2. To calculate the mechanism involved in the complexation MeJA by Mβ-CD, calculating the stoichiometry, $K_F$ values and thermodynamic parameters for the Mβ-CD/MeJA complex.
3. To propose molecular interactions for the complexation process using molecular modelling.
4. To identify the four stereoisomers of MeJA obtained in the separation process.

## 3. Materials and methods

### 3.1 Materials

The (+/-) MeJA standard (which contains 5% methyl epi-jasmonate) and Mβ-CD were purchased from Sigma (Madrid, Spain). Rosemary essential oil was purchased from a local supermarket. HPLC grade methanol was purchased from Fisher (Madrid, Spain). MQ water was obtained using a Milli-Q Advantage A10 system by Merck Millipore (Madrid, Spain). Binary mixtures of water/methanol, with methanol percentages of 05−30%, were used without further purification.

### 3.2 Inclusion complex characterization

Twenty microlitres of a 10% MeJA solution in methanol was injected for HPLC analysis using a Merck-Hitachi L-6200 pump (Merck-Hitachi, Darmstadt, Germany) and a Shimadzu SPD-M6A ultraviolet (UV) diode array detector (Shimadzu, Kyoto, Japan) with a Kromasil 150 C18 column (Análisis Vínicos S.L.Tomelloso, Spain) (150 mm x 4,6 mm, 5µm particle size). The mobile phase flow rate was set and systematically controlled at 1.50 ± 0.01 mL/min with Methanol/Water (40/60 v/v) at 25 ºC. The UV detector was operated at 210 nm.

To determine the $K_F$ value for the MeJA/Mβ-CD complex, Eq. 1 was used [15]. In this equation two conditions are assumed: 1) the complex has a 1:1 stoichiometry and 2) any interaction of the MeJA/Mβ-CD complex with the stationary phase is negligible [16].

$$\frac{1}{k} = \frac{1}{k_0} + \frac{K_F}{k_0}[CD] \qquad (1)$$

where *k* is the capacity factor of the solute, $k_0$ is the solute capacity factor in the absence of CD, $K_F$ is the apparent formation constant of the inclusion complex and [CD] is the Mβ-CD mobile-phase concentration. Values of $R^2$ close to 1 indicate a 1:1 model

We also studied the possible formation of a 1:2 MeJA/Mβ-CD complex via a precursor 1:1 complex. Eq. 2 is an extension of Eq. 1 and includes a second-order term that accounts for the possibility of a 1:2 MeJA/Mβ-CD complex formation:

$$\frac{1}{k} = \frac{1}{k_0} + \frac{K_{F12}}{k_0}[CD]^2 \qquad (2)$$

where $k_0$ is the capacity factor of MeJA in the absence of Mβ-CD modifier, $K_{F1}$ is the apparent formation apparent for the 1:1 MeJA/Mβ-CD complex and $K_{F2}$ is the apparent formation constant for the 1:2 MeJA/Mβ-CD complex. A value of $R^2$ close to 1 indicates a 1:2 model.

### 3.3 Separation and identification of stereoisomers

Five microlitres of 10% MeJA solution in methanol was injected for HPLC analysis using a Merck-Hitachi L-6200 pump (Merck-Hitachi, Darmstadt, Germany) and a Shimadzu SPD-M6A ultraviolet (UV) diode array detector (Shimadzu, Kyoto, Japan) with a Phenomenex Gemini RP18 reversed-phase column 110A (Phenomenex, Madrid, Spain) (250 × 4.6 mm inner diameter, 5 µm particle size). To identify the peaks using rosemary essential oil, a dilution of 20% in methanol was filtered through a 0,22 µm diameter filter and 20 µL was injected into the Phenomenex column. For the co-injection experiment, 20 µL of a sample with 2,5% MeJA standard and 20% of rosemary essential oil, in

methanol was injected into the Phenomenex column. The mobile phase flow rate was set and systematically controlled at 1.25 ± 0.01 mL/min with different methanol proportions (5% to 30%) in water and 16mM of Mβ-CD. The UV detector was operated at 210 nm. In addition, the temperature was controlled with the HPLC at 15 ºC, 45 ºC and 60 ºC. Whenever the mobile-phase solution was changed, the column was first conditioned for at least 1 h with the new solution mixture at a flow rate of 1.0 mL/min.

### 3.4 Molecular modeling

The molecular structures used in this study were built manually using Avogadro [17] or derived from experimental data. The structure of Mβ-CD was built adding a methyl group to the β-CD (obtained by PDB ID 1Z0N) model. The structure of MeJA was obtained from the CACTUS database (NCI/CADD group, USA), and all isomers were built in house using Avogadro. Molecular docking calculations were carried out using default parameters five times in AutoDock Vina [18], except five randomised selected seeds (one for each). Mβ-CD were explicitly considered as rigid during docking simulations. Graphical representations of the docking results were prepared using PyMOL (Molecular Graphics System, version 1.3, Schrödinger, LLC)

### 3.5 Data analysis.

All experiments were carried out three times. Graphical representations were made using SigmaPlot (Version 10.0). ANOVA analysis was carried out using Openoffice Calc (Version 4.2.8.2). Default parameters in Fityk were used for curve fitting [19].

## 4. Results and discussion

### 4.1 Effect of Mβ-CD concentration on MeJA retention

The first step of this investigation was to ascertain whether the addition to the mobile phase of Mβ-CD, a CD not previously tested with MeJA, could reduce the retention time of this elicitor [20].

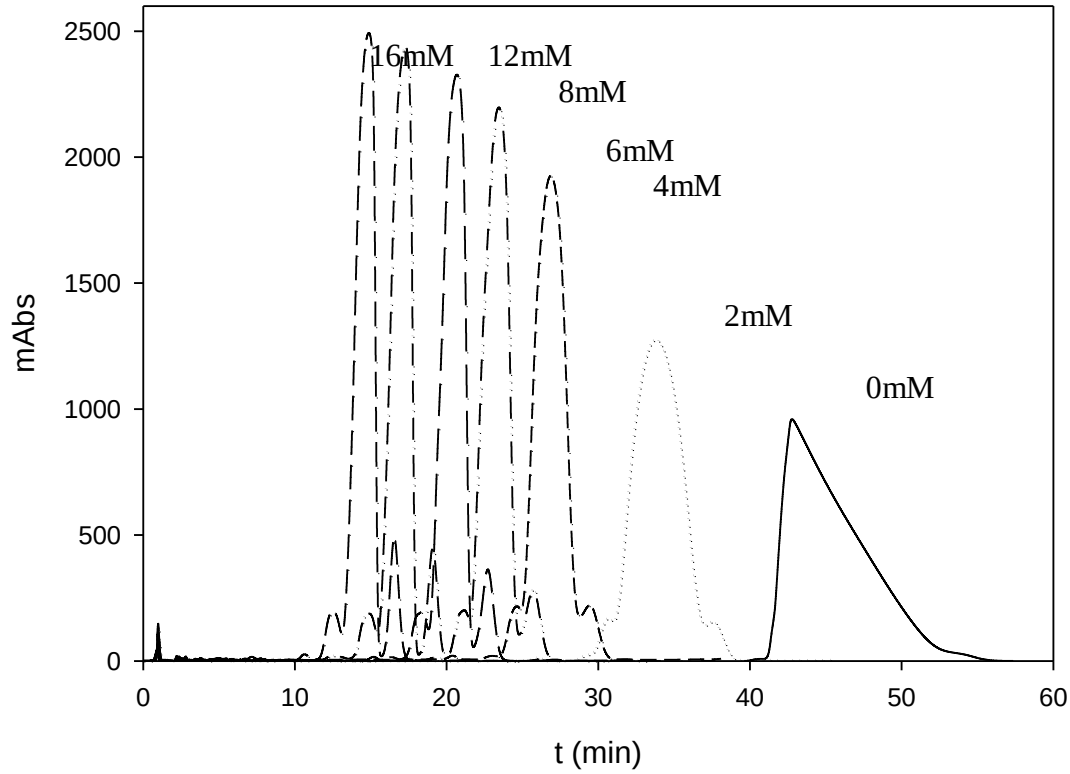


***Fig.*** *2. HPLC chromatograms of MeJA at increasing Mβ-CD concentrations (0-16mM). 150mm C18 column, 40% MeOH, 1.5mL/min at 25ºC*

The MeJA chromatograms obtained at increasing concentrations of Mβ-CD (from 0 to 16 mM) in the mobile phase are presented in **Fig.** 2, where a marked reduction from 42.8 to 14.9 minutes (around 65%) in the MeJA tR can be observed when this elicitor was determined in a C18 Sunfire column using

50:50 water–methanol proportions containing 16 mM Mβ-CD in the mobile phase. The CD reduced the *tR* of *MeJA* because the inclusion complexes between *MeJA* and Mβ-CD enhance guest solubility in the mobile phase thus reducing its residency time in the column. Moreover, the *tR* presented in this work (14.9 min. in the presence of 16 mM Mβ-CD) is the lowest reported for the analysis of MeJA.

This reduction in the *tR* of several compounds when different types of CDs are added to the mobile phases has been used by several researchers to determine the complexation constants of guest/CD complexes [15,21,22]. However, no study has suggested that this decrease in the *tR* might be used to develop a new method to separate and identify the stereoisomers of elicitor compounds.

### 4.2 Validation of the use of CDs in the new HPLC method

To validate the use of CDs as additives in the mobile phase for developing a new analysis method it was first necessary to confirm that the effect of CDs on the MeJA *tR* was not due to the glucidic nature of the CDs, but to their ability to complex hydrophobic compounds.

For this, the possible reduction of the MeJA *tR* due to the presence of D-glucose in the reaction medium was studied since glucose is a molecule included in the CD structure. Thus, various amounts of D-glucose (14 and 112 mM), corresponding to 2 and 16 mM of Mβ-CD (each molecule of Mβ-CD contains seven units of D-glucose in a ring), were added to the 40:60 (v/v) (methanol:water) mobile phase and the *tR* of MeJA was ascertained. The *tR* of MeJA in the absence of any additive was 42.8 min. but decreased in the

presence of 2 mM (33.77 min.) and 16 mM (14.9 min.) Mβ-CD, whereas the addition of D-glucose did not alter the retention times (41.9 min.) significantly**.**

4.3 Study of the complexation of MeJA by MβCD. Stoichiometry of the complex and determination of the apparent racemic complexation constant

The next step therefore was to obtain the MβCD/MeJA complexation constant ($K_F$) and the stochiomnetry of the encapsulation process. Using eq 1 and the data obtained from the chromatogram presented in **Fig.** 3, a plot of 1/k vs. [Mβ-CD] gave a straight line with a linear correlation higher than 0.99, indicating that the presumed stoichiometry of the MeJA/Mβ-CD complexes formed was 1:1 (**Fig. 3** inset, filled circles). On the other hand, when 1/k was plotted vs. $[M\beta\text{-CD}]^2$, a non-linear relationship was obtained (linear correlation of 0.82) (**Fig. 3** *inset*, filled squares), which indicates that the stoichiometry of the inclusion complex is not 2:1.

Table 1: Apparent $K_F$ values for the 3 peaks in a 150mm C18 column at 25ºC and 40% MeOH.

| Peak | $K_F$ ($M^{-1}$) | Correspond to |
|---|---|---|
| 1 | 139.78 +/- 6.98 | (-) EpiMeJA |
| 2 | 117.49 +/- 5.90 | (+/-)MeJA |
| 3 | 105.93 +/- 5.29 | (+) EpiMeJA |

Fitting the obtained data to eq. 1, the $K_F$ values were calculated for each stereoisomers (Table 1). As will be demonstrated in the following section, peak 1 could be (-) EpiMeJA, peak 3 could be (+) EpiMeJA and peak 2 could be the mix of (+/-)MeJA.

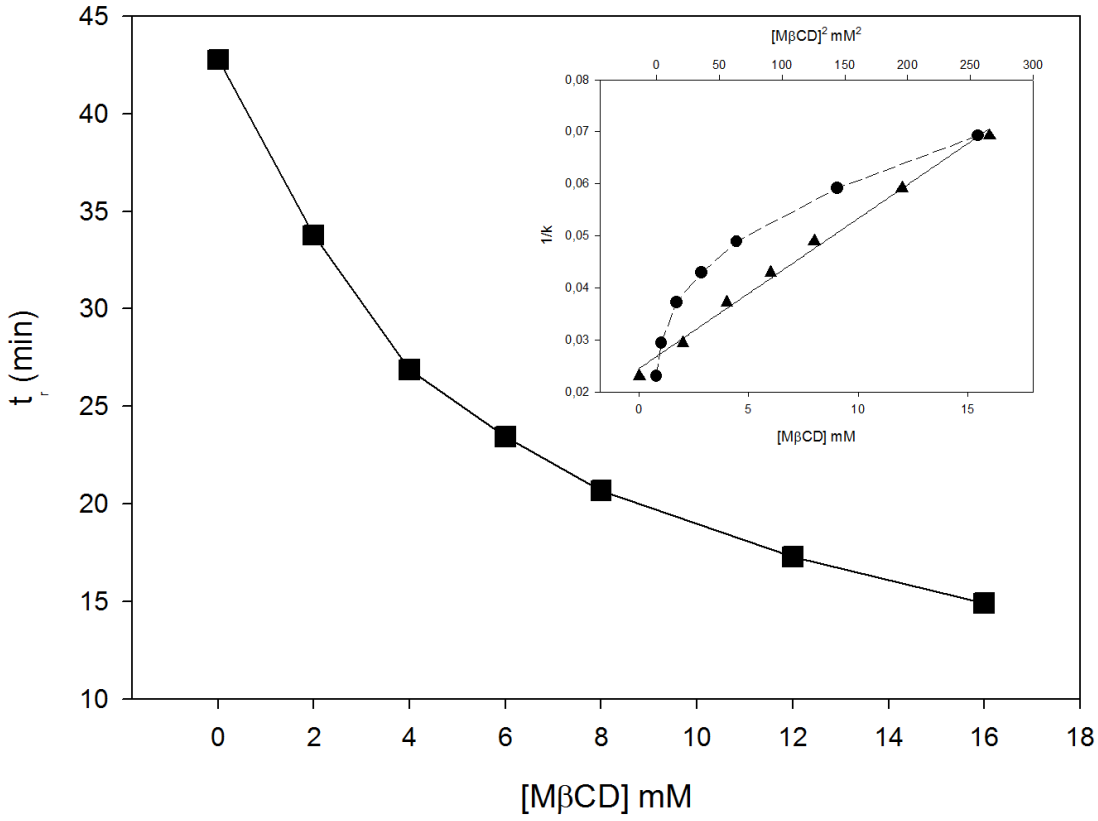


***Fig.*** *3 HPLC tR of MeJA at different Mβ-CD concentrations. Inset: Effect of Mβ-CD concentration on the reciprocal of the capacity factor (k) for a 1:1 model (●) and 2:1 model (▲).*

4.4 Effect of the cyclodextrin structure on complexation constants.

In previous sections it was described how Mβ-CD can be used for encapsulating MeJA. However, it was not clear whether this particular CD was the best for complexing this elicitor. In order to characterize the interaction between MeJA and the host CD at a molecular level, the next step was compare the $K_F$ values between MeJA and several types of CD with different structures, sizes and number of glucose units [20]. Three types of natural CD and three types of modified CDS (Mβ-CD, HPβ-CD and HEβ-CD) were used to this end. As in the previous section when determining the $K_F$ values between

Mβ-CD and MeJA, the relative intensity values calculated experimentally were fitted to the above mentioned equations. The $K_F$ values for different natural and modified species are shown in Table 2.

Table 2: Apparent $K_F$ values and correlation coefficients for different MeJA-CD complexes at 25ºC in a MeOH/water (40:60%) medium [20] compared with our results for the MeJA/MβCD complex.

| Complex | $K_F$ ($M^{-1}$) | Correlation coefficient | |
|---|---|---|---|
| | | 1:1 | 2:1 |
| MeJA/αCD | 30.4 +/- 1.5 | 0.99 | 0.91 |
| MeJA/βCD | 60.9 +/- 2.3 | 0.99 | 0.86 |
| MeJA/γCD | 9.6 +/- 0.08 | 0.99 | 0.92 |
| MeJA/HPβCD | 43.1 +/- 1.6 | 0.99 | 0.89 |
| MeJA/HEβCD | 22.8 +/- 1.1 | 0.99 | 0.89 |
| MeJA/MβCD | 117.49 +/- 5.9* | 0.99 | 0.87 |

* Major peak Used

Among the natural CDs it can be observed that the highest $K_F$ value belonged to β-CD, followed by α-CD and, finally, γ-CD (Table 2). At the molecular level, the data shows that the inner diameter of the CD formed by seven units of glucose (β-CD: 6.0-6.4 Å) fitted MeJA better than the inner diameter of six units (α-: 4.7-5.2 Å) or seven units (γ-CD: 7.5-8.3 Å) of glucose.

However, the $K_F$ obtained with modified CDs (Mβ-CD, HPβ-CD and HEβ-CD) were showed that the best type of CD for encapsulating MeJA is Mβ-CD, and whose $K_F$ was higher than that obtained with other natural and modified CDs (Table 2). Moreover, partial separation of the isomers in the MeJA sample was observed (**Fig.** 2) providing three peaks when a high concentration of Mβ-

CD is present in the mobile-phase. Since Mβ-CD was the most effective CD for complexing MeJA, this modified CD was chosen to continue the investigation.

### 4.5 Enantioseparation of MeJA stereoisomers

Our next step was to optimize separation of the isomers using HPLC-RP with Mβ-CD in the mobile-phase. In this case, the four stereoisomers of MeJA were separated for the first time using HPLC without chiral columns. Such separation was possible because Mβ-CD is a chiral agent and can distinguish between different stereoisomers.

Several mobile-phase analysis conditions were studied, including organic solvent composition (from 40 to 20 % v/v methanol concentration) MβCD concentration (from 0 to 16 mM), temperature (from 5 to 60ºC) and MeJA volume (from 2 to 20 µL). Other parameters, such as the type of column or flow rate in the HPLC system were also optimized.

The results demonstrated that the best conditions for the enantioseparation of MeJA steroisomers are: 20% methanol in the mobile phase, a temperature of 45 ºC and a 16 mM concentration of Mβ-CD. To increase the number of plates in our system, a 250 mm C18 column and a flow of 1.25 mL/min were used at first. As is shown in **Fig.** 4, these conditions permitted the four MeJA stereoisomers to be separated.

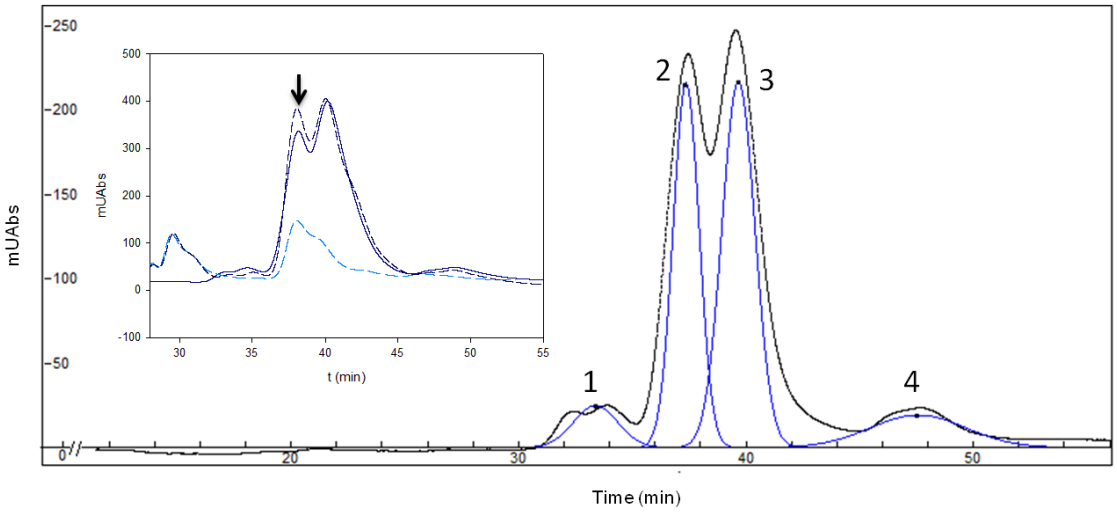


***Fig.*** *4 HPLC chromatogram of the four stereoisomers of MeJA 1) (-)EpiMeJA; 2) (-)MeJA, 3) (+)MeJA and 4) (+)EpiMeJA. Conditions: 250 mm C18 column, 16mM Mβ-CD, 20% MeOH. Flow: 1.25mL/min at 45ºC. In blue, Fityk analysis. Inset: Injection of rosemary essential oil (light blue broken line), MeJA sample (blue continuous line) and coinjection of rosemary essential oil and MeJA sample (blue discontinuous) at the same conditions. Indicated, (-)MeJA.*

## 4.6 Prediction and identification of the four stereoisomers of MeJA

In the absence of any standard, molecular docking was used to predict the order and essential oil samples were used to identify the stereoisomers. Molecular docking is a method which predicts the preferred orientation of one molecule relative to another, when they are mutually bound forming a stable complex. The average docking score was previously correlated with experimental data [23] suggesting that it could be a good manner to predict the order of the stereoisomers in question.

The order of the average docking score of the MeJA stereoisomers was: i) (-)EpiMeJA (-4.46 +/- 0.06); ii) (-)MeJA (-4.40 +/- 0.00); iii) (+)MeJA (-4.26 +/- 0.11) and iv) (+)EpiMeJA (-4.22 +/- 0.11). The quantity in the sample of (+/-

)EpiMeJA indicates that the first and fourth peaks were EpiMeJA. So the prediction could be considered very good. ANOVA analysis provided a p-value for (-)EpiMeJA and (+)EpiMeJA of $p<0.005$, indicating the strength of the prediction. ANOVA analysis of the average docking score of (-)MeJA and (+)MeJA showed $p<0.05$. Although this was also a good value, further certification of the order of the main stereoisomers was thought necessary.

As the differences between the average docking score of (+/-)EpiMeJA were excellent, we focused our interest on (+/-)MeJA. It is well known that essential oils contain many volatiles, for example MeJA. Furthermore, because rosemary essential oil might be used as a natural source of pure (-)MeJA [24], we decided to use a commercial rosemary essential oil as a standard of (-)MeJA. Co-injection of rosemary essential oil and a MeJA sample (**Fig.** 4 Inset) led to a higher second peak, as predicted by our docking study for (-)MeJA.

In conclusion, identification of the four peaks using molecular docking and coinjection of a commercial rosemary essential oil as a standard gave the following results: Peak 1: (-)EpiMeJA: Peak 2: (-)MeJA; Peak 3: (+)MeJA and Peak 4: (+)EpiMeJA.

### 4.7 Molecular modelling

Molecular docking is a good method to predict the preferred orientation of one molecule with regard to another. Therefore, in order to understand how Mβ-CD interacts with the different stereoisomers of MeJA, docking simulations were carried out (**Fig. 5**). The structural information concerning the different binding poses obtained by docking could explain the experimental data obtained.

(-)EpiMeJA docking showed the best result, perhaps because of the better collocation of this stereoisomer and the high number of hydrogen bonds. The second was (-)MeJA, perhaps because of the different orientation of its hydrogen bonds and interaction with Mβ-CD. The third, (+)MeJA, showed a lower number of hydrogen bonds than the others. The different orientation of (+)MeJA with regard to Mβ-CD could explain the score and the standard derivation. Finally, the different orientation of (+)EpiMeJA could have originated its lower degree of complexation.

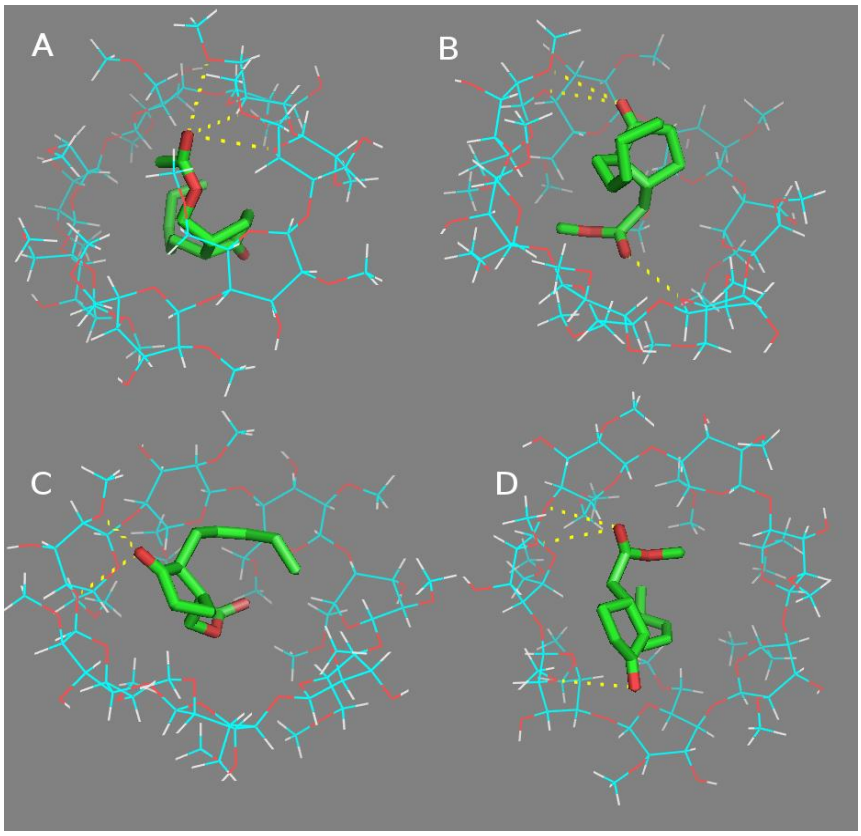


***Fig.*** *5. Docking Results of A: (-) EpiMeJA, B: (-) MeJA, C: (+) MeJA and D: (+) EpiMeJA In yellow, hydrogens bonds.*

To conclude, the use of Mβ-CD as additive in the mobile phase of an RP-HPLC system was seen to be a good alternative for separating MeJA

stereoisomers compared with other, more expensive methods. Moreover, quantification of the interaction between MeJA and Mβ-CD is necessary for inclusion complexes to be used in different areas as cell biology, chemical analysis, or the food and pharmaceutical industries. For this reason, the stoichiometry and complexation constants between both natural and modified CDs and MeJA were calculated and the interaction was modeled by computational methods. After separation, the four stereoisomers of MeJA were identified using molecular docking and coinjection of the commercial racemic mixture with a rosemary essential oil obtaining the following ordination: (-)EpiMeJA, (-)MeJA; (+)MeJA and (+)EpiMeJA. These results could be used for improving the elicitation of cell cultures by using only the best isomer.

## References

[1] A.G. Pérez, C. Sanz, D.G. Richardson, J.M. Olías, Methyl jasmonate vapor promotes β-carotene synthesis and chlorophyll degradation in Golden Delicious apple peel, J. Plant Growth Regul. 12 (1993) 163–167. doi:10.1007/BF00189648.

[2] M. Saniewski, J. Czapski, The effect of methyl jasmonate on lycopene and β-carotene accumulation in ripening red tomatoes, Experientia. 39 (1983) 1373–1374. doi:10.1007/BF01990110.

[3] E.-A.M.A.M. Pour, Effect of Methyl Jasmonate on Resveratrol Production in Leaf and Fruit of Two Iranian Grape ( Vitis vinifera L.) Cultivars, J. Sci. Technol. Agric. Nat. Resour. 12 (2008) 571–579.

[4] D. Lijavetzky, L. Almagro, S. Belchi-Navarro, J.M. Martinez-Zapater, R. Bru, M.A. Pedreno, Synergistic effect of methyljasmonate and cyclodextrin on stilbene biosynthesis pathway gene expression and resveratrol production in Monastrell grapevine cell cultures, BMC Res. Notes. 1 (2008) 132. doi:10.1186/1756-0500-1-132.

[5] H. J. D. Lalel, Zora Singh, S. C. Tan, The role of methyl jasmonate in mango ripening and biosynthesis of aroma volatile compounds, J. Hortic. Sci. Biotechnol. 78 (2003) 470–484.

[6] E.E. Farmer, C.A. Ryan, Octadecanoid Precursors of Jasmonic Acid Activate the Synthesis of Wound-Inducible Proteinase Inhibitors., Plant Cell. 4 (1992) 129–134. doi:10.1105/tpc.4.2.129.

[7] F. de la Peña Moreno, G.P. Blanch, M.L. Ruiz del Castillo, (+)-methyl jasmonate-induced bioformation of myricetin, quercetin and kaempferol in red raspberries, J. Agric. Food Chem. 58 (2010) 11639–11644. doi:10.1021/jf102875b.

[8] A. Tassoni, L. Durante, M. Ferri, Combined elicitation of methyl-jasmonate and red light on stilbene and anthocyanin biosynthesis, J. Plant Physiol. 169 (2012) 775–781. doi:10.1016/j.jplph.2012.01.017.

[9] T.E. Acree, R. Nishida, H. Fukami, Odor thresholds of the stereoisomers of methyl jasmonate, J. Agric. Food Chem. 33 (1985) 425–427. doi:10.1021/jf00063a025.

[10] M.H. Beale, J.L. Ward, Jasmonates: key players in the plant defence, Nat. Prod. Rep. 15 (1998) 533–548. doi:10.1039/A815533Y.

[11] H. Kiyota, E. Higashi, T. Koike, T. Oritani, Lipase-catalyzed preparation of both enantiomers of methyl jasmonate, Tetrahedron Asymmetry. 12 (2001) 1035–1038. doi:10.1016/S0957-4166(01)00169-0.

[12] H. Yamane, N. Takahashi, U.-I. Ueda, J. Kato, Resolution of (±)-Methyl Jasmonate by High Performance Liquid Chromatography and the Inhibitory Effect of (+)-Enantiomer on the Growth of Rice Seedlings., Agric. Biol. Chem. 45 (1981) 1709–1711. doi:10.1080/00021369.1981.10864755.

[13] G.P. Blanch, G. Flores, M. del Mar Caja, M.L. Ruiz del Castillo, Enantioselective isolation of methyl jasmonate using permethyl-β-cyclodextrin HPLC, J. Sep. Sci. 32 (2009) 180–184. doi:10.1002/jssc.200800444.

[14] G. Flores, G.P. Blanch, M.L. Ruiz del Castillo, Isolation of the four methyl jasmonate stereoisomers and their effects on selected chiral volatile compounds in red raspberries, Food Chem. 141 (2013) 2982–2987. doi:10.1016/j.foodchem.2013.05.117.

[15] J.M. López-Nicolás, E. Núñez-Delicado, A.J. Pérez-López, A.C. Barrachina, P. Cuadra-Crespo, Determination of stoichiometric coefficients and apparent formation constants for beta-cyclodextrin complexes of trans-resveratrol using reversed-phase liquid chromatography, J. Chromatogr. A. 1135 (2006) 158–165. doi:10.1016/j.chroma.2006.09.013.

[16] K. Fujimura, T. Ueda, M. Kitagawa, H. Takayanagi, T. Ando, Reversed-phase retention behavior of aromatic compounds involving .beta.-cyclodextrin inclusion complex formation in the mobile phase, Anal. Chem. 58 (1986) 2668–2674. doi:10.1021/ac00126a020.

[17] M.D. Hanwell, D.E. Curtis, D.C. Lonie, T. Vandermeersch, E. Zurek, G.R. Hutchison, Avogadro: an advanced semantic chemical editor, visualization, and analysis platform, J. Cheminformatics. 4 (2012) 17. doi:10.1186/1758-2946-4-17.

[18] O. Trott, A.J. Olson, AutoDock Vina: improving the speed and accuracy of docking with a new scoring function, efficient optimization, and multithreading, J. Comput. Chem. 31 (2010) 455–461. doi:10.1002/jcc.21334.

[19] M. Wojdyr, Fityk: a general-purpose peak fitting program, J. Appl. Crystallogr. 43 (2010) 1126–1128. doi:10.1107/S0021889810030499.

[20] J.M. López-Nicolás, M. Escorial Camps, H. Pérez-Sánchez, F. García-Carmona, Physicochemical and Thermodynamic Characterization of the Encapsulation of Methyl Jasmonate by Natural and Modified Cyclodextrins Using Reversed-Phase High-Pressure Liquid Chromatography, J. Agric. Food Chem. 61 (2013) 11347–11354. doi:10.1021/jf402920p.

[21] J.M. López-Nicolás, F. García-Carmona, Rapid, simple and sensitive determination of the apparent formation constants of trans-resveratrol complexes

with natural cyclodextrins in aqueous medium using HPLC, Food Chem. 109 (2008) 868–875. doi:10.1016/j.foodchem.2008.01.022.

[22] J.M. López-Nicolás, P. Rodríguez-Bonilla, L. Méndez-Cazorla, F. García-Carmona, Physicochemical study of the complexation of pterostilbene by natural and modified cyclodextrins, J. Agric. Food Chem. 57 (2009) 5294–5300. doi:10.1021/jf900285e.

[23] P. Sivaprakasam, P.N. Tosso, R.J. Doerksen, Structure−Activity Relationship and Comparative Docking Studies for Cycloguanil Analogs as PfDHFR-TS Inhibitors, J. Chem. Inf. Model. 49 (2009) 1787–1796. doi:10.1021/ci9000663.

[24] M.L. Ruiz Del Castillo, G.P. Blanch, Enantiomeric purity of (+/-) -methyl jasmonate in fresh leaf samples and commercial fragrances, J. Sep. Sci. 30 (2007) 2117–2122. doi:10.1002/jssc.200700115.

# Block II Part II

# Applications of cyclodextrins in Food Science.

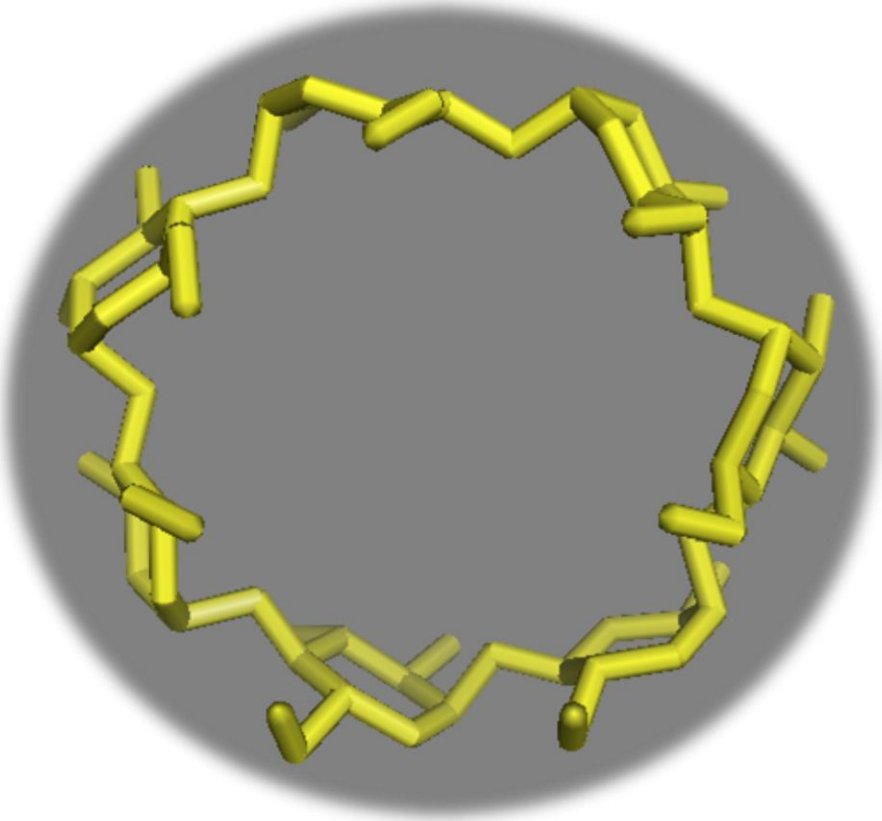

## Introduction

Food science is a multidisciplinary field. It can be defined as <<*the application of basic sciences and engineering to study the physical, chemical, and biochemical nature of foods and the principles of food processing*>> [1].

Studies of half-life of products, food composition and processing, sensory evaluation, among others are some of the topics investigated in food science.

Bearing our introduction in mind, it is obvious to find several applications of cyclodextrins on food science. From to increase bioactive compounds solubility to improve stability, cyclodextrins have a great potential in this part application.

In this section we are going to show some applications of CDs in food science such as i) the development of a nanosensor for blueberries, ii) a stabilization of a bioactive compound using CDs and iii) a food model study of stability.

## References

[1] Potter N.N., Hotchkiss J.H. Introduction: Food Science as a Discipline. In: Food Science. Food Science Text Series. (1995) Springer, Boston, MA doi: 10.1007/978-1-4615-4985-7_1

# Block II part II

# Chapter I

## *Ellagic acid-borax fluorescence interaction. Laying the foundations of a novel cyclodextrin-borax nanosensor for analyzing ellagic acid in food samples*

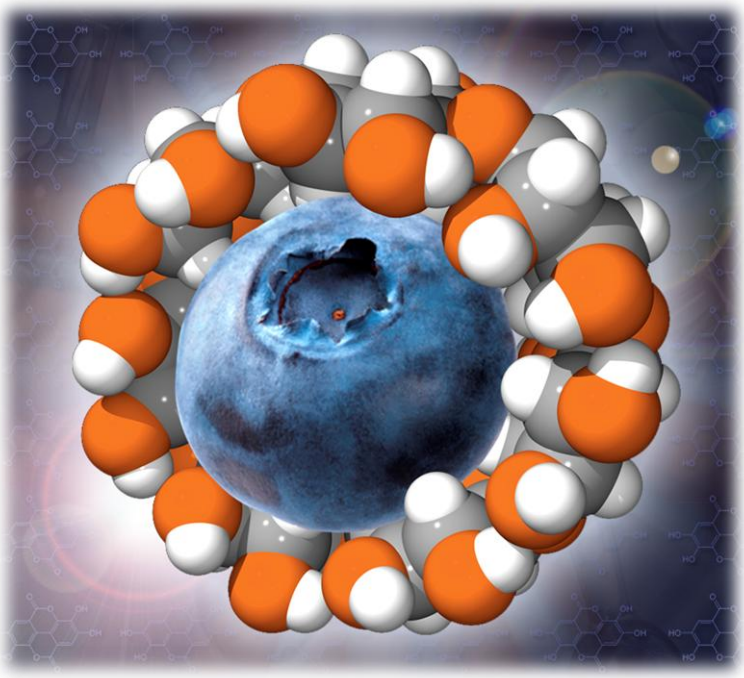

**Abstract**

This chapter describes a novel fluorecence nanosensor based on cyclodextrin (CDs) to determine ellagic acid (EA). The encapsulation of EA in the presence of borax was studied.

Firstly, the complexation of EA-borax was tested. The stoichiometry of the EA-borax complex showed a 1:2 complex, with a $K_{F1}$ = 2548 +/- 127 $M^{-1}$ and a $K_{F2}$ = 302 +/- 15 $M^{-1}$. Different CDs were used to obtain a 1:1:1 CD-EA-borax complex γ-CD providing the best complexation constant ($K_{F3}$ = 364 +/- 18 $M^{-1}$).

Furthermore, when the accuracy and sensitivity of the signal as nanosensor were tested using a crude blueberry extract , the CD/borax mixture provided an 18 times stronger signal than the crude extract alone and 7 times stronger than the obtained by borax alone.

## Index

## 1. Contextualization

Ellagic acid (**Fig**. **1**, EA, 2,3,7,8-Tetrahydroxy-chromeno[5,4,3-cde]chromene-5,10-dione) is a symmetric natural phenol bioactive compound present in pomegranates, grapes, strawberries, blueberries and raspberries [1]. It has been recently studied for its bioactive characteristics as an antioxidant [2], anti-inflammatory [3], anticancer [4], anti-lipoxidation or anti-microbial [1] agent.

At present, methods to analyze EA focus on chromatographic solutions [5,6], although other easier and cheaper methods would be welcome. In this respect, it is well known that the complex EA-borax presents fluorescence [7], the measurement of which is one of the most powerful and sensitive methods for analyzing compounds. Moreover, EA has been shown to act as a ligand of cyclodextrins (CDs) encapsulation [8]. With this idea in mind and since CDs can increase the fluorescence signal of a complex [9–11] , the possibility of creating a novel nanosensor based on fluorescence was studied.

## 2. Objectives

i) To study the fluorescence signal of the binary complex, EA-borax, and determine its stoichiometry.
ii) To evaluate the encapsulation mechanism of the binary EA-borax complex using different types of CDs.
iii) To determine the stoichiometry and $K_F$ (complexation constant) values for the ternary complex EA-borax/CD.
iv) To test the use of this complex as nanosensor using a crude extract of blueberries.

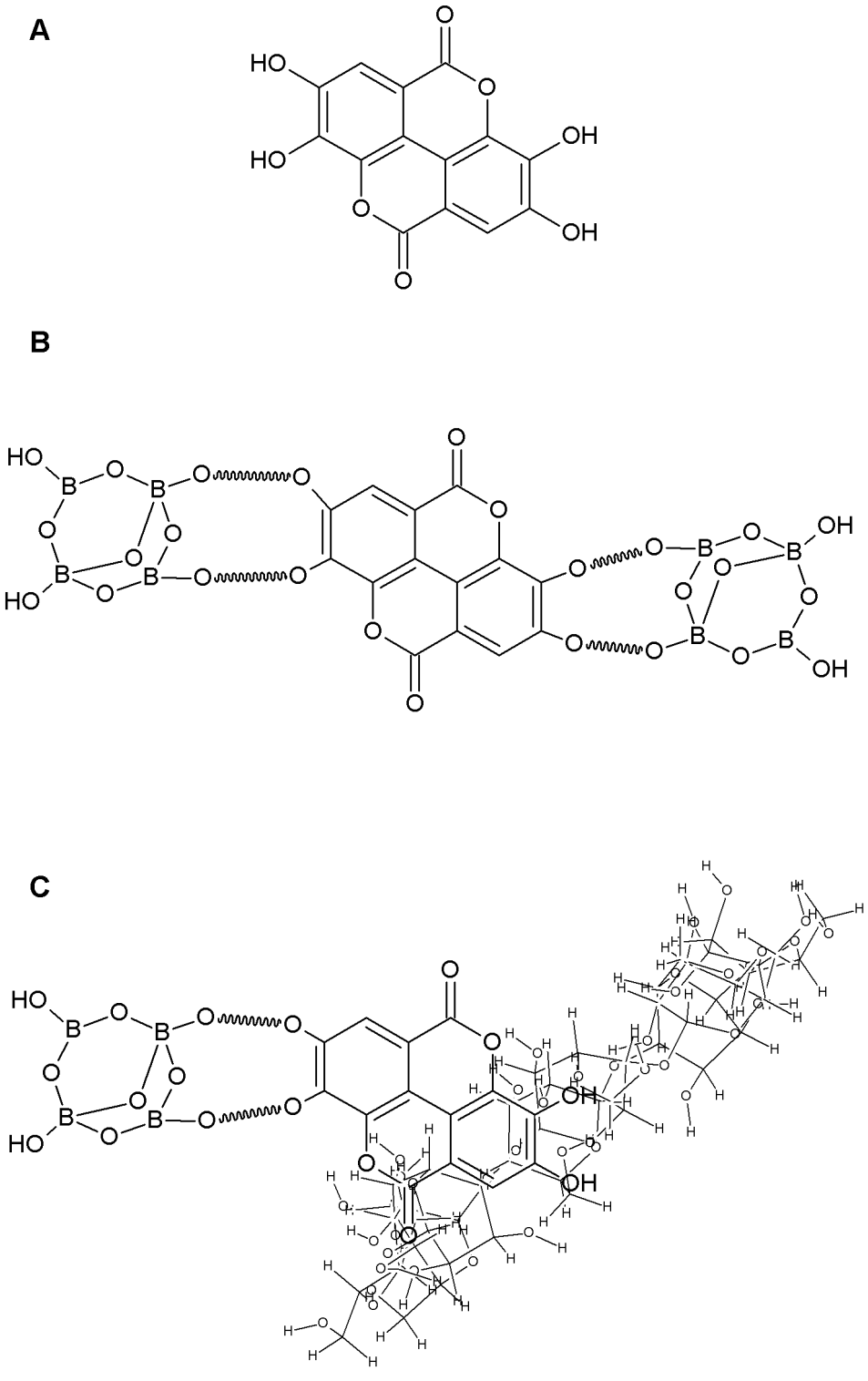


***Fig.** 1: (A) Structure of ellagic acid. (B) representation of EA-borax complex and (C) representation of CD-EA-borax complex.*

## 3. Materials and methods

### 3.1 Material

Ellagic acid (EA, ≥ 95 % purity, CID 5281855) was purchased from Sigma-Aldrich (Madrid, Spain) and kept in darkness. The CDs tested (α-, β-, γ-, 2-Hydroxypropyl-βCD and Methyl-βCD were purchased from Sigma-Aldrich. Borax (Sodium tetraborate) was purchased from Panreac (Barcelona, Spain).

### 3.2 Fluorescence studies

Maximum and minimum fluorescence were determined using a Shimazdu RF-6000 Spectrofluorimeter equipped with thermostatically controlled cells, setting both excitation and emission bandwidths were set at 5nm. Spectral measurements were made to obtain the excitation (358 nm) and emission (430 nm) maxima and the borax concentration (15 mM) studied. A 500 µL Super Micro Fluorescence cuvette from Hellma was used. The concentration of EA was fixed at 25 µM and the CD concentration range between 0 and 40 mM. All reagents were dissolved in water or buffer with the exception of EA, which was dissolved in ethanol.

The complexes were prepared using a 0.8 mM EA solution in ethanol, an appropiate (between 8-50 mM) solution of each CD, a 0.1 M sodium-phosphate buffer pH 7and 0.1 M borax in 0.1 M sodium-phosphate buffer pH 7. Different volumes of each reactant were added in the following order i) buffer, ii) borax, iii) CD (if it was necessary) and iv) EA to set the desired concentrations in each sample. Later, samples were incubated for 10 minutes in darkness before measurements were made without further purification.

## 3.3 Complexation constant determination

### *3.3.1 EA-borax interaction*

To determine the stoichiometry of the complex between the EA molecule and one or two molecules of borax, the Benesi-Hildebrand method [12] was first used. However, the symmetry of the molecule suggested two possible complexation sites, with two complexation constants ($K_{F1}$ and $K_{F2}$). So, a new model was created following the method developed for the rapid equilibrium assumption in steady state [13].

Two possible equilibria were obtained

$$\text{EA} + \text{Borax} \rightleftharpoons \text{EA-borax} \overset{\text{Borax}}{\rightleftharpoons} \text{EA-borax}_2$$

The encapsulation constant, $K_F$, is given by:

$$K_{F1} = \frac{[\text{EA}-\text{Borax}]}{[\text{Borax}]\,[\text{EA}]} \quad (1)$$

$$K_{F2} = \frac{[\text{EA}-\text{Borax}_2]}{[\text{EA}-\text{Borax}]\,[\text{Borax}]} \quad (2)$$

The mathematical model used to obtain the complexation constants was:

$$\Delta_F = 1 + \frac{\Delta_{F1}\cdot K_{F1}\cdot[\text{Borax}] + \Delta_{F2}\cdot K_{F1}\cdot K_{F2}\cdot[\text{Borax}]^2}{1 + K_{F1}\cdot[\text{Borax}] + K_{F1}\cdot K_{F2}\cdot[\text{Borax}]^2} \quad (3)$$

where [Borax] denotes the borax concentration; ΔF is the experimentally measured fluorescence intensity; $\Delta F_1$ the fluorescence intensity when one center of EA is complexed with borax; $\Delta F_2$ is the fluorescence intensity when

the two borax are linked and $K_{F1}$ and $K_{F2}$ are the complexation constants for 1 or 2 borax, respectively.

### *3.3.2 EA-borax-CD interaction*

In addition, CDs were included, and a new mathematical expression was obtained for the new equilibrium.

At high $K_{F1}$ values (see results and discussion), it is supposed that CDs

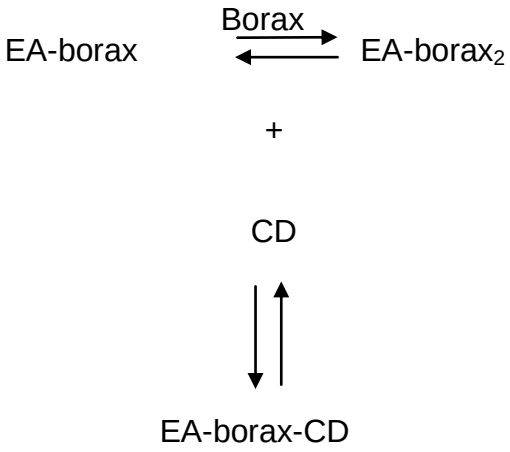


The formation of the EA-borax-CD complex is given by:

$$K_{F3} = \frac{[EA-Borax_2-CD]}{[EA-Borax]\,[CD]} \quad (4)$$

The other model used to analyze the interaction with CDs was:

$$\Delta_F = 1 + \frac{\Delta_{F2}\cdot K_{F2}\cdot[Borax] + \Delta_{F3}\cdot K_{F3}[CD]}{1 + K_{F3}\cdot[CD] + K_{F2}\cdot[Borax]} \quad (5)$$

where ΔF is the experimentally measured fluorescence intensity, $\Delta F_2$ is the fluorescence due to the interaction with borax, and $\Delta F_3$ is the fluorescence due to CD, and $K_{F3}$ is the complexation constant for the equilibrium with CDs. The pH was fixed at 7 using 0.1 M sodium-phosphate with or without borax.

### 3.4 EA purification for Blueberry

Blueberries were bought in a local supermarket. Thirty grams of blueberries were homogenized with mortar and pestle with 100 mL of MeOH at 4 ºC. The resulting mixture was incubate for 30 min and filtered using a 0.22 µm filter.

### 3.5 Crude blueberry extract analysis

0.05 mL of blueberry crude extract was analyzed using a Shimazdu RF-6000 spectrofluorimeter equipped with thermostatically controlled cells. The measurements were used to obtain the excitation (358 nm) and emission (430 nm) maxima and the borax (15 mM) and γ-CD (10 mM) concentrations. A 500 µL Super Micro Fluorescence cuvette from Hellma was used. A calibration plot was obtained using pure EA sample, with $R^2 > 0.999$, which was used to determine EA concentration.

### 3.6 Data analysis

All experiments were carried out in triplicate. Regressions, the non-linear analysis and Graphics were made using Sigma-Plot (version 10.0.0.54), except in the case of the spectra graphics, which were made by the spectrofluorimeter software. A t-test was carried out using Rstudio (version 0.99.878) with a significance of $P < 0.05$. Other mathematical operations were carried out using wxMaxima (version 12.04.0).

## 4. Results and discussion

### 4.1 Study of fluorescence behavior and stoichiometry of the binary EA-borax complex

As mentioned above, EA is only fluorescent in the presence of borax [7]. For this reason, the first step was to obtain the excitation and emission maxima, which were at 358 and 430 nm, respectively. Then, the fluorescence behavior of the binary EA-borax complex was studied using the Benesi-Hildebrand method because it correlates changes in the fluorescence with changes in the physico-chemical states obtained by adding molecules.

**Fig**. 2 presents the effect of adding borax on the EA fluorescence signal. It is clear that there is a direct correlation. That curve seems to represent a 1:2 complex between borax and EA; however, its symmetry means that the two complexation poses are difficult to study. Although the data fitted a 1:1 complex with the original Benesi-Hildebrand method (data not shown), at values below 1 mM of Borax the behavior of the curve was unusual, becoming sigmoidal, not a line. To clarify this, eq. 3 was generated to try to identify the two possible complexation constants. **Fig**. 2 also shows the fit of eq. 3 to the data, which presented an $R^2 \approx 0.99$ and a $K_{F1} = 2548 +/- 127\ M^{-1}$ and a $K_{F2} = 302 +/- 15\ M^{-1}$.

Although Wolfbeis & Hochmuth in 1986 said that the stoichiometry between EA and borax is 1:1, it is possible that they did not decrease the borax concentration enough to find the first constant. Furthermore, the fluorescence behavior of both constants is clearly different. Below 0.05 mM ($5 \cdot 10^{-5}$ M) the interaction is not strong enough to make EA fluoresce, while above 0.05 mM (5

· $10^{-5}$ M) the complex is fluorescent (**Fig**. 2 *insert*). These results would be due to the symmetry of the molecule and, perhaps, due to internal resonance.

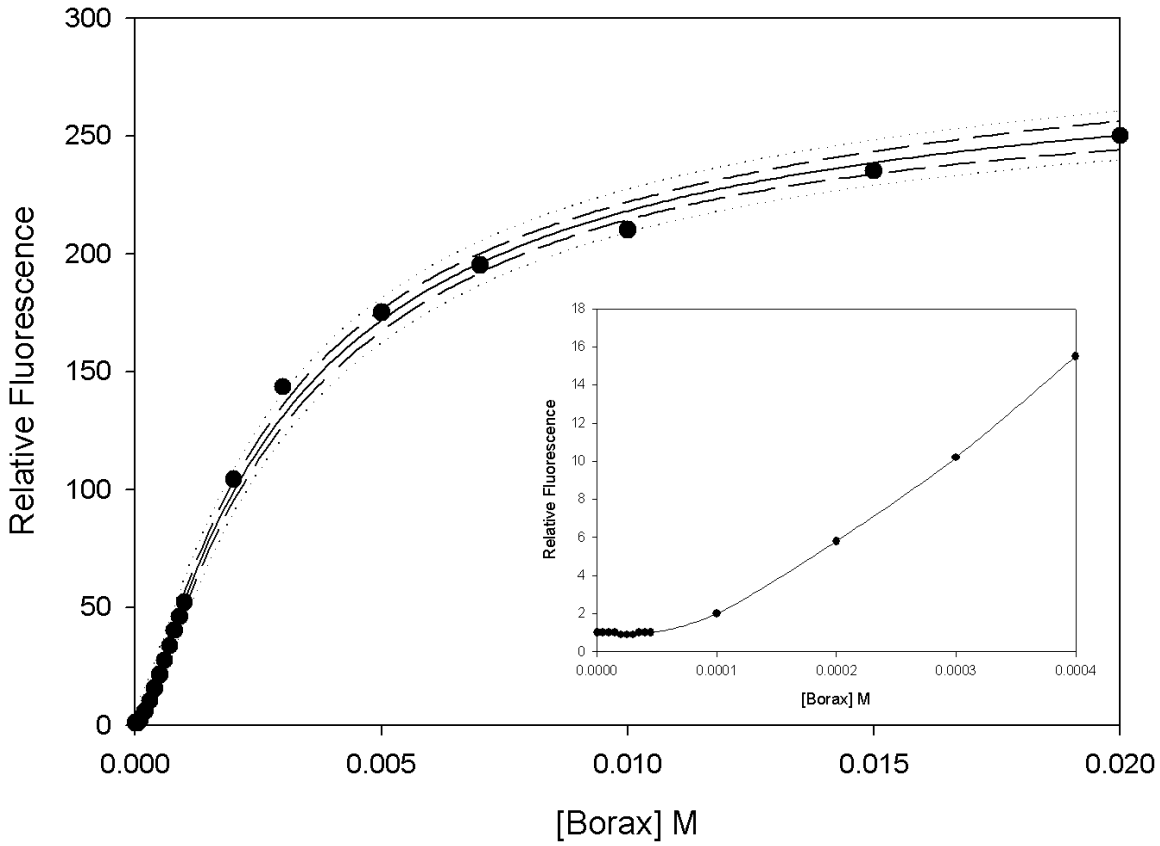


***Fig.*** *2: Ploting data of fluorescence vs Borax concentration with eq. 3 (—) is the adjust, (---) is the 95% confidence level and (···) is the 95% prediction level (EA 25 μM pH 7 and 25 ºC). Insert: dependence of emission fluorescence intensities of EA 25 μM on borax concentration.*

4.2 Study of the stoichiometry and determination of the complexation constants between EA-borax and CDs

Bearing the above in mind, we know that Borax not only increases the fluorescence behavior of EA, but also links with it through a 1:2 stoichiometry. As now is EA-borax$_2$ the ligand instead of EA, the complexation stoichiometry

between pure EA and CD might change. According to Bulani et al., 2016, a 1:2 stoichiometry occurs between EA and CD. So, the next step was to check the stoichiometry in the EA-borax-CD complex. Firstly, a suitable borax concentration was studied, where slight concentration differences could not affect the signal. As it could be saw in **Fig**. 2 *insert*, due to the slight increase of fluorescence signal later than 10 mM, 15 mM of Borax concentration was fixed.

There have been no studies of the influence of CD on EA fluorescence, especially in the presence of borax. Firstly, a study without borax but with increasing CD concentrations was carried out, finding no increase in fluorescence. Therefore, the behavior of the EA-borax complex was studied in the presence of γ-CD, the largest natural CD of those commonly used. The increase in the relative fluorescence of EA was plotted for increasing concentrations of γ-CD added to the medium (**Fig**. **3**). The curve obtained was more like a typical Benesi-Hildebrand curve [12] but was not a hyperbole presumably because of the equilibrium between the uploading of γ-CD and the release of one borax (with only cyclodextrin, the system shows no fluorescence). **Fig**. 3 also shows the plot of our data using the new equation ($R^2$ > 0.99) suggesting that the supposition is correct. The $K_{F3}$ value obtained for this neutral pH was $K_{F3}$ = 364 +/- 18 $M^{-1.}$ These results do not agree with those in the bibliography, where only EA was analyzed, because borax interacts with EA changing the complexation possibilities. When EA is combined with borax at a sufficiently high concentration, the two sites are linked by borax; the introduction of CD releases one of the borax, and the EA-borax-CD complex is created.

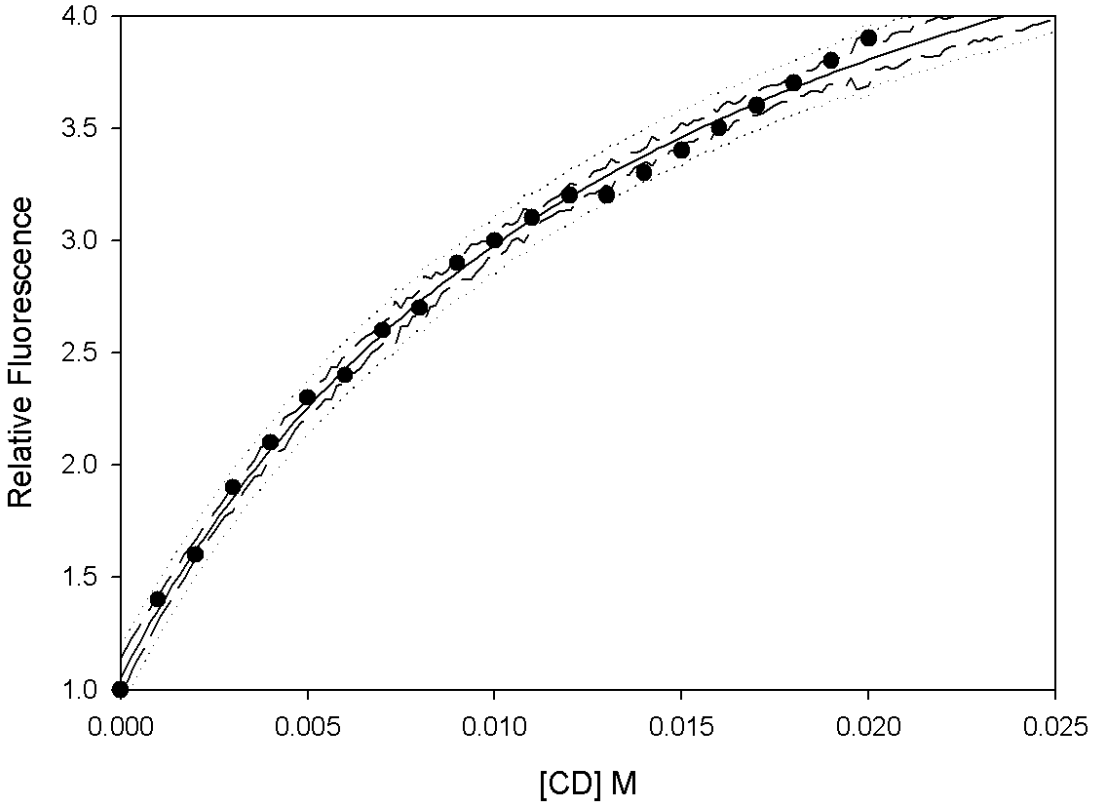


***Fig.*** *3: Ploting data of fluorescence vs γ-CD concentration with eq. 5 (—) is the adjust, (---) is the 95% confidence level and (⋯) is the 95% prediction level (EA 25 μM pH 7 and 25 ºC).*

4.3 Selection of the optimum type of CD for the encapsulation of EA-borax

To increase the efficiency of the fluorescence signal, natural (α- and β-CD) and modified ( 2-hydroxypropyl-βCD [HPβ-CD] and Methyl-βCD [Mβ-CD]) CDs were used. Whereas α-CD and β-CD did not result in a sufficient interaction to determine any $K_{F3}$, HPβ-CD and Mβ-CD showed similar values (73 +/- 6 and 81 +/- 6 $M^{-1}$ respectively). The t-test was not passed (P ≈ 0.07), so there are no differences in the strength of complexation using HPβ-CD or Mβ-CD. Our results, γ-CD > Mβ-CD ≈ HPβ-CD > α-CD and β-CD could be due to neither α-

CD or β-CD having an optimal cavity to complex EA-borax; however, when the CD presented a greather surface area (HPβ-CD or Mβ-CD) or a larger cavity (γ-CD) the complexation was more efficient.

Testing the fluorescence-based nanosensor with blueberry crude extract

The next step was to test the nanosensor using a real sample. A crude extract of blueberries in methanol was prepared mixed with a buffer of borax at our concentration (15 mM) and γ-CD (10 mM). Fluorescence excitation and emission were the same (358 and 430 nm) as for pure EA, with a deviation of +/- 3 nm in the triplicate experiment, meaning that there was no interference with any other molecule (**Fig.** 4). The increase in the fluorescence signal when15 mM borax and 10 mM of γ-CD were present was almost 18 times (3500 fluorescence units *vs*. 205) higher than with extract alone, and 7 times (3500 fluorescence units *vs*. 546) higher than with borax. A calibration curve was made with a $R^2 > 0.999$ (**Fig.** 4 *insert*), giving us a concentration of EA of 3.3 mg/mL in the crude extract. These results demonstrated the possibility of using CD and borax to analyse EA in food samples. Furthermore, the presence of CDs to create a ternary complex is highly recommended due to the pronounced increase in signal.

In conclusion, the fluorescence of EA in the presence of borax and CDs provides an excellent basis for developing a novel fluorecence nanosensor to determine EA. The results showed, fistly, that the binary complex between EA and Borax is not 1:1, but a 1:2 model with a $K_{F1}$ = 2548 +/- 127 $M^{-1}$ and a $K_{F2}$ = 302 +/- 15 $M^{-1}$.

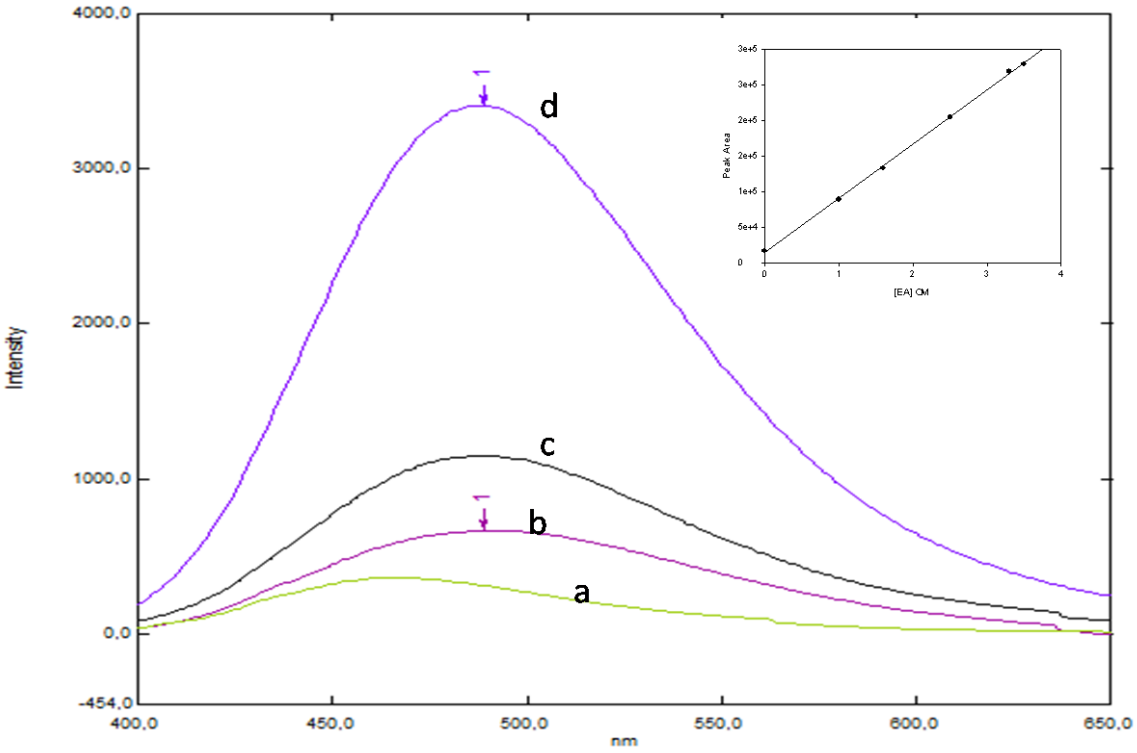


***Fig.*** *4: Fluorescence signal of Blueberry extract with a) nothing, b) 15 mM borax, c) 15 mM borax + 5 mM γ-CD and d) 15 mM borax + 10 mM at pH 7 and 25 ºC. Indicated, emission maximun. Insert: Calibration curve of EA ($R^2$ > 0.999)*

Secondly, when the effect of adding different CDs was tested to increase the fluorescence signal, the best CD to create the EA-borax-CD complex was γ-CD (complexation constant, $K_{F3}$ = 364 +/- 18 $M^{-1}$) with a 1:1:1 complex between them. The accuracy and sensitivity of the signal as nanosensor was tested using a crude blueberry extract, and was seen to provide an 18 times more potent signal than the pure extract alone, and 7 times higher than with borax alone. This work lays the basics for a novel method to determine EA and, moreover, increases of knowledge of the EA-borax interaction.

## References

[1] J.M. Landete, Ellagitannins, ellagic acid and their derived metabolites: A review about source, metabolism, functions and health, Food Res. Int. 44 (2011) 1150–1160. doi:10.1016/j.foodres.2011.04.027.

[2] I. Kilic, Y. Yeşiloğlu, Y. Bayrak, Spectroscopic studies on the antioxidant activity of ellagic acid, Spectrochim. Acta. A. Mol. Biomol. Spectrosc. 130 (2014) 447–452. doi:10.1016/j.saa.2014.04.052.

[3] M. Kassim, M. Achoui, M.R. Mustafa, M.A. Mohd, K.M. Yusoff, Ellagic acid, phenolic acids, and flavonoids in Malaysian honey extracts demonstrate in vitro anti-inflammatory activity, Nutr. Res. 30 (2010) 650–659. doi:10.1016/j.nutres.2010.08.008.

[4] N.P. Seeram, L.S. Adams, S.M. Henning, Y. Niu, Y. Zhang, M.G. Nair, D. Heber, In vitro antiproliferative, apoptotic and antioxidant activities of punicalagin, ellagic acid and a total pomegranate tannin extract are enhanced in combination with other polyphenols as found in pomegranate juice, J. Nutr. Biochem. 16 (2005) 360–367. doi:10.1016/j.jnutbio.2005.01.006.

[5] Y. Amakura, M. Okada, S. Tsuji, Y. Tonogai, High-performance liquid chromatographic determination with photodiode array detection of ellagic acid in fresh and processed fruits, J. Chromatogr. A. 896 (2000) 87–93. doi:10.1016/S0021-9673(00)00414-3.

[6] W. Mullen, T. Yokota, M.E.J. Lean, A. Crozier, Analysis of ellagitannins and conjugates of ellagic acid and quercetin in raspberry fruits by LC–MSn, Phytochemistry. 64 (2003) 617–624. doi:10.1016/S0031-9422(03)00281-4.

[7] O.S. Wolfbeis, P. Hochmuth, The fluorescence of ellagic acid and its borax complex, Monatshefte Für Chem. Chem. Mon. 117 (1986) 369–374. doi:10.1007/BF00816531.

[8] V.D. Bulani, P.S. Kothavade, H.S. Kundaikar, N.B. Gawali, A.A. Chowdhury, M.S. Degani, A.R. Juvekar, Inclusion complex of ellagic acid with β-cyclodextrin: Characterization and in vitro anti-inflammatory evaluation, J. Mol. Struct. 1105 (2016) 308–315. doi:10.1016/j.molstruc.2015.08.054.

[9] J.M. López-Nicolás, P. Rodríguez-Bonilla, F. García-Carmona, Complexation of pinosylvin, an analogue of resveratrol with high antifungal and antimicrobial activity, by different types of cyclodextrins, J. Agric. Food Chem. 57 (2009) 10175–10180. doi:10.1021/jf902519d.

[10] A. Matencio, C.J.G. Hernández-Gil, F. García-Carmona, J.M. López-Nicolás, Physicochemical, thermal and computational study of the encapsulation of rumenic acid by natural and modified cyclodextrins, Food Chem. 216 (2017) 289–295. doi:10.1016/j.foodchem.2016.08.023.

[11] A. Matencio, F. García-Carmona, J.M. López-Nicolás, Encapsulation of piceatannol, a naturally occurring hydroxylated analogue of resveratrol, by natural and modified cyclodextrins, Food Funct. 7 (2016) 2367–2373. doi:10.1039/c6fo00557h.

[12] H.A. Benesi, J.H. Hildebrand, A Spectrophotometric Investigation of the Interaction of Iodine with Aromatic Hydrocarbons, J. Am. Chem. Soc. 71 (1949) 2703–2707. doi:10.1021/ja01176a030.

[13] S. Cha, A Simple Method for Derivation of Rate Equations for Enzyme-catalyzed Reactions under the Rapid Equilibrium Assumption or Combined Assumptions of Equilibrium and Steady State, J. Biol. Chem. 243 (1968) 820–825.

# Block II part II

# Chapter II

## *Stabilization of phenylethylamine-betaxanthin using cyclodextrins for juice products*

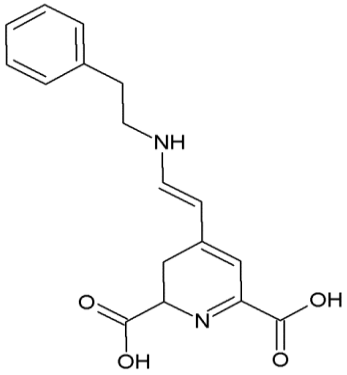


**Abstract**

Nowadays the use of betalains as bioactive compounds is highly investigated. However, its use as functional foods requires a more exhaustive study due to its low stability and photosensibility. In this work, the stabilization of a powerful betalain derivative, phenylethylamine-betaxanthin (Fetyl-Bet), was studied using cyclodextrins (CDs). A complete study of its encapsulation with natural and modified CDs was carried out. Methyl-β-CD (Mβ-CD) showed the best results at pH 3 ($K_F$ = 17.08 ± 0.85 $mM^{-1}$) and 7 ($K_F$ = 8.88 ± 0.71 $mM^{-1}$) of all CDs tested. In addition, the effect of pH and temperature was studied. $K_F$ value was increased when pH decreased.

The temperature behavior showed a decrease of $K_F$ at high temperature; moreover, thermodynamic parameters ($\Delta H^o$, $\Delta S^o$ and $\Delta G^o$) were calculated. Molecular docking calculations provided further insights into how the different interactions influence the complexation constant. Finally, the results show a strong remaining of Fetyl-Bet quantity in presence of this complexating compound. This study is a first step to introduce its type of compounds in functional foods.

## Index

## 1. Contextualization

A novel bioactive compounds family that is currently investigated is Betalains. Betalains are vacuolar nitrous pigments using betalamic acid as core structure. The betalamic acid forms a Schiff base with imino compounds such us *cyclo-Dopa*, giving a color spectra than yellow to violet [1]. It is quite safe (indeed, betanin is an FDA approved food additive, E-162). A recent review is about the bioactivities of this pigments: They are promising alternatives for antioxidants, inflammation treatment, cardiovascular protection or anticancer [2]. Among others, Phenylethylamine-betaxanthin [(2S,4E)-4-{(2E)-2-[(2-phenylethyl)imino]ethylidene}-1,2,3,4-tetrahydropyridine-2,6-dicarboxylic acid, Fetyl-Bet)] is a natural derivative of Betalamic acid (**Fig.** 1) presented in Beetroot.

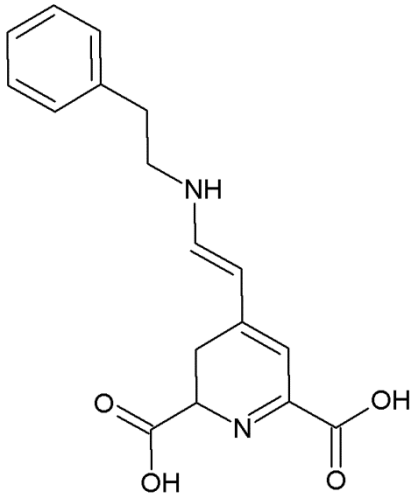


***Fig**. 1 Struture of Fetyl-Bet*

Despite all these healthy properties though it is quite soluble, the stability of its type of compounds at food pH values, oxidativity, and photosensibility must be improved. One way could be its introduction in cyclodextrins (CDs).

Although the stabilization of betalains has been studied [3], only two authors have studied the complexation of betalains in CDs and stabilization [4,5] but the results are very limited. In these papers authors described the encapsulation of the extract superficially (f.e. no complexation constant was obtained, no temperature and pH behavior were studied…). As is showed in this chapter, the knowledge of these aspects is essential if Fetyl-bet is used as an ingredient in nutraceutical industry. Indeed, it is the first work where an exhaustive stuy of the interaction between Fetyl-bet, a potent COX-2 inhibitor [6], and CDs, is carried out.

## 2. Objectives

1. To analyze the stability of Fetyl-Bet at acid pH.
2. To study the encapsulation mechanism of Fetyl-Bet by different types of natural (α-, β-, and γ-CD) and modified (HPβ-CD and Mβ-CD) CDs.
3. To evaluate the effect of temperature and pH on the encapsulation mechanism of Fetyl-Bet.
4. To determine the stoichiometry, $K_F$ values and thermodinamic parameters for the Fetyl-Bet/CD complexes.
5. To study the types of interactions between Fetyl-Bet and CD using molecular docking.
6. To analyze the stability of Fetyl-Bet in presence and absence of Cyclodextrin.

## 3. Materials and methods

### 3.1 Materials

Natural CDs (α-, β- and γ-CD, purity ≥ 97 %), modified CDs (HPβ-CD and Mβ-CD) were purchased from Sigma-Aldrich (Madrid, Spain). Fetyl-Bet was kindly supplied by Dr. F. Gandía-Herrero (University of Murcia, Spain) and used as received. The samples were stored in darkness. MQ water was obtained using a Milli-Q Advantage A10 system by Merck Millipore (Madrid, Spain).

### 3.2 Equipment and experimental procedure

#### *3.2.1 Fluorescence studies*

Fluorescence intensity was measured in a Shimazdu RF-6000 spectrofluorimeter (Shimazdu, Japan) equipped with thermostatically controlled cells and with a xenon lamp source and quartz cell, which were used to perform all the fluorescence measurements. Excitation and emission bandwidths were both set at 10 nm. The excitation and emission wavelengths for Fetyl-Bet were 460 nm and 510 nm, respectively using a 100 µL Super Micro Fluorescence cuvette from Thorlabs. The concentration of Fetyl-Bet was fixed at 5.4 µM and the CD concentration was between 0-40 mM. All reagents were dissolved in water or buffer.

#### *3.2.2 Spectrophotometric studies*

Spectrometric studies were done using a Jasco V-600 spectrophotometer (Madrid, Spain) thermostatically controlled. The wavelength fixed to stability measurement was 470 nm. For stability studies, 4 tubes, i) control, ii) 5.4 µM

Fetyl-Bet, iii) Control 25 mM Mβ-CD and iv) a mix, were incubated in triplicate at room temperature during seven days. Each 24h absorbance at 470nm was determined.

### *3.2.3 Encapsulation constant determination*

Two mathematical models were proposed to determine the encapsulation stoichiometry of the Fetyl-Bet/CD complexes: a 1:1 model where one CD complexes one molecule of Fetyl-Bet and a 2:1 model, where 2 CDs complex 1 Fetyl-Bet.

To start, a quantification of the interaction between Fetyl-Bet and CD based on the steady state fluorescence which considers the changes in the physico-chemical states was carried out. For this, the Benesi-Hildebrand method [7] to obtain the complexation constant ($K_F$) was used.

Assuming the composition of the complex to be 1:1, the following expression can be written:

$$\text{Fetyl-Bet} + \text{CD} \rightleftarrows \text{Fetyl-Bet/CD}$$

The complexation constant, $K_F$ is given by:

$$\mathrm{K_F} = \frac{[\mathrm{Fetyl-Bet/CDl}]}{[\mathrm{Fetyl-Bet}]\,[\mathrm{CD}]} \qquad (1)$$

where [Fetyl-Bet], [CD] and [Fetyl-Bet/CD] are equilibrium concentrations.

The expression corresponding to the Benesi-Hildebrand method was used to determine de $K_F$ value.

$$\frac{1}{F-F_0} = \frac{1}{(F_\infty - F_0)K_F\,[CD]} + \frac{1}{F_\infty - F_0} \qquad (2)$$

where [CD] denotes the CD concentration; $F_0$ the fluorescence intensity of Fetyl-Bet in the absence of CD; $F_\infty$ the fluorescence intensity when all of the Fetyl-Bet molecules are essentially complexed with CD; and F, is the observed fluorescence intensity at each CD concentration tested.

The other model, a 2:1 complex, can be analyzed using the following expression [8]:

$$\frac{1}{F-F_0} = \frac{1}{(F_\infty - F_0)K_{F12}([HP\beta-CD])^2} + \frac{1}{F_\infty - F_0} \quad (3)$$

For temperature studies, the complexes were studied at 278, 288, 298 and 310 K (5, 15, 25 and 37 ºC) to determine their $K_F$. Temperature was controlled using a Thermomixer confort (Eppendorf Iberica, Spain). For pH studies, different buffers were prepared: pH (5.5-7.0) sodium-phosphate 0.1 M, pH (3.0-4.0) sodium-acetate 0.1 M and pH 2 sodium-citrate 0.1 M.

### *3.2.4 Thermodynamic parameters determination*

The thermodynamic parameters, ΔHº, ΔS, and ΔGº, can be calculated using Van't Hoff expression:

$$Ln\ K_F = \frac{-\Delta H^\circ}{RT} + \frac{-\Delta S^\circ}{R} \quad (4)$$

where $K_F$ is the complexation constant of the inclusion complex, T is the temperature, R is the gas constant and Δ*H*º and Δ*S*º are standard enthalpy and entropy changes of complex formation in the mobile phase. For a linear plot of ln $K_F$ versus 1/T, the slope and intercept are –ΔHº/R and ΔSº/R, respectively.

The Gibbs free energy change for the interactions that take place during the inclusion process may be found by the following equation:

$$\Delta G^{\circ} = \Delta H^{\circ} - T\Delta S^{\circ} \quad (5)$$

### *3.2.5 Molecular docking*

The molecular structures used in this work were built using Avogadro Software [9] or were obtained by different databases. The β-CD structure was extracted from the Protein Data Bank (PDB ID: 4RER). Fetyl-Bet was created using Betalamic acid obtained from PubChem database (NCBI, USA). Mβ-CD was built by adding methyl group to the β-CD. Molecular docking was carried out using Autodock Vina [10]. All CDs were considered as flexible. Graphical representations of the docking results were prepared using PyMOL (Molecular GraphicsSystem, version 1.3, Schrödinger, LLC) .

### *3.2.6 Data Analysis*

All experiments were carried out in triplicate. Graphical representations were made using SigmaPlot (Version 10.0). An ANOVA and a Tukey Test were applied using Rstudio (version 0.99.878) fixing the significance level at $P < 0.05$. Other mathematical operations were carried out using wxMaxima software (version 12.04.0).

## 4. Results and discussion

### 4.1 Stability of Fetyl-Bet at citric pH juice

Although betalamic derivatives are generally perfectly soluble, it is clear that these family of compounds needs to be stabilized in acid pHs [3], to keep their bioactivies intact. One of the most attractive hydrophilic products to add betalains could be citric juice, which pH is around 3, although stomach pH will be also important (1.5 to 3.5). For that reason, the stability of 5.4 µM Fet-Bet was studied at pH 3. The results showed degradation around 60% in 24h. This high degree of degradation prevents the administration in food products of betalains without protection. At this moment, its complexation with CDs can be a good solution.

### 4.2 Study of the stoichiometry and determination of the encapsulation constants with different CDs

To optimize the preparation on any stable product with Fetyl-Bet, it is essential to study the encapsulation behavior and the complexation constant ($K_F$). In order to calculate $K_F$, the increase of relative fluorescence of Fetyl-Bet in presence of increasing concentrations of Mβ-CD was studied. The results showed in **Fig**. 2, reveal an increase in the signal in presence of Mβ-CD until saturation. Using eq. 2, a plot of $1/F\text{-}F_0$ vs. 1/[Mβ-CD] gave a $R^2$ coefficient close to 1 (0.99, **Fig**. 2 insert) whereas eq. 3 gave a lower $R^2$ (0.87). The $K_F$ value obtained with Mβ-CD was 8.88 +/- 0.44 $mM^{-1}$ at pH 7 and 25 ºC.

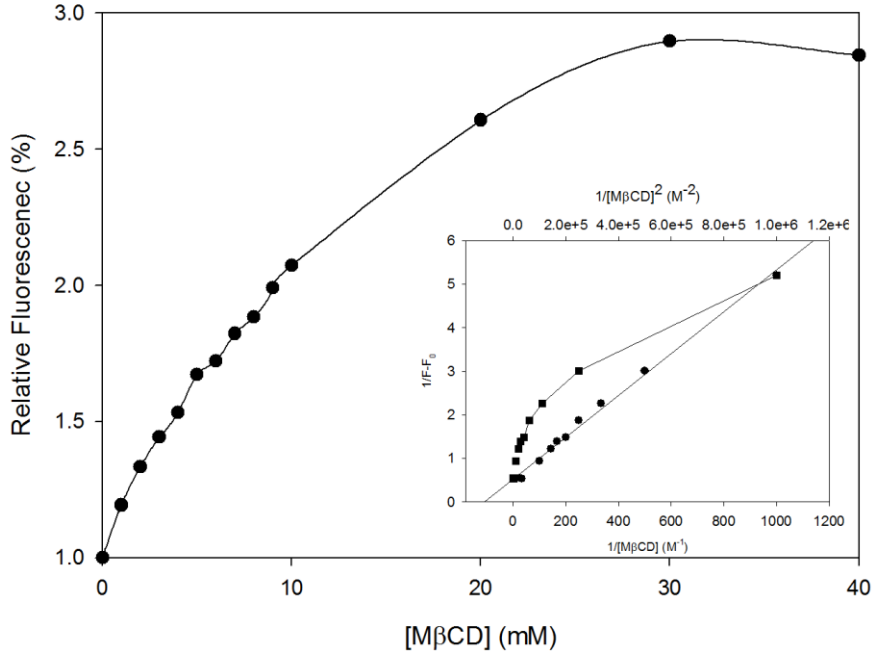


***Fig** 2. Dependence of emission fluorescenec intensities of Fetyl-Bet (5.4 μM) on Mβ-CD concentrations at pH 7 at 25 ºC. Inset. Double reciprocal plot of Fetyl-Bet complexed to Mβ-CD for determining the stoichiometry of 1:1 model (filled circles) or a 1:2 model (filled squares).*

Different natural (α-, β- and γ-CD) and modified (Mβ-CD and HPβ-CD) were tested and plotted against both equations (Table 1). All CDs showed a 1:1 complex with considerable differences in $K_F$ values. An ANOVA and Tukey were used to corroborate the differences. Only Mβ-CD and HPβ-CD did not pass the test to our significance level ($P < 0.05$. The modified CD of β-CD (Mβ-CD and HPβ-CD) showed strong encapsulation efficiency. It could be because the modification may generate better scenery for the complexation. Although β-CD had a lower $K_F$ than γ-CD, the increase of signal was higher. Maybe the lower solubility of β-CD prevents to get a higher $K_F$ value. To clarify the results obtained at pH 7, the same experiment was done at pH 3 showing that Mβ-CD

$K_F$ (17.08 +/- 0.85 $mM^{-1}$) was higher than $K_F$ (13.65 +/- 0.68 $mM^{-1}$) for HPβ-CD. So, Mβ-CD was selected as CD model for all the remaining experiments.

Table 1. Experimental $K_F$ values, correlation coefficients arising from eq (2) and (3) for 1:1 or 1:2 complexes respectively at 25 ºC and pH 7; and docking score results.

| CD type | $K_F$ ($mM^{-1}$) | SD (+/-) | Coefficient correlation | | Docking score |
|---|---|---|---|---|---|
| | | | 1:1 complex | 1:2 complex | |
| α-CD | 0.47 | 0.02 | 0.99 | 0.90 | - |
| β-CD | 4.00 | 0.20 | 0.97 | 0.92 | -9.00 |
| γ-CD | 7.49 | 0.37 | 0.98 | 0.90 | - |
| HPβ-CD | 8.22 | 0.41 | 0.99 | 0.92 | - |
| Mβ-CD | 8.88 | 0.44 | 0.99 | 0.89 | -7.90 |

### 4.3 Effect of pH on the complexation of Fetyl-Bet by Mβ-CD

CD could be a good protector of Fetyl-Bet in acid products. However, there are other types of products or conditions that must be considered. For that reason, we also evaluate the effect of pH on $K_F$ values. The results (**Fig**. 3A) showed that the lower pH we had the higher $K_F$ value we reported. The highest was at pH 2; it could be by the protonation of both carboxy groups of betalamic acid.

In addition, the fluorescence signal of Fetyl-Bet decreased with pH (**Fig**. 3A *insert*), perhaps the protonation of the molecule could affect the fluorescence yield of the molecule. This data is in accordance with our previous stability experiment where we have demonstrated that at low pH Fetyl-Bet has low stability and CDs could protect the molecule in solution.

4.4 Effect of temperature and thermodynamics parameters of Fetyl-Bet/Mβ-CD complexes.

**Fig**. 3B presents the effect of increasing temperature (5, 15 25 and 37 ºC) on $K_F$. There was a direct relationship with temperature. This lower degree of interaction at higher temperatures could be attributed to the fat that hydrogen bonds are usually weakened by heating.

To gain information on the mechanistic aspects of the affinity of Fetyl-Bet for Mβ-CD, its thermodynamic parameters (ΔHº, ΔSº, and ΔGº at 25 ºC) were studied. **Fig**. 3B *insert* shows that the Ln $K_F$ vs. 1/T plot presented a linear relationship, with a coefficient higher than 0.96. Now, using eq. 4 we can obtain the parameters.

Changes in entropy are negative in these processes (-90.40 +/- 4.52 J · $mol^{-1}$ · $K^{-1}$). This can be because that complexation decrease the degrees of freedom (translational and rotational), leading to a more ordered system. In addition, the negative values for enthalpy changes (-16.61 +/- 0.81 KJ · $mol^{-1}$) indicate the exothermic nature of the interaction between Fetyl-Bet and Mβ-CD. This behavior is typical of hydrophobic interaction because of the displacement of water from the cavity of the CD, increasing van der Walls interactions and the formation of hydrogen bonds and other interactions [11]. About Spontaneity of the process, the results show that the complexation is spontaneous at 25 ºC due to the negative value of Gibbs free energy (-19.08 ± 0.95 KJ · $mol^{-1}$)

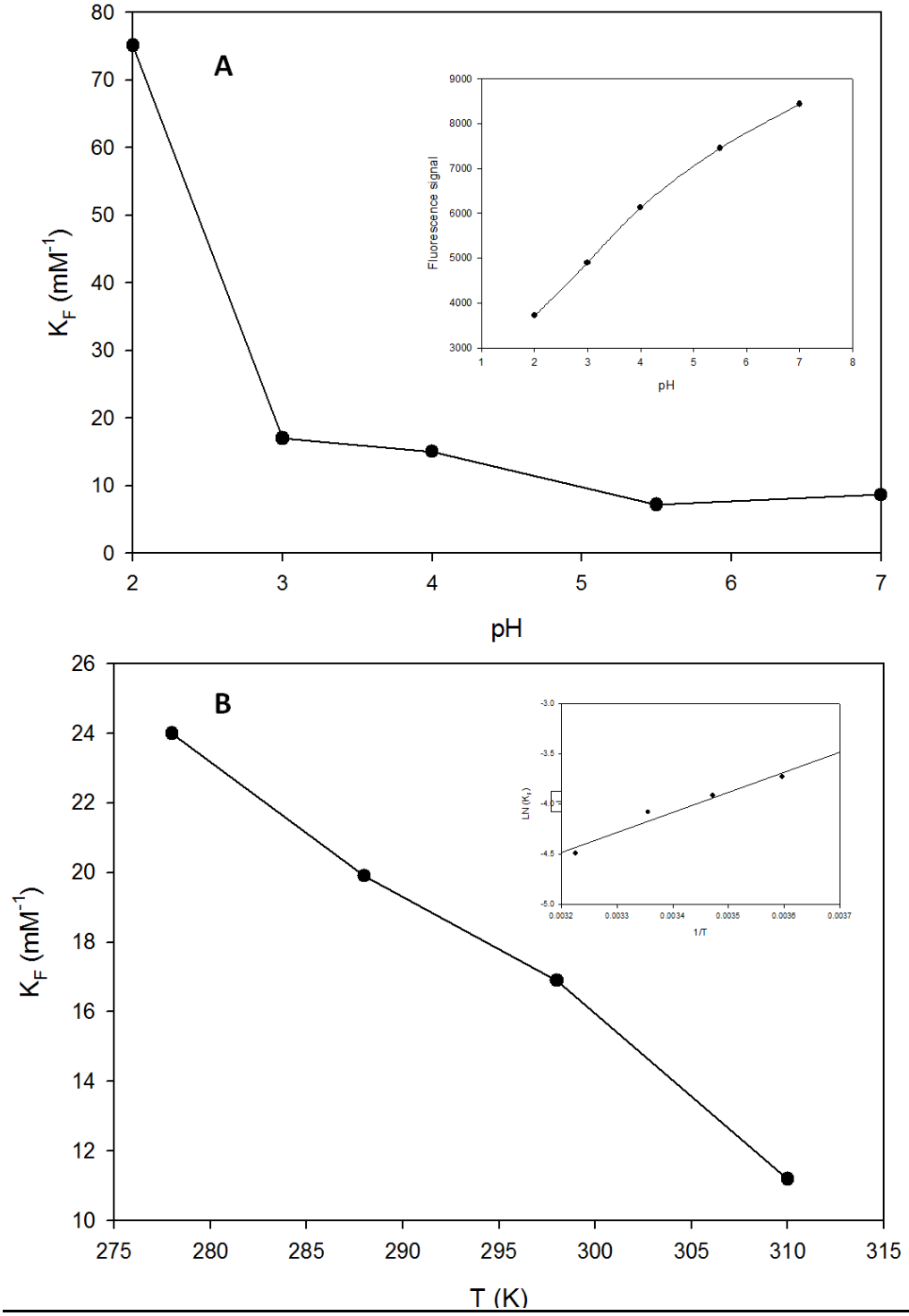


***Fig** 3. (A) Effect of pH on $K_F$ values at 25 ºC Insert. Dependence of emission fluorescence intensities of Fetyl-Bet (5.4 µM) on pH at 25 ºC. (B). Effect of temperature on $K_F$ values at pH 3. Insert. The Van't Hoff plot (LN $K_F$ vs. 1/T) for Fetyl-Bet complexes in 0.1M acetate-sodium buffer pH 3.0.*

## 4.5 Molecular modelling of the Fetyl-Bet/CD complexes

In order to understand the interactions between Fetyl-Bet and CDs, docking simulations were carried out. As the size of β-CD is the best to encapsulate Fetyl-Bet, we focused our interest on study differences between our better CD, Mβ-CD, and β-CD. **Fig**. 4 showed the most stable poses for the complexes between Fetyl-Bet with each CD.

Although our experimental data said that Mβ-CD was better than β-CD, the score docking of each pose said the contrary (Table 1). This could be because Mβ-CD is less soluble than Mβ-CD preventing to show its real encapsulation potential against Fetyl-Bet [12]. Furthermore, the poses are very clear in this respect. While Mβ-CD complex (**Fig**. 4A) presents a good fit without any hydrogen bond, the complex with β-CD (**Fig**. 4B) shows better fit than Mβ-CD, with hydrogen bonds additionally. It is important to remember that hydrogen bonds is one of the most powerful forces to stabilize complexes [13].

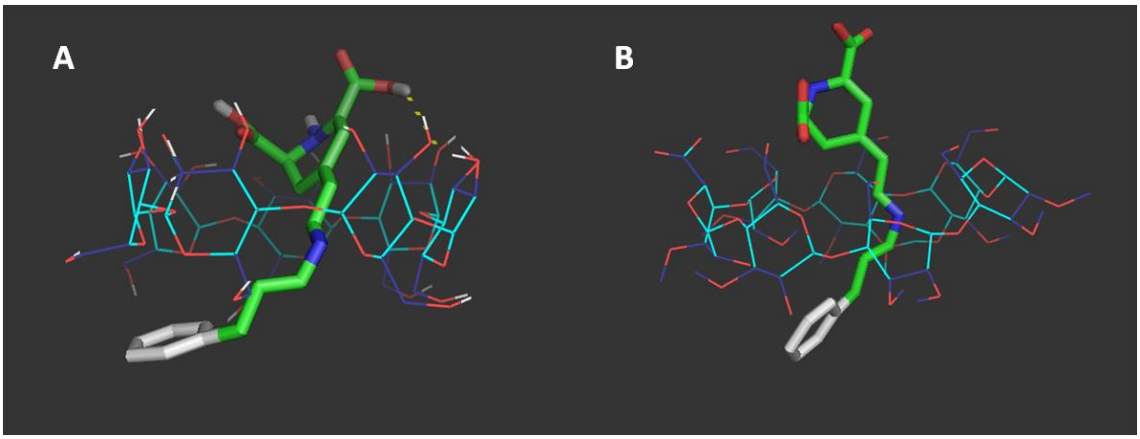


***Fig** 4. Docking results of A, βCD and B, Mβ-CD with Fetyl-Bet as ligand. In violet, flexible residues of each CD. In Yellow, hydrogen bonds.*

## 4.6 Stabilization of Fetyl-Bet in presence of Mβ-CD at citric juice pH

To conclude the study, a probe that CDs could protect Fetyl-Bet is desirable.For that reason, the stability of 5.4 μM Fet-Bet in presence and abscence of 25 mM Mβ-CD at pH 3 was analyzed. The results (**Fig**. 5) showed as whereas at day 3 no Fetyl-Bet is found without Mβ-CD, the 20 % of the initial Fetyl-Bet is remained. Furthermore, the first day the Fetyl-Bet concentration decreased 1.5 times more without Mβ-CD. This fact presumed the stabilization of Fetyl-Bet by CDs in acid products such as juice.

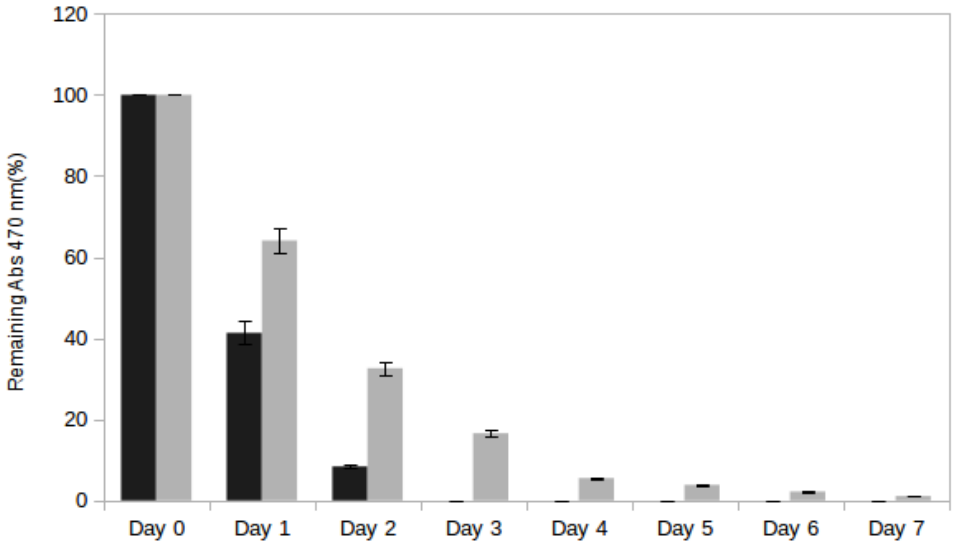


***Fig** 5. Remaining Fetyl-Bet 5.4 μM in presence (Gray) and abscence (Black) of Mβ-CD 25 mM during 7 days at pH 3 and RT.*

In conclusion, although betalains has a great solubility, its stability must be improved to establish a food or nutraceutical use. In this chapter, we have demonstrated that CDs can be used to protect and increase the stability of this type of compounds at acid pH, common in citric products. Furthermore, this work presents a physico-chemical, thermodynamic and computational study of

the encapsulation of Fetyl-Bet, naturally occurring betalains with many bioactivities, in CDs. Fetyl-Bet forms 1:1 complexes with all natural and modified CDs tested, showing the best $K_F$ value for Mβ-CD. The encapsulation process was more effective at low pH, where the carboxyl groups are partially protonated. The study of the effect of temperature on $K_F$ value showed how the efficiency decreases when temperature increased. Furthermore, a negative enthalpy and entropy was reported indicating the spontaneity of the process. Additionally, a molecular docking study was carried out showing high level of differences between β-CD and Mβ-CD complexes. The findings as a whole represent a way to introduce betalains in functional foods or nutraceutical produts preserving betalains in perfect conditions

## References

[1] F. Gandía-Herrero, J. Escribano, F. García-Carmona, Structural implications on color, fluorescence, and antiradical activity in betalains, Planta. 232 (2010) 449–460. doi:10.1007/s00425-010-1191-0.

[2] P. Rahimi, S. Abedimanesh, S.A. Mesbah-Namin, A. Ostadrahimi, Betalains, the nature-inspired pigments, in health and diseases, Crit. Rev. Food Sci. Nutr. 0 (2018) 1–30. doi:10.1080/10408398.2018.1479830.

[3] M.I. Khan, Stabilization of betalains: A review, Food Chem. 197, Part B (2016) 1280–1285. doi:10.1016/j.foodchem.2015.11.043.

[4] S. A. M. M., H. Norasiha, C.M. Rohaida, Characterization of β-Cyclodextrin Complexes with Natural Dye, in: UMP Conference Hall, Malaysia, 2009: pp. 98–106. http://umpir.ump.edu.my/4146/ (accessed April 5, 2017).

[5] D.A. Drunkler, R. Fett, M.T.B. Luiz, THE EVALUATION OF STABILITY OF BETALAINS IN BEETROOT (Beta vulgaris L.) EXTRACT ADD TO OF α-, ß- AND Y-CYCLODEXTRINS, MyScienceWork. (2006). https://www.mysciencework.com/publication/show/85dc725aa0b087f4316e067e9018af28 (accessed April 5, 2017).

[6] P.J. Vidal, J.M. López-Nicolás, F. Gandía-Herrero, F. García-Carmona, Inactivation of lipoxygenase and cyclooxygenase by natural betalains and semi-synthetic analogues, Food Chem. 154 (2014) 246–254. doi:10.1016/j.foodchem.2014.01.014.

[7] H.A. Benesi, J.H. Hildebrand, A Spectrophotometric Investigation of the Interaction of Iodine with Aromatic Hydrocarbons, J. Am. Chem. Soc. 71 (1949) 2703–2707. doi:10.1021/ja01176a030.

[8] A.M. Rimando, M. Cuendet, C. Desmarchelier, R.G. Mehta, J.M. Pezzuto, S.O. Duke, Cancer Chemopreventive and Antioxidant Activities of Pterostilbene, a Naturally Occurring Analogue of Resveratrol, J. Agric. Food Chem. 50 (2002) 3453–3457. doi:10.1021/jf0116855.

[9] M.D. Hanwell, D.E. Curtis, D.C. Lonie, T. Vandermeersch, E. Zurek, G.R. Hutchison, Avogadro: an advanced semantic chemical editor, visualization, and analysis platform, J. Cheminformatics. 4 (2012) 17. doi:10.1186/1758-2946-4-17.

[10] O. Trott, A.J. Olson, AutoDock Vina: improving the speed and accuracy of docking with a new scoring function, efficient optimization, and multithreading, J. Comput. Chem. 31 (2010) 455–461. doi:10.1002/jcc.21334.

[11] C. Ravelet, A. Geze, A. Villet, C. Grosset, A. Ravel, D. Wouessidjewe, E. Peyrin, Chromatographic determination of the association constants between nimesulide and native and modified β-cyclodextrins, J. Pharm. Biomed. Anal. 29 (2002) 425–430. doi:10.1016/S0731-7085(02)00088-2.

[12] E.M.M. Del Valle, Cyclodextrins and their uses: a review, Process Biochem. 39 (2004) 1033–1046. doi:10.1016/S0032-9592(03)00258-9.

[13] W. Saenger, Cyclodextrin Inclusion Compounds in Research and Industry, Angew. Chem. Int. Ed. Engl. 19 (1980) 344–362. doi:10.1002/anie.198003441.

# Block II part II

# Chapter III

## *An evaluation of juice and milk "food models" fortified with oxyresveratrol and β-Cyclodextrin*

**Abstract**

The food market is saturated. A huge quantity of “novel” functional food products reaches the food market every day and companies are looking for new products to catch their attention. In the present study i) 0.2 mM oxyresveratrol, ii) 0.2 mM oxyresveratrol complexed with 8 mM β-CD and iii) 4 mM oxyresveratrol solubilized with 8 mM β-CD were used to fortify, juice and milk food models, and kept in the most typical storage conditions (darkness and/or refrigerated) conditions for one month.

The results showed that the CD supplementation can lead to a higher oxyresveratrol concentration and antioxidant capacity than when they are not used. Oxyresveratrol/β-CD food models were stable for five weeks. The most typical variables measured were comparable. An *in vitro* digestion pointed to similar bioaccessibility. The bacteriostatic effect was also studied showing an increase of the effect of oversaturated solutions. These results showed to be useful for the food industry in order to design hydrophilic products containing oxyresveratrol.

## Index

## 1. Contextualization

The society is increasingly demanding healthier food products and one way to satisfy this demand could be the fortification of foods by bioactive compounds, which are common or novel molecules that have demonstrated bioactivities such us antioxidant or anticancer activities. A well known bioactive compound family is stilbene (e.g. resveratrol, oxyresveratrol), which is presents in grapes, mulberry fruits, among others [1], and several have authors reported the high number of bioactivities for these compounds such us anticancer, antioxidant or antimicrobial activities [2–4].

However, this family of compounds presents low solubility, which may obscure good organoleptic properties and hinder the arrival of the molecule at the target tissue. Moreover, these products could lose the stilbene before consumption.

An interesting strategy to increase the stilbene concentration of a product and protect them is the complexation with cyclodextrins (CDs). It is important to remember that natural CDs appear in the lists of additives approved for alimentary use with the corresponding E-numbers for α-, β- and γ-CD: E-457, E-459 and E-458, respectively.

Oxyresveratrol was selected because it has four hydroxyl groups and would be the most sensitive of the family; moreover its complexation with CDs were previously characterized in this thesis (*Block I, part I, chapter III*) and by some authors [5,6]. Food models are an easy way to evaluate the behavior of a sample without the interference of other metabolites [7]. For example, they have

been previously used to evaluate the antimicrobial effect of resveratrol [8], but its stability was not evaluated.

## 2. Objectives

1. To evaluate the fortification of food model samples with oxyresveratrol and β-CD using the most common techniques in the industry, the following secondary objectives were proposed:
    a. To determine the increase in solubility and antioxidant capacity of oxyresveratrol complexed with β-CD.
    b. To understand the interactions of the oxyresveratrol/β-CD complex.
    c. To study, for one month, the stability of different oxyresveratrol/β-CD combinations in different food models and storage conditions.
    d. To determine the bioaccessibility of oxyresveratrol/β-CD complexes in *in vitro* digestion.
    e. To show the antimicrobial effect of food model samples

## 3. Materials and methods

### 3.1 Materials

Oxyresveratrol was purchased from TCI (Belgium). β-CD, citric acid, pepsin, pancreatin and bilis extract were purchased from Sigma-Aldrich (Madrid, Spain). Acetic acid was from Panreac S.A. (Spain). MQ water was obtained using a Milli-Q Advantage A10 system by Merck Millipore (Madrid, Spain).

### 3.2 Experimental procedures

#### *3.2.1 Solubility studies*

Tubes with 1 mg/mL of oxyresveratrol were incubated at increasing β-CD concentrations in water at 25 ºC using a Thermomixer Comfort system at 650 rpm (Eppendorf) for 24 h in darkness (after 10 minutes sonication). The tubes were centrifugated at 5000 g's for 10 minutes to remove non-soluble oxyresveratrol, and the spectrum of the supernatant was measured. The concentration of oxyresveratrol was measured at 328 nm.

#### *3.2.2 Food model preparation*

Food samples including milk and orange juices were prepared [7]. Food models were developed based on the pH. In order to eliminate any chemical interactions between our samples and the food ingredients, an appropriate quantity of citric acid and acetic acid buffer at pH 6.51 and 3.27 were prepared. All samples were sterilized by autoclave. Prior and final concentration of the samples was checked to prevent degradation. Independently of food model

type, five doses were prepared: i) control, ii) oxy 0.2 mM, iii) β-CD 8 mM, iv) 0.2 mM oxyresveratrol and β-CD 8 mM and v) oxyresveratrol 4 mM solubilized by β-CD 8 mM (24 hours solubilization in food model buffer was required). Samples were stored in four conditions to reflect the most common storage modes: i) Darkness refrigerated, ii) Darkness non-refrigerated, iii) refrigerated and iv) non-refrigerated. All samples were prepared in quintuplicate.

### *3.2.3 Time course measurements*

Four variables were measured at 0, 1, 3 and 5 weeks: pH, using a Crison pH-meter GLP 21+; Degrees Brix, using a refractometer PAL-3 (Atago, Japan) using MQ water as blank, spectra and absorbance at 328 and 600 nm using a Jasco V-630 Spectrophotometer (with Thorlabs cuvettes CV10Q1400) .

### *3.2.4 In vitro digestion*

Four samples, i) control, ii) 0.2 mM oxyresveratrol, iii) 8 mM β-CD, iv) a mixture of both and v) 4 mM oxyresveratrol solubilized by β-CD 8 mM, were subjected to the *in vitro* digestion model to assess the behavior of the complexes [9]. The protocol was the same as that described by Ilyasoglu (2014) with a few modifications: First, samples were prepared in saline at pH 3 with pepsin-HCl to simulate the gastric phase before incubating in a shaking water bath at 37 °C for 1 h. The incubation was stopped by adding 1 mol/$m^3$ $Na_2CO_3$ to increase the pH to 6.9. In the subsequent intestinal phase, the pH was adjusted to 6.9 and a pancreatin–bile extract–lipase mixture was added before incubating at 37 °C for 2 h. Tubes were placed in an ice bath to stop digestion and the contents were diluted in phosphate-Na buffer pH 7.4 and filtered. The samples were analyzed using the remaining antioxidant capacity in ABTS assay

using sample not digested as reference as described by Rodriguez-Bonilla *et al.* (2017), [10]: Briefly, it was evaluated by following their effect on free radical ABTS.+ [2,2´-azino-bis(3-ethylbenzothiazoline-6-sulfonic acid)] in a assay based on the reduction in absorbance of ABTS• + radical cation solutions, which has a broad absorption spectrum. The ABTS•+ radical was prepared from 2mM ABTS through peroxidase activity (88 units/L commercial horseradish peroxidase type VI) in the presence of $H_2O_2$ (45 µM), in sodium acetate buffer, (pH 5.0; 0.2 M). The reagent was then diluted by adding the samples, carrying out the reactions in sodium phosphate buffer, pH 7.0. The final volume was 300 µL with a 1/100 dilution of the sample. Other conditions are specified in that paper. The reaction was monitored spectrophotometrically at 414 nm [15]. The measurements were carried out in 96 well plates at 24 hours at 20 °C in a Synergy HT plate reader (Bio-Tek Instruments, Winooski).

### *3.2.5 Antimicrobial analysis*

A culture of *Escherichia coli* DH5α was used as antimicrobial control. Cultures at 0.25 O.D. from fresh culture in LB medium were incubated in 96 well plates with appropriate addition of food model samples for 24 hours at 37 ºC. Abs 600nm was automatically measured each 15 minutes using a Synergy HT plate reader (Bio-Tek Instruments, Winooski). Border plates were filled with sterile water to prevent evaporation. Antibiogram petri dishes were made using a filter paper previously sterilized (impregnated with food model sample) in a surface-spread DH5α culture and incubated at 37 ºC for 24 hours.

### *3.2.6 Molecular docking*

The molecular structures used in this work were obtained from several databases. β-CD was obtained from the Protein Data Bank (ID 4RER). Oxyresveratrol was downloaded from the PubChem database (NCBI, USA). Input files for docking were generated using Autodock tools (version 1.5.6) with default parameters and charges. Molecular docking was carried out using Autodock Vina [12] using default parameters. CDs were considered as flexible. Graphical representations of the docking results were prepared using PyMOL (Molecular GraphicsSystem, version 1.3, Schrödinger, LLC) with default parameters to display hydrogen bonds.

### *3.2.7 Data analysis*

Regressions and graphs were made with Sigma-Plot (version 10.0.0.54) and OpenOffice (version 6.0.3.2). Statistical evaluation was carried out using Rstudio (version0.99.878). Other mathematical operations were carried out using wxMaxima (version 12.04.0).

## 4. Results and discussion

### 4.1 β-CD increases the apparent solubility and antioxidant capacity of oxyresveratrol solutions

The bioactivities of stilbene are well documented and products based on these compounds could be welcome. However, the correct concentration of the compound is difficult to attach due to its water insolubility. This may prevent the desired concentration from reaching the target tissue. Complexation of stilbene with a matrix to increase its apparent solubility could increase the final concentration in the tissue. The oxyresveratrol complex with β-CD was previously characterized [5], but the increase in solubility was not demonstrated. Which is why, a serial oxyresveratrol solution at increasing β-CD concentration was prepared.

Results (**Fig.** 1) showed that β-CD can completely dissolve at least 1 mg/mL (≈ 4.09 mM) concentration of oxyresveratrol (**Fig.** 1. *Insert*). At the same time, the antioxidant capacity of solutions using ABTS+ was also evaluated (**Fig.** 1B). It was found that the antioxidant capacity increased as β-CD solubilizes oxyresveratrol in the final solution. Recently the oral pharmacokinetic parameters of oxyresveratrol in rats has been evaluated, where oxyresveratrol blood concentration increased as the oral dosage increased [13] without toxicity (maxima dose used: 97.6 mg/kg). The combination of these data suggest that β-CD, as one of the approved food additives, could increase not only the final concentration in the food product, but also its bioavailability and bioactivity.

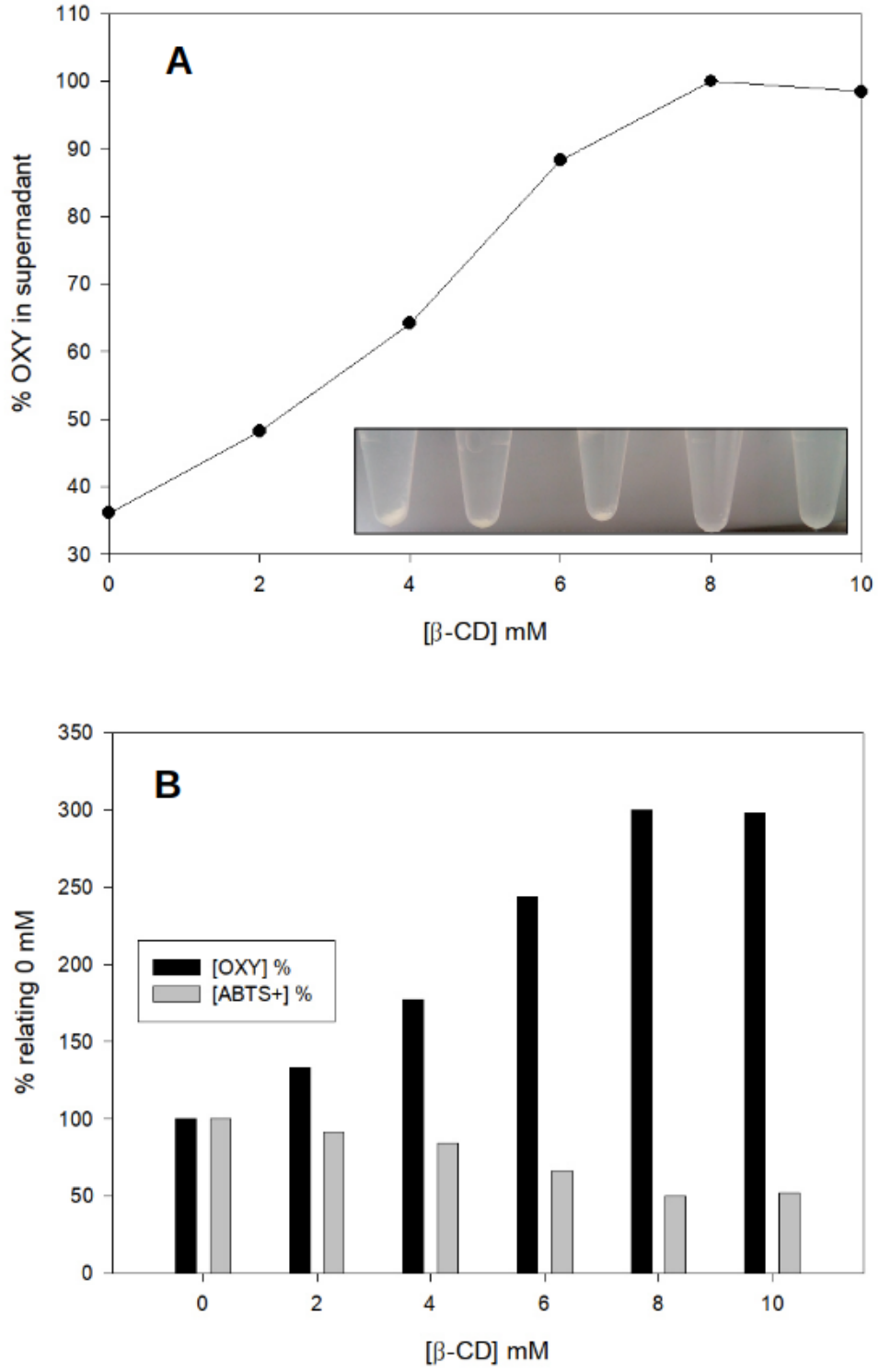


***Fig**. 1. (A) Effect of β-CD on oxyresveratrol solubilization after 24 mixing at 25ºC. Insert, details of oxyresveratrol precipitate. (B) Effect of higher concentration of oxyresvertrol on free radical abts quantity.*

### 4.2. Molecular modeling of Oxyresveratrol/β-CD complex.

In order to understand better the possible interactions between oxyresveratrol and β-CD complex, a molecular docking was carried out [14]. The results (**Fig.** 2A) showed that oxyresveratrol would fit perfectly inside β-CD. Recently, it was demonstrated that oxyresveratrol forms two possible complexes with Mβ-CD [15] and it is reflected in our case with β-CD (**Fig.** 2B). Furthermore, a hydrogen bond was found that helping the system stabilization.

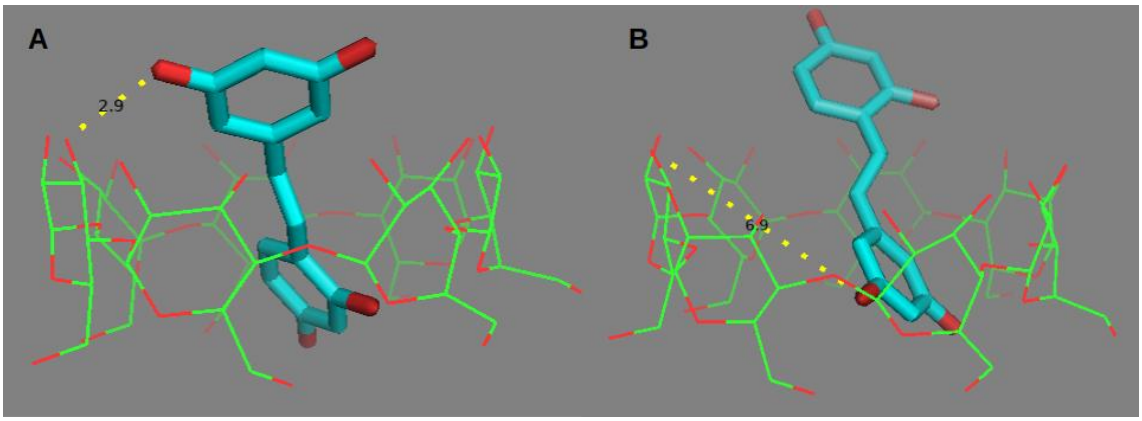


***Fig**. 2. (A) Pose of oxyresveratrol/β-CD complex. In yellow, the hydrogen bond finded. (B) Pose of oxyresveratrol/β-CD complex. In yellow, the previous hydrogen bond indicating the change of conformation.*

### 4.3 Food model preparation and evaluation, a time course experiment.

Several storage conditions and food products were evaluated using juice and milk as pH-based food models (citric acid 0.1 M pH 3.73 and 6.51 respectively). As citric acid could be complexed by β-CD [16], an acetic acid food model at pH 3.73 was also made (in this way, the influence of co-complexable agents would also be evaluated). For each food model, four condition were evaluated, i) Darkness refrigerated, ii) Darkness non-

refrigerated, iii) refrigerated and iv) non-refrigerated. These conditions attempt to study the most typical storages condictions (for example, a juice may be found in a transparent bottle or tetra-bricks). Five solutions were measured: i) control, ii) oxy 0.2 mM, iii) β-CD 8 mM, iv) oxy 0.2 mM and β-CD 8 mM and v) oxy 4 mM solubilized by β-CD 8 mM. In short, 60 different samples (type of food model, type of storage condiction and solution) were evaluated (Table 1).

Table 1. A scheme of conditions evaluated.

| Food model | Stogage | Solution |
|---|---|---|
| **Acetic acid 0.1 M pH 3.73** | Darkness & Refrigerated | Control |
| | Darkness & Non-Refrigerated | Oxyresveratrol 0.2 mM |
| **Juice food model (citric acid 0.1 M pH 3.73)** | No-darkness & Refrigerated | β-CD 8 mM |
| | No-darkness & Non-Refrigerated | 0.2 mM oxyresveratrol & β-CD 8 mM |
| **Milk food model (citric acid 0.1 M pH 6.51)** | | Oxyresveratrol 4 mM & β-CD 8 mM |

### *4.3.1 pH evaluation*

The pH is one of the most common variables used by the food industry to check the quality of its products (for example, for possible biotic contamination). The addition of our molecules could affect the initial pH value and/or its evolution, for which reason, the pH was measured at 0, 1, 3 and 5 weeks. The Results (**Fig.** 3A, 3B and 3C) showed that i) the addition of the molecules did not change the pH value of the food model sample and ii) there was no variation during the time course experiment. These results demonstrate that the addition of oxyresveratrol and/or β-CD would not change the natural pH value of the food product for at least five weeks.

### *4.3.2 Evaluation of ºBrix*

To check the quantity of sugar in a food sample, the most common parameter measured, is its Brix, a non-spectroscopic technique based on refractometry. However, the addition of other molecules could alter the value changing the target value for industry. So, prior evaluation of the solution is desirable. The results (**Fig.** 3D, 3E and 3F) demonstrated that the addition of the molecules alter the Brix value although it remarked constant throughout the experiment. These results confirm the idea that the Brix value must be corrected previously.

### *4.3.3 Oxyresveratrol concentration*

The remaining concentration of oxyresveratrol in the samples was measured by reference to their spectra. Oxyresveretrol presents three points at 328nm (maximum), 301 and 290 nm; the quotient of abs_301/abs_290 is the relationship between cis/trans oxyresveratrol [17]. The results showed that i) the cis/trans relationship was almost completely stable (**Fig.** 4A), with the exception of milk model (**Fig.** 4B and *insert*). **Fig.** 4C presents the degradation of oxyresveratrol for five weeks: 0.2 mM oxyresveratrol samples showed in general a 90 % of remaining concentration, but “non-darkness & refrigerated” presented the highest degradation ($P < 0.05$). Oxyresveratrol 0.2 mM & 8 mM β-CD samples presented in general lower degradation at acid pH (≈ 95 % remaining, orange model, $P < 0.05$) than free oxyresveratrol, but similar degradation at little acid pH (milk model). Oxyresveratrol 4 mM & 8 mM β-CD samples showed the same degradation rate than Oxyresveratrol 0.2 mM & 8 mM β-CD samples although milk model presents higher degradation ($P < 0.05$)

than Oxyresveratrol 0.2 mM & 8 mM β-CD. However, a higher total quantity of oxyresveratrol is in the solution.

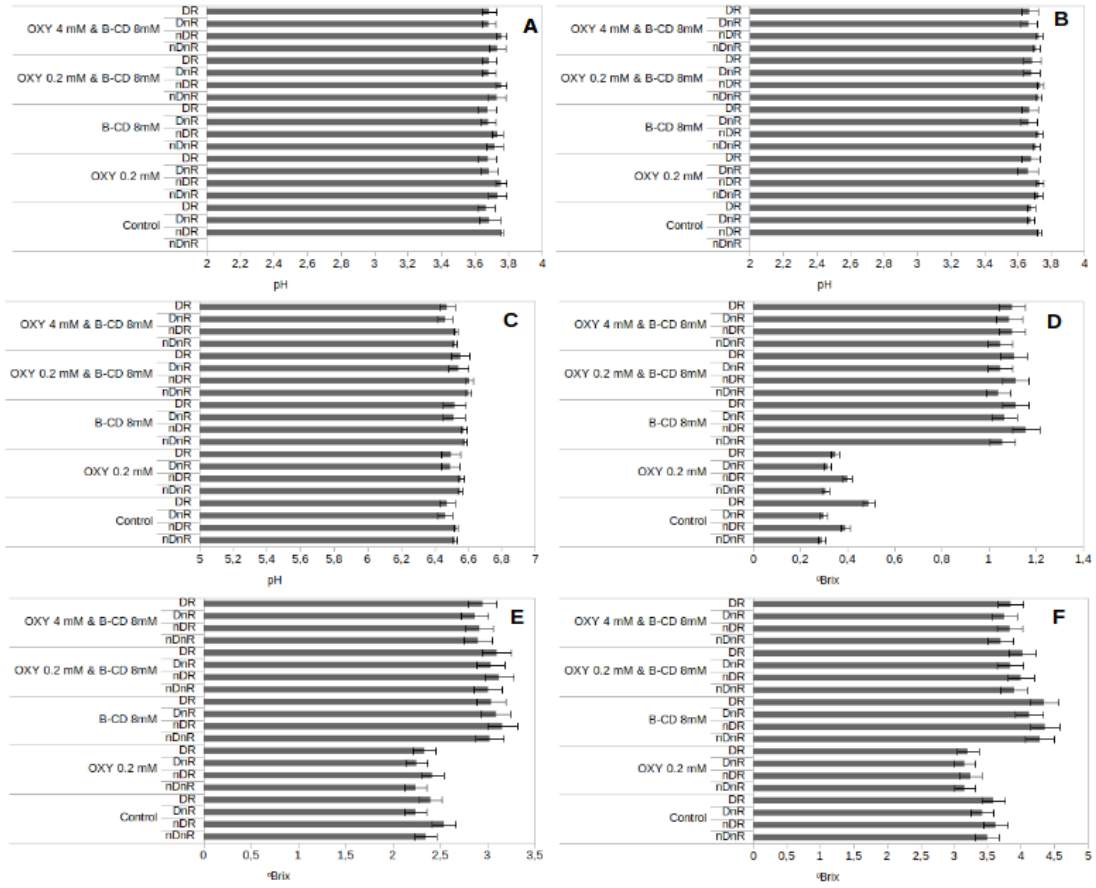


***Fig**. 3. (A) Mean pH value of samples in acetic acid pH 3.73 for five weeks. (B) Mean pH value of samples in citric acid pH 3.73 (Orange model) for five weeks. (C) Mean pH value of samples in citric acid pH 6.51 (Milk model) for five weeks. (D) Mean ºBrix value of samples in acetic acid pH 3.73 for five weeks. (E) Mean ºBrix value of samples in citric acid pH 3.73 (Orange model) for five weeks. (F) Mean pH value of samples in citric acid pH 6.51 (Milk model) for five weeks. Legend: DR = darkness & refrigerated, nDR = Non-darkness & refrigerated, DnR = Darkness & non-refrigerated and nDnR = Non-darkness & Non-refrigerated. OXY = oxyresveratrol*

In general, a degradation around 5-10 % in five weeks were reported although it was also higher in citric pH 6.51 and ii) the oxyresveratrol milk model (pH 6.51) samples stored in darkness non-refrigerated showed the most stable

storage condition, a decrease in oxyresveratrol quantity since the 3rd week were reported. These data pointed to the alteration of oxyresveratrol stability at pH 6.51 at high concentrations because at pH 3.73 the oxyresveratrol was not degradated and at 0.2 mM it did not present so much degradation. Perhaps the deprotonation of last citric acid pKa (6.4) enhances the oxyresveratrol oxidation in the presence of light. Sequential spectra measurement were carried out using citrate and phosphate buffer giving a 5% of degradation with citrate vs 0.5% with phosphate (**Fig.** 4D, $P<0.05$), these data suggest that citric acid could be affected oxyresveratrol in presence of light. In addition, food model data suggest an increase of degradation at low temperatures in presence of citric acid pH 6.51. In other words, dark storage could solve this problem. These results demonstrated that fortified and oversaturated oxyresveratrol solutions would be almost completely stable at least 5 weeks in darkness, enabling storage for at least this time.

### 4.4 Study of bioaccesibility using *in vitro* digestion

To evaluate the stability of solutions during digestion, an *in vitro* approximation was applied. The concentration of samples was added in pepsin-pH 3 solution and the samples were then incubated at 37 ºC for 1 hour. Then they were incubated with a mixture of pancreatine, bilis extract and lipase pH 7 at 37ºC for 2 hours [9].

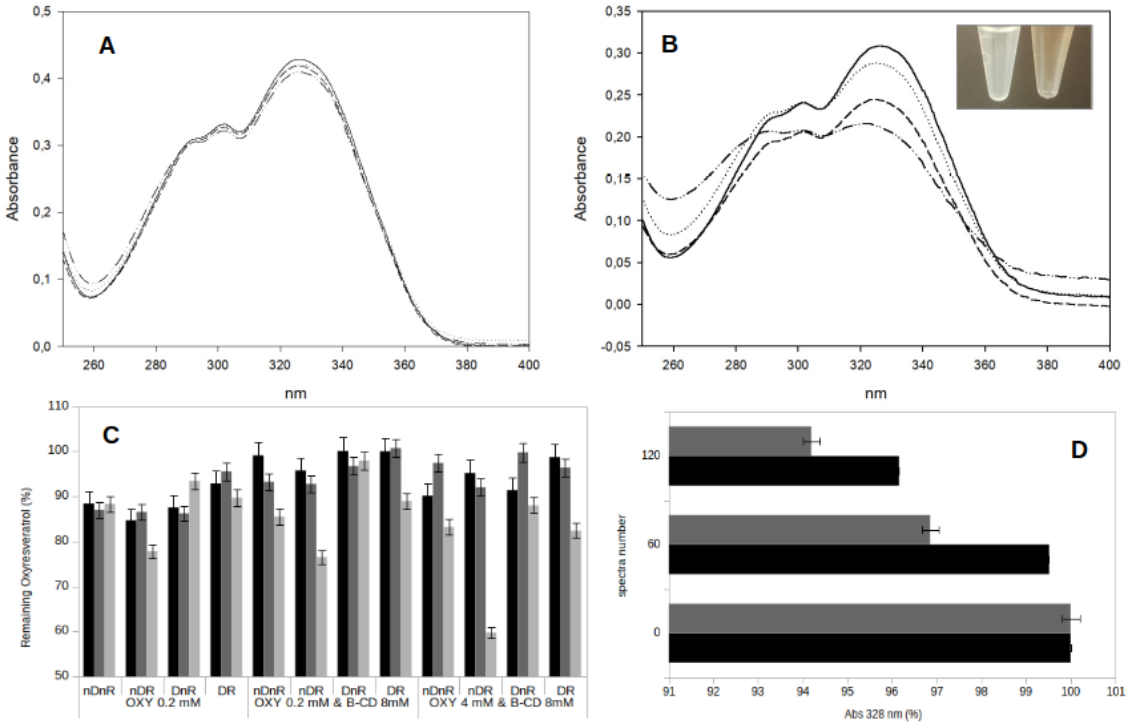


***Fig**. 4. (A) Spectra of orange model 4 mM oxyresveratrol & 8 mM β-CD non-darkness & refrigerated at week 0, 1, 3 and 5. (B) spectra of milk model 4 mM oxyresveratrol & 8 mM β-CD non-darkness & refrigerated at week 0, 1, 3 and 5. Insert, detail of darkness & non-darkness samples. (C) Remaining quantity of initial oxyresveratrol at the end of experiment of acetate 3.73 (black), orange model (pH 3.73 gray) and milk model (pH 6.51, light grey). Legend: DR = darkness & refrigerated, nDR = Non-darkness & refrigerated, DnR = Darkness & non-refrigerated and nDnR = Non-darkness & Non-refrigerated. OXY = oxyresveratrol (D) Effect of phosphate (black) and citric (gray) buffer on oxyresveratrol absorbance after repetitive spectra measurement.*

The ABTS measurement was used to determine the quantity of oxyresveratrol remaining based on its antioxidant capacity. In all samples, the antioxidant capacity was preserved. These data suggest the complete bioaccesiblity of oxyresveratrol. Our results and those of Lin and co-workers [13], lead to the conclusion that the huge increase of oxyresveratrol after using

β-CD in food products remains totally bioaccesibility and would increase its bioavailability in plasma.

### 4.5 Antimicrobial evaluation of food model samples.

The next step of our research was to evaluate the antimicrobial effect of the food model samples. A 96 LB well plate with *E.coli* DH5α (as bacterial witness), was incubated with increasing oxyresveratrol concentrations. Although oxyresveratrol did not stop the *E.coli* growing (**Fig.** 5A), the doubling time of *E.coli* was significantly increased in presence of 2.5 % and 5% of 4 mM food models ($P<0.05$). In this case, as was recently reported [18], there was an equilibrium between the increases in carbon source with β-CD, and the antimicrobial activity of oxyresveratrol. It is clear that β-CD promotes *E.coli* growth ($P<0.005$) Additionally, an antibiogram was also carried out using Petri dishes and circular filters impregnated by food model solutions which showed a slight bacteriostatic halo (**Fig.** 5B. Curiously, filters with “β-CD 8 mM” and “0.2 mM oxyresveratrol β-CD 8 mM” were completely covered by *E.coli* although “oxyresveratrol 0.2 mM” not (**Fig.** 5C) as a misbalance of growing/die equilibrium [18]. To sum up, the results demonstrated that fortification with oversaturated oxyresveratrol and β-CD could prevent the contamination of food products due to its antimicrobial capacity.

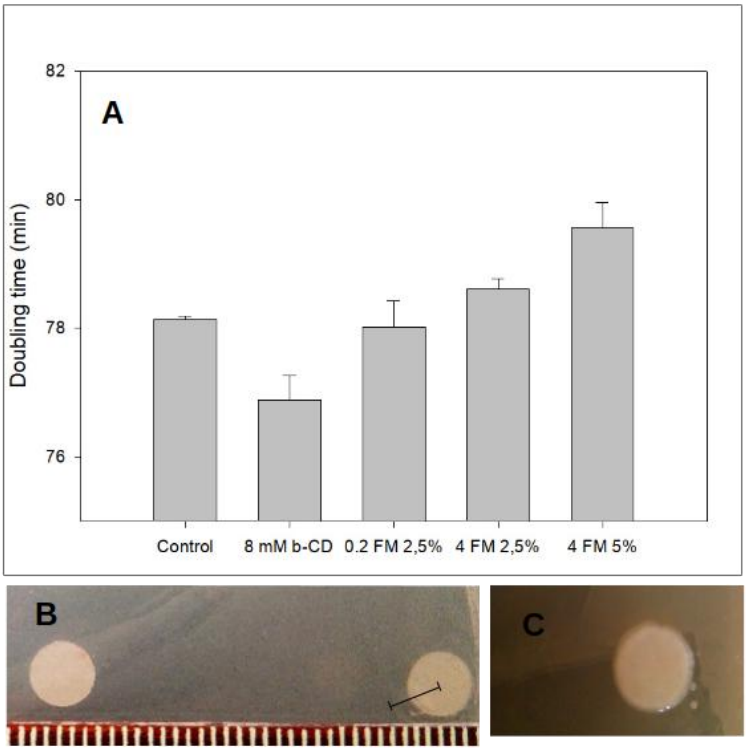


***Fig**. 5. (A) Doubling time of E.coli in presence of 2.5% of initial solution of 8 mM β-CD, food model 0.2 mM oxyresveratrol & 8 mM β-CD , food model 4 mM oxyresveratrol & 8 mM β-CD and finally 5% of 4 mM oxyresveratrol & 8 mM β-CD. (B) Antibiogram of food models, indicated, the bacteriostatic halo. (B) Detail of 0.2 mM oxyresveratrol & 8 mM β-CD filter*

In summary, the solubility of oxyresveratrol was increased by β-CD, an approved food additive, leading to a final concentration of 4 mM of oxyresveratrol, which was perfectly soluble, and presented higher antioxidant capacity than the intrinsic soluble sample. Different food models and condition were evaluated to compare the storage conditions of new functional foods based on oxyresveratrol. The results showed the samples to be perfectly stable for 5 weeks in all the conditions tested with the exception of the “oversaturated non-darkness stored milk food model samples” after 3 week, when partial

degradation started. Using dark storage an oversaturated oxyresveratrol solution solubilized by β-CD can be preserved at least 5 weeks.

All food models showed complete bioaccesibility which would also the increase of blood oxyresveratrol bioavailability in the blood. Finally, oversaturated oxyresveratrol/β-CD samples showed an antimicrobial effect higher than soluble oxyresveratrol. The findings as a whole represent a way for the food industry to improve the functional food market with oxyresveratrol (and stilbenes) products.

## References

[1] T. El Khawand, A. Courtois, J. Valls, T. Richard, S. Krisa, A review of dietary stilbenes: sources and bioavailability, Phytochem. Rev. 17 (2018) 1007–1029. doi:10.1007/s11101-018-9578-9.

[2] A.Y. Berman, R.A. Motechin, M.Y. Wiesenfeld, M.K. Holz, The therapeutic potential of resveratrol: a review of clinical trials, Npj Precis. Oncol. 1 (2017) 35. doi:10.1038/s41698-017-0038-6.

[3] H. Piotrowska, M. Kucinska, M. Murias, Biological activity of piceatannol: Leaving the shadow of resveratrol, Mutat. Res. Mutat. Res. 750 (2012) 60–82. doi:10.1016/j.mrrev.2011.11.001.

[4] Y.H. Lim, K.H. Kim, J.K. Kim, Source, biosynthesis, biological activities and pharmacokinetics of oxyresveratrol, Korean J. Food Sci. Technol. 47 (2015) 545–555. doi:10.9721/KJFST.2015.47.5.545.

[5] P. Rodríguez-Bonilla, J.M. López-Nicolás, F. García-Carmona, Use of reversed phase high pressure liquid cromatography for the physicochemical and thermodynamic characterization of oxyresveratrol/β-cyclodextrin complexes, J. Chromatogr. B. 878 (2010) 1569–1575. doi:10.1016/j.jchromb.2010.04.016.

[6] J. He, Z.-P. Zheng, Q. Zhu, F. Guo, J. Chen, Encapsulation Mechanism of Oxyresveratrol by β-Cyclodextrin and Hydroxypropyl-β-Cyclodextrin and Computational Analysis, Mol. Basel Switz. 22 (2017). doi:10.3390/molecules22111801.

[7] A. Babazadeh, B. Ghanbarzadeh, H. Hamishehkar, Novel nanostructured lipid carriers as a promising food grade delivery system for rutin, J. Funct. Foods. 26 (2016) 167–175. doi:10.1016/j.jff.2016.07.017.

[8] S. Ferreira, F. Domingues, The antimicrobial action of resveratrol against Listeria monocytogenes in food-based models and its antibiofilm properties, J. Sci. Food Agric. 96 (2016) 4531–4535. doi:10.1002/jsfa.7669.

[9] H. Ilyasoglu, S.N. El, Nanoencapsulation of EPA/DHA with sodium caseinate–gum arabic complex and its usage in the enrichment of fruit juice, LWT - Food Sci. Technol. 56 (2014) 461–468. doi:10.1016/j.lwt.2013.12.002.

[10] P. Rodríguez-Bonilla, F. Gandía-Herrero, A. Matencio, F. García-Carmona, J.M. López-Nicolás, Comparative Study of the Antioxidant Capacity of Four Stilbenes Using ORAC, ABTS+, and FRAP Techniques, Food Anal. Methods. 10 (2017) 2994–3000. doi:10.1007/s12161-017-0871-9.

[11] J. Escribano, M.A. Pedreño, F. García-Carmona, R. Muñoz, Characterization of the antiradical activity of betalains from Beta vulgaris L. roots, Phytochem. Anal. 9 (1998) 124–127. doi:10.1002/(SICI)1099-1565(199805/06)9:3<124::AID-PCA401>3.0.CO;2-0.

[12] O. Trott, A.J. Olson, AutoDock Vina: improving the speed and accuracy of docking with a new scoring function, efficient optimization, and multithreading, J. Comput. Chem. 31 (2010) 455–461. doi:10.1002/jcc.21334.

[13] W. Chen, S.C.M. Yeo, M.G.A.A. Elhennawy, H.-S. Lin, Oxyresveratrol: A bioavailable dietary polyphenol, J. Funct. Foods. 22 (2016) 122–131. doi:10.1016/j.jff.2016.01.020.

[14] A. Matencio, S. Hernández-García, F. García-Carmona, J. Manuel López-Nicolás, An integral study of cyclodextrins as solubility enhancers of α-methylstilbene, a resveratrol analogue, Food Funct. 8 (2017) 270–277. doi:10.1039/C6FO01677D.

[15] A. Matencio, F. García-Carmona, J.M. López-Nicolás, The inclusion complex of oxyresveratrol in modified cyclodextrins: A thermodynamic, structural, physicochemical, fluorescent and computational study, Food Chem. 232 (2017) 177–184. doi:10.1016/j.foodchem.2017.04.027.

[16] E. Fenyvesi, M. Vikmon, J. Szeman, E. Redenti, M. Delcanale, P. Ventura, J. Szejtli, Interaction of Hydroxy Acids with β-Cyclodextrin, J. Incl. Phenom. Macrocycl. Chem. 33 (1999) 339–344. doi:10.1023/A:1008094702632.

[17] M. Maafi, M.A. Al-Qarni, Φ-order spectrophotokinetic characterisation and quantification of trans-cis oxyresveratrol reactivity, photodegradation and actinometry, Spectrochim. Acta. A. Mol. Biomol. Spectrosc. 188 (2018) 64–71. doi:10.1016/j.saa.2017.06.067.

[18] C. Abril-Sánchez, A. Matencio, S. Navarro-Orcajada, F. García-Carmona, J.M. López-Nicolás, Evaluation of the properties of the essential oil citronellal nanoencapsulated by cyclodextrins, Chem. Phys. Lipids. 219 (2019) 72–78. doi:10.1016/j.chemphyslip.2019.02.001.

# Block II Part III

# Application of cyclodextrins to Pharmaceutical Science.

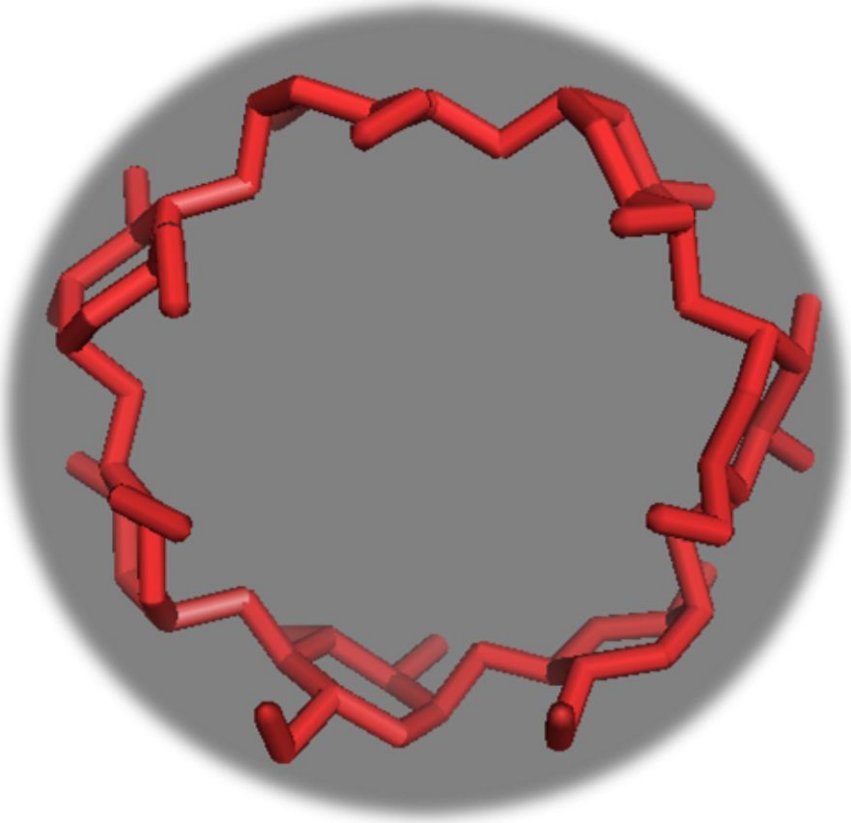

## Introduction

Pharmaceutical applications are always in our mind, everyone wants to live longer and healthier. The University of California describes pharmaceutical science as <<*a broad range of scientific disciplines that are critical to the discovery and development of new drugs and therapies*>> [1]. The great quantity of study areas could be classified within following categories: Drug discovery and design, drug delivery, drug action, bioavailability, analysis, clinical traits, toxicity, etc.

In the present thesis introduction was underlying the applications of CDs. As reader surely intuits, CDs have a great potential for pharmaceutical applications (e.g. some drugs improves their bioavailability complexed by CDs). In this section, we are going to show some application of CDs not only as drug nanocarrier, but also as a drug itself.

## References

[1] What are the Pharmaceutical Sciences? -, (n.d.). http://pharmsci.uci.edu/what-are-the-pharmaceutical-sciences/ (accessed April 22, 2019).

# Block II part III

# Chapter I

## *A clinical use of Hydroxypropyl-β-Cyclodextrin for treating a case of Niemann–Pick disease type C. Analysing urine using HPLC–LS in a novel way*

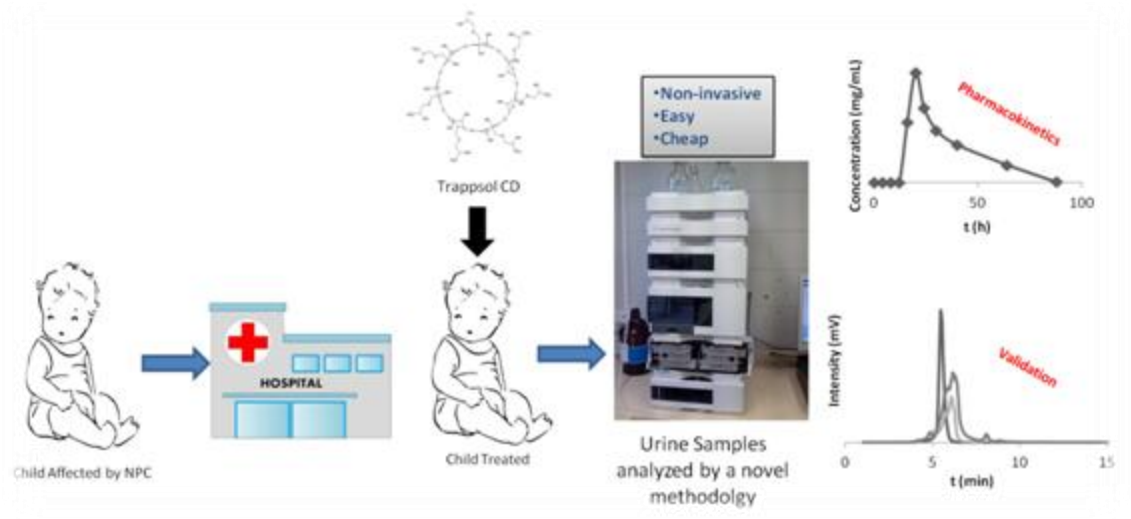


*Rest in peace*

**Abstract**

The Food and Drug Administration (FDA) and The European Medicines Agency (EMA) have granted Hydroxypropyl-beta-Cyclodextrin (HPβ-CD) orphan drug status for treating NPC because of its ability to mobilize cholesterol and improves the life quality in patients. In this chapter, a new methodology based on high resolution liquid chromatographic (HPLC) with light scattering detector was designed specifically to analyze HPβ-CD in urine samples of a child affected by NPC treated in Sanitas La Zarzuela Hospital (Madrid, Spain).

The treatment not only stopped disease progression, but also has increased the life expectancy and quality of our patient. The pharmacokinetic of HPβ-CD in the child was defined, with 92.8 % recovered after treatment. At 88 hours, no HPβ-CD was found in the urine. During the treatment, HPβ-CD has not shown toxicity. This study could improve the child treatment shortening the period between injections.

## Index

## 1. Contextualization

Niemann-Pick Type C disease (NPC) is a rare metabolomic disorder characterized by progressive ataxia, dementia, learning difficulties and intellectual decline, accompanied by short life expectancy [1,2]. Mutant *NPC1* and *NPC2* genes cause an accumulation of cholesterol (**Fig.** 1A) and a several glycosphingolipids in tissues such as the liver or brain [2,3].

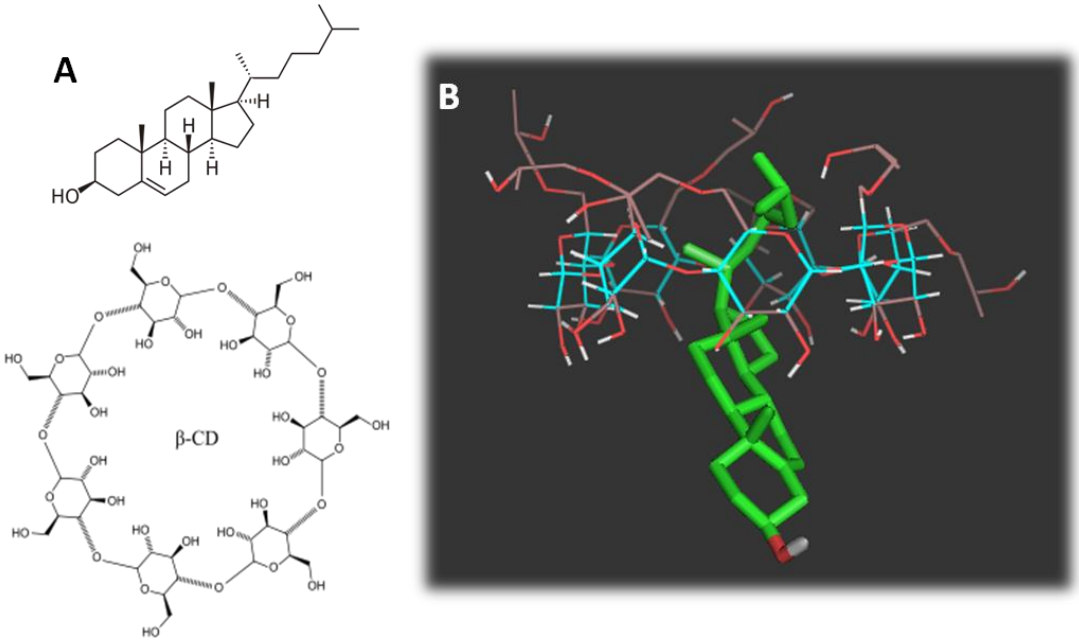


***Fig. 1:*** *(A) Cholesterol and β-CD. (B) Docking results of the Cholesterol/HPβ-CD complex (in pink, flexible atoms of HPβ-CD).*

The more cholesterol trapped in tissues, the greater its diffusion [4]. For this reason, in the absence of any therapy, the current focus is to reduce the degree of cholesterol accumulation [5]. Recently, The Food and Drug Administration (FDA) and The European Medicines Agency (EMA) granted Hydroxypropyl-beta-Cyclodextrin (HPβ-CD), a type of Cyclodextrin (CD, **Fig. 1A**), orphan drug status for treating NPC due to its well-known cholesterol solubilization (Fig. 1B) capacity [6,7] and low toxicity [8].

The action mechanism of HPβ-CD in tissues is not totally clear since it cannot cross membranes; however, a recent study suggested that it is delivered via pinocytosis to late endosomes/lysosomes [9].

Many papers have described the use of HPβ-CD in animal models [10,11] and in clinical cases [12,13], where treatment has demonstrated to be very effective. But, since an accumulation of HPβ-CD in the body could have unwanted side effects, it is essential to monitor its elimination. It has been measured in urine [14], although the method required indirect determination using phenolphthalein, thus increasing the possibility of errors. Matsuo et al. (2014) studied the pharmacokinetics of HPβ-CD with this method using cerebrospinal fluid (CSF). Nevertheless, as CDs can exit across the blood brain barrier [15], alternative, preferably non-invasive, techniques are necessary that the present study describes such a methodology. Furthermore, as we demonstrate if the time between injections is reduced to four days, the results will be better.

## 2. Objectives

1. To prepare a new method to measure HPβ-CD directly using HPLC-LS.
2. To try to use the method with other cyclodextrins.
3. To study its accuracy, sensibility and reproducibility
4. To check its method using real samples of a child affected with Niemman Pick type C.
5. To understand the complex Cholesterol/HPβ-CD.

## 3. Materials and methods

### 3.1 Patient

As a baby, the patient in question suffered cholestatic jaundice liver failure at 3 months and psychomotor retardation. As the patient had marked hepatosplenomegaly with a history of liver failure during breast feeding and suffered neurological deterioration, the possibility of NPC disease was studied, and NPC1 was diagnose at two years of age. Treatment with Miglustat® was carried out with no result (9/45 to 18/45 Disability Rating Scale [DRS, [16]] scale in 9 months). For this reason, the administration of HPβ-CD was considered at 3 years.

### 3.2 Materials

All CDs were purchased from Sigma-Aldrich (Madrid, Spain). Methanol, ethanol, isopropanol and acetonitrile were purchased from Fisher Chemical (U.K). Urine samples to make a linear regression were kindly supplied by a healthy volunteer. HPβ-CD was administrated as Trappsol ® (CTD Holdings, Alachua, USA).

### 3.3 Treatment

Trappsol® was administrated every fortnight (400 mg) intrathecally using an Ommaya device. Doses were prepared in saline solutions using sterile conditions and materials in the hospital pharmacy. Urine samples from the child were taken using a sterile tube during the course of four treatments. The research was carried out according to The Code of Ethics of the World Medical Association (Helsinki Declaration) and the informed consent was obtained. The

Sanitas-Hospital and "*Agencia Española de Medicamentos y productos sanitarios*" review board approved the study (Treatment code TRT585600308651).

### 3.4 Equipment and experimental procedures

Urine samples were filtered (0.22 µm diameter) and analyzed without further purification by HPLC a using a LC-20AD Shimadzu HPLC (Shimadzu, Japan) and an ELSD-LT II (Shimadzu, Japan) detector at 80 ºC drift tube temperature and $N_2$ pressure of 3.9 bar. A Unison UK-amino column (Imtakt, USA) 250 mm x 3 mm, 3 µm particle size, was used at 37 ºC injecting 1µL of the sample in a mobile phase of acetonitrile:water (70:30) at 0.4 mL/min.

For the calibration curve, 1 µL of different concentrations of HPβ-CD (0.5-5 mg/mL) were dissolved in the volunteer's urine. The method used was the same as above. For the coinjection experiment, 5 µL of the samples at an appropriate percentage of urine and pure HPβ-CD were injected using the same conditions. For the pharmacokinetics, different samples were taken over a period of 88 hours and 1µL was injected into the HPLC-LS system using the described method.

### 3.5 Molecular docking

HPβ-CD was built using Avogadro Software (version 2.3.2), adding the hydroxyl group to a β-CD obtained from the Protein Data Bank (PDB ID: 4RER). Cholesterol molecule was downloaded from the PubChem database (NCBI, USA). Molecular docking was carried out using Autodock Vina [17] and default parameters. HPβ-CD was considered as flexible. Graphical representations of

the docking results were prepared using PyMOL (Molecular GraphicsSystem, version 1.3, Schrödinger, LLC).

### 3.6 Data analysis

The samples were taken during the course of four treatments, and the data were analyzed and graphs constructed using Microsoft Excel (Version 2007). Pharmacokinetics study was carried out using PKsolved [18].

## 4. Results and discussion

### 4.1 Optimization of the HPLC-LS conditions

A UK-amino column was used because it separates oligosaccharides and derivates better than other column types such as the C18 column. Because of the direct method used, and the absence of a clear wavelength, a light scattering detector was considered the best option. After trying methanol, ethanol, isopropanol and acetonitrile at different proportions as solvent, acetonitrile:water (70:30) was chosen for its good HPβ-CD retention time (**Fig.** 2) and good symmetric. Similarly, after testing different temperatures (5, 20, 25, 30 and 37 ºC), 37 ºC was selected because it gave the best resolution. LS conditions were 80 ºC and $N_2$ pressure of 3.9 bars.

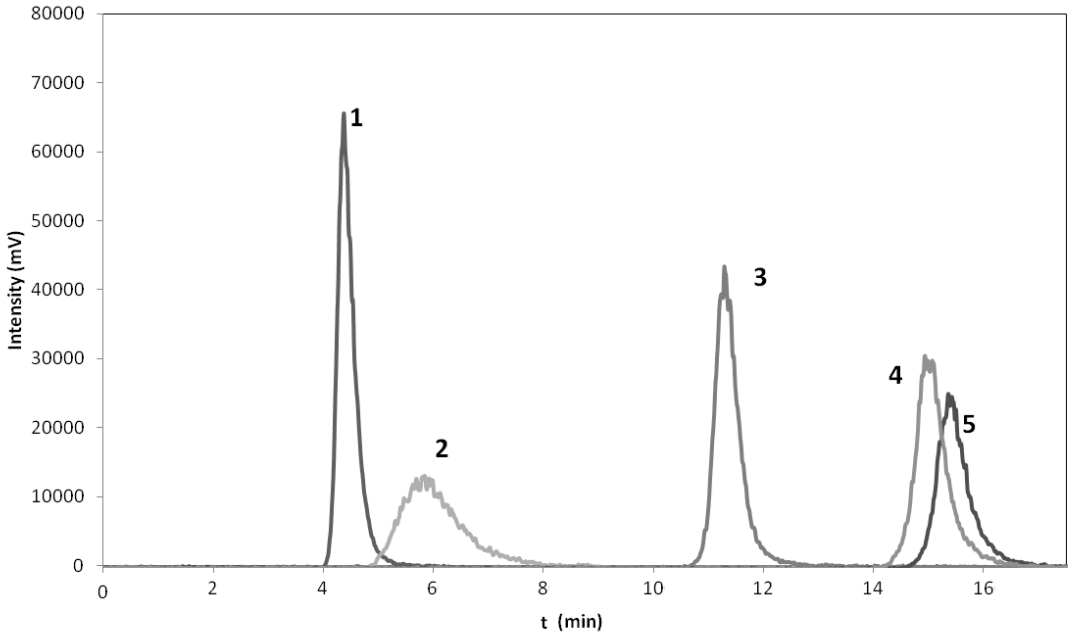


***Fig.** 2: Results of the injection of (1) MβCD, (2) HPβ-CD, (3) αCD, (4) βCD and (5) γCD using our method with 70 % acetonitrile and at 37 ºC and 0.4 mL/min.*

4.2 Testing the method with different types of cyclodextrins.

It is clear that other types of CD can be used as carriers for nutraceutics [19], for which reason, other CDs such as α-CD, β-CD and γ-CD and Mβ-CD were tested in the optimized conditions showing good results. As Fig. 2 shows, the first CD to be separated in urine was Mβ-CD (4.3 +/- 0.2 min), followed by HPβ-CD (5.8 +/- 0.2 min), α-CD (9.6 +/- 0.3 min), γ-CD (13.0 +/- 0.3 min) and β-CD (12.8 +/- 0.2 min) in urine.

4.3 Method validation and HPβ-CD identification of patient's urine.

The relative standard deviation (RSD) of the *Rt* of α-CD (3.1 %), β-CD (1.6 %) and γ-CD (2.3 %) and Mβ-CD (4.6 %) and HPβ-CD (3.4 %) was determined. The sensitivity of the method for HPβ-CD was tested satisfactorily up to $3.4 \cdot 10^{-10}$ mols (**Fig.** 4. *Insert*). In addition, a co-injection experiment with (1) HPβ-CD , (2) Urine and (3) HPβ-CD plus urine was carried out. The results (**Fig.** 3) showed that a peak in the urine alone (2) that was very close to that of the pure HPβ-CD alone (1) but with a different form. However, following co-injection (3), the peak observed for the urine increased. Adding the first peak area (peak 1) to the second (peak 2); an error of 3 % can be observed when comparing the sum with the area of third peak. These data demonstrated the accuracy, reproducibility precision of the new method.

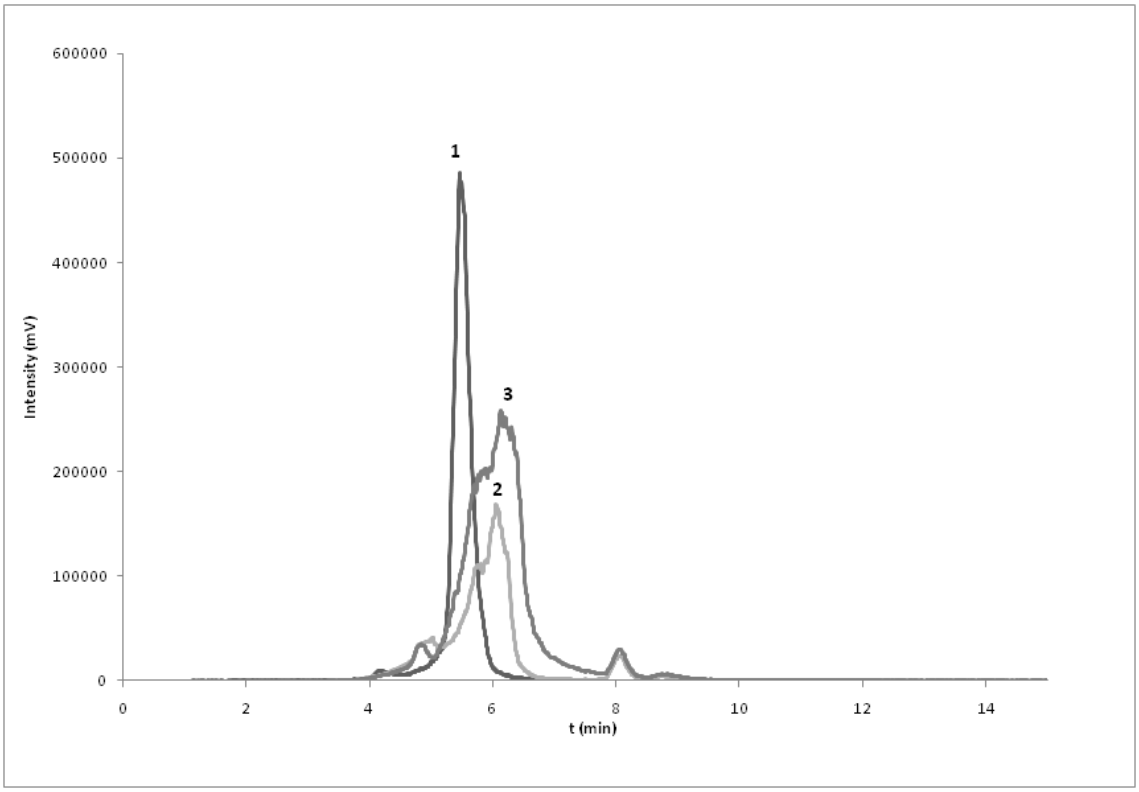


***Fig.*** *3: Injection of (1) HPβ-CD, (2) Urine and (3) mix of both. 70 % acetonitrile at 37 ºC and 0.4 mL/min.*

4.4 Cholesterol/HPβ-CD complex modeling

Although cholesterol cannot be eliminated by urine [20], it is important to study how the complex is formed. Molecular docking was carried out for this purpose, and the results (**Fig.** 1B) showed that HPβ-CD changed its conformation to when cholesterol was introduced without many modifications in cholesterol structure. Indeed, no hydrogens bonds were found probably because most of the forces involved in its complexation are Van der Walls interactions [21].

4.5 Quantification and pharmacokinetics of HPβ-CD in the subject's urine.

A calibration curve was constructed (**Fig.** 4. Inset) and then different samples of patient urine were taken and injected over a period of 88 h. The calibration curve was able to detect 0.5 µg efficiently. As **Fig.** 4 shows, the highest HPβ-CD concentration was found at 20h ($C_{max}$ = 2.5+/- 0.1 mg/mL) after which it gradually decreased until 88h, when no HPβ-CD was observed. The integration of the curve provided the mg/mL for 72h (when the HPβ-CD was still observed), with a result of 49.8mg/mL. As the average volume of urine for an NPC child is 0.5 mL/(kg body weight · h) [22], and the weight of the child was 13 kg at that moment, elimination was around 92.8% of the total HPβ-CD injected.

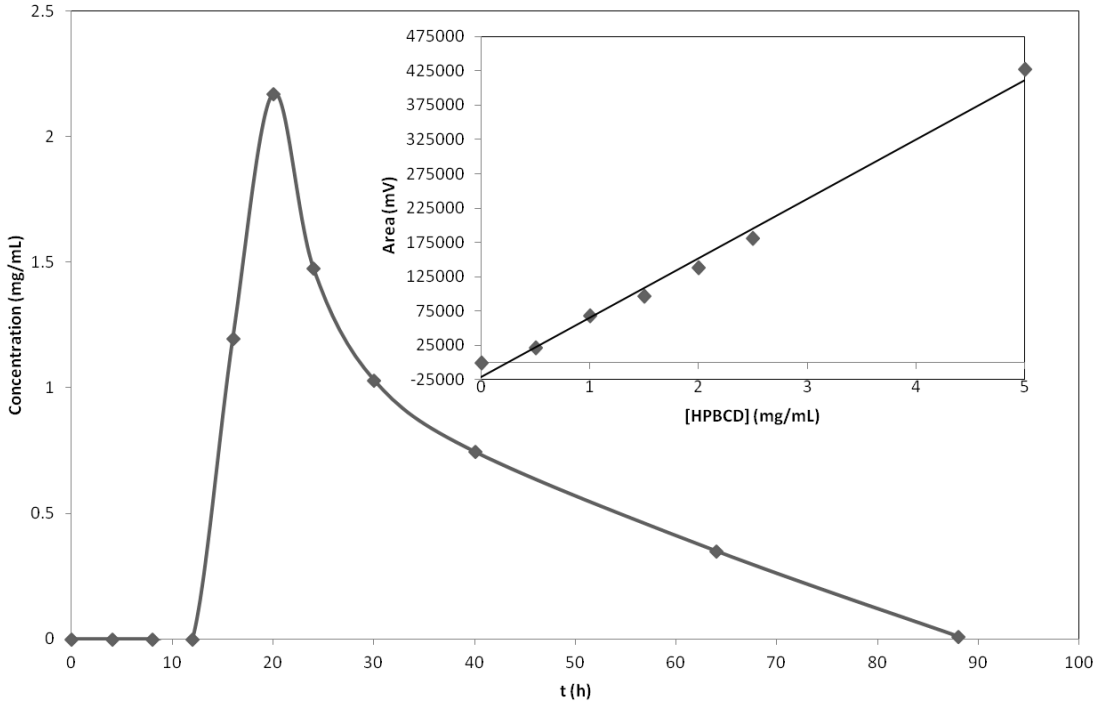


***Fig.** 4: Pharmacokinetics of HPβ-CD in the subject's urine. Inset. Linear regression of HPβ-CD in urine.*

Furthermore, at 88 hours, HPβ-CD was not found in the urine. By analyzing CSF Matsuo *et al*., (2014) described an HPβ-CD concentration decrease of 90% inside the brain after 1h. However our results suggest that HPβ-CD remains in the body a minimum of fifteen hours after which it begins to be eliminated. The results suggest that HPβ-CD in the blood could help to mobilize the cholesterol from other tissues[12], because it can complex and to make more soluble cholesterol, preventing their damage.

### 4.6 Patient evolution

At the beginning of HPβ-CD administration, our patient had an 18/45 score on the Disability Rating Scale (DRS) scale, where it has remained fairly stable during the previous 5 years. No toxicity or secondary effect for the treatment was found.

While it was not able to return the patient to her previous physical and mental stage; it clearly offered an increase in her life expectancy and life quality: the patient was 7 years old, while her life expectancy before the treatment was 6 years maximum. Recently, Santed *et al*., (2016) reported a case of a girl with NPC treated with HPβ-CD [23] administrated every fortnight without toxicity. However, the treatment was suspended a year and 8 month after starting because they reported progressive clinical deterioration. These data corroborate our pharmacokinetic results. It was demonstrated how at 88h no HPβ-CD was found in the body, so, it is clear that by shortening periods between injections the effectiveness of HPβ-CD can be improved.

In conclusion, a novel, fast, easy and direct HPLC methodology using a light scattering detector was designed for analyzing HPβ-CD in urine samples of a child affected by NPC. The method was extended to other types of CDs. According to the results, our method is sufficiently sensitive to detect HPβ-CD in urine. The pharmacokinetics of HPβ-CD in the subject was studied, showing 92.8% HPβ-CD recovery after treatment. At 88 hours, HPβ-CD was not found in the urine. No toxicity was observed during the treatment. The results show the injection of HPβ-CD could be increased from fortnight to every four days.

## REFERENCES

[1] P.G. Pentchev, M.E. Comly, H.S. Kruth, M.T. Vanier, D.A. Wenger, S. Patel, R.O. Brady, A defect in cholesterol esterification in Niemann-Pick disease (type C) patients, Proc. Natl. Acad. Sci. U. S. A. 82 (1985) 8247–8251.

[2] M.T. Vanier, Niemann-Pick disease type C, Orphanet J. Rare Dis. 5 (2010) 16. doi:10.1186/1750-1172-5-16.

[3] S. Cruz-Pardos, P.G.-P. y F.-J. Sánchez-García, Tratamiento con ciclodextrina para la enfermedad de Niemann Pick, Farm. Hosp. 37 (2013). doi:10.7399/FH.2013.37.3.555.

[4] J.J. Repa, H. Li, T.C. Frank-Cannon, M.A. Valasek, S.D. Turley, M.G. Tansey, J.M. Dietschy, Liver X receptor activation enhances cholesterol loss from the brain, decreases neuroinflammation, and increases survival of the NPC1 mouse, J. Neurosci. Off. J. Soc. Neurosci. 27 (2007) 14470–14480. doi:10.1523/JNEUROSCI.4823-07.2007.

[5] A. Santos-Lozano, D. Villamandos García, F. Sanchis-Gomar, C. Fiuza-Luces, H. Pareja-Galeano, N. Garatachea, G. Nogales Gadea, A. Lucia, Niemann-Pick disease treatment: a systematic review of clinical trials, Ann. Transl. Med. 3 (2015). doi:10.3978/j.issn.2305-5839.2015.12.04.

[6] R.O. Williams, V. Mahaguna, M. Sriwongjanya, Characterization of an inclusion complex of cholesterol and hydroxypropyl-beta-cyclodextrin, Eur. J. Pharm. Biopharm. Off. J. Arbeitsgemeinschaft Für Pharm. Verfahrenstechnik EV. 46 (1998) 355–360.

[7] Y. Yu, C. Chipot, W. Cai, X. Shao, Molecular Dynamics Study of the Inclusion of Cholesterol into Cyclodextrins, J. Phys. Chem. B. 110 (2006) 6372–6378. doi:10.1021/jp056751a.

[8] S. Gould, R.C. Scott, 2-Hydroxypropyl-beta-cyclodextrin (HP-beta-CD): a toxicology review, Food Chem. Toxicol. Int. J. Publ. Br. Ind. Biol. Res. Assoc. 43 (2005) 1451–1459. doi:10.1016/j.fct.2005.03.007.

[9] A.I. Rosenbaum, G. Zhang, J.D. Warren, F.R. Maxfield, Endocytosis of beta-cyclodextrins is responsible for cholesterol reduction in Niemann-Pick type C mutant cells, Proc. Natl. Acad. Sci. 107 (2010) 5477–5482. doi:10.1073/pnas.0914309107.

[10] C.H. Vite, J.H. Bagel, G.P. Swain, M. Prociuk, T.U. Sikora, V.M. Stein, P. O'Donnell, T. Ruane, S. Ward, A. Crooks, S. Li, E. Mauldin, S. Stellar, M. De Meulder, M.L. Kao, D.S. Ory, C. Davidson, M.T. Vanier, S.U. Walkley, Intracisternal cyclodextrin prevents cerebellar dysfunction and Purkinje cell death in feline Niemann-Pick type C1 disease, Sci. Transl. Med. 7 (2015) 276ra26. doi:10.1126/scitranslmed.3010101.

[11] C.M. Ramirez, B. Liu, A.M. Taylor, J.J. Repa, D.K. Burns, A.G. Weinberg, S.D. Turley, J.M. Dietschy, Weekly cyclodextrin administration normalizes cholesterol metabolism in nearly every organ of the Niemann-Pick type C1 mouse and markedly prolongs life, Pediatr. Res. 68 (2010) 309–315. doi:10.1203/PDR.0b013e3181ee4dd2.

[12] M. Matsuo, M. Togawa, K. Hirabaru, S. Mochinaga, A. Narita, M. Adachi, M. Egashira, T. Irie, K. Ohno, Effects of cyclodextrin in two patients with Niemann-Pick Type C disease, Mol. Genet. Metab. 108 (2013) 76–81. doi:10.1016/j.ymgme.2012.11.005.

[13] M. Matsuo, K. Shraishi, K. Wada, Y. Ishitsuka, H. Doi, M. Maeda, T. Mizoguchi, J. Eto, S. Mochinaga, H. Arima, T. Irie, Effects of intracerebroventricular administration of 2-hydroxypropyl-β-cyclodextrin in a patient with Niemann–Pick Type C disease, Mol. Genet. Metab. Rep. 1 (2014) 391–400. doi:10.1016/j.ymgmr.2014.08.004.

[14] H.W. Frijlink, J. Visser, N.R. Hefting, R. Oosting, D.K.F. Meijer, C.F. Lerk, The Pharmacokinetics of β-Cyclodextrin and Hydroxypropyl-β-cyclodextrin in the Rat, Pharm. Res. 7 (1990) 1248–1252. doi:10.1023/A:1015929720063.

[15] M. Vecsernyés, F. Fenyvesi, I. Bácskay, M.A. Deli, L. Szente, É. Fenyvesi, Cyclodextrins, Blood–Brain Barrier, and Treatment of Neurological Diseases, Arch. Med. Res. 45 (2014) 711–729. doi:10.1016/j.arcmed.2014.11.020.

[16] M. Rappaport, K.M. Hall, K. Hopkins, T. Belleza, D.N. Cope, Disability rating scale for severe head trauma: coma to community, Arch. Phys. Med. Rehabil. 63 (1982) 118–123.

[17] O. Trott, A.J. Olson, AutoDock Vina: improving the speed and accuracy of docking with a new scoring function, efficient optimization, and multithreading, J. Comput. Chem. 31 (2010) 455–461. doi:10.1002/jcc.21334.

[18] Y. Zhang, M. Huo, J. Zhou, S. Xie, PKSolver: An add-in program for pharmacokinetic and pharmacodynamic data analysis in Microsoft Excel, Comput. Methods Programs Biomed. 99 (2010) 306–314. doi:10.1016/j.cmpb.2010.01.007.

[19] R. Challa, A. Ahuja, J. Ali, R.K. Khar, Cyclodextrins in drug delivery: An updated review, AAPS PharmSciTech. 6 (2005) E329–E357. doi:10.1208/pt060243.

[20] K. Einarsson, K. Nilsell, B. Leijd, B. Angelin, Influence of Age on Secretion of Cholesterol and Synthesis of Bile Acids by the Liver, N. Engl. J. Med. 313 (1985) 277–282. doi:10.1056/NEJM198508013130501.

[21] A. Matencio, F. García-Carmona, J.M. López-Nicolás, Aggregation of t10,c12 conjugated linoleic Acid in presence of natural and modified cyclodextrins. A physicochemical, thermal and computational analysis, Chem. Phys. Lipids. 204 (2017) 57–64. doi:10.1016/j.chemphyslip.2017.03.008.

[22] V. Ruiz-Rodado, R. Marcos Luque-Baena, D. te Vruchte, F. Probert, R. H. Lachmann, C. J. Hendriksz, J. E. Wraith, J. Imrie, D. Elizondo, D. Sillence, P.

Clayton, F. M. Platt, M. Grootveld, 1H NMR-Linked Urinary Metabolic Profiling of Niemann-Pick Class C1 (NPC1) Disease: Identification of Potential New Biomarkers using Correlated Component Regression (CCR) and Genetic Algorithm (GA) Analysis Strategies, Curr. Metabolomics. 2 (2014) 88–121.

[23] M.R. Santed, M.J.C. Poy, M.D.T. Riera, C.C. Ramírez, A.F. Polo, S.C. Bautista, Intrathecal cyclodextrin in the treatment of Niemann-Pick disease type C, Eur. J. Hosp. Pharm. (2016) ejhpharm-2016-001067. doi:10.1136/ejhpharm-2016-001067.

# Block II part III

# Chapter II

## *A novel way to improve the bioaccesibility and photostability of roflumilast by cyclodextrins*

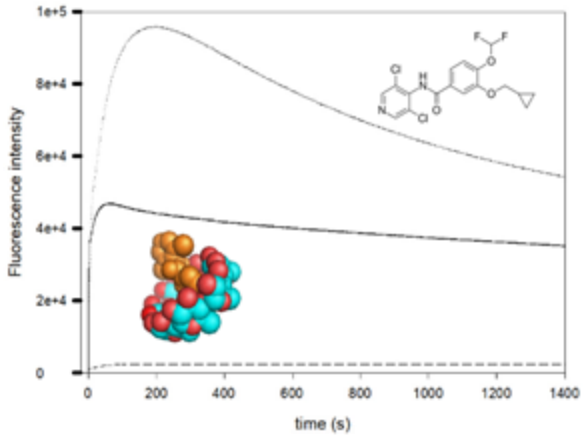


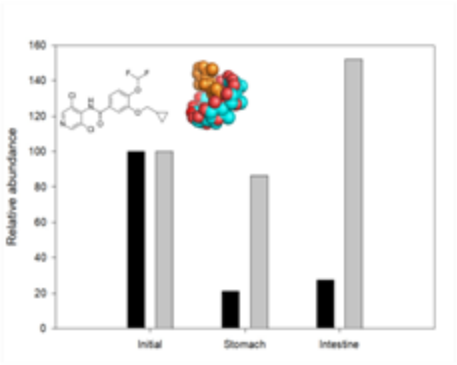

**Abstract**

Roflumilast is an orally available inhibitor of phosphodiesterase (PDE) type 4, which is widely used in chronic obstructive pulmonary diseases. However, it has low solubility and adverse effects include diarrhea and nausea. Since its solubilization may improve treatment and, dismissing any adverse effects, its interaction with cyclodextrins (CDs) was studied. The Higuchi-Connors method was used to determine the complexation constant with different CDs, pH values and temperatures. Molecular docking was used to predict interaction between the complexes. An in vitro digestion experiment was carried out to test roflumilast protection. Finally, the photostability of the complex was evaluated.

The complex formed with β-CD had the highest K11 value (646 +/- 34 M-1), although this value decreased with increasing temperature. Similarly, K11 decreased as the pH increased. In vitro digestion showed that CDs protect the drug during digestion and even improve its bioaccessibility. Finally, CDs reduced the drug's extreme photosensitivity, originating a fluorescence signal, which is described for first time. The kinetic parameters of the reaction were obtained.

This study not only completes the complexation study of roflumilast-CD, but also points to the need to protect roflumilast from light, suggesting that tablets containing the drug might be reformulated

## Index

## 1. Contextualization

### 1. Introduction

Roflumilast (**Fig.** 1) is an orally available, long-acting inhibitor of phosphodiesterase (PDE) type 4 (PDE4), with anti-inflammatory and potential antineoplastic activities [1]. Roflumilast and its active metabolite roflumilast N-oxide are selective and competitive inhibitors of PDE4 [1], which leads to an increase in both the intracellular levels of cyclic-3',5'-adenosine monophosphate (cAMP) and cAMP-mediated signaling. A recent review focused on its use in chronic obstructive pulmonary disease (COPD, [2]), for which it has been commonly administered since its approving in 2010 (EU) and 2011 (FDA) approving.

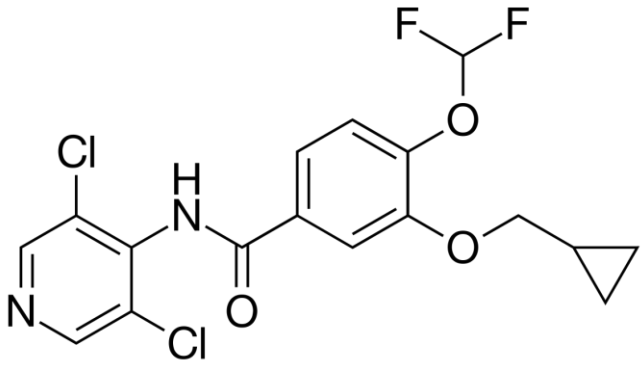


***Fig.*** *1 Structure of Roflumilast.*

Despite its good bioavailability, adverse effects such as diarrhea or nausea have been reported [3], its low solubility could originate an osmotic diarrhea [4] while the increase in concentration of cAMP probably has the same effect [5]. Whatever the case, these observations suggest that treatment with roflumilast might improve if its solubility could be improved (and fewer drugs would be necessary). However, this bioactive molecule is easily oxidized and so

any new strategy to improve its solubility and bioavailability must be able to limit any undesirable oxidation. In this chapter, we analyze the encapsulation of roflumilast in a molecule with a known high complexation capacity: cyclodextrin (CD).

Recently, an article described how roflumilast was prepared with hydroxypropyl-β-CD (HPβ-CD), demonstrating that the CD can be a good carrier and that the resulting complex has a good apparent transepithelial permeability coefficient, similar to that of another drugs [6]. However, the study was only performed with HPβ-CD, overlooking a large number of CDs that might offer even better results. For example no natural CDs were studied and, furthermore, the effect of temperature (a very important variable for release) was not studied.

## 2. Objectives

1. To analyze the encapsulation mechanism of roflumilast by different types of natural and modified CDs.
2. To evaluate the effect of temperature and pH on the encapsulation mechanism of roflumilast.
3. To study the physical interactions between roflumilast and CDs using molecular docking.
4. To determine the stability and bioaccessibilityof the complex in digestion.
5. To understand the increased photostability of the complex.

## 3. Materials and Methods

### 3.1. Materials

α-, β- and γ-CD, pepsin-HCl, pancreatine and bilis were purchased from Sigma-Aldrich (Madrid, Spain). Hydroxypropyl-beta- and methyl-beta-cyclodextrin (HPβ-CD and Mβ-CD DS) were purchased from Carbosynth (Berkshire, UK). Roflumilast (CID 5281717) was purchased from Xi An Kerui Biochemical CO (Xi'an, China) and used as received. The samples were stored in darkness. Ethanol (absolute, analysis grade) was purchased from Panreac (Madrid, Spain).

### 3.2. Equipment and Experimental Procedure

#### *3.2.1. Inclusion complex characterization.*

To characterize the encapsulation process, the method of Higuchi and Connors [7] was used. Tubes with specific quantities of CDs were prepared at a fixed quantity of roflumilast (8 mg/mL). Using different incubation times, it was demonstrated that a minimum of 10 h was necessary to achieve equilibrium, so, all the samples in this experiment were incubated for 12 h. A calibration curve was used to obtain roflumilast concentration (using roflumilast dissolved in 5% EtOH).

This method is able to evaluable a 1:1 stoichiometry (1 CD per molecule).

$$\text{CD} + \text{roflumilast} \leftrightarrow \text{CD-roflumilast} \qquad (1)$$

Total solubility ($S_t$) of the drug in solution with CDs was evaluated using the equation:

$$S_t = S_0 + \frac{K_F S_0}{1 + K_F S_0}[CD] \quad (2)$$

where $S_0$ is the intrinsic solubility of the drug, $K_{11}$ is the apparent 1:1 complex stability constant and CD is the concentration of CD in the tube. Plotting the solubilized/complexed guest *vs*. solubilizer provides a "solubility isotherm" that can be fitted to equation 2. This giving a slope that can be used to obtain K11 using the Higuchi and Connors method:

$$K_{F11} = \frac{Slope}{S_0(1 - Slope)} \quad (3)$$

*3.2.2. Temperature and pH*

To study the effect of temperature on roflumilast encapsulation by CD, increasing temperatures of 278, 283, 288, 293, 298, 303, 310 and 318 K (5, 10, 15, 20, 25 30, 37 and 45 ºC) were assayed. The thermodynamic relationship shown in equation 3 was used to determine the standard thermodynamic parameters of enthalpy and entropy of roflumilast complexation in CD:

$$Ln\, K_{F11} = -\frac{\Delta H^\circ}{RT} + \frac{\Delta S^\circ}{R} \quad (4)$$

where $K_{11}$ is the complexation constant of the inclusion complex, T is the temperature in Kelvin, R is the gas constant, $\Delta H^\circ$ and $\Delta S^\circ$ are the standard enthalpy and entropy changes of the complexes formed in the mobile phase. For a linear plot of ln $K_{11}$ *vs.* 1/T, the slope and intercept were $-\Delta H^\circ/R$ and $\Delta S^\circ/R$, respectively. To determine the Gibbs free energy change for the interactions that take place during the inclusion process, equation 5 was used:

$$\Delta G^{\circ} = \Delta H^{\circ} - T\Delta S^{\circ} \quad (5)$$

For the pH studies, the same method as that described in the above section was followed at pH 6, 7.4 and 8 (although the incubation time was three hours due to the drug's stability at pH 8). The following buffers were used i) pH {6-7.4} 100 mM Phosphate-Na and ii) pH 8 100 mM Borate-Na.

### *3.2.3. Molecular docking*

The molecular structures used in this work were obtained from several databases. β-CD was obtained from Protein Data Bank (ID 4RER) and used without modification. Roflumilast was downloaded from the PubChem database (NCBI, USA). HPβ-CD was build using Pymol (Molecular GraphicsSystem, version 1.3, Schrödinger, LLC) from β-CD. Input files for docking were generated using Autodock tools (version 1.5.6) with default parameters and charges. Molecular docking was carried out using Autodock Vina [8] using default parameters. CDs were considered as flexible. A graphical representation of the docking result was prepared using PyMOL with default parameters to display hydrogen bonds.

### *3.2.4. In vitro digestion*

Three samples i) control, ii) roflumilast 0.2 mg/mL and iii) roflumilast 0.2 mg/mL in the presence of 17.5 mg/mL of HPβ-CD (in a volume ingestion of 0.24 L) were subjected to the *in vitro* digestion model to assess the behavior of the complexes [9]. The protocol was the same as that described by Ilyasoglu (2014) with a few modifications: First, samples were prepared in saline at pH 3 with pepsin-HCl to simulate the gastric phase before incubating in a shaking water

bath at 37 °C for 1 h. The incubation was stopped by adding 1 mol/$m^3$ $Na_2CO_3$ to increase the pH to 6.9. In the subsequent intestinal phase, the pH was adjusted to 6.9 and a pancreatin–bile extract–lipase mixture was added before incubating at 37 °C for 2 h. Tubes were placed in an ice bath to stop digestion and centrifuged at 10,000 × g at 4 °C for 35 min and the contents were diluted in phosphate-Na buffer pH 7.4 to achieve the same final concentration and filtered. The samples were analyzed using an Agilent HPLC 1200 series equipped with a TOF 6220 (acquisition range 100-1100) in negative mode. Six microliters of the soluble part were injected using 40/60 $H_2O$/MeOH with 20 mM ammonium acetate as mobile phase at 0.6 mL/min and 25 ºC. The ratio of the roflumilast content of the *in vitro* digested sample to the initial content was taken to represent its bioaccessibility.

### *3.2.5. Photostability study*

The spectra of roflumilast with or without CDs were obtained using a Jasco V-650 Spectrophotometer (Jasco, Spain) between 200 and 400 nm. Fluorescence spectra were obtained in a Shimazdu RF-6000 spectrofluorimeter (Shimadzu, Japan) equipped with thermostatically controlled cells. Excitation and emission bandwidths were both set at 2 nm. The excitation and emission wavelengths for roflumilast were 290 nm and 380 nm, respectively. The relative fluorescence intensity values were recorded at 25 ºC. To avoid inner filter effects, 2 mm quartz cells were used. The concentration of roflumilast was fixed at 8 µM and the CD concentration was varied between 0 and 5 mM. All reagents were dissolved in 0.1 M pH 7 sodium-phosphate buffer 4 % EtOH.

The HPLC-MS sample was prepared by exposing the sample at 290 nm for 30 min and analyzed using an Agilent 1200 series HPLC equipped with a TOF 6220 (acquisition range 100-1100) in positive mode. Six microliters of 8 µM irradiated roflumilast were injected using a 40/60 H2O/MeOH mixture with 20 mM ammonium acetate as mobile phase at 0.6 mL/min and 25 ºC.

*3.2.6. Photodegradation kinetic study*

The kinetic parameters of the reaction were obtained from consecutive reaction kinetics:

$$A \xrightarrow{k1} I \xrightarrow{k2} P \quad (4)$$

where "A" was roflumilast, "I" the intermediate, "P" the product of the reaction and $k_n$ the reaction rate constants. [I] and [P] can be expressed using the following equations:

$$[\mathrm{I}] = [\mathrm{A_0}]\frac{k_1}{k_2 - k_1}(e^{-k_1 t} - e^{-k_2 t}) \quad (7)$$

$$[\mathrm{P}] = [\mathrm{A_0}](1 + \frac{1}{k_2 - k_1})(k_2 e^{-k_1 t} - k_1 e^{-k_2 t}) \quad (8)$$

The fluorescent signal is the product of each concentration and its fluorescence yield,

$$F = Fi[I] + Fp[P] \quad (9)$$

where Fi and Fp are the fluorescent yield of each product. Adding equations 7 and 8 in 9, a novel equation can be obtained:

$$F = Fi[A_0]\frac{k_1}{k_2 - k_1}(e^{-k_1 t} - e^{-k_2 t}) + Fp[A_0](1 + \frac{1}{k_2 - k_1})(k_2 e^{-k_1 t} - k_1 e^{-k_2 t})$$

(10)

*3.2.7. Data analysis.*

The HPLC-MS experiments were carried out once, while the remaining experiments were carried out in triplicate. Graphical representations were made using SigmaPlot (Version 10.0) and GraphPad Prism (version 5.03) was used for the kinetic fitting. A t-test was applied using Rstudio (version 0.99.878), fixing the significance level at $P < 0.05$. Other mathematical operations were carried out using wxMaxima software (version 12.04.0).

## 4. Results and discussion

### 4.1. Effect of CDs on the solubility of roflumilast

The first step was to study the effect of CDs on the solubility of roflumilast. The first candidate selected was β-CD because it has a similar inner cavity to HPβ-CD. Different tubes at a fixed roflumilast quantity (8 mg/mL) were prepared with increasing β-CD concentrations and mixed for 12 h. **Fig.** 2A shows the variations in the apparent solubility of roflumilast in these conditions. A linear regression was carried out to obtain the slope for the $K_{11}$ calculation, which gave a value of 646+/- 32 $M^{-1}$. In order to increase the number of CDs evaluated with roflumilast, different natural (α- and γ-) and modified (HPβ-CD and Mβ-CD) CDs were used. The results (table 1) showing great variability.

**Table 1.** Apparent $K_{11}$ values and SD for Higuchi and Connors method (1:1 complex).

| | B-CD | Mβ-CD | HPβ-CD | γ-CD | α-CD |
|---|---|---|---|---|---|
| $K_{11}$ ($M^{-1}$) | 646 | 418 | 329 | 300 | 143 |
| SD (+/-) | 32 | 20 | 16 | 15 | 7 |

As can be seen in **Fig.** 2A the solubility presented a behavior of a typical AL-type curve. Moreover, the solubility with 8mM was 6 times higher than without β-CD A value that reflects the normal $K_{11}$ values (between 50 and 2000 $M^{-1}$ [10]) obtained with this technique. Of all the CDs tested, β-CD provided the highest values of $K_{11}$ followed by Mβ-CD and HPβ-CD, the two modified CDs

studied. It seems that the cavity of β-CD was optimal for encapsulating roflumilast; by contrast, the extra polarity of the hydroxypropyl substituent may prevent a better fit. The γ-CD presented a very close value to HPβ-CD (ANOVA, p≈0.08), not statistically significant. The cavity of γ-CD may be sufficient for a good fit, although not optimal. Finally, α-CD presented the worst result. These observations demonstrated that the addition of CD to the solution can increase the apparent solubility of roflumilast, although, the complexation strength is not the same for all CDs.

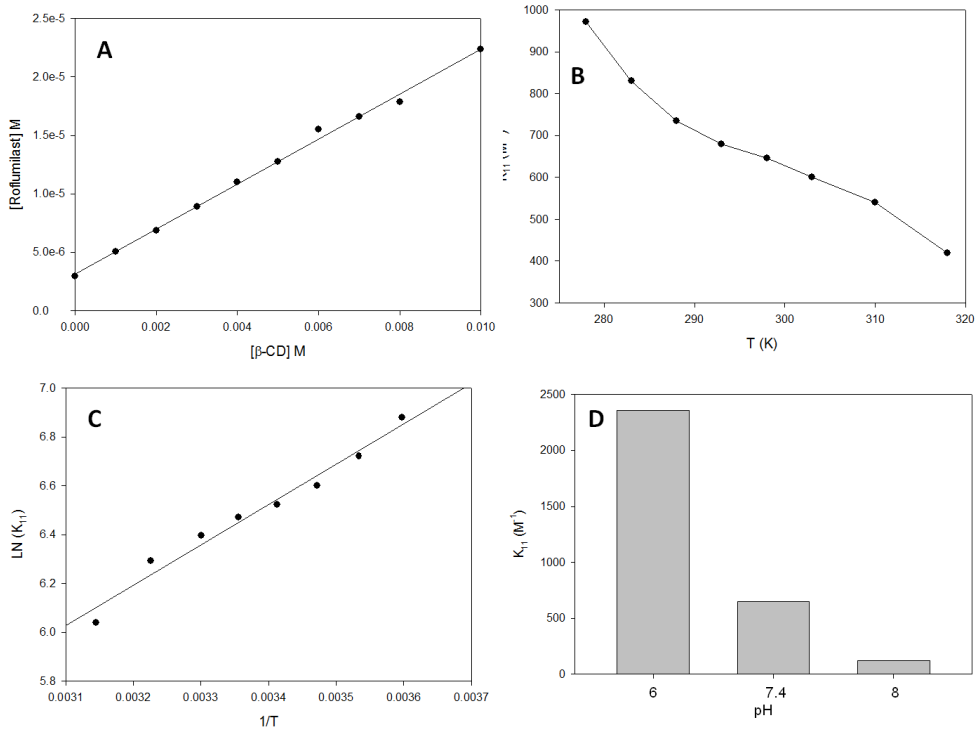


***Fig 2.*** *(A) Effect of β-CD concentration on roflumilast solubility at pH 7.4 25ºC. (B) Effect of temperature on $K_{11}$ values for roflumilast and β-CD complexes at pH 7.4. (C) Van't Hoff plot. (D) Effect of pH on $K_{11}$ values for roflumilast and β-CD complexes at 25 ºC.*

4.2. Effect of temperature on roflumilast and β-CD complexation.

One of the most important parameters that must be studied when using complexes as ingredients in the pharmaceutical industry is the effect of temperature on the complexation mechanism, which must be tested at different temperatures. **Fig.** 2B shows an inverse relationship between temperature and $K_{11}$, while a direct relationship was obtained for $S_{int}$ (the theoretical solubility obtained from the intercept regression) or $S_0$. The encapsulation process is more efficient at low temperatures.

4.3. Thermodynamic parameters for the roflumilast- β-CD complexes

The next step was to study the main thermodynamic parameters of the complexation process (***ΔHº, ΔSº*** and ***ΔGº*** at 25 ± 0.2 ºC) in order to study mechanistic aspects of the affinity of roflumilast for β-CD. For this, a van´t Hoff plot (eq. 4) was used and the Ln $K_{11}$ was plotted *vs.* 1/T. The data showed a lineal behavior, with a correlation coefficient higher than 0.96 (**Fig.** 2C). Results showed the following values: ΔHº = –13.7 +/- 0.9 KJ $mol^{-1}$, ΔSº = 7.4 +/- 0.4 J $mol^{-1}$ $K^{-1}$ and ΔGº = -15.7 +/- 0.8 KJ $mol^{-1}$.

The thermodynamic values obtained led to three main conclusions being drawn concerning the nature of the complexation of roflumilast by β-CD: i) the process is *exothermic,* as deduced from the negative values obtained for enthalpy changes. This indicate the exothermic nature of the interaction processes of roflumilast with β-CD. This behavior is typical of hydrophobic interactions, van der Waals interactions and the displacement of water molecules from the cavity of β-CD or the formation of hydrogen bonds. ii) The process presents a positive value for entropy changes possibly due to the water

released from the β-CD cavity and/or the increase of hydrophobic interactions [11]; iii) The process is *spontaneous*, as seen from the negative value obtained for the Gibbs free energy change (for the interactions that take place during the inclusion process at 25 ± 0.2 ºC.

### 4.4. Effect of pH on complexation constant of roflumilast with β-CD

As shown in **Figure** 2D, $K_{11}$ values are closely dependent on pH, passing from a value of 2356 +/- 118 $M^{-1}$ (when the medium pH is 6) to about 121 +/- 6 $M^{-1}$ (medium pH 8).

The sharp decrease in the $K_{11}$ value observed in **Fig.** 2D coincides with the region where the roflumilast could be influenced by its pKa (8.74, pubchem). A possible cause for this pH-dependence of $K_{11}$ would be the formation of a hydrogen bond between roflumilast and CD, since hydrogen bonding is one of the most important types of interaction in the stabilization of inclusion complexes [12,13]. The fact that the complexes between β-CD and roflumilast were more stable below 7.4 is of great interest for the industry, because lower CD concentrations are necessary for roflumilast to be administered.

### 4.5. Molecular docking simulations of roflumilast/β-CD complex

One of the most widely used techniques for predicting the host/guest interactions resulting from complexation with CDs is molecular docking [14,15]. After preparing the inputs, Vina software was used. The function score is a fast mathematical methods used to predict the strength of the non-covalent interaction (also referred to as binding affinity). The score for the roflumilast/β-

CD complex was -8.9 and for HPβ-CD it was -6.9. **Fig.** 3A shows the most probable pose of the Vina software. Furthermore, the amine atom was seen to be near (2.5 Å) a hydroxyl part of CD. **Fig.** 3B shows the vina pose for the roflumilast/HPβ-CD complex. The pose showed three possible hydrogen bonds.

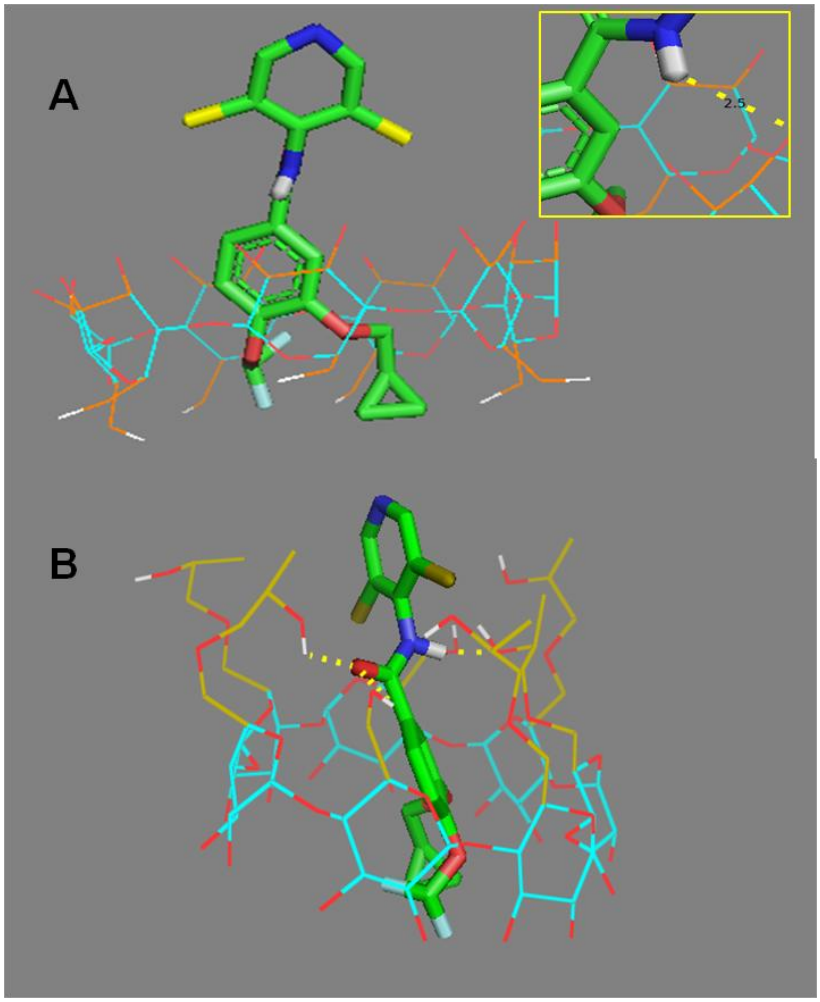


***Fig 3.*** *(A) Result for roflumilast/β-CD docking pose simulation, interactions are in yellow. Flexible atoms are coloured orange. Insert. Details of interaction. (B) (A) Result for roflumilast/HPβ-CD docking pose simulation, interactions are in yellow. Flexible atoms are coloured orange.*

The molecular docking score indicated that the encapsulation is spontaneous. The fact that the data correlated perfectly with the $K_{11}$ value indicates that the predictions provided the essential interaction information between CD and roflumilast. The complete encapsulation of roflumilast by β-CD was observed, especially of the most hydrophobic part. The same profile was found for HPβ-CD. The chlorine atoms remained outside in the figure, perhaps because they are more hydrophilic than the other parts. Furthermore, the amine atom was seen to be near (2.5 Å) a hydroxyl part of CD, where it probably contributed an important function to the stabilization of the complex. Although HPβ-CD/roflumilast showed more hydrogen bonds than β-CD complex, some interference with hydroxypropyl substituent (e.g steric hindrance) could affect negatively to the complexation.

4.6. Effect of CD addition on the roflumilast digestion.

Roflumilast is an orally administrated drug: for example DAXAS® is administrated as a 500 mg tablet (1.24 µmols/day). Although the tablets are usually film coated, CDs could be considered as a carrier for oral administration (alone or in combination) of roflumilast. An experimental *in vitro* digestion was carried out for i) roflumilast 0.2 mg/mL and ii) roflumilast 0.2 mg/mL in the presence of 17.5 mg/mL of HPβ-CD in 0.24 L of final volume [16]. The CD concentration was the 50 % of the legally limited level [17]. In both cases roflumilast was supersaturated and only the soluble part was analyzed. The solution was filtered and diluted using phosphate-Na buffer pH 7.4 for analysis by LC-MS.

**Fig.** 4 shows the [Roflumilast-H]-abundance, shows the abundance of the roflumilast ion and the adducts formed normalized with their abundance at $t_0$. The results showed that CDs not only protected roflumilast at pH 3, but also increased its solubility. Indeed, at pH 6.9, the solubility of roflumilast may increase explaining the increase of roflumilast/CD sample and roflumilast alone. Roflumilast in acid (1 N HCl) conditions gives 3,5-dichloropyiridin-4-amine [18], and as HCl was used to adjust the pH in the *in vitro* stomach simulation maybe this products might appear. 3,5-dichloropyiridin-4-amine sodium adduct was obtained with an abundance of 9320 without HPβ-CDs *vs* 273 with HPβ-CD at the end of the digestion, a 34.13 fold increase.

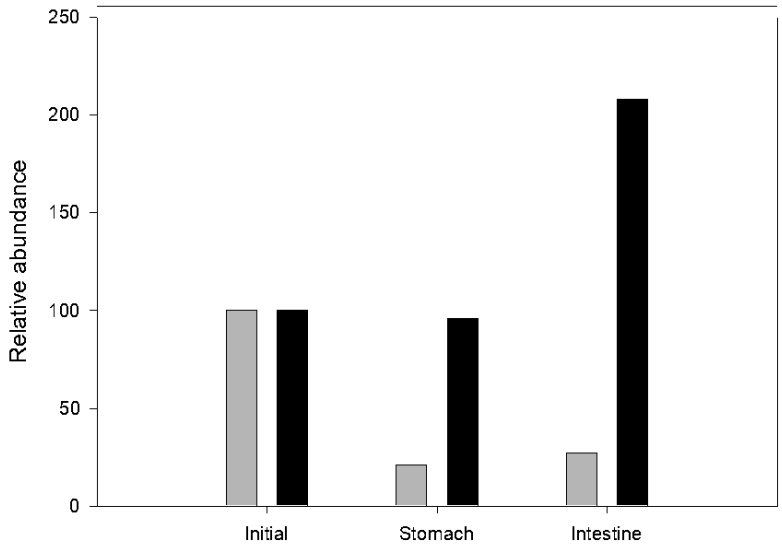


***Fig 4.*** *Relative abundance of roflumilast ions after stomach and intestine digestion without CD (gray) and with HPβ-CD (black). The data are normalized using initial roflumilast abundance.*

Our results indicate that the stomach part might be the most aggressive. For that reason, a film-coated tablet for the stomach part would be desirable if

CDs are used. Even so, our results were quite good. The increase in roflumilast solubility demonstrated that CDs not only partially protect roflumilast during digestion, but increase its solubility and bioaccesibility, information that may be used to reformulate tablets because the same results can be obtained using less roflumilast.

4.7. Effect of CD addition on roflumilast photostability.

The photostability of chlorine-containing drugs is well-documented [19]. For this reason, the photostability of complexed roflumilast was studied. **Fig.** 5A and 5B shows the effect of the complexation on the consecutive absorbance signal. The decrease in absorbance was slower with HPβ-CD, reflecting the apparent greater protection of the drug. Moreover, at around 240 nm, an apparent isopectic point was observed, suggesting a destructive reaction is ocurring.

It is well known that the fluorine atom is fluorescent. So, the next step was to study the possible fluorescence of roflumilast. The results showed for the first time that roflumilast is fluorescent. The excitation and emission wavelengths for roflumilast were 290 nm and 380 nm, respectively. No phosphorescence was found. At these nm values, a time course analysis showed that the signal increased with time (25min) (**Fig.** 5C). The signal presented a maximum around 180 seconds of irradiation followed by a gradual decrease. Stopping the reaction before the maxima excitation, did not return the drug to its original state. The reaction was slower in the presence of HPβ-CD, possibly due to the encapsulation and protection. Furthermore, an experiment without $O_2$ (Inner $N_2$

atmosphere) pointed to the absence of a fluorescence signal and no degradation of the drug.

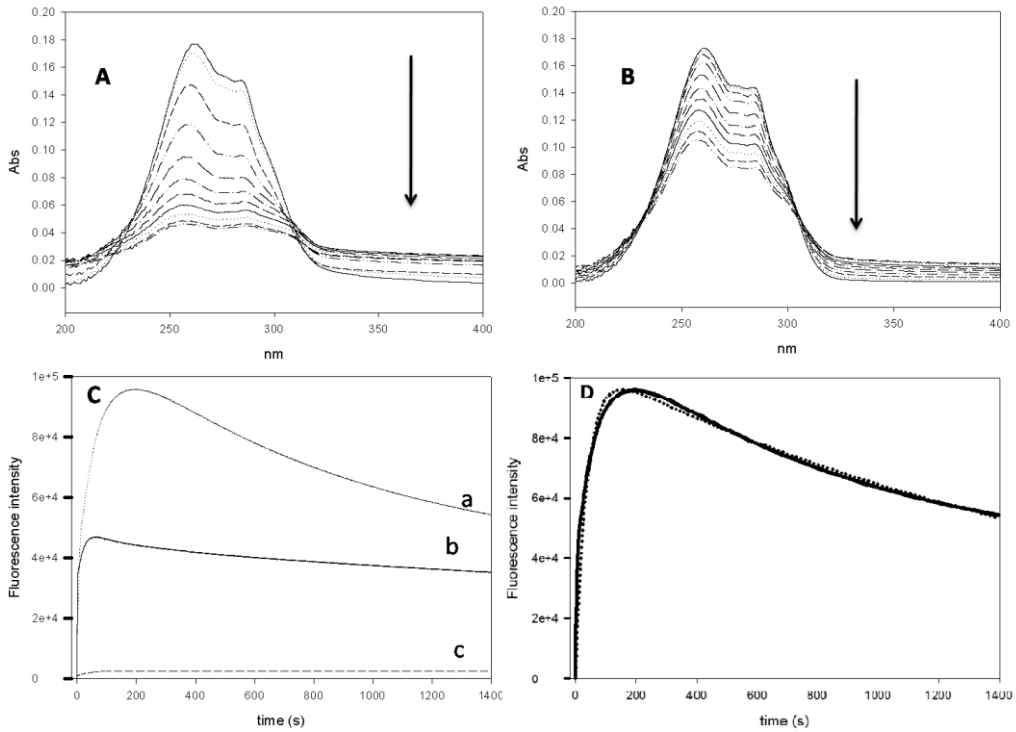


***Fig 5. (****A) Spectra of roflumilast 24 µM at 4% EtOH pH 7.4 and 25 ºC every 2 minutes.* ***(****B) Spectra of roflumilast 24 µM at 4% EtOH with 5 mM β-CD at pH 7.4 and 25 ºC every 2 minutes. (C) Fluorescence time-course for (a) roflumilast 8 µM at 4% EtOH pH 7.4 and 25 ºC; (b) roflumilast 8 µM at 4% EtOH with 5 mM β-CD pH 7.4 and 25 ºC and (c) roflumilast 8 µM at 4% EtOH pH 7.4 and 25 ºC in $N_2$ atmosphere. (D) Experimental fluorescence time course for roflumilast 8 µM at 4% EtOH pH 7.4 and 25 ºC (represented by a line) and the fit (represented by dots).*

As the fluorescence signal did not return to basal state, an irreversible change must have occurred. An HPLC-MS analysis of the reaction showed an interesting peak at 367.0661 (*data not showed*), which presented exactly the mass as roflumilast without one chlorine atom. This product was suggested by Paul in (2015) as a fragment of their MS/MS studies [18].

4.8. Kinetics analysis of the reaction

In the previous section we explained the phenomena that occurred when roflumilast was irradiated. There seemed to be a consecutive reaction pathway where a substrate "A" reacts to give an unstable intermediate "I" and a stable "P" product. Our data suggest that the intermediate product must be more fluorescent than the final product; so, this signal could be used to obtain the kinetic parameters ($k_1$ and $k_2$) of the reaction by using Eq. 10. Graphpad iterated the data and predicted the values of $F_i = 1.28 \cdot 10^{10}$ +/- 6.4 $10^8$ a.u., $k_1 = 2.86 \cdot 10^{-2}$ +/- 1.43 +/- $10^{-3}$ $s^{-1}$, $k_2 = 4.83 \cdot 10^{-4}$ +/- 2.42 +/- $10^{-5}$ $s^{-1}$and $F_p = 8.5 \cdot 10^4$ +/- $4 \cdot 10^2$ a.u. with a $R^2 > 0.97$ (**Fig.** 5D). These results demonstrated that the conversion of roflumilast in the intermediate (A → I) is the most important contribution to the fluorescence signal. Furthermore, $k_1$ is 56 times higher than $k_2$; So, the formation of the product would be the rate-determining step (RDS) of the reaction. With this in mind, a possible reaction scheme was formed (**Fig**. 6*)* where roflumilast, in the presence of oxygen and light, is irradiated giving an intermediate molecule, whose degradation releases one chlorine atom.

The problem of photostability must be taken into account during the manufacture and administration of the drug. The use of CDs was seen to decrease the effect of light on roflumilast. The reaction was irreversible because no return to initial drug state was observed. These facts suggest that oxygen is crucial to the reaction mechanism, in contrast of chlorpromazine or hydrochloryhiazide [19]. The reaction released chlorine after light irradiation in the presence of oxygen, generating a fluorescent signal. This reaction can be prevented an inner atmosphere. CDs showed a protective effect on the reaction

although the docking results suggested that the chlorine part remains outside the complex, perhaps because the protection of fluorine atoms prevents its irradiation.

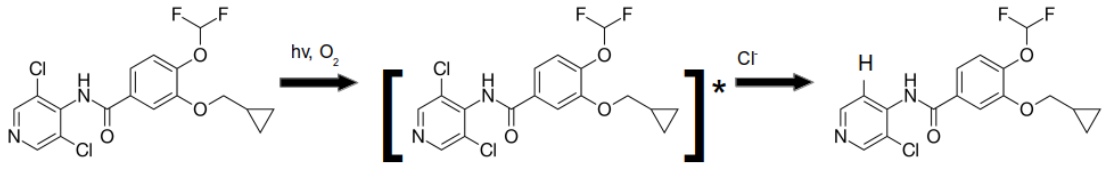


***Fig 6.*** *Plausible simplified reaction mechanism.*

In conclusion, the Higuchi-Connors method was used to obtain the values of $K_{11}$ of natural and modified CDs with roflumilast; β-CD was the best CD tested with a value of 684.55 +/- 34.23 $M^{-1}$. The effect of temperature and pH on the encapsulation process was also evaluated. The $K_{11}$ values increased at low temperatures. The thermodynamic parameters were also evaluated ($\Delta H^o$ = – 12.21 +/- 0.6 KJ $mol^{-1}$, $\Delta S^o$ = 12.93 +/- 0.6 J $mol^{-1}$ $K^{-1}$ and $\Delta G^o_{(25)}$ = -15.73 +/- 0.8 KJ $mol^{-1}$). The effect of pH was inversely proportional. These data agree with the increase in roflumilast solubility at higher temperature and pH values. Besides, molecular docking simulations were carried out to study their interactions. A high degree of correlation was observed between the computed score and experimental value. An *in vitro* digestion showed that CDs could protect this drug during digestion and improve its bioaccessibility. Finally, when the effect of CDs on the photostability of roflumilast was evaluated CDs were seen to reduce the photosensitivity of roflumilast. These changes originated a fluorescence signal, which is described for first time in this compound (λ excitation 290, λ emission 380). The fluorescence was seen to be dependent on $O_2$ and to release one chlorine atom. Kinetic parameters calculated for a

consecutive reaction showed that the formation of the intermediate is 53 times faster than the corresponding of the product formation and is responsible for the signal. This study not only completes the complexation study of roflumilast-CD, but also reveals the need to protect roflumilast from light and degradation.

## References

[1] A. Hatzelmann, C. Schudt, Anti-Inflammatory and Immunomodulatory Potential of the Novel PDE4 Inhibitor Roflumilast in Vitro, J. Pharmacol. Exp. Ther. 297 (2001) 267–279.

[2] J.A. Wedzicha, P.M. Calverley, K.F. Rabe, Roflumilast: a review of its use in the treatment of COPD, Int. J. Chron. Obstruct. Pulmon. Dis. 11 (2016) 81–90. doi:10.2147/COPD.S89849.

[3] DailyMed - DALIRESP- roflumilast tablet, (n.d.). https://dailymed.nlm.nih.gov/dailymed/drugInfo.cfm?setid=c9a1d0a8-581f-4f91-a2b8-f419192d0ebf (accessed October 11, 2018).

[4] T.A. Woods, Diarrhea, in: H.K. Walker, W.D. Hall, J.W. Hurst (Eds.), Clin. Methods Hist. Phys. Lab. Exam., 3rd ed., Butterworths, Boston, 1990. http://www.ncbi.nlm.nih.gov/books/NBK414/ (accessed April 6, 2019).

[5] B. Beghè, K.F. Rabe, L.M. Fabbri, Phosphodiesterase-4 inhibitor therapy for lung diseases, Am. J. Respir. Crit. Care Med. 188 (2013) 271–278. doi:10.1164/rccm.201301-0021PP.

[6] É.Y. Suzuki, M.I. Amaro, G.S. de Almeida, L.M. Cabral, A.M. Healy, V.P. de Sousa, Development of a new formulation of roflumilast for pulmonary drug delivery to treat inflammatory lung conditions, Int. J. Pharm. 550 (2018) 89–99. doi:10.1016/j.ijpharm.2018.08.035.

[7] H.T. Connors KA, Phase solubility techniques, Adv. Anal. Chem. Instrum. 4 (1965) 117–210.

[8] O. Trott, A.J. Olson, AutoDock Vina: improving the speed and accuracy of docking with a new scoring function, efficient optimization, and multithreading, J. Comput. Chem. 31 (2010) 455–461. doi:10.1002/jcc.21334.

[9] H. Ilyasoglu, S.N. El, Nanoencapsulation of EPA/DHA with sodium caseinate–gum arabic complex and its usage in the enrichment of fruit juice, LWT - Food Sci. Technol. 56 (2014) 461–468. doi:10.1016/j.lwt.2013.12.002.

[10] K.A. Connors, Population characteristics of cyclodextrin complex stabilities in aqueous solution, J. Pharm. Sci. 84 (1995) 843–848. doi:10.1002/jps.2600840712.

[11] M.V. Rekharsky, Y. Inoue, Complexation Thermodynamics of Cyclodextrins, Chem. Rev. 98 (1998) 1875–1918. doi:10.1021/cr970015o.

[12] R. Bru, J.M. López-Nicolás, E. Núñez-Delicado, D. Nortes-Ruipérez, A. Sánchez-Ferrer, F. Garciá-Carmona, Cyclodextrins as hosts for poorly water-soluble

compounds in enzyme catalysis, Appl. Biochem. Biotechnol. 61 (1996) 189–198. doi:10.1007/BF02785701.

[13] W. Saenger, Cyclodextrin Inclusion Compounds in Research and Industry, Angew. Chem. Int. Ed. Engl. 19 (1980) 344–362. doi:10.1002/anie.198003441.

[14] A. Matencio, C.J.G. Hernández-Gil, F. García-Carmona, J.M. López-Nicolás, Physicochemical, thermal and computational study of the encapsulation of rumenic acid by natural and modified cyclodextrins, Food Chem. 216 (2017) 289–295. doi:10.1016/j.foodchem.2016.08.023.

[15] A. Matencio, F. García-Carmona, J.M. López-Nicolás, Encapsulation of piceatannol, a naturally occurring hydroxylated analogue of resveratrol, by natural and modified cyclodextrins, Food Funct. 7 (2016) 2367–2373. doi:10.1039/c6fo00557h.

[16] D.M. Mudie, K. Murray, C.L. Hoad, S.E. Pritchard, M.C. Garnett, G.L. Amidon, P.A. Gowland, R.C. Spiller, G.E. Amidon, L. Marciani, Quantification of Gastrointestinal Liquid Volumes and Distribution Following a 240 mL Dose of Water in the Fasted State, Mol. Pharm. 11 (2014) 3039–3047. doi:10.1021/mp500210c.

[17] Questions and answers on cyclodextrins used as excipients in medicinal products for human use, (n.d.) 9.

[18] S.K. Paul, U.N. Dash, Identification of Degradation Products in the Phosphodiesterase (PDE-4) Inhibitor Roflumilast Using High Resolution Mass Spectrometry and Density Functional Theory Calculations, Mass Spectrom. Lett. 6 (2015) 38–42. doi:10.5478/MSL.2015.6.2.38.

[19] D.E. Moore, S.R. Tamat, Photosensitization by drugs: photolysis of some chlorine-containing drugs, J. Pharm. Pharmacol. 32 (1980) 172–177. doi:10.1111/j.2042-7158.1980.tb12884.x.

# Block III

# Synthesis and application of cyclodextrin based nanosponges polymer

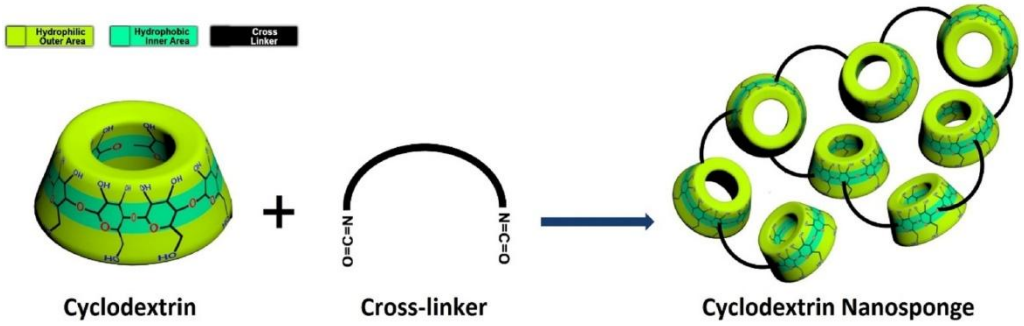


*Obtained from [1]*

**Block Introduction**

In this block, we are going to work with cyclodextrin (CDs) not commercially available. Indeed, a polymer based on CDs will be synthesized in collaboration with Prof. Dr. Francesco Trotta group (University of Turin, Italy). The polymer synthesized will be CD based nanosponges (CD-NS). Recent reviews [1,2] point to the wide potential, applications of these polymers that include i) increasing the apparent solubility of poorly soluble drugs, ii) modulating drug release and activity, iii) protecting drugs against several agents, iv) enhancing bioactivities, v) the ability to absorb contaminants, vi) drug delivery, etc.

Cross-linking CDs brings significant benefits to CD-NSs compared with the respective native CDs used. In general, CD-NSs are able to form complexes with a wider series of molecules due to the presence of interstitial spaces among CDs, which can host more hydrophilic guests. A further advantage of using NSs, is the polymer network that surrounds the cavities and hampers the diffusion of entrapped guest molecules, thus promoting slower release kinetics.

For these reasons, in this block a synthesis of CD-NS will be carried out to study the complexation of oxyresveratrol with soluble and insoluble CD-NS and applied in anticancer and lifespan studies.

## References

[1] A.P. Sherje, B.R. Dravyakar, D. Kadam, M. Jadhav, Cyclodextrin-based nanosponges: A critical review, Carbohydr. Polym. 173 (2017) 37–49. doi:10.1016/j.carbpol.2017.05.086.

[2] S. Swaminathan, R. Cavalli, F. Trotta, Cyclodextrin-based nanosponges: a versatile platform for cancer nanotherapeutics development, Wiley Interdiscip. Rev. Nanomed. Nanobiotechnol. 8 (2016) 579–601. doi:10.1002/wnan.1384.

# Block III

## Chapter I

## Study of oxyresveratrol complexes with insoluble cyclodextrin based nanosponges. Application in an anticancer study.

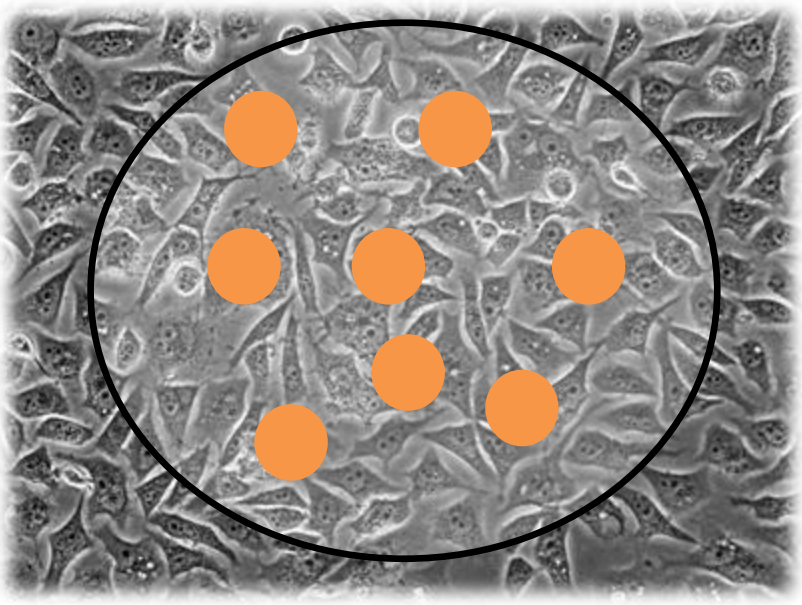

**Abstract**

We have used a polymer called cyclodextrin-based nanosponge (CD-NS) to establish a stable complex. Because no method is currently available to study the complexation formulation a new methodology is used to calculate, for the first time, an apparent inclusion complex constant ($K_{Fapp}$) between a ligand and CD-NSs using UV-Vis measurement and the Benesi-Hildebrand technique with modifications. The constant was evaluated with different CD-NSs, its value depended on the type of cyclodextrin or number of bridges. Moreover, the $K_{Fapp}$ of other drugs such as resveratrol was also evaluated and compared.

The complex of OXY with the nanosponge β-CDI 1:4 (one CD per CDI linker), was studied *in vitro* using DSC, TGA and FTIR techniques and its encapsulation efficiency and release behavior were studied. Finally, an anticancer study against PC-3 prostate cancer cell line was carried out showing higher inhibition of cell viability (42 % free oxy *vs.* 58% complexed). These data demonstrated the potential of CD-NS to enhance oxyresveratrol stability and bioactivities.

## Index

## 1. Contextualization

Oxyresveratrol (*trans*-3,5,2′,4′-tetrahydroxystilbene, OXY, **Fig**. 1A) a stilbenoid present in mulberry fruits (*Morus alba* L.) and twigs is a naturally occurring resveratrol analogue with an additional hydroxyl group in the aromatic ring. A recent review [1] showed that OXY exhibits a wide range of biological activities, such as antioxidant, antiviral, anti-inflammation, anti-obesity, cholesterol lowering, hepatoprotection, neuroprotection and photo-protective effects. Furthermore, OXY presents cyclooxygenase and tyrosinase-inhibitory activities. Indeed, OXY has demonstrated great potential in several pre-clinical studies [2,3].

Previously has been characterized the inclusion complexes of OXY with modified CDs (block I, Part II, chapter III), and our research group characterized OXY/natural CDs complexes [4]. The results obtained with this commonly used matrix were very good and considerably improved oxyresveratrol qualities. However, when bioactive compounds are to be used as a pharmaceutical product, sometimes is desirable a slower release than the obtained by CD complexes [5]. For that reason this chapter describes a new approach using Cyclodextrin-based nanosponges (CD-NSs). CD-NSs are innovative cross-linked polymer structures with a three-dimensional network with a crystalline and amorphous structure, spherical in shape and possessing good swelling properties [6]. Recent reviews [7,8] point to the wide potential, applications of these polymers that include i) increasing the apparent solubility of poorly soluble drugs, ii) modulating drug release and activity, iii) protecting drugs against

several agents, iv) enhancing bioactivities, v) the ability to absorb contaminants, vi) drug delivery, etc.

Cross-linking CDs brings significant benefits to CD-NSs compared with the respective native CDs used. In general, CD-NSs are able to form complexes with a wider series of molecules due to the presence of interstitial spaces among CDs, which can host more hydrophilic guests. A further advantage of using NSs, is the polymer network that surrounds the cavities and hampers the diffusion of entrapped guest molecules, thus promoting slower release kinetics. No less important is the fact that CD-NSs are insoluble; hence they can be easily recovered from aqueous media and recycled

While CD-NSs have previously been used to encapsulate the stilbene resveratrol [9] there is a gap in the characterization of CD-NS complexes that have not been studied yet due to the difficulty in knowing the molecular weight of CD-NSs: the establishment of a protocol to calculate the encapsulation constant. This lack of knowledge makes it difficult to know the exact quantities of each reactant to add and its extrapolation to bigger volumes.

**2. Objectives**

1) To establish a methodology to calculate the $K_{app}$ between OXY and CD-NSs, and to compare its value with others.

2) To characterize the structure of the OXY/CD-NSs complex by FTIR, DSC and TGA

3) To study the release profile and uploading of the OXY/CD-NSs complex

4) To study the anticancer effect of CD-NS complexes *in cellulo*.

## 3. Materials and methods

### 3.1 Materials

α-Cyclodextrin (α-CD), β-Cyclodextrin (β-CD) and γ-Cyclodextrin (γ-CD) were purchased from Roquette (France). 1,1′-Carbonyldiimidazole (CDI), Dimethylformamide (DMF), ethanol and dialysis membranes were purchased from Sigma-Aldrich. Oxyresveratrol (OXY, CID 5281717) was purchased from TCI Europe and used as received. The samples were stored in darkness

### 3.2 Equipment and Experimental Procedure

#### *3.2.1 Preparation of nanosponges.*

Different CDI nanosponges (α-, β- and γ-) were prepared as reported [10]. Briefly, 100 mL of anhydrous DMF was placed in a round bottom flask and 10 g of the appropriate CD was added until complete dissolution. Then, the required quantity of CDI was added in a different molar ratio of 1:4 or 1:8 (CD:linker), respectively [10] and the solution was allowed to react for 4 h at 72 ºC. Once the reaction was completed, the transparent block of the cross-linked CD was roughly ground and an excess of water was added during filtration to remove DMF.

Finally, residuals and unreacted reagents were completely removed by Soxhlet extraction with ethanol for 24 h. The white powder was dried and ground in a mortar and preserved in darkness and dry conditions.

### *3.2.2 Inclusion complex characterization: obtaining an apparent encapsulation constant between a ligand and CD-NSs.*

To obtain the apparent encapsulation, the methodology described by Benesi-Hildebrand was used [11] with slight modifications:

i) Although CD-NSs have a random number of cavities, it was simulated that each cavity, which has its own microscopic encapsulation constant, to give a global apparent (macroscopic) encapsulation constant. Using this approximation only a 1:1 complex could be evaluated, where $R^2$ is the degree of alteration between each microscopic constant.

$$\frac{\sum_{i=0}^{n} K_n}{n} = K_{Fapp} \quad (1)$$

ii) To it is impossible to know the molecular weight of CD-NSs accurately. However, it is possible to know the molecular weight of the guest (in our case, OXY). As is reported to fullerenes [12], the guest was used as a variable parameter of the system.

iii) As our CD-NSs are insoluble and, as is the complex too, the quantity encapsulated would be eliminated from the dissolution. So, we can measure the [OXY] before and after the equilibrium. Its variation is proportional to CDNS-OXY formed.

$$[OXY]_{Final} - [OXY]_{Initial} \propto [CDNS - OXY]_{Formed} \quad (2)$$

So, assuming a 1:1 complex, the following equilibrium is presented

$$\text{CD-NS + OXY} \rightleftharpoons \text{CDNS-OXY}$$

The apparent encapsulation constant, $K_{Fapp}$ is given by:

$$K_{Fapp} = \frac{[CDNS-OXY]}{[OXY][CDNS]} \quad (3)$$

where [CDNS], [OXY] and [CDNS-OXY] are equilibrium concentrations.

To calculate $K_{Fapp}$, eppendorfs with increasing OXY (or RES) concentration (from 2 to 400 µM) at 1 % CD-NSs in water were left in a Thermomixer Comfort(R) (Eppendorf) at 25 ºC and 800 rpm during 48 hours to measure the respective absorbances ($t_0$). After this time, the eppendorfs were centrifuged in refrigerated conditions at 7500 x g for 15min and the absorbance of the supernatant was measured in an appropriate dilution (always below 2.5 abs units). Finally, the expression corresponding to the Benesi–Hildebrand method was used to determine the $K_{Fapp}$ value.

$$\frac{1}{A-A_0} = \frac{1}{(A_\infty-A_0)K_{Fapp}[OXY]} + \frac{1}{A_\infty-A_0} \quad (4)$$

where [OXY] denotes the OXY concentration; $A_0$ the absorbance of OXY in solution without CDNS; $A_\infty$ the absorbance when all CD-NSs is complexed with OXY; and A, is the absorbance of any sample at each OXY indicated.

### *3.2.3 Preparation of OXY Loaded with β-CDI*

OXY with β-CDI 1:4 complexes were prepared in the following way: 100 mg of pure drug was added to 150 mL of *miliQ* water and sonicated for 15 min.

After that, 500 mg of β-CDI 1:4 nanosponges were added and kept for 24 h under stirring conditions in the dark. This suspension was centrifuged and the nanosponges containing OXY below was collected and dried overnight in an oven at 60 ºC.

### *3.2.4. Loading efficiency of OXY in β-CDI*

The weighed amount of OXY loaded NS (10 mg) was taken in 1 mL of ethanol. This was sonicated for 3 hours and then centrifuged to remove the solid part. The supernatant was diluted and its absorbance was measured at 301 nm; the following equation was applied to obtain the drug loading.

$$Drug\ loading\ (\%) = \frac{Quantity\ in\ the\ sonicated\ supernatant}{initial\ quantity}\ x\ 100 \qquad (5)$$

### *3.2.5 In vitro OXY release profile*

The release of OXY from the complex and free OXY was studied using dialysis membranes (cut-off 12000 Da) submerged in different stirred flasks at 37 ºC with 40 mL of 0.1M phosphate-sodium-potassium buffer at pH 7.4 and 5.5 respectively. The donor phase comprised different nanosuspensions: 2mL of buffer with 1.5 mg of OXY and/or an appropriate quantity of the complex (20 mg complex ≈ 1.5 mg OXY). The receptor phase also contained the same medium. Different samples were taken and the receptor phase was diluted with the same amount of fresh buffer. The samples were diluted and its absorbance was recorded at 301 nm.

*3.2.6 Differential scanning microcalorimetry (DSC).*

Thermograms were recorded using a DSC 200 (TA instruments, EEUU). OXY, β-CDI 1:4 nanosponge and the OXY loaded NS complex were analyzed with an aluminum pan as reference material. The samples were scanned at the rate of 10ºC/min in the range of 30 to 250 ºC under nitrogen.

*3.2.7. Fourier-transform infrared spectroscopy*

OXY, β-CDI 1:4 nanosponge and the OXY loaded NS complex were subjected to Fourier transform infrared (FTIR) spectroscopic studies using Perkin-Elmer spectrum 100 FT-IR spectrophotometer in the region of 4000 to 650 $cm^{-1}$ under nitrogen (50 mL/min).

*3.2.8 Thermal gravimetric analysis*

OXY, β-CDI 1:4 and the OXY loaded NS complex were subjected to thermal gravimetric analysis using TGA 2050 thermogravimetric analyzer (TA instruments) from 40 to 700 ºC at 10 ºC/min.

*3.2.9 Anticancer study using PC-3 cell line.*

PC-3 prostate cancer cell lines were purchased from ATCC (Manassas, VA, USA). PC-3 prostate cancer cell lines were seeded into a 96-well plate and incubated for 24 hours at 37 ℃ in a 5 % CO2 atmosphere. The cells were treated with OXY and OXY/CD-NS in the concentration range of 10-100 µM for 96 hours. After 96 hours, cell viability was evaluated using MTT by recording the absorbance at 570 nm according to the manufacturer's protocol. The cells treated with culture medium alone considered as a control and the reading

obtained from treated cell were expressed as % inhibition of cell viability. All the experiments were performed in triplicate.

### *3.2.10Data analysis*

The experiments were carried out in triplicate. Graphical representations were made using SigmaPlot (Version 10.0) and Graphpad Prism (version 5.03). A t-test was applied using Rstudio (version 0.99.878) fixing the significance level at $P < 0.05$. Other mathematical operations were carried out using wxMaxima software (version 12.04.0).

## 4. Results and discussion

### 4.1 Apparent encapsulation constant determination

Our first objective after synthesizing the nanosponges was to try to determine for the first time a model to calculate the encapsulation constant using the approximation described in the material and methods section.

Different samples with 1% of β-CDI 1:4 nanosponge were taken at increasing OXY concentrations, and incubated for 48 hours (measuring OXY concentration after and before that time). The results (**Fig**. 1) showed the effect of the β-CDI 1:4 on OXY concentration. From plotting $1/(A-A_0)$ vs 1/[OXY] it can be observed how the OXY concentration was decreased with encapsulation and precipitation (**Fig.** 1 *Insert*).

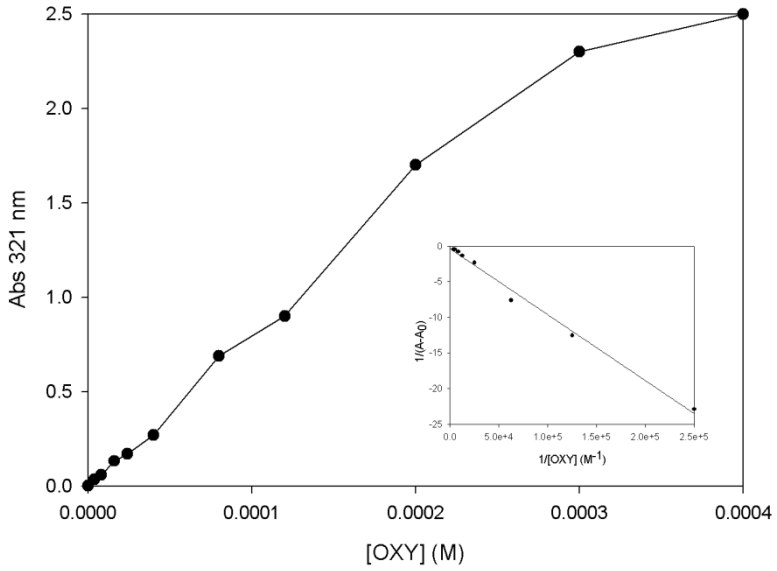


***Fig 1****. Effect of increasing OXY concentration on absorbance at 48 h with 1% of β-CDI 1:4 in water at 25 ºC. Insert. Benesi-Hildebrand plot of OXY complexed to β-CD-CDI 1:4.*

Using eq. 4 a $K_{Fapp}$ was obtained with a value of 3917.89 +/- 391.79 $M^{-1}$. Other types of CD-NSs were tested in a similar manner (**Table** 1). The $K_F$ of stilbenoids with natural and modified cyclodextrin has a $10^4$ order (as is showed in block I, part I chapter I) while CD-NSs has a $10^3$ order. Perhaps because only a few number of cavities are available to complex OXY through polymerization.

The β-CDI 1:8 nanosponge showed the highest $K_{Fapp}$, perhaps due to its higher number of CDs per gram. While α-, β-and γ- CDI 1:4. α- and γ- CDI 1:4 obtained similar and lower $K_{Fapp}$ values, possibly due to an inadequate cavity for OXY complexation, as occurs with natural CD [13]. Among the all the tested CD-NSs, β-CDI 1:4 nanosponge was selected due to a combination of low toxicity [6] and good complexation.

Table 1. Apparent $K_F$ ($M^{-1}$), SD (+/-) values and correlation coefficients for OXY/CD complexes at 25 °C in water.

| Guest | CDNS | Kapp | SD | $R^2$ 1:1 |
|---|---|---|---|---|
| **OXY** | β-CDI 1:4 | 3917.89 | 391.79 | 0.99 |
| **OXY** | β-CDI 1:8 | 5575.52 | 557.55 | 0.98 |
| **OXY** | α-CDI 1:4 | 1595.08 | 159.51 | 0.99 |
| **OXY** | γ-CDI 1:4 | 1718.64 | 171.86 | 0.99 |
| **RES** | β-CDI 1:4 | 4466.48 | 446.65 | 0.99 |

Furthermore, the complex with resveratrol, which was previously characterized, gave a $K_{Fapp}$ of 4466.48 +/- 446.65 $M^{-1}$. Although OXY has an extra hydroxyl group, both constants are very close (T-test P≈0.09), compared with natural CDs [14]. This could be because a great number of hydroxyl-groups of CD-NSs are polymerized and fewer hydrogen bonds are formed.

4.2 Loading efficiency of OXY with β-CDI 1:4 nanosponge

Drug loading is a very important parameter when preparing an inclusion complex, because bioactive compound waste should be minimized. Using Eq. 5, the results pointed to 39.75 +/- 3.8 % of OXY loading. This value is very close to the value reported previously for resveratrol for a ratio of 1:5 w/w [9] possibly due to the small difference between both $K_{Fapp}$.

4.3 Characterization of OXY loaded β-CDI 1:4 nanosponge complex: FTIR, DSC and TGA studies

The next step was to characterize our complex. Firstly, FTIR data (**Fig**. 2A) demonstrated the binding between CDI and β-CD (peak of 1746 $cm^{-1}$). For its part, OXY was demonstrated to have a peak of 1591 (aromatic C=C). This peak is also presented in the OXY loaded NS complex but with lower intensity because of the possible encapsulation of OXY with nanosponges.

DSC could be used to verify the existence of the complex instead of a physical mixture. **Fig**. 2B shows the DSC results for β-CDI 1:4, OXY and OXY loaded NS complex. β-CDI 1:4 data showed a peak at around 100 ºC; which is typical for the release of water by evaporation. Moreover, no melting or degradation was reported. OXY showed an endothermic melting peak at 199.94 ºC, which was not present in the thermogram of OXY loaded β-CDI 1:4 NS due to masking of endothermic melting of OXY. This reflects the encapsulation of OXY by β-CDI 1:4. The disappearance of the entire peak could be the result of the amorphous state of OXY [15].

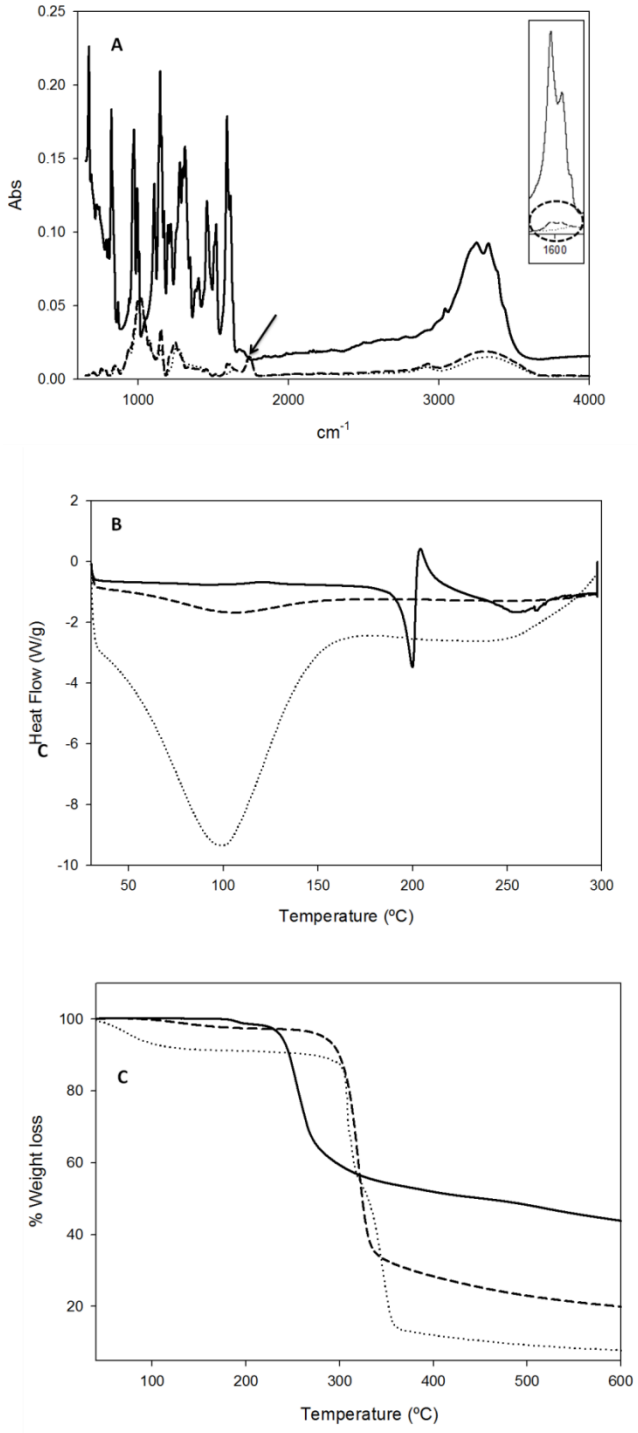


***Fig.2.*** *(A) FTIR spectrum of OXY, β-CDI 1:4 and OXY loaded β-CDI 1:4. Arrow: peak of linked β-CDI 1:4, circle, changes in complex. (B) DSC profile of OXY, β-CDI 1:4 and OXY loaded β-CDI 1:4. (C) TGA results of OXY, β-CDI 1:4 and OXY loaded β-CDI 1:4. Legend: (—) OXY, (···) β-CDI 1:4 and (·—·—·) OXY loaded β-CDI 1:4.*

Additionally, TGA studies were carried out (**Fig**. 2C). While pure β-CDI 1:4 nanosponge presented two degradation peaks (possibly due to different intramolecular binding strengths) and a mass reduction of 79.29%, the presence of OXY not only decreased the mass reduction (69.62%), but the two peaks became one. Such observations lend weight to the complexation.

4.4 *In vitro* Release profile of OXY loaded β-CDI 1:4 nanosponge

When a new pharmaceutical product is presented, the pharmacokinetics is exhaustively studied and the release of the drugs into tissues is thoroughly characterized. To study the release of our complex in tissues, an *in vitro* approximation was carried out. Different membranes (cut-off 12000 Da) were prepared at physiological pH 7.4 and at pH 5.5 (slightly acid). Different samples were taken and OXY concentration was measured (**Fig**. 3).

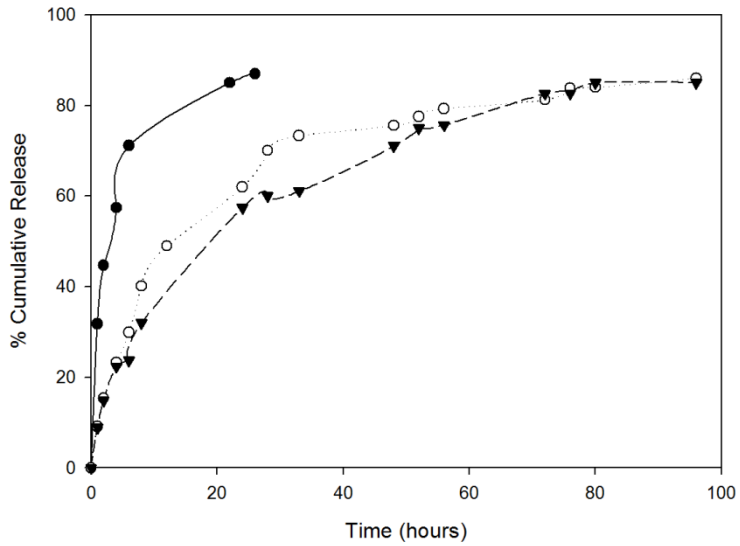


***Fig.3.*** *In vitro release profile of OXY or complex at pH 7.4 and 5.5 at 37 ºC.*

*Legend: (●) Free OXY at pH 7.4, (○) OXY loaded β-CDI 1:4 at pH 7.4 and (▲) OXY loaded β-CDI 1:4 at pH 5.5.*

The free OXY released more than 70 % with in 12 hours at both pH however, the slow and prolonged release was achieved with OXY loaded NS. The OXY loaded NS released upto 45 % at pH 7.4 and 39 % at pH 5.5 respectively, with in 12 hours which is due to encapsulation of OXY inside the cavities of β-CDs.

The OXY loaded β-CDI 1:4 nanosponge did not release the same quantity until 80 hours had passed. Furthermore, the release was slower than free OXY, suggesting a continuous dose of OXY in the sample. These data present a good approximation to real release and confirm the potential of β-CDI 1:4/OXY complexes for nutraceutical application.

4.5 *In vivo* anticancer activity of OXY loaded β-CDI 1:4 nanosponge against PC-3 cell line

The percent inhibition of cell viability is shown below. PC-3 cell lines were incubated for 96 hours and it was observed that OXY or OXY-NS showed toxicity to PC-3 cell lines (**Fig**. 4) in dose dependant manner.

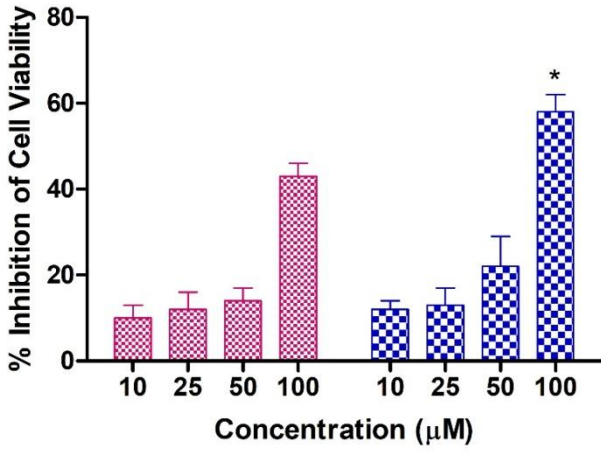


***Fig**.4 Effect of OXY (pink) and OXY/CD-NS (blue) on PC-3 viability.*

Moreover, OXY-NS showed higher toxicity compared to free OXY at all concentration range. However, only a significant difference between OXY and OXY-NS was observed at a concentration of 100 µM (43 +/-3 % *vs*. 58 +/- 4 %, $P<0.05$). Furthermore, Blank NS does not give any significant toxicity compared to OXY-NS (Data not shown).

Cancer cell are slightly acid [16], for that reason Our *in vitro* controlled release results at pH 5.5 could help to discuss results. The release demonstrated a slower release of OXY in presence of CD-NS. These facts suggest an slower release of the complexes than free drug, which in combination of a higher stability of the complex, pointed a better inhibitory effect [8,9] in cancer cells.

In conclusion, this chapter studied and applied a new methodology to calculate, for the first time, an apparent inclusion complex constant ($K_{Fapp}$) between OXY and CD-NSs using UV-Vis measurement and the Benesi-Hildebrand method with a few modifications. The $K_{Fapp}$ of OXY, with different CD-NSs was evaluated showing that the $K_{Fapp}$ is dependent on the type of cyclodextrin, bridges and type of linker. Moreover, the $K_{Fapp}$ of other drugs such as resveratrol was also evaluated and compared (3917.89 +/- 391.79 $M^{-1}$ vs 4466.48 +/- 446.65 $M^{-1}$) finding no relevant differences . The complex OXY/β-CD-CDI 1:4 was studied *in vitro* with DSC, TGA and FTIR and its loading efficiency and release behavior were studied. Finally, an anticancer study against PC-3 prostate cancer cell line was carried out showing higher inhibition of cell viability (43 +/- 3 % free oxy *vs.* 58 +/- 4% complexed). The findings as a whole represent a new opportunity to further study the complexation of drugs in CD-NSs and the use of oxyresveratrol as anticancer drug.

## References

[1] Y.H. Lim, K.H. Kim, J.K. Kim, Source, biosynthesis, biological activities and pharmacokinetics of oxyresveratrol, Korean J. Food Sci. Technol. 47 (2015) 545–555. doi:10.9721/KJFST.2015.47.5.545.

[2] R.M. Bertram, J.K. Takemoto, C.M. Remsberg, K.R. Vega-Villa, S. Sablani, N.M. Davies, High-performance liquid chromatographic analysis: applications to nutraceutical content and urinary disposition of oxyresveratrol in rats, Biomed. Chromatogr. 24 (2010) 516–521. doi:10.1002/bmc.1320.

[3] W. Chen, S.C.M. Yeo, M.G.A.A. Elhennawy, H.-S. Lin, Oxyresveratrol: A bioavailable dietary polyphenol, J. Funct. Foods. 22 (2016) 122–131. doi:10.1016/j.jff.2016.01.020.

[4] P. Rodríguez-Bonilla, J.M. López-Nicolás, F. García-Carmona, Use of reversed phase high pressure liquid cromatography for the physicochemical and thermodynamic characterization of oxyresveratrol/β-cyclodextrin complexes, J. Chromatogr. B. 878 (2010) 1569–1575. doi:10.1016/j.jchromb.2010.04.016.

[5] F. Hirayama, K. Uekama, Cyclodextrin-based controlled drug release system, Adv. Drug Deliv. Rev. 36 (1999) 125–141. doi:10.1016/S0169-409X(98)00058-1.

[6] R. Cavalli, F. Trotta, W. Tumiatti, Cyclodextrin-based Nanosponges for Drug Delivery, J. Incl. Phenom. Macrocycl. Chem. 56 (2006) 209–213. doi:10.1007/s10847-006-9085-2.

[7] A.P. Sherje, B.R. Dravyakar, D. Kadam, M. Jadhav, Cyclodextrin-based nanosponges: A critical review, Carbohydr. Polym. 173 (2017) 37–49. doi:10.1016/j.carbpol.2017.05.086.

[8] S. Swaminathan, R. Cavalli, F. Trotta, Cyclodextrin-based nanosponges: a versatile platform for cancer nanotherapeutics development, Wiley Interdiscip. Rev. Nanomed. Nanobiotechnol. 8 (2016) 579–601. doi:10.1002/wnan.1384.

[9] K.A. Ansari, P.R. Vavia, F. Trotta, R. Cavalli, Cyclodextrin-Based Nanosponges for Delivery of Resveratrol: In Vitro Characterisation, Stability, Cytotoxicity and Permeation Study, AAPS PharmSciTech. 12 (2011) 279–286. doi:10.1208/s12249-011-9584-3.

[10] W.T. Francesco Trotta, Cross-linked polymers based on cyclodextrins for removing polluting agents, 2005. http://www.google.com/patents/US20050154198.

[11] H.A. Benesi, J.H. Hildebrand, A Spectrophotometric Investigation of the Interaction of Iodine with Aromatic Hydrocarbons, J. Am. Chem. Soc. 71 (1949) 2703–2707. doi:10.1021/ja01176a030.

[12] S.P. Sibley, R.L. Campbell, H.B. Silber, Solution and Solid State Interactions of C60 with Substituted Anilines, J. Phys. Chem. 99 (1995) 5274–5276. doi:10.1021/j100015a007.

[13] P. Rodríguez-Bonilla, J.M. López-Nicolás, F. García-Carmona, Use of reversed phase high pressure liquid cromatography for the physicochemical and thermodynamic characterization of oxyresveratrol/β-cyclodextrin complexes, J. Chromatogr. B. 878 (2010) 1569–1575. doi:10.1016/j.jchromb.2010.04.016.

[14] A. Matencio, F. García-Carmona, J.M. López-Nicolás, The inclusion complex of oxyresveratrol in modified cyclodextrins: A thermodynamic, structural,

physicochemical, fluorescent and computational study, Food Chem. 232 (2017) 177–184. doi:10.1016/j.foodchem.2017.04.027.

[15] Y. Sangsen, K. Wiwattanawongsa, K. Likhitwitayawuid, B. Sritularak, R. Wiwattanapatapee, Modification of oral absorption of oxyresveratrol using lipid based nanoparticles, Colloids Surf. B Biointerfaces. 131 (2015) 182–190. doi:10.1016/j.colsurfb.2015.04.055.

[16] P. Swietach, R.D. Vaughan-Jones, A.L. Harris, A. Hulikova, The chemistry, physiology and pathology of pH in cancer, Philos. Trans. R. Soc. B Biol. Sci. 369 (2014). doi:10.1098/rstb.2013.0099.

# Block III,

# Chapter II

## *Lifespan extension in Caenorhabditis elegans by oxyresveratrol supplementation complexed in soluble cyclodextrin-based nanosponges. In vitro PDE4 inhibition characterization and in vivo approach*

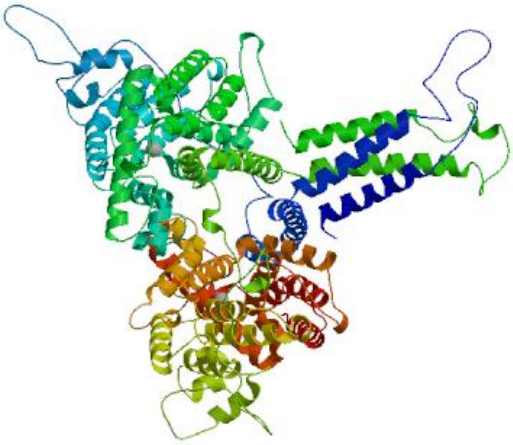

**Abstract**

In this chapter, the use of soluble nanosponges (CD-NS) to complex oxyresveratrol (OXY) was evaluated to study the lifespan extension of the mix in *Caenorhabditis elegans* (*C.elegans*) due to its phosphodiesterase type 4 (PDE4) inhibition. The titration displacement of fluorescein was used to calculate the complexation constant (KF) between CD-NS and OXY. Moreover, C.elegans PDE4 was heterologously expressed in *E.coli*, purified and refolded in presence of cyclodextrins (CDs). The apparent activity was characterized (Km = 230 ± 9 µM) and the inhibitory effect of OXY displayed *in vitro* and *in silico*. The results demonstrated a competitive inhibition fitting perfectly in our molecular docking study.

A maximum increase of the life expectancy about 6.5% was obtained in presence of OXY alone and 9.6% when is complexated with CD-NS. Surprisingly, HPβ-CD showed adverse effect agains *C.elegans*. These results as a whole represent a new opportunity to use OXY and CD-NS in lifespan products.

## Index

## 1. Contextualization

It is clear that to increase the life expectancy is a humanity desire. One of the most important environment to get it would be Dietary restriction (DR), which extending lifespan and health span [1]. However, a pharmacological approach would be more interesting to prevent strict diets. In this sense, stilbenes has been proposed and demonstrated to act as one such mimetic [2].

Nowardays, *Caenorhabditis elegans* (C.elegans) has been successfully tested for health-promoting and anti-aging potential of molecules because is transparent, small size, well-annotated genome. presents a lot of tissues similar to animals and rapid life cycle [3]. Indeed, stilbenes has been tested as lifespan agent in C.elegans previously [4], showing their capacity to lifespan extension and a plausible mechanism dependent of SIR-2.1. However, upstream the mechanism remains unclear. The first target of stilbenes in this pathway (**Fig**. 1) are the cyclic nucleotide phosphodiesterases (PDE) family [2,5]. The cyclic nucleotide phosphodiesterases comprise a group of enzymes that degrade the phosphodiester bond in the second messenger molecules cAMP and cGMP. They regulate the localization, duration, and amplitude of cyclic nucleotide signaling within subcellular domains. PDEs are therefore important regulators of signal transduction mediated by these second messenger molecules.

Some phosphodiesterases (type 1, 3 and 7) inhibition has showed to extend lifespan [6], but the paper of PDE4 has not well studied. In mice, the pharmacological inhibition of PDE4 reproduces the benefits of stilbene inhibition [7]. This data suggest that its paper on *C.elegans* lifespan should be studied.

Although stilbenes are interesting molecules, its hydrophobicity makes difficult its solubilization. For that reason, an administration using cyclodextrins (CD) and soluble cyclodextrin based nanosponges (CD-NSs) would be desirable. It would make more effective and stable the drug administration. As stilbene model oxyresveratrol (OXY) will be used, an interesting molecule which effect on lifespan has been previously studied [4].

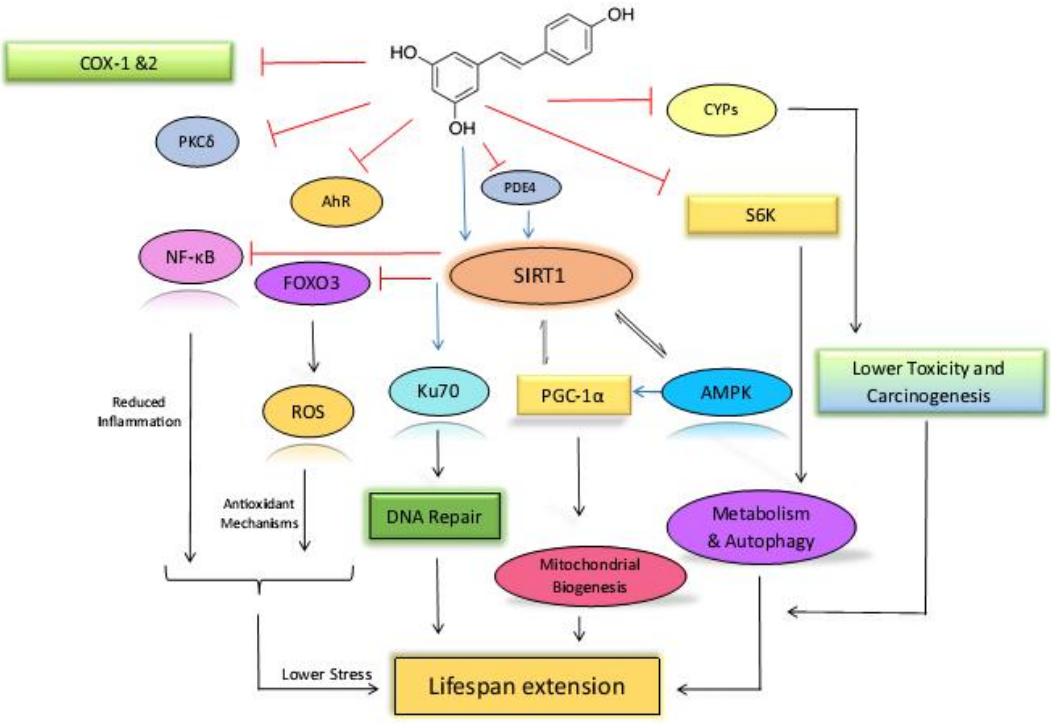


***Fig**. 1. Molecular targets of resveratrol,an OXY analogue for lifespan extension and age-related diseases [8].*

## 2. Objectives

1) To study the complexation between OXY and CD-NSs.

2) To characterize the enzymatic activity of PDE4 and its inhibition by OXY.

3) To study the mechanistic of the inhibition using molecular docking techniques.

4) To carry out an exhaustive study of lifespan in presence of CDs and CD-NSs on *C.elegans*.

## 3. Materials and methods

### 3.1 Materials

β-Cyclodextrin (β-CD) was purchased from Roquette (France). Hydroxypropyl-beta- (HPβ-CD) was purchased from Carbosynth (Berkshire, UK). Oxyresveratrol (OXY, CID 5281717) was purchased from TCI Europe and used as received. The remaining chemicals were purchased from Sigma-Aldrich (Madrid, Spain). The samples were stored in darkness

### 3.2 Equipment and Experimental Procedure

#### *3.2.1 Preparation of soluble nanosponge*

Hyper-branched water-soluble β-CD nanosponge was prepared as reported [9]. Briefly, 6 mL of anhydrous DMSO and 1 mL of triethylamine were placed in a glass scintillation vials round bottom flask and 0.997 g of β-CD was added until complete dissolution. Then, the required quantity of PMDA (pyromellitic dianhydride) was added for a 1:12 (CD:linker) ratio and the solution was allowed to react for 24 h at RT. Once the reaction was completed, the product was precipitated adding ethyl acetate and an excess of ethyl acetate was added during filtration to remove impurities. After dry, it was solubilized in deionized water, lyophilized and finally, residuals and unreacted reagents were completely removed by Soxhlet extraction with acetone for 24 h. The white powder was dried and ground in a mortar and preserved in darkness and dry conditions.

### *3.2.2 Fluorescein as displacement signal of CD-NS/OXY complex*

To verify the complexation of Fluorescein by CD-NS, the fluorescence of 25 µM of Fluorescein (ex 494 em 521) were monitored at increasing CD-NS quantities using a Shimazdu RF-6000 spectrofluorimeter (Shimadzu, Kyoto, Japan) equipped with thermostatically controlled cells was used to obtain its fluorescence spectra. Excitation and emission bandwidths were both set at 5 nm. The displacement was carried out studying the effect of increasing OXY concentration on a 25 µM of Fluorescein mixed with 200 ppm CD-NS. All samples were prepared in water with the exception of fluorescein (acetone). The apparent complexation constant of OXY/CD-NS was calculated using the equations developed by Leroy *et al.,* in 1985 for CD/ligands interactions [10]. The average molecular weight of CD-NS [9] was used to obtain the concentration of polymer and its apparent complexation constant ($K_1$) with fluorescein using Benesi-Hildebrand plot [11] as intrinsic average constant. After that, the following algebraic solution was applied to obtain the OXY/CD-NS apparent constant ($K_2$):

$$K_2 = \frac{[CDNS]_0 - \frac{v}{K_1(1-v)} - v[Fluorescein]_0}{\frac{v}{K_1(1-v)}([OXY]_0 - [CD-NS]_0 + v[Fluorescein]_0 + \frac{v}{K_1(1-v)})} \quad (1)$$

where $[CD\text{-}NS]_0$, $[Fluorescein]_0$ and $[OXY]_0$ are the initial concentration of each reactant and v is the fraction of fluorescein bound to CD-NS.

### *3.2.3. PDE4 expression*

The sequence of PDE4 (Uniprot code Q22000) was optimized and synthesized by Genscript and cloned in pET-28(a) vector to yield an N-

terminally His6-tagged protein. The final vector was transformed into *Escherichia coli* (strain Rosetta 2, DE3). To express the protein, the cells were grown with Terrific Broth (Fisher Scientific) at 37 ºC until an optical density around 1 from 0.3 abs. When the culture reached 1 D.O., ethanol was slowsly added (2% w/w final proportion) and the temperature was changed to 18 ºC. After 1 h, the cells were induced with 0.25 mM isopropyl β-D-1-thiogalactopyranoside for 16 h. Finally, the cells were centrifugated at 2500 g and 4 ºC to be stored in -80 ºC for at least two hours.

### *3.2.4. PDE4 purification and refolding*

Cells were lysed by sonication in 5 pulses of 15 s in a Branson Digital sonifier (Branson Ultrasonic Corporation, Connecticut, USA) and centrifugated at 8000 g for 30 min at 4ºC. The resulting pellet was dissolved in 0.3 M NaCl, 6 M Urea, 1 % Triton X-100, 0.05 M phosphate buffer pH 7.4 with 0.5 mM benzamidine for 30 min at 500 rpm and 20 ºC in a thermomixer confort (Eppendorf). It was centrifugated at 8000 g's for 30 min at 4ºC and the remaining pellet was dissolved in 0.3 M NaCl, 2.5 % Triton X-100, 0.05 M phosphate buffer pH 7.4 with 0.5 mM benzamidine for 150 min at 500 rpm and 20 ºC in a thermomixer confort (Eppendorf). The sample was centrifugated at 8000 g for 30 min at 4ºC to remove pellet. The supernatant was incubated [12] adding 2 mM β-CD (15 min at 35 ºC) and after β-CD until 4 mM (15 min at 35 ºC). The final solution was concentrated using Amicon Ultra15 50KDa until 100 uL and added to 5 mL of binding buffer (0.3 M NaCl, 0.05 M phosphate buffer pH 7.4 with 0.5 mM benzamidine) and purified using a His GraviTrap TALON ® column (GE Healthcare, Germany) using a wash buffer (0.3 M NaCl, 25 mM

imidazole, 0.05 M phosphate buffer pH 7.4 with 0.5 mM benzamidine) and elution buffer (0.3 M NaCl, 300 mM imidazole, 0.05 M phosphate buffer pH 7.4 with 0.5 mM benzamidine). The final solution was concentrated again with another Amicon Ultra15 50KDa to 100 uL and dissolved in binding buffer (3 mL) twice to remove salt contaminations. A 10% SDS-PAGE was carried out to check purify and the molecular weight of the final protein. The concentration of PDE4 was determined by the Bradford assay (Biorad) using bovine serium albumin as standard.

### *3.2.5. PDE4 activity assay*

The assay of PDE4 activity was as described [13]: Briefly, the desirable cAMP concentration incubated with PDE4 in sample buffer (7.5 mM $Mg_2SO_4$ 0.1 M Tris-HCl pH 7) were incubated and 15 µL were directly injected in an Agilent 1100 series HPLC system (CA, USA) and a 1200 series module UV–VIS detector with a Kromasil Hydro 150 C18 column (150 mm × 4,6 mm, 5 µm particle size) equipped with a Optiguard® C18 precolumn (Supelco) to prevent entering proteins or contaminants. The conditions were established in the following gradient: solvents A, mQ water with 0.1% acetic acid, and B solvent, 85/15 MeOH/THF w/w with 0.1% acetic acid. Conditions: 0–3 min, 0% B at 1 mL/min; for 3–12.5 min, 5% B at 2 mL/min; for 12.5–17 min, 50% B at 2 mL/min and for 17–20 min, 0% B at 2 mL/min all at 30 °C.

The effect of pH and Mg2SO4 concentration were studied changing their concentrations in sample buffer.

For $K_m$, $V_{max}$ and $k_{cat}$ (product generated per enzyme and time) determination, a non-linear plot using Michaelis-Menten kinetic was used.

$$V = \frac{V_{max}[S]}{K_m+[S]} = \frac{k_{cat}[E][S]}{K_m+[S]} \quad (2)$$

Where [S] is the subtract concentration and [E] the enzyme concentration.

For OXY inhibition assay, the $I_{50}$ (value where the 50% of the enzyme is inhibited) was studied. To obtain $K_i$ (the concentration required to produce half maximum inhibition), a conversion from $I_{50}$ to $K_i$ for competitive inhibition was applied [14].

$$K_i = \frac{I_{50}}{1+\frac{[S]}{K_m}} \quad (3)$$

*3.2.6. Molecular modeling and docking*

The sequence reported by Genscript after optimization was uploaded to Swiss-Model [15] with default parameters using PDB ID 4WZI as template. The resulting protein was used to carry the molecular docking experiments out. Our model and the ligand (cAMP or OXY, obtained from ZINC database) were uploaded to Swiss-Dock [16] with default parameters. The results were analyzed using Chimera (Version 1.9) and Pymol (version 1.9).

*3.2.7 In vivo Lifespan assay in C.elegans*

The protocol was carried out as reported [17] using *lifespan machine* [18] with slight modifications; briefly: After 48 h in liquid media, the synchronic worms (strain N2) were centrifuged at 2.000 g and washed with M9 buffer three times. 70-80 worms were then transferred to 35 mm analysis plates, containing 8 mL of NGM agar, supplemented with 30 µg/mL of nystatin, 100 µM of ampicillin and 10 µg/mL of FUdR (2′-Deoxy-5-fluorouridine) to avoid progeny.

Plates were seeded with 100 µL of *E. coli* OP50 from an overnight culture in LB at 37 °C; the culture was concentrated 10× in a sterile M9 buffer and was inactivated using the heat shock method (incubation at 65 °C for 30 min). Then, the samples were administrated. The samples were prepared to achieve 1% DMSO in plates and sterilized by filtration (CD or CD-NS) or autoclave (OXY).

All the experiment plates were done in triplicate. Plates were closed and incubated for 20 min at 20 °C. Plates that present condensation were open under sterile conditions and the lids dried with disposable sterile wipers. Closed lid plates were loaded into the scanners of the lifespan machine. The machine acquired an image of each loaded plate every hour for the duration of the experiment and the analysis detected the time of the death for each worm. The experiments were set at 25 °C for 25 days.

### *3.2.8 Data analysis*

Mathematical analysis of the obtained data in *Lifespan Machine* was performed using the online application for survival analysis OASIS 2 [19] with the Kaplan-Meier estimator, Boschloo's Test, Kolmogorov-Smirnov Test and Survival Time F-Test.

The remaining experiments were carried out in triplicate. Graphical representations and kinetic were made using SigmaPlot (Version 10.0). A t-test was applied using Rstudio (version 0.99.878) fixing the significance level at $P < 0.05$. Other mathematical operations were carried out using wxMaxima software (version 12.04.0).

## 4. Results and discussion

### 4.1 Fluorescein as a nanosensor for soluble CD-NS complexation

Our first objective in this chapter was to demonstrated that soluble CD-NS could also complex OXY. For that reason, we used a host displacement with fluorescein, which is a well studied CD complexated molecule [20,21], whose complexation quenches the fluorescence signal.

The effect of CD-NS on fluorescein is showed in **Fig**. 2A. The results showed that the fluorescein signal is decreased by CD-NS. No scattering were reported by CD-NS. This data suggests that the decrease on fluorescein signal is due to its complexation. This data was used to obtain $K_1$ ($K_1 = 5.6 \times 10^4 \pm 2.5 \times 10^3$ $M^{-1}$, $R^2 > 0.99$) using Benesi-Hildebrand assay as an intrinsic average complexation constant.

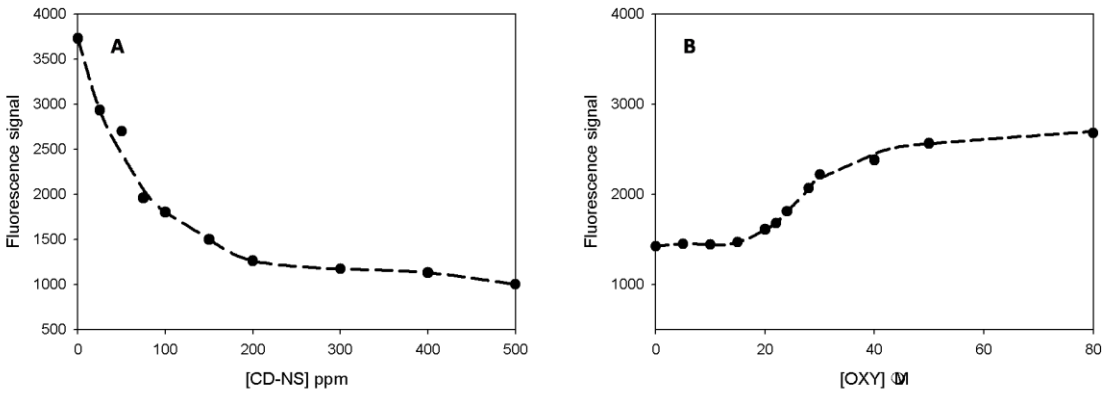


*Fig. 2. (A) Effect of CD-NS on fluorescein fluorescence signal (conditions: water at 25 ºC). (B) Effect of OXY on fluorescein/CD-NS complex fluorescence signal (condition: water at 25 ºC)*

Now, the effect of OXY on fluorescein/CD-NS signal is studied. 200 ppm of CD-NS was selected because it was the concentration where the asymptote

starts. **Fig**. 2B shows that the fluorescein signal is increased as a consequence of the entrance of OXY and fluorescein release. Using **Eq**. 1 at several OXY concentrations [10], the average $K_2$ value was $1.20 \times 10^5$ $M^{-1} \pm 1.23 \times 10^4$ $M^{-1}$.In general terms, these data support the idea that CD-NS can complex OXY.

4.2 PDE4 purification and refolding

This is the first time that the complete PDE4 of *C.elegans* is expressed heterologously. We selected *E.coli* to manage this expression. Although it was a eukaryotic protein, *E.coli* is easily handling [22]. The uniprot Q22000 was used to create a heterologous expression vector for *E.coli*. Several tries always gave the same profile; the protein formed inclusion bodies. For that reason, our strategy changed to be focused on purifying the inclusion bodies and refold the protein. In the bibliography there are a lot of possibilities and strategies to purify inclusion bodies and try to recover the activity of proteins [22], however, the use of CDs as chaperons was previously reported [12] and attracted our attention. The protocol (**Fig**. 3A) described the possibility of i) using detergents to purify and separate proteins from the inclusion bodies and ii) with CDs, removing the detergent slowly starting the refolding process. Firstly, treatment with urea was used to remove impurities of pellet. After that, increasing concentrations of triton X-100 were tested to recover the protein, selection 2.5% as optimal (**Fig**. 3B). After purification and refolding, the protein showed a good purity (**Fig**. 3C). It is clear that there was a decrease of apparent molecular weight, perhaps some aggregation of other proteins or by the presence of detergents [23].

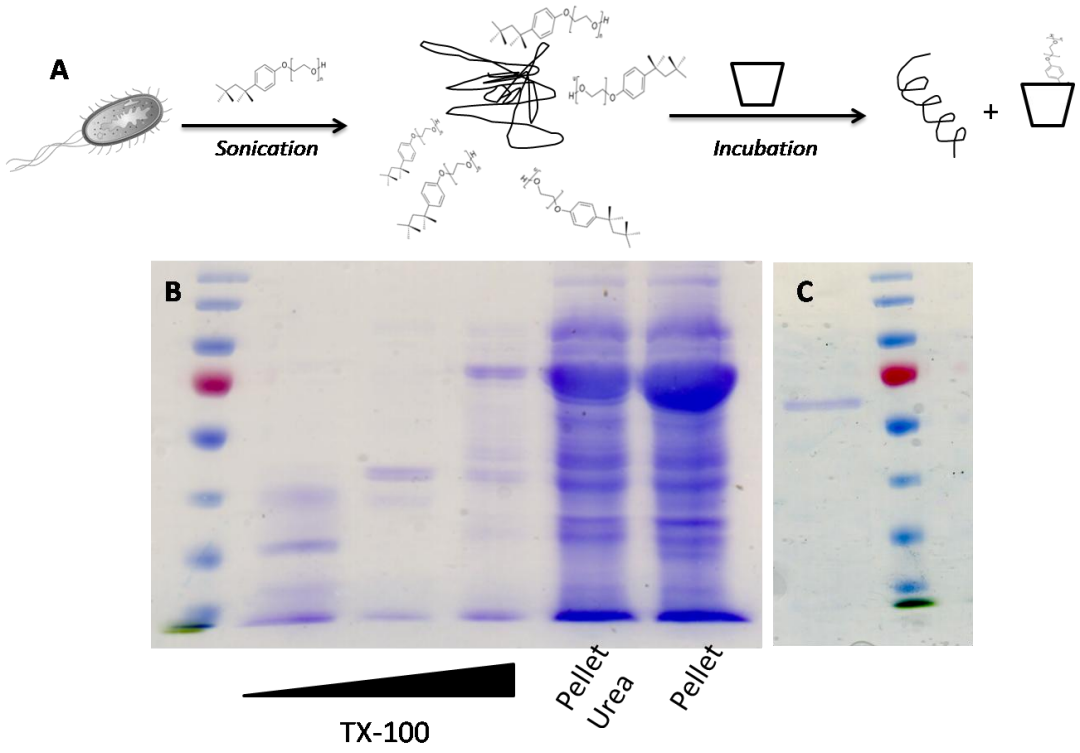


***Fig**.3. (A) Scheme of the refolding process. (B) SDS-PAGE of different TX-100 % for purifying PDE4. (C) SDS-PAGE of refolded and pure PDE4.*

4.3 PDE4 activity assay and inhibition

Our next step was to check the activity of the pure refolded PDE4 against cAMP. The protein was able to convert cAMP to AMP; for that reason, the optimal pH and [$Mg^{2+}$], because the zinc ion is strongly linked to the catalytic center, [24,25] were studied to proceed the characterization (data not showed). **Fig**. 4A shows the typical Michaelis-Menten kinetics of the curve at the optimal conditions (pH 7 and 7.5 mM $Mg_2SO_4$). The results gave a $K_{mapp}$ = 230 ± 9 µM, $V_{maxapp}$ = 3.3 x $10^{-8}$ ± 0.1 x $10^{-8}$ mols/s/mg and $k_{catapp}$ 0.001 ± 3 x $10^{-5}$ $s^{-1}$ ($R^2$ ≈ 0.98). After enzymatic characterization, the next step was to study the effect of OXY on the enzymatic activity (**Fig**. 4B). The $I_{50}$ = 10 ± 0.6 µM suggests a powerful inhibition. Recently, it was reported that human PDE4 presents a

resveratrol competitive inhibition [5], for that reason, it is reasonable to manage the same inhibition. The calculation of $K_i$ was carried out using Eq.3, with a $K_{iapp}$ of 3.2 ± 0.16 µM.

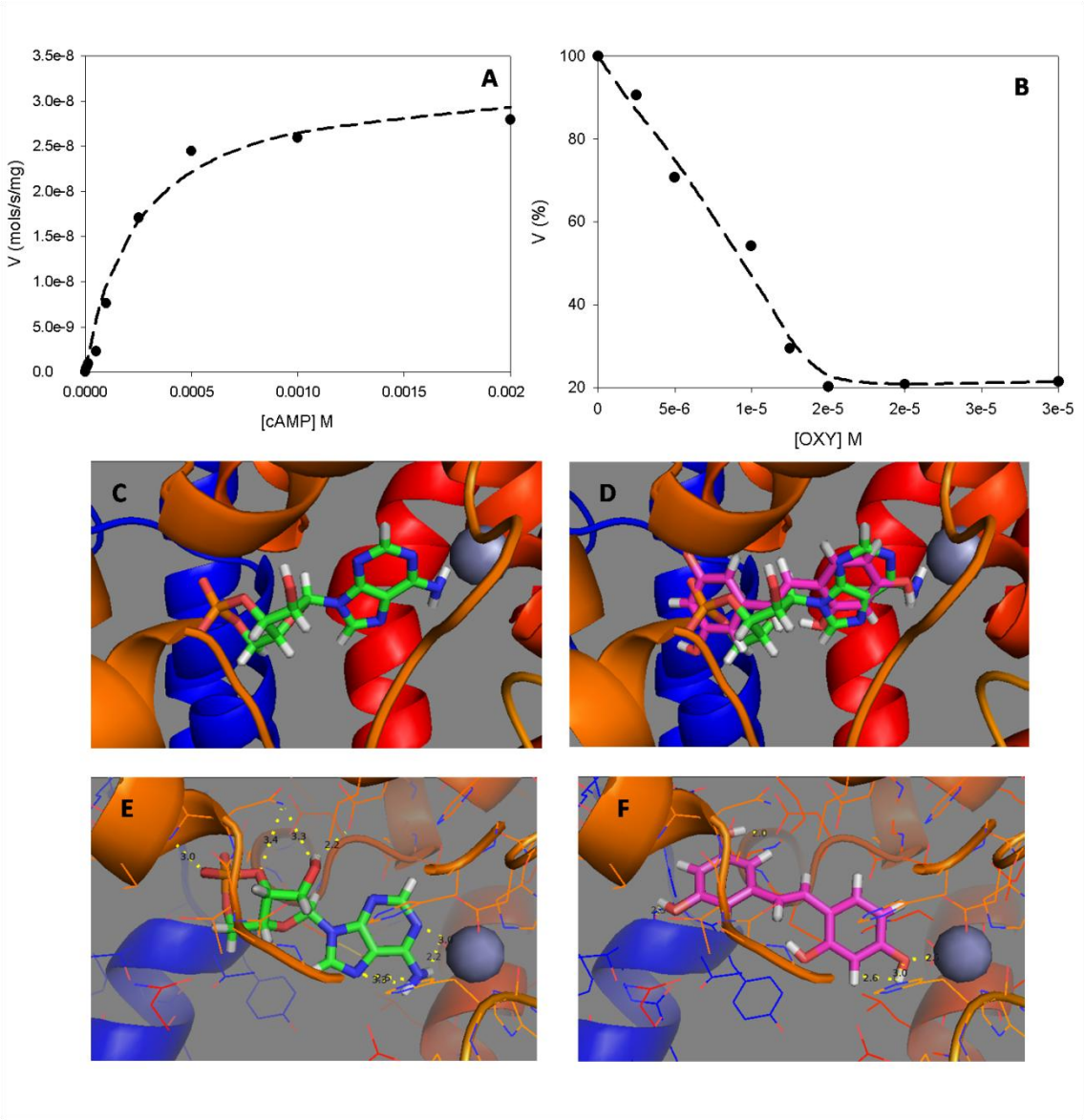


***Fig**. 4. (A) Michaelis-Menten fit of the Effect of cAMP on PDE4 activity (sample buffer at 25 ºC). (B) Effect of OXY on PDE4 activity at 4 x $10^{-4}$ M of cAMP (sample buffer at 25 ºC). (C) Molecular docking of cAMP/PDE4, (D) Overlapping OXY and cAMP docking results. (E) Polar interactions of cAMP with PDE4 and (F) Polar interactions of OXY with PDE4.*

4.4 Molecular modeling of PDE4

Our molecular modeling of PDE4 also demonstrated that oxy enter in the active site of PDE4 to inhibit the protein (**Fig**. 4C and D). The score docking of cAMP (-8.18) and OXY (-8.56) could also justify the lower concentration of OXY to fit PDE4 than cAMP. In addition, a practical perfect overlapping was achieved for both molecules. The interaction (Table 1, **Fig.** 4E and 4F) of cAMP and OXY with $Zn^{2+}$ ion demonstrate that $Zn^{2+}$ is essential for its bioactivity, which is intrinsic linked to the enzyme in collaboration with $Mg^{2+}$ [24]. Moreover, both molecules interact also with His347 of the protein and an internal bound in OYX and cAMP is formed (**Fig.** 4E and 4F), being this Hys the UNIPROT proposal active site of this enzyme. Perhaps this structure (internal bond+Hys347+Zn) is essential to the activity. Two last sections demonstrated that i) PDE4 has an important role on OXY bioactivities, ii) the refolding was enough to elucidate the inhibition strength and iii) OXY inhibits PDE4 using an almost perfect competitive interaction.

Table 1. Distance of polar contact of cAMP and OXY with PDE4 residues.

| Residue | cAMP (Å) | OXY (Å) |
|---|---|---|
| **His 347** | 3.3 | 3.0 |
| **$Zn^{2+}$** | 2.7 | 3.0 |
| **Glu 417** | 2.2 | - |
| **Asn 396** | 3.3 and 3.4 | - |
| **Gln 37** | 3.0 | - |
| **Asp 459** | - | 3.0 |
| **Thr 209** | - | 2.3 |

4.5 In vivo Lifespan

After to demonstrate that PDE4 can be inhibited by OXY, being an important regulator of the pathway (**Fig**. 1); an *in vivo* study of the effect of OXY supplementation (alone or complexated, increasing its stability) on *C.elegans* lifespan was carried out (**Fig**. 5A). The results showed that OXY increases the average life expectancy around 6.5% ($P<0.05$) with maximum at 25 µM (**Fig** 5B). Our research group has demonstrated that stilbenes could form aggregates [26] and this fact could prevent their bioavailability. To demonstrate these aggregates, different spectra at increasing OXY concentration was done and after 32 µM started to change, perhaps by the existence of other OXY forms (**Fig**. 5C).

This fact can prevent to see the real oxyresveratrol capacity. In these cases, the supplementation in presence of HP-βCD and soluble CD-NS must be evaluated. HP-βCD demonstrated to be toxic ($P<0.05$, **Fig**. 5D) for *C.elegans*, perhaps by the complexation of some essential compounds inside worms like membrane cholesterol [27]. However, soluble CD-NS would not be toxic; its polymeric nature would have less absorption capacity by the worm. Effectively, **Fig**. 5E showed that our polymer did not present any adverse effect on *C.elegans.* Furthermore, the effect of the polymer on C.elegans in presence of OXY caused an increase of life expentancy higher than free OXY, around 9.6% (**Fig**. 5F). As can be seen, the more polymers you have the lower effect you have. This is because OXY complexation is much higher than the release and *C.elegans* cannot absorb OXY.

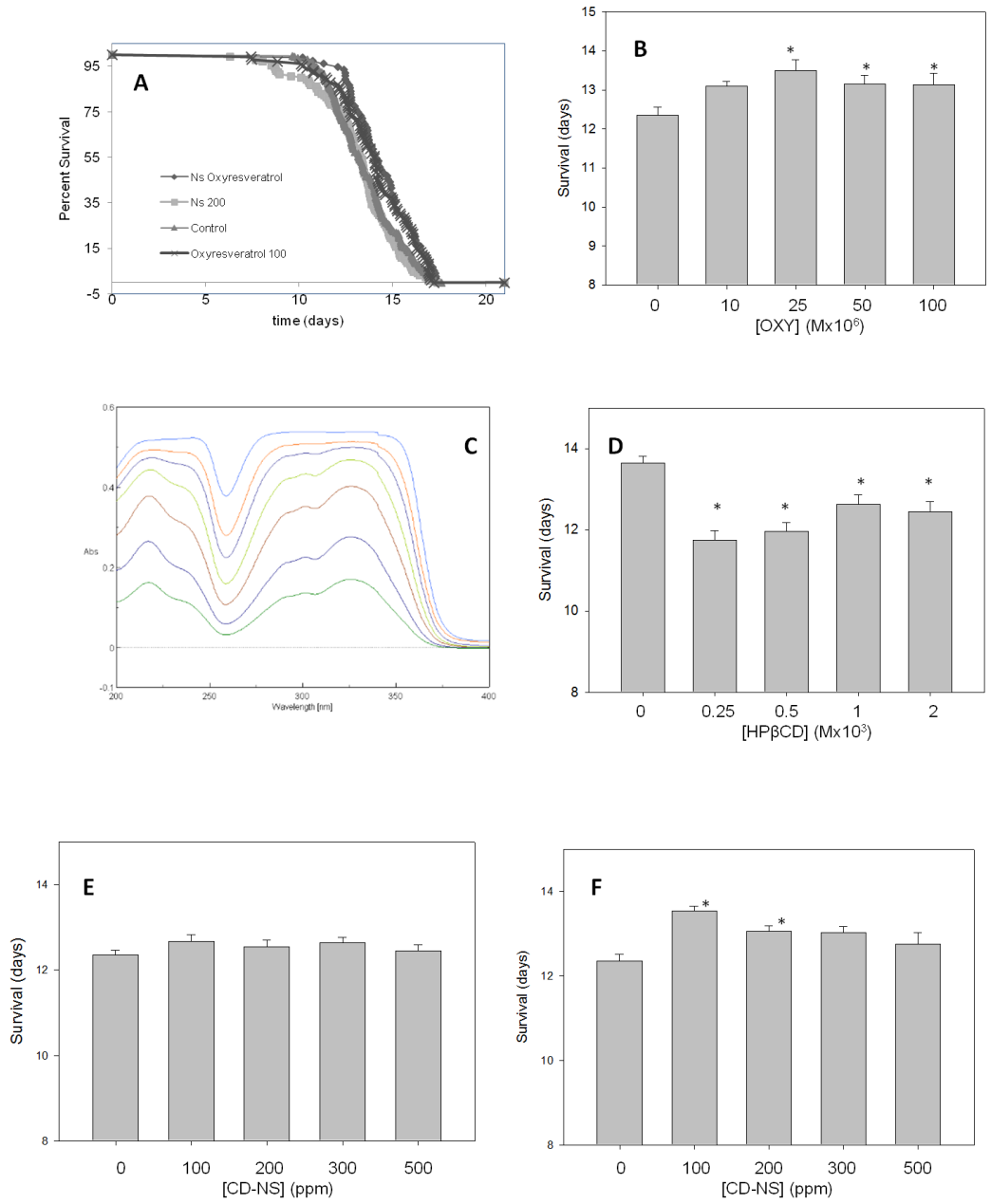


***Fig**. 5. (A)Percent of survival worms in presence of CD-NS 200 ppm, OXY 100 µM, and a mixture of them. (B) Mean lifespan of C.elegans in presence of different OXY concentrations. (C) Successive spectra at 8, 16, 32, 48, 72, 100 and 140 µM OXY concentrations (water, 25 ºC). (D) Mean lifespan of C.elegans in presence of different HPβ-CD concentrations, (E) Mean lifespan of C.elegans in presence of different CD-NS concentrations. (F) Mean lifespan of C.elegans in presence of different CD-NS concentrations at 100 µM OXY (even the control). (* = P<0.05 related to control)*

To finish, our data demonstrated that i) OXY improves life expectancy on *C.elegans*, ii) the CDs monomers are toxic for *C.elegans* and iii) the supplementation of OXY with soluble CD-NS enhanced the beneficial effects to OXY supplementation.

To conclude, in this chapter we have synthesized soluble CDs polymers, which has been used to supplement OXY to *C.elegans*. The complexation of OXY by CD-NS was demonstrated using fluorimetric displacement of fluorescein. On the other hand, *C.elegans* PDE4 was heterologously expressed, refolded and purified. The refolding with CDs acting as molecular chaperons was enough to characterize the enzyme activity and its inhibition by OXY, showing its potential as a key of the regulation on lifespan extension. The combination of CD-NS/OXY increased more the life expectancy than free OXY. The findings as a whole represent a new opportunity to use OXY as an ingredient of nutraceutical products focused on lifespan.

## References

[1] E.L. Greer, D. Dowlatshahi, M.R. Banko, J. Villen, K. Hoang, D. Blanchard, S.P. Gygi, A. Brunet, An AMPK-FOXO pathway mediates longevity induced by a novel method of dietary restriction in C. elegans, Curr. Biol. CB. 17 (2007) 1646–1656. doi:10.1016/j.cub.2007.08.047.

[2] M. Reinisalo, K&#xe5, A. Rlund, A. Koskela, K. Kaarniranta, R.O. Karjalainen, M. Reinisalo, K&#xe5, A. Rlund, A. Koskela, K. Kaarniranta, R.O. Karjalainen, Polyphenol Stilbenes: Molecular Mechanisms of Defence against Oxidative Stress and Aging-Related Diseases, Polyphenol Stilbenes: Molecular Mechanisms of Defence against Oxidative Stress and Aging-Related Diseases, Oxidative Med. Cell. Longev. Oxidative Med. Cell. Longev. 2015, 2015 (2015). doi:10.1155/2015/340520, 10.1155/2015/340520.

[3] A.K. Corsi, B. Wightman, M. Chalfie, A Transparent Window into Biology: A Primer on Caenorhabditis elegans, Genetics. 200 (2015) 387–407. doi:10.1534/genetics.115.176099.

[4] J. Lee, G. Kwon, J. Park, J.-K. Kim, Y.-H. Lim, Brief Communication: SIR-2.1-dependent lifespan extension of Caenorhabditis elegans by oxyresveratrol and resveratrol, Exp. Biol. Med. Maywood NJ. 241 (2016) 1757–1763. doi:10.1177/1535370216650054.

[5] S.-J. Park, F. Ahmad, A. Philp, K. Baar, T. Williams, H. Luo, H. Ke, H. Rehmann, R. Taussig, A.L. Brown, M.K. Kim, M.A. Beaven, A.B. Burgin, V. Manganiello, J.H. Chung, Resveratrol ameliorates aging-related metabolic phenotypes by inhibiting cAMP phosphodiesterases, Cell. 148 (2012) 421–433. doi:10.1016/j.cell.2012.01.017.

[6] X. Ye, J.M. Linton, N.J. Schork, L.B. Buck, M. Petrascheck, A pharmacological network for lifespan extension in Caenorhabditis elegans, Aging Cell. 13 (2014) 206–215. doi:10.1111/acel.12163.

[7] J.H. Chung, Metabolic benefits of inhibiting cAMP-PDEs with resveratrol, Adipocyte. 1 (2012) 256–258. doi:10.4161/adip.21158.

[8] K.S. Bhullar, B.P. Hubbard, Lifespan and healthspan extension by resveratrol, Biochim. Biophys. Acta BBA - Mol. Basis Dis. 1852 (2015) 1209–1218. doi:10.1016/j.bbadis.2015.01.012.

[9] F. Trotta, F. Caldera, R. Cavalli, A. Mele, C. Punta, L. Melone, F. Castiglione, B. Rossi, M. Ferro, V. Crupi, D. Majolino, V. Venuti, D. Scalarone, Synthesis and

characterization of a hyper-branched water-soluble β-cyclodextrin polymer, Beilstein J. Org. Chem. 10 (2014) 2586–2593. doi:10.3762/bjoc.10.271.

[10] L.A. Selvidge, M.R. Eftink, Spectral displacement techniques for studying the binding of spectroscopically transparent ligands to cyclodextrins, Anal. Biochem. 154 (1986) 400–408. doi:10.1016/0003-2697(86)90005-9.

[11] H.A. Benesi, J.H. Hildebrand, A Spectrophotometric Investigation of the Interaction of Iodine with Aromatic Hydrocarbons, J. Am. Chem. Soc. 71 (1949) 2703–2707. doi:10.1021/ja01176a030.

[12] D. Rozema, S.H. Gellman, Artificial chaperone-assisted refolding of carbonic anhydrase B, J. Biol. Chem. 271 (1996) 3478–3487.

[13] A. Matencio, F. García-Carmona, J.M. López-Nicolás, An improved "ion pairing agent free" HPLC-RP method for testing cAMP Phosphodiesterase activity, Talanta. 192 (2019) 314–316. doi:10.1016/j.talanta.2018.09.058.

[14] C. Yung-Chi, W.H. Prusoff, Relationship between the inhibition constant (KI) and the concentration of inhibitor which causes 50 per cent inhibition (I50) of an enzymatic reaction, Biochem. Pharmacol. 22 (1973) 3099–3108. doi:10.1016/0006-2952(73)90196-2.

[15] A. Waterhouse, M. Bertoni, S. Bienert, G. Studer, G. Tauriello, R. Gumienny, F.T. Heer, T.A.P. de Beer, C. Rempfer, L. Bordoli, R. Lepore, T. Schwede, SWISS-MODEL: homology modelling of protein structures and complexes, Nucleic Acids Res. 46 (2018) W296–W303. doi:10.1093/nar/gky427.

[16] A. Grosdidier, V. Zoete, O. Michielin, SwissDock, a protein-small molecule docking web service based on EADock DSS, Nucleic Acids Res. 39 (2011) W270-277. doi:10.1093/nar/gkr366.

[17] M.A. Guerrero-Rubio, S. Hernández-García, F. García-Carmona, F. Gandía-Herrero, Extension of life-span using a RNAi model and in vivo antioxidant effect of Opuntia fruit extracts and pure betalains in Caenorhabditis elegans, Food Chem. 274 (2019) 840–847. doi:10.1016/j.foodchem.2018.09.067.

[18] N. Stroustrup, B.E. Ulmschneider, Z.M. Nash, I.F. López-Moyado, J. Apfeld, W. Fontana, The *Caenorhabditis elegans* Lifespan Machine, Nat. Methods. 10 (2013) 665–670. doi:10.1038/nmeth.2475.

[19] S.K. Han, D. Lee, H. Lee, D. Kim, H.G. Son, J.-S. Yang, S.-J.V. Lee, S. Kim, OASIS 2: online application for survival analysis 2 with features for the analysis of maximal lifespan and healthspan in aging research, Oncotarget. 7 (2016) 56147–56152. doi:10.18632/oncotarget.11269.

[20] I.R. Politzer, K.T. Crago, T. Hampton, J. Joseph, J.H. Boyer, M. Shah, Effect of β-cyclodextrin on the fluorescence, absorption and lasing of rhodamine 6G, rhodamine B and fluorescein disodium salt in aqueous solutions, Chem. Phys. Lett. 159 (1989) 258–262. doi:10.1016/0009-2614(89)87420-2.

[21] L. Flamigni, Inclusion of fluorescein and halogenated derivatives in .alpha.-, .beta.-, and .gamma.-cyclodextrins: a steady-state and picosecond time-resolved study, J. Phys. Chem. 97 (1993) 9566–9572. doi:10.1021/j100140a006.

[22] J. Kaur, A. Kumar, J. Kaur, Strategies for optimization of heterologous protein expression in E. coli: Roadblocks and reinforcements, Int. J. Biol. Macromol. 106 (2018) 803–822. doi:10.1016/j.ijbiomac.2017.08.080.

[23] A. Rath, M. Glibowicka, V.G. Nadeau, G. Chen, C.M. Deber, Detergent binding explains anomalous SDS-PAGE migration of membrane proteins, Proc. Natl. Acad. Sci. U. S. A. 106 (2009) 1760–1765. doi:10.1073/pnas.0813167106.

[24] K. Suoranta, J. Londesborough, Purification of intact and nicked forms of a zinc-containing, Mg2+-dependent, low Km cyclic AMP phosphodiesterase from bakers' yeast, J. Biol. Chem. 259 (1984) 6964–6971.

[25] Y. Xiong, H.-T. Lu, Y. Li, G.-F. Yang, C.-G. Zhan, Characterization of a Catalytic Ligand Bridging Metal Ions in Phosphodiesterases 4 and 5 by Molecular Dynamics Simulations and Hybrid Quantum Mechanical/Molecular Mechanical Calculations, Biophys. J. 91 (2006) 1858–1867. doi:10.1529/biophysj.106.086835.

[26] J.M. López-Nicolás, F. García-Carmona, Aggregation state and pKa values of (E)-resveratrol as determined by fluorescence spectroscopy and UV-visible absorption, J. Agric. Food Chem. 56 (2008) 7600–7605. doi:10.1021/jf800843e.

[27] D. Castagne, M. Fillet, L. Delattre, B. Evrard, B. Nusgens, G. Piel, Study of the cholesterol extraction capacity of β-cyclodextrin and its derivatives, relationships with their effects on endothelial cell viability and on membrane models, J. Incl. Phenom. Macrocycl. Chem. 63 (2008) 225–231. doi:10.1007/s10847-008-9510-9.

# Conclusions

This thesis focused on the different uses of CDs in basic and applied studies. In our first block, several inclusion complexes characterizations were carried out for understanding CDs capacities. After that, in the second block we studied the application of CDs in different fields such as analytical chemistry, food science and pharmaceutical science. Finally, our third block studied the synthesis of a polymer called CDs-based nanosponge and its applications.

A considerable quantity of CD advances was obtained, which can be cleared up:

1. For the first block, different CDs were used to obtain and characterize the inclusion complex of some stilbenes such as piceatannol, trans-α-methylstilbene, oxyresveratrol, resveratrol sterate and resveratrol oleate and fatty acids such as rumenic acid and t10,c12 Conjugated linoleic acid.
    a. For fatty acids, the effect of CDs on the critical micellar concentrations of the lipids was used to calculate the complexation constant of the fatty acids. The effect of temperature and pH was studied showing an interesting conformational changing in rumenic acid depending on temperature. The best CD tested was HPβ-CD in both cases giving similar $K_F$ results, although rumenic acid complex was the strongest.
    b. For stilbenes, commercial stilbenes and synthethized (using Steglich esterification) were studied using two principal strategies (spectrometric and HPLC) in combination with a lot of techniques (DSC, NMR, molecular docking, quenching, etc.) to clarify the complex. In general, β-CD modified cyclodextrins have been the

best for stilbene complexing. Our results demonstrated as the displacement of quinine can be used to confirm the complexation of drugs in CD. In addition, NMR was used to study the structure of a complex for the first time in our research group. Finally, molecular docking strategy was applied to predict the interactions successfully.

2. The applications of the second block were focused in three fields:
    a. Our analytical chemistry application was to study the enantioseparation of methyl jasmonate isomers using a combination of HPLC-RP, Mβ-CD and molecular docking technique. We were able to separate and identify them successfully with an easy and reproducible method when CDs were added to mobile phase and rosemary essential oil sample was used in combination of molecular docking to number the molecules.
    b. The applications of the food science studied three different uses of CDs:
        i. The ternary complex between ellagic acid, γ-CD and borax was evaluated and exhaustively studied and the resulting signal probed in blueberries successfully. A novel mathematical model was used to determine the encapsulation constant. The signal sensitivity was lineal and accurate. No interferences were obtained in the application.

ii. The effect of CDs protection on betalain derivates at citric pH was evaluated. The complex of Phenylethylamine-betaxanthin with different CDs was studied. β-CD derivates showed to be the best option to complex the molecule. Its complexation is a good strategy to protect the molecule in aqueous solutions.

iii. Finally, the food model strategy was applied to fortify juice and milk with oxyresveratrol and β-CD. The results showed the samples to be perfectly stable for 5 weeks in all the conditions tested with the exception of the "oversaturated non-darkness stored milk food model samples" after 3 week, when partial degradation started. Using dark storage an oversaturated oxyresveratrol solution solubilized by β-CD can be preserved at least 5 weeks. The samples were also perfectly bioaccessible and its antimicrobial properties were increased.

c. The pharmaceutical applications were:

i. The establishing of an easy methodology to measure HPβ-CD in Niemman Pick Type C patient. Indeed, the method was applied in a clinical case. An almost complete HPβ-CD elimination was showed in 3 days but we have demonstrated that this can be increased to every four days.

ii. The increase of bioaccesibility and photostability of roflumilast, a potent Chronic obstructive pulmonary disease (COPD) treatment, was carried out complexing this drug

with several CDs. These data could improve the tablets and therapy to improve the treatment.

3. The third block studied the synthesis and application of soluble and insoluble nanosponges on OXY encapsulation and bioactivities.
    a. Insoluble nanosponges were used to complex OXY creating a novel methodology to determine the complexation constant for the first time in nanosponges. The complexation efficiency and uptake were also obtained. TGA, DSC and FTIR experiment were carried out to check the complex. An *in vitro* controlled release showed the slower release of complexated drug than free drug. The anticancer test demonstrated higher inhibition of complexed drug (58 %) than free drug (42%) representing a novel possibility to enhance its bioactivities.
    b. Soluble nanosponges were used to study the lifespan of OXY supplementation on *C.elegans*. A displacement of fluorescein was used to verify the encapsulation of OXY on CD-NS. PDE4 of *C.elegans* was heterologous expressed, purified and refolded to determine its enzymatic parameters and OXY inhibition. An *in silico* study was carried out showing the essential of the inhibition. The combination of OXY and CD-NS increased the effect of OXY on lifespan in contrast to CDs monomers that affected negatively to *C.elegans*.

This thesis as a whole represents an important advance on the knowledge of CDs in several fields and establishes new methodologies to work with CDs

monomers and polymers in analytical chemistry, food and pharmaceutical Science.